INVESTIGATION ON DIELECTRIC PROPERTIES OF SOLID SILICONE RUBBER PARTICULATE COMPOSITES

Thesis

Submitted in partial fulfilment of the requirements for the degree of

DOCTOR OF PHILOSOPHY

by

B.S. MANOHAR SHANKAR

MECHANICAL ENGINEERING DEPARTMENT
NATIONAL INSTITUTE OF TECHNOLOGY
KARNATAKA,
SURATHKAL, MANGALORE -575025
OCTOBER, 2020

DECLARATION

by the Ph.D. Research Scholar

I hereby *declare* that the Research Thesis titled "**Investigation on dielectric properties of solid silicone rubber particulate composites.**" which is being submitted to the **National Institute of Technology Karnataka, Surathkal,** in the partial fulfilment of the requirements for the award of the degree of **Doctor of Philosophy** in the **Department of Mechanical Engineering**, is a *bonafide report of the work carried out by me*. The material contained in this Research Thesis has not been submitted to any University or Institution for the award of any degree.

Register Number: **145042ME14P02**

Name of the Research Scholar: **B.S. Manohar Shankar**

Signature of the Research Scholar: 

Department of Mechanical Engineering

Place: NITK, SURATHKAL

Date: 28/10/2020

CERTIFICATE

This is to *certify* that the Research Thesis titled "**Investigation on dielectric properties of solid silicone rubber particulate composites**" submitted by **Mr. B.S. Manohar Shankar** (**Register number: 145042ME14P02**) as the record of the research work carried out by him, is *accepted as the Research Thesis submission* in partial fulfilment of the requirements for the award of degree of Doctor of Philosophy.

Research guide

Dr. S.M. Kulkarni
Professor
Dept. of Mechanical Engineering,
NITK, Surathkal.

Chairman – DRPC

ACKNOWLEDGEMENT

I take this opportunity to express my gratitude to my Guide and mentor Professor S.M. Kulkarni, Professor, Department of Mechanical Engineering who has hand held me through this enriching research journey. I learnt the art of research under his tutelage. His guidance is acknowledged not only on the professional front but also on the human and personal aspects as well. My gratitude to Prof. Dwarakish G. S., Professor in Department of Applied Mechanics and Hydraulics for having been the motivating and guiding force throughout my stay at NITK. The research path was shaped with the guidance and motivation of the RPAC members, Prof. Vijay Desai and Prof. K.P. Vittal who wholeheartedly gave constructive suggestions for improving my work.

I have learnt a lot from the course instructors namely Prof. A.H. Sequeira, Prof. Suresh H. Hebbar at NITK during my course work. My co-research scholars, Shri Kevin A. Mathias, Dr. Sangameshwar Rajole, Shri Shivshankar Hiremath, Shri Vishwas M and Shri Shrikumar Biradar at the MST Laboratory were instrumental in opening up my research options through healthy and fruitful discussions. I am indebted to Prof. Ravishankar K.S. and Prof. Udaya Bhat K. from the Department of Metallurgical and Materials Engineering for allowing me to use their facilities for research work. I express my sincere thanks to present HOD Prof. Shrikantha S. Rao, previous HOD's Prof. Narendranath S and Prof. Gangadharan K V, Academic section, Library, Computer centre, Registrar, Dean and Director of NITK Surathkal for providing all academic and administrative support during the course of my study.

My colleagues at Goa College of Engineering were instrumental in my pursuit of research at NITK. I would like to thank the Director of Technical education, Asst. Director of Technical education (Colleges), Principal, Head of Mechanical Engineering department, colleagues at Mechanical and Electrical Engineering Departments of Goa College of Engineering.

Shri G.K. Navelkar allowed me to use his facilities for fabricating the samples and Shri M.G. Lanjewar from Goa university helped me with micrographs. I am grateful to them. I would like to express my gratitude to Prof. Ganesh Hegde, Prof.

Adlete Mascarenhas, Prof. Ujwala Phadke, Shri Sandip Kerkar and Shri Suresh and family.

The support, wishes and encouragement of Prof. Ulhas Sawaikar, Prof Ranjita Sawaikar, my in-laws and brother's family throughout my research journey is gratefully acknowledged. My son and wife were very supportive throughout this fruitful journey by undertaking all the other tasks upon themselves and allowing me to concentrate on my work. I offer my gratitude and salutations to my parents Late Shri B.S. Shankar and Late Smt B.S. Uma who shaped my personality and capabilities with which I could undertake this task.

I offer this work to the lotus feet of my Lord for providing all of the above in right proportion and at the right time.

Date: 28/10/2020 B.S. Manohar Shankar

ABSTRACT

Dielectric elastomers belong to the class of electroactive polymers that respond to electrical stimulus by undergoing change in shape. These materials also produce electrical signal on being deformed mechanically. The objective of the present study is to investigate the solid silicone rubber composites as candidate materials for use as dielectric elastomers. Solid silicone rubber along with barium titanate as dielectric and ketjenblack as conductive fillers is processed through high temperature compression moulding to obtain dielectric-dielectric, conductive-dielectric and conductive-dielectric-dielectric composites.

Property-processing relationships are investigated for these composites by studying the influences of various factors such as type and amount of fillers, amount of curing agent, mixing time and curing temperature using Taguchi design of experiments. The properties investigated include physical, mechanical, dielectric and electromechanical. Various dielectric mixing rules have been evaluated for the dielectric filler composites. Dielectric spectroscopy and SEM characterization have also been carried out on these composites in order to study filler-matrix interactions.

Results show that the processing parameters along with fillers have influence on physical, mechanical, dielectric and electromechanical properties of the composites. Conductive fillers have a prominent influence on permittivity of the composites as compared to dielectric fillers. However, they are more reinforcing than dielectric fillers. The investigations reveal improved dielectric permittivity and electromechanical sensitivity of 390% and 100% respectively. Piezoresistive and piezo capacitive sensitivities of 3.7E-3 kPa^{-1} and 3.9E-3 kPa^{-1} respectively were achieved in the 0-20 kPa range of pressure for the composites. The processing method adopted ensures uniform distribution and wetting of the fillers in the solid silicone rubber matrix as confirmed through SEM characterisation. Thus, solid silicone rubber composites can be used as promising materials for use as dielectric elastomers.

Keywords: Solid silicone rubber composites, Electromechanical sensitivity, Piezo resistive sensitivity, Piezo capacitive sensitivity, Capacitive pressure sensors.

Table of Contents

List of Figures iv

List of Tables vii

1. INTRODUCTION 1

1.1. Dielectric Elastomer Applications 2

1.1.1. Working principle in actuator mode 3

1.1.2. Electromechanical sensitivity 5

1.1.3. Working principle in sensor mode 5

1.1.4. Piezoresistive mechanism 6

1.1.5. Piezo capacitive mechanism 8

1.1.6. Performance improvement of dielectric elastomers 11

1.1.7. Dielectric mixing rules 13

1.1.8. Dielectric relaxations 15

1.1.9. Matrix materials 16

1.2. Silicone Rubber Composites 18

1.3. Dielectric Filler Composites 23

1.4. Conductive Filler Composites 25

1.5. Conductive-Dielectric Filler Composites 29

1.6. Research Gap 33

1.7. Objectives of Present Research Work 33

1.8. Scope of Present Research Work 34

2. METHODOLOGY 37

2.1 Raw Materials 38

2.2 Taguchi Design of Experiments 39

2.3 Processing of Composites 40

2.3.1 Dielectric filler composites 41

2.3.2 Conductive filler composites 42

2.3.3 Conductive-dielectric filler composites 43

2.3.4 Samples for dielectric relaxation and comparative studies 44

2.3.5. Sample preparation and coding 45

2.4 Testing of Composites 46

2.4.1 Physical properties 46

2.4.2 Mechanical properties 47

2.4.3 Dielectric properties 49

2.4.4 Electromechanical properties 50
3. RESULTS AND DISCUSSION 52
3.1 Dielectric Filler Composites 52
3.1.1 Physical properties 52
3.1.2 Mechanical properties 57
3.1.3 Dielectric properties 61
3.1.4 Electromechanical properties 74
3.2 Conductive Filler Composites 83
3.2.1 Physical properties 83
3.2.2 Mechanical properties 86
3.2.3 Dielectric properties 90
3.2.4 Electromechanical properties 99
3.3 Conductive-Dielectric Filler Composites 106
3.3.1 Physical properties 106
3.3.2 Mechanical properties 110
3.3.3 Dielectric properties 114
3.3.4 Electromechanical properties 123
3.4 Confirmatory Tests 131
3.5 Comparison of Performance 134
4. CONCLUSION 143
4.1 Dielectric Filler Composites 143
4.1.1 Physical properties 143
4.1.2 Mechanical properties 143
4.1.3 Dielectric properties 144
4.1.4 Electromechanical properties 144
4.2 Conductive Filler Composites 145
4.2.1 Physical properties 145
4.2.2 Mechanical properties 145
4.2.3 Dielectric properties 145
4.2.4 Electromechanical properties 146
4.3 Conductive-Dielectric Filler Composites 146
4.3.1 Physical properties 146
4.3.2 Mechanical properties 146
4.3.3 Dielectric properties 147
4.3.4 Electromechanical properties 147

4.4 Scope for Further Research 148
A. APPENDIX 149
RESEARCH OUTCOMES 151
REFERENCES 153
BIO-DATA 168

List of Figures

Figure 1.1 Deactivated state of dielectric elastomer 4
Figure 1.2 Activated state of dielectric elastomer 4
Figure 1.3 Investigated silicone rubber as dielectric elastomers 19
Figure 2.1 Methodology of the study undertaken 38
Figure 2.2 Processing of solid silicone rubber composites 41
Figure 2.3 Processing of DDC composites 42
Figure 2.4 Processing of CDC composites 43
Figure 2.5 Processing of CDDC composites 44
Figure 2.6 Composite samples for physical and mechanical tests (A: DDC, B: CDC and C: CDDC) 45
Figure 2.7 Composite samples for dielectric and electromechanical tests (A: DDC, B: CDC and C: CDDC) 45
Figure 2.8 Set up for SEM characterisation of the composites 47
Figure 2.9 Set up for testing Young's modulus in compression 48
Figure 2.10 Shore A hardness tester 48
Figure 2.11 Test set up for determining dielectric properties of the composite specimens 49
Figure 2.12 Setup for determining the piezoresistive and piezo capacitive characteristics 50
Figure 3.1 Main effects plot for density of DDC composites 54
Figure 3.2 Interactions plot for density of DDC composites 54
Figure 3.3 SEM micrograph of 3.5 phr DDC composites 55
Figure 3.4 SEM micrograph of 7.75 phr DDC composites 56
Figure 3.5 SEM micrograph of 12 phr DDC composites 56
Figure 3.6 Stress strain plots of DDC composites 58
Figure 3.7 Main effects plot for Young's modulus of DDC composites 59
Figure 3.8 Interactions plot for Young's modulus of DDC composites 59
Figure 3.9 Main effects plot for shore A hardness of DDC composites 60
Figure 3.10 Interactions plot for shore A hardness of DDC composites 61
Figure 3.11 Main effects plot for permittivity for DDC composites 64
Figure 3.12 Interactions plot for permittivity for DDC composites 64
Figure 3.13 Comparison of dielectric mixing rules for DDC composites 66
Figure 3.14 Characteristic response of permittivity as a function of frequency for DDC composites 67
Figure 3.15 Main effects plot for dielectric loss of DDC composites 69
Figure 3.16 Interactions plot for dielectric loss of DDC composites 69
Figure 3.17 Characteristic response of dielectric loss as a function of frequency for DDC composites 70
Figure 3.18 Main effects plot for effective resistivity of DDC composites 72
Figure 3.19 Interactions plot for effective resisitivity of DDC composites 72
Figure 3.20 Characteristic response of AC conductivity as a function of frequency for DDC composites 73
Figure 3.21 Main effects plot for electromechanical sensitivity of DDC composites 76
Figure 3.22 Interactions plot for electromechanical sensitivity of DDC composites 76
Figure 3.23 Piezoresistive characteristics of DDC composites 78

Figure 3.24 Main effects plot for piezoresistive sensitivity of DDC composites 79
Figure 3.25 Interactions plot for piezoresistive sensitivity of DDC composites..... 79
Figure 3.26 Piezo capacitive characteristics of DDC composites..... 81
Figure 3.27 Main effects plot for piezo capacitive sensitivity of DDC composites 82
Figure 3.28 Interactions plot for piezo capacitive sensitivity of DDC composites..... 82
Figure 3.29 Main effects plot for density of CDC composites 84
Figure 3.30 Interactions plot for density of CDC composites..... 84
Figure 3.31 SEM micrograph of 3.5 phr CDC composites..... 85
Figure 3.32 SEM micrograph of 7.75 phr CDC composites..... 85
Figure 3.33 SEM micrograph of 12 phr CDC composites..... 86
Figure 3.34 Stress strain plots of CDC composites..... 87
Figure 3.35 Main effects plot for Young's modulus of CDC composites 88
Figure 3.36 Interactions plot for Young's modulus of CDC composites..... 88
Figure 3.37 Main effects plot for shore A hardness of CDC composites 89
Figure 3.38 Interactions plot for shore A hardness of CDC composites..... 90
Figure 3.39 Main effects plot for permittivity of CDC composites..... 92
Figure 3.40 Interactions plot for permittivity of CDC composites 92
Figure 3.41 Characteristic response of permittivity as a function of frequency for CDC composites 93
Figure 3.42 Main effects plot for dielectric loss of CDC composites..... 94
Figure 3.43 Interactions plot for dielectric loss of CDC composites..... 95
Figure 3.44 Characteristic response of dielectric loss as a function of frequency for CDC composites 96
Figure 3.45 Main effects plot for effective resistivity of CDC composites 97
Figure 3.46 Interactions plot for effective resistivity of CDC composites 97
Figure 3.47 Characteristic response of AC conductivity as a function of frequency for CDC composites 98
Figure 3.48 Main effects plot for electromechanical sensitivity of CDC composites. 100
Figure 3.49 Interactions plot for electromechanical sensitivity of CDC composites..... 100
Figure 3.50 Piezoresistive characteristics of CDC composites..... 101
Figure 3.51 Main effects plot for piezoresistive sensitivity of CDC composites..... 102
Figure 3.52 Interactions plot for piezoresistive sensitivity of CDC composites..... 103
Figure 3.53 Piezo capacitive characteristics of CDC composites..... 104
Figure 3.54 Main effects plot for piezo capacitive sensitivity of CDC composites..... 105
Figure 3.55 Interactions plot for piezo capacitive sensitivity of CDC composites..... 105
Figure 3.56 Main effects plot for density of CDDC composites 107
Figure 3.57 Interactions plot for density of CDDC composites..... 107
Figure 3.58 SEM micrographs for 3.5 phr CDDC composites..... 108
Figure 3.59 SEM micrographs for 7.75 phr CDDC composites..... 109
Figure 3.60 SEM micrographs for 12 phr CDDC composites..... 109
Figure 3.61 Stress strain plots of CDDC composites..... 111
Figure 3.62 Main effects plot for Young's modulus of CDDC composites 112
Figure 3.63 Interactions plot for Young's modulus of CDDC composites..... 112
Figure 3.64 Main effects plot for shore A hardness of CDDC composites 113
Figure 3.65 Interactions plot for shore A hardness of CDDC composites..... 113

Figure 3.66 Main effects plot for permittivity of CDDC composites 116
Figure 3.67 Interactions plot for permittivity of CDDC composites 116
Figure 3.68 Characteristic response of permittivity as a function of frequency for CDDC composites..... 117
Figure 3.69 Main effects plot for dielectric loss of CDDC composites 118
Figure 3.70 Interactions plot for dielectric loss of CDDC composites 119
Figure 3.71 Characteristic response of dielectric loss as a function of frequency for CDDC composites..... 119
Figure 3.72 Main effects plot for effective resistivity of CDDC composites 121
Figure 3.73 Interactions plot for effective resistivity of CDDC composites..... 121
Figure 3.74 Characteristic response of AC conductivity as a function of frequency for CDDC composites..... 122
Figure 3.75 Main effects plot for electromechanical sensitivity of CDDC composites..... 124
Figure 3.76 Interactions plot for electromechanical sensitivity of CDDC composites..... 125
Figure 3.77 Piezoresistive characteristics of CDDC composites 126
Figure 3.78 Main effects plot for piezoresistive sensitivity of CDDC composites..... 127
Figure 3.79 Interactions plot for piezoresistive sensitivity of CDDC composites 127
Figure 3.80 Piezo capacitive characteristics of CDDC composites. 129
Figure 3.81 Main effects plot for piezo capacitive sensitivity of CDDC composites..... 130
Figure 3.82 Interactions plot for piezo capacitive sensitivity of CDDC composites 131
Figure 3.83 Comparison of density of composites for varying filler loading 135
Figure 3.84 Comparison of Young's modulus of composites for varying filler loading 135
Figure 3.85 Comparison of shore A hardness of composites for varying filler loading 136
Figure 3.86 Comparison of permittivity of composites for varying filler loading..... 137
Figure 3.87 Comparison of dielectric loss of composites for varying filler loading..... 138
Figure 3.88 Comparison of effective resistivity of composites for varying filler loading 139
Figure 3.89 Comparison of electromechanical sensitivity of composites for varying filler loading 140
Figure 3.90 Comparison of piezoresistive sensitivity of composites for varying filler loading 141
Figure 3.91 Comparison of piezo capacitive sensitivity of composites for varying filler loading 141
Figure A.1 Schematic of the specimen with dimensions for evaluating mechanical properties (Dimensions in mm). 149
Figure A.2 Schematic of the specimen with dimensions for evaluating dielectric and electromechanical properties (Dimensions in mm)..... 150

List of Tables

Table 1-1 Summary of the Literature survey of piezo capacitive sensitivity of unstructured capacitive sensors 9
Table 1-2 Summary of the Literature survey of DDC composites 23
Table 1-3 Summary of the Literature survey of CDC composites 26
Table 1-4 Summary of the Literature survey of CDC composites for flexible pressure applications 28
Table 1-5 Summary of the Literature survey of CDDC composites 32
Table 2-1 Materials used for development of dielectric elastomer composites 38
Table 2-2 Factors and levels selected for study as per L_8 orthogonal array for DDC composites 42
Table 2-3 Factors and levels selected for study as per L_8 orthogonal array for CDC composites 43
Table 2-4 Factors and levels selected for study as per L_9 orthogonal array for CDDC composites 44
Table 3-1 Density of DDC composites 53
Table 3-2 Mechanical properties of DDC composites 57
Table 3-3 Dielectric properties of DDC composites as per L_8 orthogonal array 63
Table 3-4 Exponent of AC universality law of DDC composites 74
Table 3-5 Electromechanical sensitivity of DDC composites 75
Table 3-6 Piezoresistive sensitivity of DDC composites 78
Table 3-7 Piezo capacitive sensitivity of DDC composites. 81
Table 3-8 Density of CDC Composites 83
Table 3-9 Mechanical properties of CDC Composites. 86
Table 3-10 Dielectric properties of CDC composites as per L_8 orthogonal array 90
Table 3-11 Exponent of AC universality law of CDC composites 99
Table 3-12 Electromechanical sensitivity of CDC composites 99
Table 3-13 Piezoresistive sensitivity of CDC composites 102
Table 3-14 Piezo capacitive sensitivity of CDC composites 104
Table 3-15 Density of CDDC composites 106
Table 3-16 Mechanical properties of CDDC composites 110
Table 3-17 Dielectric properties of CDDC composites as per L_9 orthogonal array 114
Table 3-18 Exponent of AC universality law of CDDC composites 123
Table 3-19 Electromechanical sensitivity of CDDC composites 123
Table 3-20 Piezoresistive sensitivity of CDDC composites 126
Table 3-21 Piezo capacitive sensitivity of CDDC composites 129
Table 3-22 Piezo capacitive sensitivity values of unstructured capacitive sensors from literature 131
Table 3-23 Confirmatory tests of DDC composites 132
Table 3-24 Confirmatory tests of CDC composites 133
Table 3-25 Confirmatory tests of CDDC composites 133
Table A-1 Volume fraction equivalent to phr 149

NOMENCLATURE

p – Maxwell pressure

U – Electrostatic energy

C - Capacitance

V - Voltage

R - Resistance

ε_0 - Permittivity of free space

ε' - Real part of the permittivity

ε'' - Imaginary part of permittivity

ε^* - Complex permittivity

σ_{AC} - AC conductivity

ρ – Effective resistivity

S - Sensitivity

β – Electromechanical sensitivity

DDC – Dielectric Dielectric Composites

CDC – Conductive Dielectric Composites

CDDC – Conductive Dielectric Dielectric Composites

RTV – Room temperature vulcanised

HTV – High temperature vulcanised

BT – Barium titanate

SCCB – Super conductive carbon black

DCP – Dicumyl peroxide

MT – Mixing time

CT – Curing temperature

phr – Parts per hundred rubber

PDMS - Polydimethylsiloxane

CF - Carbon fiber

SSF- Stainless steel fiber

NBR - Acrylonitrile butadiene rubber

NR- Natural rubber

SR - Silicone rubber

VMQ- Methyl vinyl silicone rubber

SBR- Styrene–butadiene rubber

SBS - Styrene–butadiene–styrene

PR – Piezoresistive

CHAPTER 1

1. INTRODUCTION

Polymers and polymer composites are increasingly replacing metals and their alloys in all fields of technological advancements, such as automobiles, aerospace, biomedical, household appliances and electronics. They have attractive properties that enable them to replace the conventional materials. They are light weight, pliable, inexpensive and offer simple processing techniques that can be scaled for mass production. Their properties can be tailored and can be configured into complex shapes(Kim and Tadokoro 2007). A number of processing techniques have been developed to enable production of polymers with tailored properties.

Functional polymer composites have an active phase embedded into the passive polymer phase(Tressler et al. 1999). Functional composites respond to external stimuli by changing shape or size. They respond to the stimuli such as electrical field, magnetic field and light. These materials are also addressed to as active polymers. They convert energy from one form to another directly through the response of the material. This capability enables shrinking mechanical components and use of simple linkages thus offering miniaturization of products.

Polymers that change shape or size in response to electrical fields are called electroactive polymers (EAP). They are further classified as electronic EAPs (driven by electric field) and ionic EAPs (change shape by diffusion of ions).

The electronic EAPs work on electrostatic, electrostrictive, piezoelectric and ferroelectric phenomena. They offer high energy density, lower density, rapid response time, develop large strains and can be operated in air. The driving currents are very low and the device is electrostatic in nature(Brochu and Pei 2012), so it will theoretically only consume power during an active expansion mode and no power will be consumed to maintain them at a stable actuated state. Also, some of the energy can be recovered after the actuation cycle is complete. In practice, however, there will be some leakage current through the material, the amount of which will depend on the

material and its thickness. Thus, will consume a small amount of power when maintained in a stable actuation state. However, the disadvantage is that they operate at high activation fields(>150V/μm), which are close to electric breakdown levels of the material and offer low actuation force. Viscoelastic effects too play a role in efficiency of conversion.

Types of electronic EAPs include dielectric elastomers, ferroelectric polymers, electrostrictive graft elastomers, electrostrictive paper, electroviscoelastic elastomers, liquid crystal elastomers.

Among electronic EAPs, dielectric elastomers offer high actuation speeds, high work densities, large strains and higher degree of electromechanical coupling. Their low weight coupled with flexibility are added advantages. Dielectric materials are used as actuators, sensors and energy harvesters. They are also referred to as deformable dielectric capacitors. Dielectric elastomers consist of a flexible dielectric elastomer sandwiched between two flexible and compliant electrodes, forming a capacitor. As actuators they convert electrical energy directly into mechanical energy. When an electric voltage is applied across the electrodes, electrostatic forces are generated on account of like and unlike charges on the electrodes. This acts like a pressure on the elastomer film, squeezing in the thickness direction. As elastomers are incompressible materials, hence this results in elongation along in-plane direction. Thus, electrical energy is converted into mechanical energy. This results in corresponding reduction of charge density due to expansion of electrode area. On account of the elasticity, the film returns to its original size on switching off the external voltage.

In comparison to shape memory alloys and piezoelectric ceramics, dielectric elastomers can induce large strains of up to 300 %. They are inexpensive, light weight, scalable and offer high electromechanical coupling efficiencies(Romasanta et al. 2015).

1.1. Dielectric Elastomer Applications

Dielectric elastomers (DE) are used in novel applications on account of this direct energy conversion process. They are used as actuators, sensors and energy harvesters. They can change shape as a response to electrical stimuli, hence are investigated for

applications that mimic human muscle. They are used as flat screen loud speakers(Heydt et al. 2000), prosthetic structures(Madsen et al. 2016a), microvalves(Kovacs et al. 2009), refreshable braille displays(Chakraborti et al. 2012), active vibration control(Sarban et al. 2011), robotics(Horne et al. 2020), micro-optical zoom and adaptable lenses(Maffli et al. 2015), variable diffraction gratings(Wolf et al. 2018), microfluidic devices(Pelrine et al. 2000).

These stretchable materials are also used in tactile sensing applications(Kollosche et al. 2011) such as electronic robot skins(Maiolino et al. 2015), smart fabric sensors(Castano and Flatau 2014), health monitoring of humans and structures(Laflamme et al. 2013), tactile sensing applications such as from product manufacturing (Vandeparre et al. 2013) to object recognition(Kappassov et al. 2015). Textile pressure sensors for measuring pressure distribution on the human body(Guo et al. 2016). Other applications of flexible large area sensing involve monitoring of elderly people, occupant detection in vehicles, inventory detection, haptic interfaces, wearable communication devices. Wearable health monitoring systems continuously monitor vital signals from human body that are important in health care management. Body worn sensors provide data for applications such as fire fighters, sports and personal health care(Liu et al. 2018a). Sensors for monitoring fluid dynamics environments(Zagnoni et al. 2005), pressure sensors(Maiolino et al. 2013) for portable devices, human and animal biometric applications, physiological(Zhuo et al. 2017) and physical activity monitoring.

Energy harvesting applications(Brochu et al. 2014) include energy from human walking(Kornbluh 2004) and ocean waves(Chiba et al. 2011).

1.1.1. Working principle in actuator mode

When an external electric field is applied across the dielectric elastomer, opposite charges induced on the electrodes cause electrostatic attraction. This generates electrostatic pressure (referred to as Maxwell pressure) that causes the elastomer to contract in thickness and expand in area as shown in Figures 1.1 & 1.2(Madsen et al. 2016a). The material is coated with conducting paint, grease or powder to act as compliant electrodes (Pelrine et al. 2000). The strain induced in the material is

proportional to the permittivity and square of the electric field. Hence strains can be increased by increasing electric fields, improving the permittivity or reducing its thickness(Sahu et al. 2019).

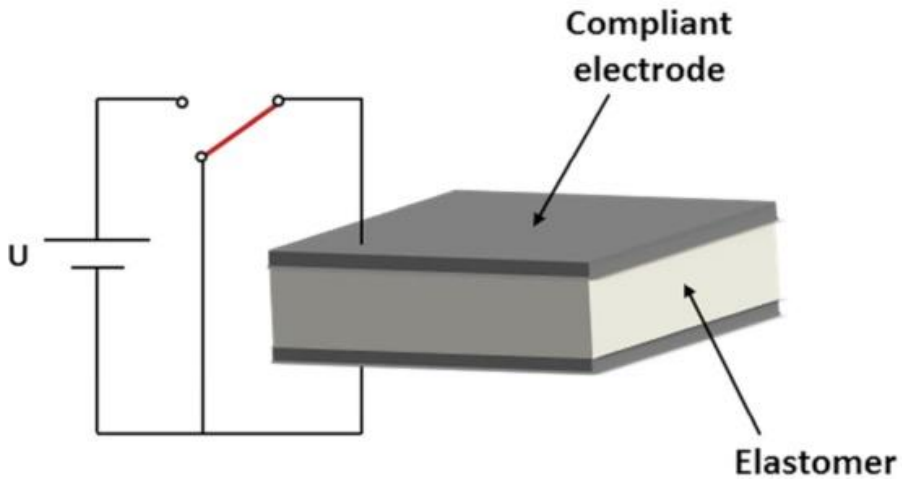

Figure 1.1 Deactivated state of dielectric elastomer

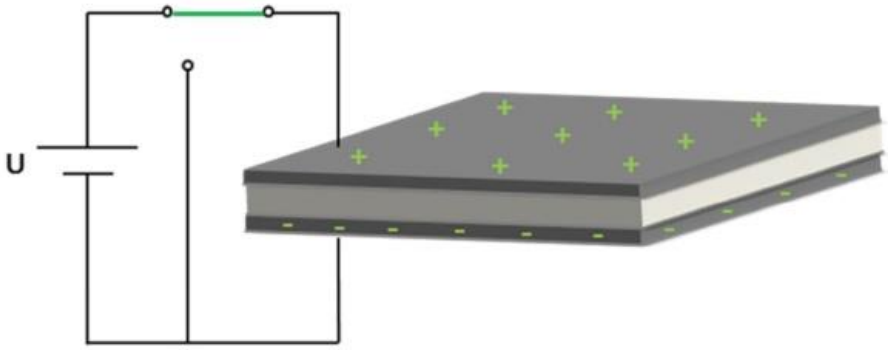

Figure 1.2 Activated state of dielectric elastomer

The Maxwell pressure p, operating on the elastomer film in terms of electric field is given by Equation 1.

$$p = \varepsilon' \varepsilon_0 E^2 \quad (1)$$

E is the electric field over the dielectric elastomer, ε_0 = 8.854E-12 F/m is the vacuum permittivity and ε' is the real part of dielectric permittivity (henceforth referred to as permittivity). Loss tangent of the material is expressed as Equation 2.

$$tan\delta = \varepsilon^{"}/\varepsilon' \quad (2)$$

ε'' is the dielectric loss of the material, also referred to as imaginary part of the complex dielectric permittivity. The complex dielectric permittivity of the material is stated as Equation 3.

$$\varepsilon^* = \varepsilon' - j\varepsilon^{"} \quad (3)$$

The dielectric loss arises on account of dipole relaxation phenomena, that contributes to the energy loss of the material. AC conductivity (σ_{AC}) of the elastomer depends on the dielectric loss along with frequency (ω) which is given as Equation 4.

$$\sigma_{AC} = 2\pi\omega\varepsilon"\varepsilon_0 \quad (4)$$

1.1.2. Electromechanical sensitivity

For a given electric field strength, Maxwell pressure can be increased by increasing permittivity. This pressure would induce a larger strain provided the material has high mechanical compliance as determined by its Young's modulus(Poudel et al. 2019). Thus, a figure of merit taking permittivity and Young's modulus into account is the electromechanical sensitivity (β) (Bele et al. 2014). It is the material's ability to provide more deformation at a lower electric field. It is regarded as a significant value in the determination of voltage induced deformation, to achieve high actuation performance in a lower electric field. It is defined as ratio of permittivity to Young's modulus(Zhao et al. 2013a)(Yang et al. 2015a)(Bele et al. 2015a).

1.1.3. Working principle in sensor mode

Dielectric elastomers are used for flexible pressure sensing applications. The mechanism involves piezoresistive and piezo capacitive energy conversion, wherein strain is converted into related resistance and capacitance change of the material respectively. While, piezoelectric sensors generate a signal only when there is

pressure variation, dielectric elastomers generate electrical signals even for static applications. Other advantages over piezoelectric mechanism are in terms of cost, flexibility and stability.

Two class of contacts based on pressure regimes are grouped as gentle touch (0 - 10 kPa)(Yang et al. 2019) and manipulation touch (>10 kPa) for robot applications, while fluid dynamics sensing for automotive applications involve pressures up to 30 kPa(Zagnoni et al. 2005).

1.1.4. Piezoresistive mechanism

The resistance of the composites varies with the pressure applied; this effect is known as piezoresistive effect(Dahiya et al. 2010). Piezoresistive (PR) sensors have been researched due to simple structure and low cost in addition to simpler read out electronics(Santos et al. 2019). For PR pressure sensors, the mechanism involves change in resistance (dR) of the sensing material with mechanical deformation on account of pressure. Two types of PR pressure sensors are evident from the literature: 1) Negative type piezoresistive pressure sensor (NPS), whose resistance decreases with increase in pressure and 2) Positive type piezoresistive pressure sensor (PPS), whose resistance increases with increase in pressure. Sensitivity is one of the important parameters relating to the output signal for PR pressure sensors. The sensitivity (S) based on the PR effect is defined in literature as Equation 5.

$$S = \frac{dR}{R_0 dP} \tag{5}$$

Where dR is the resistance change with pressure change dP and R_0 is the resistance at no pressure. A higher sensitivity allows for a high-resolution sensing however, with a lower limit of detection. Most of the available literature on flexible pressure sensors involve various ways of improving this sensitivity.

From the literature review two approaches to sensor designs are evident. One is micro structured and other unstructured thin films. Micro structured PR sensors show improved sensitivity and linearity as they depend on the form and size of the microstructures that are imprinted on the flexible substrates. This improvement is on account of the change in the contact area between the electrodes. Photolithography and low-cost molds are utilized for micro structuring that translates into fabrication

complexities and higher cost. Flexible piezoresistive pressure sensors based on porous 3D material structure(Liu et al. 2018b), hybrid foam(Tolvanen et al. 2017)(Luheng et al. 2009) have been investigated. Micro structured sensors are not scalable for large surfaces and hostile environments and the sensitivity improvement comes at the cost of flexibility in terms of allowable strains(Chowdhury et al. 2019). The micro structured piezoresistive sensors with pores and pyramids structures in the elastomer have achieved high sensitivity only in the low-pressure regimes (< 10 kPa). With the increase in pressure, the sensitivity rapidly decreases showing non-linearity(Liu et al. 2018a).

The unstructured approach to PR sensor development offer ease of fabrication and low cost, however at the expense of sensitivity. They can be scaled up for complicated surface contours and harsh environments. Huang et. al. (Huang et al. 2016) demonstrated PPS and NPS with CNT and CB/CNT fillers respectively. NPS with filler volume fraction of 26% was demonstrated by Cai et.al.(Cai et al. 2014). Piezoresistive effects have been demonstrated for cementitious composites with CNT as fillers(Cha et al. 2014). PR sensors have been used to detect human joint movements by incorporating CNF into PDMS matrix(Chowdhury et al. 2019). Magnetite particles with around 50 % volume fractions into PU matrix have been investigated for hydrostatic response(Carlson et al. 2006). PPS with PANI fibers in PU matrix has shown large strains(Fan et al. 2012). CB along with graphene nano platelets with PDMS matrix was investigated for NPS for pressures up to 1 MPa with filler loading of up to 19 % volume fraction(Cai et al. 2014).

Piezoresistive behaviors of composites with different carbon based fillers such as carbon black(Mei et al. 2015b)(Zhu et al. 2018)(Knite et al. 2004), Carbon fibers(Guo et al. 2017), carbon nanotube(Sun et al. 2018b)(Huang et al. 2016), graphite(Sun et al. 2018a) have been investigated. Composites using carbon nano particles as fibers, tubes have been investigated due to their higher aspect ratios(Huang et al. 2016). They show promising results however at a high cost of raw material and processing facilities that are also difficult to scale. Ketjenblack as a promising filler for piezoresistive applications have been investigated(Madhanagopal et al. 2017)(Yoshimura et al. 2012) due to its high aspect ratio, better dispersion properties,

easy availability and low cost. While the wealth of research is concentrated on the use of conductive fillers, there is scant literature on the use of dielectric fillers such as barium titanate for piezoresistive applications.

1.1.5. Piezo capacitive mechanism

The piezo capacitive effect can be visualised by the capacitance equation of a parallel plate capacitor. The capacitance across the elastomer increases with permittivity, area and decreases with thickness (Wang et al. 2015a). With the application of pressure, thickness of the elastomer sample reduces hereby increasing the capacitance (Weadon et al. 2014). Capacitive pressure sensors offer advantages of long-term drift stability coupled with low power consumption. They have been investigated for their simple structure, temperature independence and low cost. They offer fast response rates and are sensitive in low stress regime(Kollosche et al. 2011).

The basic sensing mechanism of piezo capacitive sensors can be modeled as a parallel plate capacitor, with the relative dielectric constant being referred to as effective permittivity(Guo et al. 2016), that depends on the dielectric constant of the active sensing material and its deformation under applied pressure. With the application of pressure, the capacitive pressure sensor responds with an increase in capacitance. Piezo capacitive sensitivity (Fan et al. 2018) is defined as the normalized capacitance change ($\Delta C/C_o$) with pressure change (ΔP) as given in Equation 6.

$$S = \frac{\Delta C / C_0}{\Delta P} \tag{6}$$

where ΔC is change in capacitance, C_o is the capacitance at no pressure.

Researchers have investigated structured and unstructured approaches to capacitive pressure sensor development. Flexible pressure sensors based on the micro structured elastomers(Cagatay et al. 2015) need elaborate microstructure design and thus are expensive and complicated to manufacture and are difficult to scale up(Shuai et al. 2017). The sensing mechanism employed is the change in permittivity on account of compressing the fabricated microstructures in the elastomer under pressure. Structured designs involve the use of following microstructures such as microspheres(Li et al. 2016), air-dielectric(Pyo et al. 2018), truncated cones(Rana et

al. 2016), pillar, wave structure(Shuai et al. 2017), porous elastomer(Liu et al. 2018a; Park et al. 2018), pyramids(Mannsfeld et al. 2010). These designs provide for lesser elastic resistance with greater air entrapment using complex fabrication processes that gives rise to enhanced increase in capacitance.

While unstructured approaches utilize mature fabrication techniques involving simpler methods and low costs, while being applicable for large area deployment, however at the expense of sensitivity (Table 1.1). Unstructured approaches utilized by researchers include bulk and porous PDMS(Chen et al. 2016), Dragon skin 10 & Ecoflex(Cheng et al. 2017), Ni-PDMS composites(Fan et al. 2017), magnetically structured Ni-PDMS composites(Fan et al. 2018), carbon black-PDMS composites(Guo et al. 2016), SomaFoama, Ecoflex, Polytek(Maiolino et al. 2015) and pre-stretching(Cheng et al. 2018). These designs involve improvement in dielectric constant of sensing materials thereby giving rise to enhanced increase in capacitance.

Table 1-1 Summary of the Literature survey of piezo capacitive sensitivity of unstructured capacitive sensors

Author	Matrix	Fillers	Remarks
Chen et. al., 2016	PDMS	--	Unstructured PDMS ($S = 0.0003\ (kPa)^{-1}$)
Guo et. al., 2016	RTV SR	Carbon black	Unstructured textile sensor ($S = 0.00025\ (kPa)^{-1}$)
Cheng et. al., 2017	Ecoflex	--	Unstructured Ecoflex ($S = 0.0011(kPa)^{-1}$
Fan et. al., 2017	RTV SR	Nickel	Unstructured SR/Ni ($S = 0.004(kPa)^{-1}$) (18% vol fraction)
Fan et. al., 2018	RTV SR	Nickel	Magnetically structured during curing ($S = 0.0036$ to $0.029\ (kPa)^{-1}$)
Liu et. al., 2018	PDMS	Ag	Unstructured PDMS/Ag ($S = 0.0014\ (kPa)^{-1}$)

A large area and low cost pressure sensor based on flexible piezo capacitive mechanism using flexible pressure sensitive materials can be produced with sufficient sensitivity(Yao et al. 2013). The sensitivity of piezo capacitive sensor depends on effective permittivity(Maheshwari and Saraf 2008). Hence unstructured approach to sensor development involves improving the permittivity of the sensing material. Two approaches for improving the permittivity are followed in literature, one is by adding high dielectric constant fillers such as barium titanate(Rana et al. 2016) to obtain dielectric-dielectric composites (DDC) and other by adding conductive fillers such as nickel(Fan et al. 2018) and carbon black(Guo et al. 2016) to obtain conductor-dielectric composites (CDC)(Zhang et al. 2015)(Guo et al. 2018). Barium titanate has been used to improve the permittivity(Liu *et al.* 2010) of the composite for sensor application due to high dielectric constant, low cost and wide availability(Rana et al. 2016). These fillers are dispersed in flexible dielectric materials that act as either substrates or as matrix materials for DDC and CDC composites. Most of the studies have reported the use of two-part PDMS which is a room temperature vulcanized silicone rubber as matrix for above applications.

Capacitive pressure sensors respond to change in pressure by an increase in capacitance on account of decrease in thickness of element and corresponding increase in effective permittivity. This effective permittivity is on account of apparent increase in volume fraction of the composite loaded with fillers. Capacitive pressure sensors show relatively low sensitivity due to higher Young's modulus(Li et al. 2015) and thereby lesser compressive strain(Yu et al. 2017). Hence researchers have investigated methods of reducing Young's modulus by structured approach, wherein, microstructures are fabricated on the elastomers and electrodes. From the literature it is observed that high sensitivity is obtained for lower pressure ranges, which decrease with increased pressure sensing range. This is also accompanied by complication and expensive fabrication process. Pyramid microstructures has attained sensitivity of around 0.55 kPa^{-1} for pressures < 2 kPa. Another method adopted is that of introducing pores into elastomers. This reduces the modulus and also increases the change in effective permittivity of porous elastomers. This method demonstrated a sensitivity of 0.01 kPa^{-1} for pressure up to 250 kPa(Chen et al. 2016). PU foams were

demonstrated as capacitive pressure sensor with sensitivity of 0.015 pF/kPa(Vandeparre et al. 2013). Polyolefin foams achieved sensitivity of 0.75 fF/g/cm^2(Metzger et al. 2008). Hemispheric micro-structured PDMS was demonstrated as a capacitive sensor with sensitivity of 2.05 N^{-1} (Zhang et al. 2012). Unstructured and structured PDMS was investigated for capacitive sensing applications by Mannsfeld et.al.(Mannsfeld et al. 2010). They reported sensitivities of 0.02 and 0.55 kPa^{-1} respectively.

Other methods investigated in literature include improving the permittivity of the elastomers(Liu et al. 2018a). They reported the influence of permittivity on the sensitivity of porous elastomers. They demonstrated that increase in permittivity leads to higher capacitance along with higher capacitance variation, resulting in higher pressure sensitivity.

It has been observed from literature that sensor sensitivity is compared among various materials. However, along with improvement in sensor sensitivity other requirements such as linear responsive behaviour in the pressure range has to be satisfied. Hence, for practical applications pressure sensors with good linearity, large sensing range and high sensitivity are desirable(Liu et al. 2018c). However, due to practical limitations from materials perspective, the sensors that are reported possess high sensitivity at low working range and low sensitivity for large sensing range. Low range high sensitivity sensors find applications for blood pressure and breathe monitoring, while large range sensors find applications for hand gestures and sports performance among others.

1.1.6. Performance improvement of dielectric elastomers

Dielectric elastomer functions as a stretchable resistor and capacitor, whose performance is determined by permittivity, dielectric loss and Young's modulus of the elastomer. Hence dielectric properties play an important role in the development of these materials. The various approaches to developing sensor and actuator applications for these materials involve improvements in permittivity, dielectric loss and Young's modulus of the materials.

From the literature, it can be observed that performance of these dielectric elastomers can be increased by;

- **Reducing elastomer thickness**

Pre-stretching has been used to reduce the thickness of the film(Matsuhisa et al. 2019). This reduces the breakdown electric field, thus allowing for greater driving voltages, thereby greater strains. The main drawback of this method is the requirement of rigid frame, that adds to complexity, space and cost(Sahu et al. 2019). Other drawbacks include increasing fatigue and reducing the effective work density of these dielectric elastomer actuators.

- **Reducing mechanical stiffness**

Reducing mechanical stiffness provides for large strains at the given actuation voltages(Sheima et al. 2019). However, this comes at the cost of force applied. Also, for applications that require very high sensor sensitivity and low-pressure sensing, Young's modulus of the elastomers have to be reduced. The strategy employed include use of plasticisers to lower stiffness(Yang et al. 2018). Varying concentration of hardeners are employed to tune the stiffness of the elastomers during curing. The disadvantage with this approach is that these plasticisers affect the working life of the actuators.

Other strategies employed include tuning the cross-linking density(Bele et al. 2018) and chemical modification of molecular weight of the elastomers(Bele et al. 2015b). By varying the amount of cross-linker, the stiffness of the elastomers can be altered. Silicone network are cured with copolymer as cross-linker for achieving improved electromechanical response. Thus, stiffness can be decreased with these approaches. However, elastomer that are soft exhibit viscoelastic effects, thus decreasing output force and breakdown strength.

- **Improving permittivity**

Permittivity enhancement improves the Maxwell pressure applied on the elastomer for the given driving voltage for actuator applications. Permittivity improvement is also sought for in sensor applications involving piezo capacitive sensing. Other applications that look for improved permittivity are capacitors, electronic packaging materials.

This methodology has been investigated through development of chemical modification of elastomer(Ellingford et al. 2018), elastomer blends(Skov and Yu 2018) and elastomer composites(Panahi-Sarmad et al. 2019d).

1.1.7. Dielectric mixing rules

The prediction of permittivity of the developed composites with various filler loading is sought by applying various dielectric mixing rules(Carpi and De Rossi 2005). Theoretical studies have been conducted on the permittivity of the composites in order to describe its dependence on the volume fraction of dielectric fillers, the permittivity of the polymer and filler. Design of polymer composites for specific applications depend on the accuracy of predicting the permittivity of the composite, using various theoretical models(Araújo et al. 2014).

The filler in the form of particles dispersed in the continuous polymer matrix has been classified as 0-3 composites by Newnham et. al(Newnham 1986). For predicting the permittivity of these composites various models have been proposed in literature. Two simplified models that define the limits of permittivity variation in the composites are series and parallel models. The effective permittivity (ε_c) of the composite consisting of filler volume fraction of υ_1 and matrix volume fraction of υ_2 is given as in Equation 7. ε_1 and ε_2 being the permittivity of filler and matrix respectively.

$$\varepsilon_c^n = \upsilon_1 \varepsilon_1^n + \upsilon_2 \varepsilon_2^n \tag{7}$$

n = -1, for series and n = 1 for parallel case.

Wiener introduced the above limits and it is widely believed that effective permittivity of the 0-3 composites should lie between these limits(Zhang and Cheng 2011).

Some of the models considered in the literature include;

- Maxwell-Wagner model:

This model is developed assuming that filler particles can be modelled as dielectric sphere surrounded by a concentric spherical shell. The model is expressed as Equation 8.

$$\epsilon_c = \epsilon_1 \left[1 + \frac{3\nu_2(\epsilon_2 - \epsilon_1)}{2\epsilon_1 + \epsilon_2 - \nu_2(\epsilon_2 - \epsilon_1)}\right] \quad (8)$$

The spherical fillers are assumed to be well separated by distances greater than their size.

- Lichtenecker model:

Lichtenecker proposed the logarithmic mixing model (Equation 9).

$$\log \varepsilon_c = v_1 \log \varepsilon_1 + v_2 \log \varepsilon_2 \quad (9)$$

Lichtenecker model has been validated by various researchers for dielectric filler composites. This model is used when particle shape and orientation can be considered to be statistically random. The fillers are considered to be embedded in an isotropic dielectric medium and that no interactions between its constituents are considered.

- Sillars model:

Is an expression (Equation 10) for dielectric inclusions that are embedded in dielectric medium.

$$\epsilon_c = \epsilon_1 \left[1 + \frac{3\nu_2(\epsilon_2 - \epsilon_1)}{2\epsilon_1 + \epsilon_2}\right] \quad (10)$$

- Bruggeman model:

This equation (Equation 11) is obtained as symmetrical expression for a spherical dielectric filler embedded in dielectric matrix.

$$\frac{\epsilon_2 - \epsilon_c}{\epsilon_c^{1/3}} = \frac{(1 - \nu_2)(\epsilon_2 - \epsilon_1)}{\epsilon_1^{1/3}} \quad (11)$$

- Landauer model:

This equation (Equation 12) is deduced for composites that have interactions between domains and when the fillers do not form continuous networks.

$$\nu_1 \frac{(\epsilon_c - \epsilon_1)}{2\epsilon_c + \epsilon_1} + \nu_2 \frac{(\epsilon_c - \epsilon_2)}{2\epsilon_c + \epsilon_2} = 0 \quad (12)$$

- Coherent potential equation:

Is an expression (Equation 13) developed for random distribution of filler particles in matrix.

$$\frac{\epsilon_c - \epsilon_1}{4\epsilon_c - \epsilon_1} = \nu_2 \frac{(\epsilon_2 - \epsilon_1)}{3\epsilon_c + \epsilon_2 - \epsilon_1} \tag{13}$$

- Jayasundere-Smith equation:

The interactions among the filler particles are considered for predicting the effective permittivity of the composites (Equation 14).

$$\epsilon_c = \frac{\epsilon_1 \nu_1 + \epsilon_2 \nu_2 \frac{3\epsilon_1}{(2\epsilon_1+\epsilon_2)}\left[1 + 3\nu_2 \frac{(\epsilon_2-\epsilon_1)}{(2\epsilon_1+\epsilon_2)}\right]}{\nu_1 + \nu_2 \frac{3\epsilon_1}{(2\epsilon_1+\epsilon_2)}\left[1 + 3\nu_2 \frac{(\epsilon_2-\epsilon_1)}{(2\epsilon_1+\epsilon_2)}\right]} \tag{14}$$

Dielectric loss is another important parameter that has to be considered for electromechanical transduction applications(Madsen et al. 2016b). Dielectric losses result in heat generation that leads to increase in temperature and conductivity. This produces a cascading effect that leads to thermal or electrical breakdown. Hence reduction in dielectric losses is crucial to the development of dielectric elastomers. There are few detailed studies on the dielectric loss for dielectric elastomer composites(Zhang and Cheng 2011).

Electrical conductivity is another important property investigated for these dielectric elastomers(Madsen et al. 2016a). Although silicone rubber is electrically insulating, the addition of fillers creates unwanted conductive paths through the matrix. This leads to charge transport resulting in further dielectric losses. Effective resistivity and AC conductivity are the measures of the electrical conductivity of the materials(Güler et al. 2019). The effect of variation of filler loading and frequency on the electrical conductivity of the composites has been investigated in the literature.

1.1.8. Dielectric relaxations

The electrical properties that determine the suitability of materials for electromechanical transduction applications are permittivity, dielectric loss and AC conductivity. Electrical relaxation behaviour of these materials is obtained from the

variation of these electrical properties with frequency(Raptis et al. 2010). These properties help to define the capacitive nature, which represents its ability to store or lose electrical charge and to ascertain the conduction nature that represents its ability to transfer electric charges(Shukla and Dwivedi 2016). Polarisation is responsible for permittivity, while leakage current is responsible for the dielectric loss and AC conductivity of the elastomers. The variation of dielectric properties with frequency is due to the following mechanisms(Panahi-Sarmad et al. 2019d): a) Polarisation causes the rotation of dipoles with variation of the frequency of electric field, b) With the increase in frequency, it is difficult for the dipoles to catch up with the field due to material properties and c) Immobilisations of some dipoles when very high frequencies are attained. Thus, the permittivity of dielectric elastomers tends to fall with the frequency of the electrical field. This dispersion is on account of losses of certain characteristic polarization abilities of the material(Dabros et al. 2009).

1.1.9. Matrix materials

Matric materials investigated include epoxides(Fan et al. 2013), polystyrenes(Zhang et al. 2018), polyimides(Wang et al. 2015b), polyurethane(Renard et al. 2017), acrylics(Sahoo et al. 2012), natural rubber(Tangboriboon et al. 2013), EPDM, ABR(Nguyen et al. 2014), PDMS(Nayak et al. 2012)(Stiubianu et al. 2016), LSR(Yu and Skov 2015) and PVDF(Shirinov and Schomburg 2008).

Researchers have thus studied elastomer composites with matrix materials like acrylics, polyurethanes and silicones for the above applications. These materials, however, suffer from lower permittivity, hence development of dielectric elastomer (DE) composites for such applications have been pursued(Madsen et al. 2016a)(Zhang et al. 2015). The improvement in permittivity of dielectric composites is due to three mechanisms: a) Intrinsic dielectric properties of filler and matrix, b) Micro-capacitors that are formed within the composite and c) Interfacial polarisation effect between mediums having different permittivity. Researchers have studied the influence of different fillers which include conductive fillers such as MWCNT, carbon black (CB), metals and metal oxides, whereas dielectric fillers investigated include barium titanate. Sheng et. al. (Sheng et al. 2012) studied the dielectric relaxation for the well-known dielectric elastomer namely VHB 4910, which is a

commercially available acrylic copolymer from 3M. They reported permittivity of 4.75 at 20 Hz. Natural rubber along with greater than 40 phr Al_2O_3 fillers were investigated for electromechanical applications by Tangboriboon(Tangboriboon et al. 2013). Stiubianu et. al.(Stiubianu et al. 2016) reported a maximum permittivity of 3.8 at 8 weight fraction of complexes of cobalt. However, they were accompanied with higher losses. Ecoflex as a matrix along with PMN-PT fillers loaded at 50 % loading achieved a permittivity of 5.4 along with low dispersion in the frequency domain(Maiolino et al. 2015). Carpi et. al. (Carpi and De Rossi 2005) showed an increase in permittivity of 30 % for 30 % weight fraction of TiO_2 filler in PDMS matrix. BaTiO3 and CB fillers were combined with NBR to obtain dielectric elastomers. They provided higher permittivity at 20 phr of BaTiO3 and 4 phr of CB loadings(Nguyen et al. 2014). Dang et. al. investigated the influence of $BaTiO_3$ along with Ni metallic inclusions in PVDF matrix that showed greater permittivity at percolation threshold, but at the cost of increased conductivity(Dang et al. 2003). Leyva et. al. presented the dielectric relaxations of carbon black/styrene-butadiene-styrene composites, and attributed the decrease in permittivity with increase in frequency to interfacial polarization(Leyva et al. 2003). Carpi et. al. investigated the dielectric relaxations of Silicone-Poly(hexylthiophene) Blends(Carpi et al. 2008) and reported single dipolar relaxation process with lesser Maxwell-Wagner polarization effects. Dielectric relaxation of silicone-barium titanate composites were studied by Bele et. al.(Bele et al. 2014). Gallone et.al investigated the dielectric relaxations of PDMS/PU blends and composites(Gallone et al. 2010).They compared blends versus composites for development of dielectric elastomers and proposed that blends provide a promising alternative.

Stiffness characteristics of the polymer chains around the filler particles also determine the degree of polarization as observed by Javadi et. al. in the case of titania-PDMS composites(Javadi et al. 2018). They observed improved segmental mobility on account of loose interfacial layers around the fillers. Researchers are of the opinion that there exists a large fraction of chains around fillers called the interphase, that reflect different behaviour than the bulk properties. The polymer chains adsorb to these filler surfaces resulting in the formation of the interfacial layer. The role of filler

morphology and polymer chain dynamics in the interfacial zone have a bearing on the macro properties of the composites(Panahi-Sarmad et al. 2019c). Dielectric broadband spectroscopy is one of the tools that has been used to investigate polymer chain dynamics in interfacial layers(Renukappa et al. 2009).

Dielectric elastomers have been fabricated using dielectric, conductive and conductive-dielectric fillers into the above matric materials to obtain dielectric-dielectric composites (DDC), conductive-dielectric composites (CDC) and conductive-dielectric-dielectric composites (CDDC) respectively(Zhang et al. 2015).

1.2. Silicone Rubber Composites

The most important component of a dielectric elastomer transducer is the elastomer. It governs the permittivity and strain. Various materials investigated for use as dielectric elastomers include polyurethane (PU)(Renard et al. 2017), natural rubber(Sahu et al. 2016), acrylic (including VHB)(Giousouf and Kovacs 2013) and silicone rubber.

Initial research was concentrated around commercial acrylic elastomer from 3M (VHB 4910). It had permittivity of around 4.5 @ 1kHz and displayed good electromechanical performance in terms of actuation strains, however slow response and sensitivity to humidity and temperatures restricted their use.

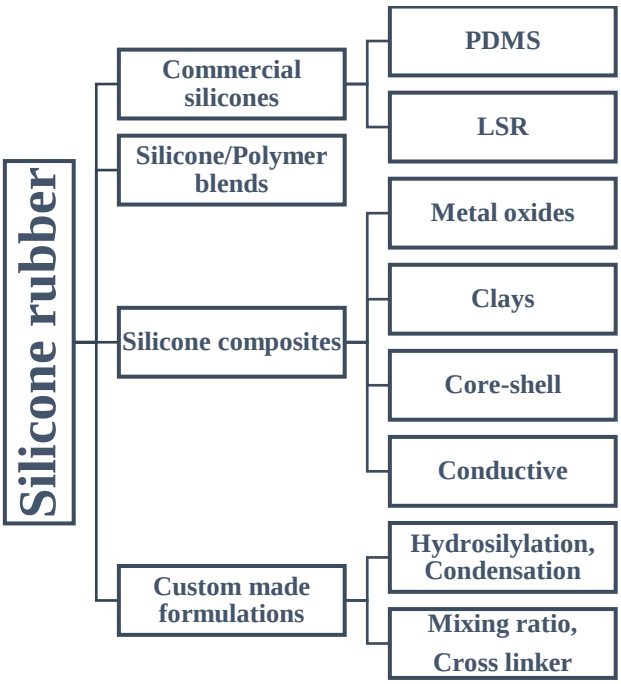

Figure 1.3 Investigated silicone rubber as dielectric elastomers

Silicones are polyorganosiloxanes with inorganic siloxane bonds as the main backbone and lateral chains of organic groups. Silicones are thus a mixture of inorganic-organic elastomer based on silicon and oxygen backbone. Hence, they possess good elastic properties due to high flexibility of siloxane bond. Most of the studies performed on silicone-based composites have used room temperature vulcanised (RTV) Polydimethylsiloxane (PDMS) (Figure 1.3). PDMS are widely researched polymers among silicone elastomers (Pignanelli et al. 2019). They have repeating units of RR'SiO, where R groups contain the methyl groups. PDMS are cross-linked into 3-dimensional polymer networks. The network possesses elasticity, thereby can return to its original shape upon stress removal. This addition cured elastomers are commercially available as two-part systems, wherein one part contains polymer and cross linker while other part contains catalyst. Curing is initiated upon mixing of the two parts in proportions as specified by the manufacturer.

Among the various promising candidate materials for dielectric elastomers, silicone elastomers stand out due to their superior properties and for ease of fabrication. They offer higher reliability, high efficiency, long term stability and fast response times. Their light weight and large strains are their inherent advantages(Madsen et al.

2016a).They produce reproducible actuation upon activation, show little ageing effects and long stable shelf life. As compared to acrylics silicones possess lower viscous losses, hence can be operation with lesser heat generation at higher frequencies. They have low rates of moisture absorption and can be used in a wide temperature range(Romasanta et al. 2015). They are stable and elastic over a broader temperature range.

Silicone elastomers are viscoelastic and hence show both elastic and viscous behaviours. Molecular weight of the elastomer chains governs its mechanical properties. They become brittle when short length polymers are cross-linked. The functionality of the crosslinker is also important for its curing characteristics. A reduction in the Young's modulus is obtained by lowering the amount of the cross linker. In the case of the elastomer matrix, polymerization results in crosslinking of side chains between adjacent long chains. These side chains prevent the long polymer chains from slipping, thereby providing the elasticity to these elastomers. Depending on the type of interactions between the adjacent chains, crosslinking is classified as physical/chemical. In the case of physical crosslinking as seen in styrenic elastomers, polymer chains are connected by relatively weak interactions such as hydrogen bonding. In chemical crosslinking, long polymer chains are connected by strong covalent bonds as in the case of silicone rubbers. The strong bonding between these long chains gives them mechanical and thermal stability. As crosslinking reactions are influenced by curing agents, their mechanical properties are tuned by adjusting weight fractions of curing agent or the reaction temperature(Kim et al. 2019). When crosslinking is weak, elastomers tend to be softer and also prone to mechanical failures. The elastomer matrix fully embraces the fillers and the interfacial filler-polymer fraction may not be completely immobile as seen from literature in the case of silicone rubber(Klonos et al. 2019). An excessive filler content in the composites lowers the crosslinking density and also restricts the long chains from migration resulting in decreased toughness of the elastomer. This limits the amount of filler loading in the composites. Mixing time influences the dispersion of fillers in the matrix, hence it is one of the important process parameters.

RTV elastomers however suffer from low tensile and tear strength, hence they are considered weak. This is on account of low melting point. Hence these elastomers cannot reinforce themselves at room temperatures and require reinforcement of particles such as silica, titania and zirconia among others. Reinforcement depends on interaction between the base polymer and the fillers, such as hydrogen bonding and van der Waals forces. Fillers immobilise the polymer chains and hence reinforce the elastomer. This reflects in improved extensibility of reinforced elastomers as compared to unfilled elastomers.

Silicone rubber are commercially available in two classes as room temperature vulcanised rubber (RTV) and high temperature vulcanised rubber (HTV) depending on their curing characteristics. RTV elastomer studied in literature include Sylgard 184, Elastosil RT625 and Nusil CF15. These elastomers are cured at room temperature. The curing reaction time can be decreased by application of heat. However, this comes at the cost of reduction in elasticity. These fast cures change the particle-particle and particle-polymer interactions, due to polymer chain entanglements.

HTV elastomers contain polymers with high molecular weight and relatively long polymer chains and are cured by addition cure or peroxides(Lin et al. 2019). These elastomers are divided into liquid silicone rubber (LSR) and solid silicone rubber based on the degree of polymerization and viscosity(Chi et al. 2019). Solid silicone rubber offers established and mature production capabilities, fast cure and high precision products. They remain elastic even for very thin dimensions with good tear resistance. It also permits incorporation of wide range of additives and fillers, with minimal changes to toughness and elastic properties(Lin et al. 2019).

Commercial silicones such as Nusil CF and Dow Corning's DC 3481 have also been investigated. Wacker Silpuran 6000 which is a medical grade LSR was studied by Stoyanov et. al. for energy harvesting applications(Stoyanov et al. 2013). Silicone elastomer from Danfoss PolyPower for actuation performance was studied by Jordi et.al(Jordi et al. 2011). Skov et. al. investigated LSR elastomers for energy harvesting applications on account of its high electrical and mechanical strengths(Yu and Skov 2015).

As against the commercially available silicones only a few cases of custom-made formulations for use as dielectric elastomers have been researched in literature(Cazacu et al. 2014). This is on account of many factors, including the economics of fabricating them on mass scale and other tests that make them robust. The chemical modifications route has achieved reasonable permittivity values, while maintaining other properties such as stiffness and dielectric losses at required values(Kim et al. 2019). These custom-made materials would achieve economies of scale upon mass production and development of matured industrial processes.

Another approach seen in literature, involve blending silicone rubber with polymers possessing high permittivity such as highly conjugated, undoped poly(3-heylthiophene) (PHT)(Carpi et al. 2008). These techniques offer the advantage of reducing the Young's modulus while simultaneously increasing permittivity. However, they suffer from high dielectric losses. Chloropropyl-functional silicone oil was blended with a commercial elastomer from Wacker Chemie by Madsen et. al. They reported higher permittivity with these blends(Madsen et al. 2016b). PDMS/PU blend was studied by Gallone et. al. Permittivity higher than pure PU was observed for the blend, which the authors ascribed it to Maxwell-Wagner-Sillars polarisation mechanism at the interphases of the blend(Gallone et al. 2010).

Pure silicone elastomers possess low permittivity, hence to achieve a given strain a higher driving voltage has to be applied. To overcome this limitation fillers are added in order to improve its permittivity giving rise to silicone elastomer composites. This method is highly researched in the literature for developing materials with high permittivity while still retaining flexibility. These fillers are added through in-situ condensation reactions or directly blended. The improvement in permittivity often comes at the cost of increase in Young's modulus and dielectric loss. Hence there is a need to optimise the permittivity increase while not compromising with Young's modulus and dielectric losses of the composites. The properties depend on the matrix, type and loading of filler, processing conditions and the interaction among them.

Silicone elastomer composites are developed using silicone elastomer as the matrix with either dielectric filler or conductive fillers to obtain dielectric filler and conductive filler composites. These are referred to in literature as dielectric-dielectric

composites and conductor-dielectric composites. Also, some studies have been conducted using both dielectric and conductive fillers to obtain conductive-dielectric-dielectric composites.

Silicones are dielectric materials. However, upon adding dielectric or conductive fillers to these pure matrix, undesirable conductive paths can occur. This undesired conductivity leads to large dielectric losses. Hence these properties have to be investigated, along with permittivity and Young's modulus.

1.3. Dielectric Filler Composites

Dielectric filler composites, referred in literature as dielectric-dielectric composites (DDC) are obtained by incorporation of dielectric fillers into the silicone elastomer matrix (Table 1.2). In this approach, high permittivity fillers are combined with high breakdown strength flexible polymers. Dielectric filler composites have been investigated with fillers such as titanium dioxide(Zakaria et al. 2017), lead magnesium niobate(Gallone et al. 2007), alumina(Tangboriboon et al. 2013) and barium titanate (BT) (Bele et al. 2015a)(Nayak et al. 2014b)(Poudel et al. 2019).

Table 1-2 Summary of the Literature survey of DDC composites

Author	Matrix	Fillers	Remarks
Bele et. al., 2018	PDMS	TiO_2 nanoparticles	ε' = 4 (5 wt.%) and ε" = 0.1
Jiang et. al., 2015	PDMS	BT	ε' = 6.3 and tanδ = 0.005 @ 50 % wt. fraction.
Yang et. al., 2018	HTV SR	BT (30 phr)	ε' = 3.85 and tanδ = 0.3
Zhu and Zhang, 2017	NBR	BT	ε' = 28 and ε'' = 3 @ 30% vol. fraction.
Ruan et. al.,2018	NBR	Al_2O_3	ε' = 11 and tanδ = 0.025 @ 30 phr.
Madsen et. al., 2016	LSR	TiO_2, silicone oil (30 phr)	ε' = 4.4
Zhao et. al.,2013	PDMS	TiO_2 (30 phr)	ε' = 4.9
Poudel et. al.,2019	SEBS-g-MA	BT	ε' = 5.06 (@10% wt. fraction)

Natural rubber along with 40 parts per hundred rubber (phr) Al_2O_3 fillers were investigated for electromechanical applications by Tangboriboon(Tangboriboon et al. 2013). Ecoflex as a matrix along with PMN-PT fillers loaded at 50 % loading achieved a permittivity of 5.4 along with low dispersion in the frequency domain(Maiolino et al. 2015). Carpi et. al. (Carpi and De Rossi 2005) showed an increase in permittivity of 30 % for 30 phr of TiO_2 filler in PDMS matrix. Dielectric relaxation of silicone-barium titanate composites was studied by Bele et. al.(Bele et al. 2014). They used high molecular weight PDMS along with surface treated BT nanoparticles and concluded that BT nanorods produced the highest permittivity of 9.04 as compared with commercial and cubic forms of BT particles. Silicone composites with BT fillers show comparable permittivity as compared to TiO_2 fillers even with lower filler loadings (Madsen et al. 2016a). Calcium copper titanate (CCTO) was used as a dielectric filler in PDMS matrix to obtain composites with frequency and temperature independent dielectric properties (Romasanta et al. 2012).

Fillers in the form of powders used include barium titanate(Khastgir and Adachi 1999), titanium dioxide(Cazacu et al. 2014). Home grown BT nano particles in the shape of bamboo leaf were incorporated in large amounts into high temperature vulcanized (HTV) solid silicone rubber matrix(Nayak et al. 2012). These composites showed improved permittivity but greater dielectric loss at these high filler loadings. Star shaped BT multipods were incorporated into HTV silicone rubber in large amounts and these composites were investigated for energy harvesting applications(Nayak et al. 2014a). NBR-BT composites were evaluated as promising DE materials for use in oily environments(Zhu and Zhang 2017). The permittivity of these composites more than doubled with the addition of 30% volume fraction of BT fillers but caused a significant drop in mechanical properties and effective resistivity. Also, at higher filler loadings formation of filler clusters and negligible wetting of fillers (dilution effects) is observed. Custom made HTV silicone rubber-titania composites were investigated as DE materials(Cazacu et al. 2014). However even with filler loading of 50 parts per hundred rubber (phr), composites achieved permittivity of around five. Poudel et. al.(Poudel et al. 2019) fabricated poly(styrene-

ethylene/butylene-styrene) grafted maleic anhydride composite with BT fillers and achieved an improvement of 34.9% in permittivity at 10 phr BT filler loading.

The effect of zinc borate on dielectric properties of metallocene linear low density polyethylene was investigated by Alwaan et. al(Alwaan et al. 2015). They reported an increase in effective resistivity, dielectric loss and Young's modulus of the composites, while the permittivity of the composite decreased with filler loading. Titanium dioxide nanotubes were incorporated into PDMS matrix and investigated for dielectric properties(Bele et al. 2018). They reported an increase of 33% in permittivity of the composites. This also resulted in an increase in Young's modulus of the material, which is a disadvantage for actuator applications.

Laflamme et.al.(Laflamme et al. 2013) investigated DDC composites for force sensing applications by incorporating TiO_2 fillers into SEBS matrix. They reported a sensitivity of 415 N/pF. Kim et.al..(Kim et al. 2018) reported micro structured pressure sensor of sensitivity 1 $(kPa)^{-1}$ using PDMS matrix filled with SiO_2 fillers.

Thus, incorporation of dielectric fillers showed an improvement in permittivity, however with a corresponding increase in Young’s modulus. The dielectric breakdown strength was also reduced.

1.4. Conductive Filler Composites

Conductive fillers such as graphite, carbon nanotubes, conductive polymers and carbon black have been incorporated into silicone matrix to obtain conductive-dielectric composites (CDC) as shown in Tables 1.3 & 1.4. At low filler concentration the electrical properties are dominated by the matrix. With the increase in filler loading, a three-dimensional network though the matrix is formed, thereby increasing the electrical conductivity of the composite. Thus, these conductive fillers have to be loaded below a threshold in order to prevent conductive paths being formed in the composites, also referred to as percolation threshold. This threshold reflects into a sudden rise in conductivity of the composites, where insulator to conductor transition occurs. This results in short-circuiting of the composite. Hence, researchers keep the conductive filler loadings below its percolation threshold or encapsulate them with

dielectric fillers. These composites offer higher permittivity as compared to dielectric filler composites, however at the cost of substantial dielectric losses.

Table 1-3 Summary of the Literature survey of CDC composites

Author	Matrix	Fillers	Remarks
Renukappa et. al., 2009	SBR	CB (90 phr)	ε' = 100 and tanδ = 1
Li et. al., 2006	PVDF	SSF (10 vol %)	ε = 427 @ 50 Hz
Hassan et. al., 2013	NBR	Al (150 phr)	ε’ = 55
Saji et. al., 2016	HTV SR	Nanographite (8 phr)	ε’ = 150 and tanδ = 0.45
Leyva et. al., 2003	SBS	CB (1.5 vol%)	ε’ = 11
Ardimas et. al., 2018	PU	GRN (2 %wt.)	ε’ = 9
Shakun et. al., 2006	ACM	CB	ε’ = 9.5 and tanδ = 0.04 (@ 5 phr)
Panahi-Sarmad and Razzaghi-Kashani, 2018	PDMS	rGO (1 vol%)	ε’ = 60 and ε” = 4

The development of CDC composites has seen the investigation of conductive fillers such as graphene(Panahi-Sarmad et al. 2019d)(Dimiev et al. 2013)(Romasanta et al. 2011), reduced graphene oxide(Panahi-Sarmad et al. 2019c), CNT(Zheng et al. 2019), metal(Ali et al. 2019)(Romasanta et al. 2015)(Hassan et al. 2013), metal oxides(Wang and Facchetti 2019), metal fibres(Li et al. 2006), transition metal complexes(Stiubianu et al. 2016), silver powder(Ding et al. 2015), graphite(Saji et al. 2016), Nano fillers(Yang et al. 2019)(Zheng et al. 2019)and carbon black(Madhanagopal et al. 2017)(Renukappa et al. 2009). Stiubianu et. al.(Stiubianu et al. 2016) reported a maximum permittivity of 3.8 at 8 weight fraction of complexes of cobalt. However, they were accompanied by higher losses.

Various types of carbon black(Madsen et al. 2016a) investigated as conductive fillers are acetylene black(Princy et al. 1998), HAF carbon black(Abu-Abdeen et al. 2007), carbon black fibres(Ding et al. 2015) and carbon nanotubes(Brochu et al. 2014).

Researchers opine that carbon-based materials are more effective than metal as conductive fillers owing to the greater affinity between carbon fillers and polymer(Panahi-Sarmad et al. 2019d) and due to the lower density of carbon materials(Zhang et al. 2019a). Panahi-Sarmad et. al.(Panahi-Sarmad and Razzaghi-Kashani 2018) reported that reduced graphene oxide nano-platelets produced enhancement of permittivity in the composites. Addition of 0.5 weight fraction of MWCNT increased the permittivity from 3 to 5 of a PDMS matrix(Park et al. 2008). These composites provide high permittivity near the percolation threshold accompanied by high dielectric loss. The dielectric loss is due to leakage current on account of conductive paths provided through the dielectric elastomer matrix. This threshold is related to the filler dispersion, content and electrical properties. The interfacial resistance between fillers is determined by the contact area, inter-filler gap and the conductivity of the fillers(Zhang et al. 2019a).

Table 1-4 Summary of the Literature survey of CDC composites for flexible pressure applications

Author	Matrix	Fillers	Remarks
Al-Hartomy et. al., 2012	NR	CB (5 phr)	$\sigma = 10^{-14}$ S/m
Knite et. al., 2004	Polyisoprene	CB (10 wt%) nanoparticles	R changes three orders with 0.30 MPa
Zhu et. al., 2018	SR	CB(50 vol %)	GF = 2.6
Liu et.al., 2017	silk fabric	GO	$S = 0.4\ kPa^{-1}$,
Liu et. al., 2018	Porous PDMS	Ag nano particles	$S = 0.0072\ kPa^{-1}$
Wang et. al., 2018	SR	CB	$\Delta R = 2\ k\Omega$ for $\Delta P = 2$ MPa.
Chowdhury et. al., 2019	PDMS (micro structured)	CNF	GF = 18.3 & 6.3
Madhanagopal et. al., 2017	NR	CB (6 wt%)	$S = 1.1\ MPa^{-1}$ (up to 2 MPa)
Yoshimura et.al., 2012	SR	CB (6.5 wt%)	60% decrease in resistivity with 10% compressive strain
Shang et. al., 2014	HTV SR	CNT (11 wt%)	R decreased from 10^{15} to $10^{2}\ \Omega$

Leyva et. al. presented the dielectric relaxations of carbon black/styrene-butadiene-styrene composites and attributed the decrease in permittivity with increase in frequency to interfacial polarization(Leyva et al. 2003). Graphene oxide sheets maintained in liquid crystal state were incorporated into PDMS(Zhang et al. 2019b), achieving an improvement of 800% in permittivity values as compared to that of pure PDMS. The surface chemistry of graphene oxide was manipulated by functionalization to minimize the dissipation effects and to create strong interactions between graphene nanosheets and matrix by Panahi-Sarmad et. al.(Panahi-Sarmad et

al. 2019b). They reported that this method also impairs the conductivity of the fillers, hence suggest that optimum properties be achieved through surface functionalization.

CNT and graphene possess excellent mechanical and dielectric properties. Larger surface area and aspect ratios are suggested as responsible for improved electrical and mechanical properties of these composites. These fillers have tendency of agglomeration and their compatibility to polymer matrices are still of prime concern to researchers(Balasubramanian and Burghard 2008). Their application to a macroscopic world still provides a big challenge(Zhang et al. 2019a) as they are prone to severe entanglements due to their large aspect ratio and Van-der-Waals forces between them(Klonos et al. 2019). Chemical modification of these surfaces is resorted to deal with these issues.

Even though carbon black fillers don't possess aspect ratio as high as CNT or graphene, but availability, ease of fabrication and cost benefits outweigh their disadvantages(Panahi-Sarmad et al. 2019a). Ketjenblack having a high structure, with increased surface area has been used as conductive filler for piezoresistive sensing application(Madhanagopal et al. 2017). This superconducting carbon black shows better results on account of its unique morphology.

Thus, the challenge with conductive filler composites is that of preventing percolation and short circuiting. The increase in permittivity occurs at percolation threshold, that is characterised by high losses and increase in conductivity due to insulator-conductor transition. This loading is very sensitive as small deviations results in serious drop of permittivity along with short circuiting(Dang et al. 2012). This is safeguarded in literature by loading conductive filler below percolation threshold or encapsulating them with dielectric fillers(Madsen et al. 2016a)

1.5. Conductive-Dielectric Filler Composites

Dielectric fillers improve the permittivity of the composites only when filler loading is high. Whereas, the addition of conductive fillers improves the permittivity at lower filler loading, while increasing the dielectric losses and reducing its breakdown strength. Also, the stiffness of the composites increases due to the reinforcing nature of the fillers.

Hence, to overcome both the above limitations, researchers have investigated simultaneous incorporation of both dielectric and conductive fillers into the dielectric elastomers to achieve conductor-dielectric-dielectric composites (CDDC) as shown in Table 1.5. These hybrid fillers significantly influence the electrical and mechanical properties of the polymer composites(Panahi-Sarmad et al. 2019a). Here conductive fillers are separated by dielectric fillers, thus preventing the formation of conductive pathways(Ma et al. 2019).

Hybrid fillers have been investigated for the following matrix materials: Epoxy resin(Tsangaris and Psarras 1999), VMQ(Dang et al. 2009), ACM(Poikelispää et al. 2016), SBR(Abu-Abdeen et al. 2007), PVDF(Jiang et al. 2009), PU(Huang et al. 2004), PDMS(Zhao et al. 2013b), PI(Yang et al. 2015b). Acrylic rubber as a dielectric matrix was investigated as a CDDC by incorporating high mass fractions of barium titanate as dielectric filler and carbon black as conducting filler(Poikelispää et al. 2016). An interesting phenomenon observed was that, for CDDC composites with 20 phr CB loading, permittivity showed an initial decrease with the addition of BT fillers followed by an increase after 5 phr BT loading. The authors attribute it to reduced Maxwell-Wagner polarization effects. Room temperature vulcanized silicone rubber was incorporated with BT and low mass fractions of acetylene carbon black to produce CDDC composite(Zhao et al. 2013b). They reported an increase in permittivity with CB at fixed BT mass fraction. However, at a fixed CB, the permittivity showed unusual behavior with BT, which showed an initial increase followed by a decrease with BT content. Similar behavior was observed for Young's modulus. They reported an initial decrease of Young's modulus followed by an increase with CB for a given BT mass fraction. This unusual behavior was attributed to interaction between dielectric and conductive fillers. Transition metal complexes along with silica nanoparticles were incorporated into HTV silicone rubber and studied for dielectric properties(Stiubianu et al. 2016). These composites showed enhanced permittivity but at the cost of large dielectric losses. HTV silicone rubber with two active fillers namely BT and silica was fabricated as DE composites(Bele et al. 2015b). They reported low dielectric loss and marginal increase in permittivity. PVDF as a matrix for two nano fillers namely BT and carbon nanotubes were reported

as DE materials(Li et al. 2018a). Dielectric properties of CDC composites made of carboxyl-functionalized multi-walled nanotubes together with BT in a PDMS matrix were investigated(Guan et al. 2018). The composite showed high permittivity but was accompanied with high dielectric loss.

Hybrid fillers investigated also include BT-Ag(Fang et al. 2014), CNT-BT(Liu et al. 2015)(Jin et al. 2016), BT-GO(Li et al. 2018b). BT and CB fillers were combined with NBR to obtain dielectric elastomers. They provided higher permittivity at 20 phr of BT and 4 phr of CB loadings(Nguyen et al. 2014). Dang et. al. investigated the influence of BT along with Ni metallic inclusions in the PVDF matrix that showed greater permittivity at percolation threshold but at the cost of increased conductivity(Dang et al. 2003). PVDF hybrid composites showed permittivity of 71.7 and dielectric loss of 0.045 at 37.1 and 3 volume fractions of BT and MWCNT respectively (Jin et al. 2016). PVDF along with BT and $LaNiO_3$ nanocrystals hybrid composite was reported with permittivity increase of 9 times as that of PVDF matrix(Jaschin et al. 2018).

Hence, several studies were undertaken to develop hybrid conductive-dielectric filler composites consisting of encapsulating the conductive particles with passivation layers before they are dispersed in matrix. PANI particles were encapsulated with insulating shell and dispersed in PDMS oligomer(Molberg et al. 2010). They reported improved dispersion of fillers with lower dielectric losses, but at the cost of stiffened composites.

Table 1-5 Summary of the Literature survey of CDDC composites

Author	Matrix	Fillers	Remarks
Abu-Abdeen et. al., 2007	SBR	BT (10 phr), HAF CB (40 phr)	$\varepsilon' = 130$ and $\sigma = 10^{-4}$ S/m
Dang et. al., 2003	PVDF	BT (20 vol%), Ni (15 vol%)	$\varepsilon' = 100$ and $\tan\delta = 0.1$
Yao et. al.,2010	PVDF	MWCNT, BT nanoparticle	$\varepsilon' = 637$ and $\sigma = 3.5x10^{-4}$ S/m
Dang et. al., 2009	VMQ	BT (40 vol%), CB (3.5 vol%) nanoparticles	$\varepsilon' = 960$ and $\sigma = 10^{-3}$ S/m
Sanches et. al., 2017	PU	PZT (30 vol%), CB (40 vol%)	$\varepsilon' = 80$
Poikelispaa et. al., 2016	ACM	BT (10 phr), CB (20 phr)	$\varepsilon' = 50$ and $\tan\delta = 0.2$
Li et. al., 2018	PVDF	CNT (0.41 vol%), BT (2.8 vol%) nanoparticles	$\varepsilon' = 70$ and $\tan\delta = 0.04$
Guan et. al., 2018	PDMS	Functionalised MWCNT (0.33 vol%), BT (1.53 vol%)	$\varepsilon' = 424$ and $\varepsilon'' = 8.5$

Hence by tuning the composition of both dielectric and conductive fillers and through the selection of appropriate matrix material, optimum values of permittivity and Young's modulus as desired for DE applications can be achieved.

1.6. Research Gap

From the above review of literature in the area of dielectric polymer composites, the following are the research gaps identified.

1) Most of the researchers have worked with room temperature vulcanized two part castable grade silicone elastomers. Few have worked with high temperature molded silicone rubber especially for pressure sensor applications.

2) Few researchers have worked with three component composites involving both dielectric and conductive fillers.

3) The structured design of experiments for evaluating the property-processing relationships by varying the processing factors for different levels and determining the interaction of the factors on the dielectric properties is not observed in the literature surveyed. This method can explore the synergy between different types of fillers and showcase some fillers with high impact on dielectric properties.

4) Dielectric mixing models for solid silicone rubber dielectric composites have to be evaluated.

5) There is scope to develop materials with improved electromechanical, piezo resistive and piezo capacitive sensitivity.

1.7. Objectives of Present Research Work

The objectives of the study are:

1. To propose a suitable composite material for electromechanical transduction.
2. Prepare composite samples with different compositions and processing parameters.
3. Test the composite samples for physical, mechanical and dielectric properties.
4. To determine the transduction properties of these composites and identify the best combination for improved transduction.

This study therefore investigates the property-processing relationships for solid silicone rubber composites processed through high temperature compression molding method. The experimental design is based on Taguchi design of experiments and analyzed using commercially available tools. Dielectric relaxation studies are conducted for these composites. The suitability of these composites as an actuator and pressure sensing material are investigated using electromechanical sensitivity, piezoresistive and piezo capacitive characterization. The effects of various factors such as type of fillers, filler and curing agent loading, mixing time and curing temperature on these characteristics are evaluated.

1.8. Scope of Present Research Work

Although there is abundant literature on the use of room temperature vulcanized PDMS as matrix materials for dielectric elastomer applications, there is scant literature involving commercially available HTV solid silicone rubber composites with conductive and dielectric filler put together especially focused on electromechanical applications. HTV rubber is a promising candidate(Madsen et al. 2016a) for such applications. Various attributes such as excellent dielectric strength, biocompatibility, thermal stability for a wide temperature range, low temperature flexibility, resistance to sunlight and weathering, water repellence make them favorable candidates for use as dielectric elastomers. They can be fabricated using mature and low cost processes that can be scaled up for industrial production(Madsen et al. 2016a). Other beneficial properties include excellent heat resistance, large area deployment, excellent aging resistance and performance at elevated temperature with continuous operation(Zhang and Feng 2003). It is physiologically safe for humans. However, their permittivity is low at around 2.5. With the appropriate amount of fillers and other additives for reducing stiffness the favourable properties of commercial silicones can be utilised for dielectric elastomer applications(Zakaria et al. 2015). Very few studies have been conducted on dielectric and mechanical properties of solid silicone rubber composites with the incorporation of both dielectric and conductive fillers.

Methods employed for mechanical dispersion of fillers in the matrix are varied, from laboratory scale to full scale production methods. Ultra-sonication in the presence of solvents, ball milling, laboratory mixers and two roll mills. Some of these processes are only effective on a laboratory scale and would be difficult to upscale for industrial production. Present study involves roll mill mixing and compression molding, which are industrial processes for the manufacture of these composites, thereby assuring of seamless industrial implementation. The comparatively high viscous solid silicone rubber provides a dry mixing production method that maintains the dispersed filler networks intact during the hot compression moulding. Thus, no filler functionalization is required to prevent the fillers from agglomerating in the polymer matrix. Also, it facilitates the use of industrial production processes such as roll-mill and compression moulding in place of laboratory-based solvent methods.

There are few studies on the application of both commercially available BT and Ketjenblack as fillers to improve the dielectric properties of dielectric elastomer composites. Electrical characterization and relaxation behaviour of these composites have been carried out using dielectric spectroscopy. The influence on the type of filler, filler loading, curing agent loading, mixing time and curing temperature on the dielectric properties of these composites are reported. Incorporation of fillers does alter the mechanical properties hence effect of filler type and loading on Young's modulus of the composites have been reported. Interfacial microstructures of solid silicone rubber composites for dielectric, conductive and conductive-dielectric fillers is reported.

Hence the focus of our study is in developing solid silicone rubber composites as dielectric elastomers and investigating the influence of dielectric, conductive and conductive-dielectric fillers and processing parameters on the its physical, mechanical, dielectric and electromechanical properties. The study involves improving its permittivity though development of DDC composites using BT as a dielectric filler, CDC composites using Ketjenblack as a conductive filler and CDDC composites using BT as dielectric and Ketjenblack as a conductive filler. Effect of factors such as amount of fillers, amount of curing agent, mixing time in the roll mill (MT) and curing temperature (CT) on the physical, mechanical, dielectric and

electromechanical properties are reported. The novelty of this study is in investigating the HTV solid silicone rubber composites fabricated with readily available and low-cost BT and ketjenblack fillers for use as dielectric elastomers. The study shows the synergistic interactions among the dielectric and conductive fillers on the properties of dielectric elastomers.

The study also reports the evaluation of piezoresistive and piezo capacitive properties of solid silicone rubber composites for flexible pressure sensing applications. The effects of filler loading and other processing parameters on sensor sensitivity of these materials as flexible pressure sensors are reported. These composites offer use of off-the-shelf materials and inexpensive, scalable and simple industry scalable manufacturing processes, resulting in cost effective and simple installation procedures for flexible sensors(Laflamme et al. 2013).

From the above it is observed that solid silicone rubber composites are candidate materials for use as dielectric elastomers. There is scope in investigating the properties of DDC, CDC and CDDC composites of solid silicone rubber for determining their suitability for such applications.

Thus, further chapters deal with processing, testing and results of these DDC, CDC and CDDC composites. The chapter on Methodology details out the raw materials, their processing methods, Taguchi design of experiments, sample preparation and testing methods employed. The chapter on results and discussions detail out the results obtained under different factors levels and discusses the property-processing relationships for each of the properties for the three types of composites. The concluding chapter summarises the properties of each of the three types of composites and presents scope for further research in this area.

CHAPTER 2

2. METHODOLOGY

The methodology employed for our study involves, solid silicone rubber as matrix material with dielectric, conductive and conductive-dielectric fillers using compression moulding to obtain dielectric-dielectric composites (DDC), conductive-dielectric composites (CDC) and conductive-dielectric-dielectric composites (CDDC) respectively. In order to investigate the property-processing relationships, the factors employed include filler type, filler amount, amount of curing agent, mixing time, curing temperature. These composites are prepared with each of the above factors set at two levels, thus giving eight different combinations. Dielectric and electromechanical sensitivity investigations are employed, that are required for its application as actuator materials. In order to characterise them for use as sensor materials, piezoresistive and piezo capacitive characterisations are employed in the pressure range of 0-20 kPa. For undertaking the above the following properties has been obtained: 1) Density and SEM characterization. 2) Mechanical properties such as Young's modulus and shore A hardness. 3) Dielectric properties such as permittivity, dielectric loss, effective resistivity and AC conductivity with frequency and 4) Electromechanical properties such as electromechanical sensitivity, piezoresistive and piezo capacitive sensitivity has been obtained for each of these composites as shown in Figure 2.1.

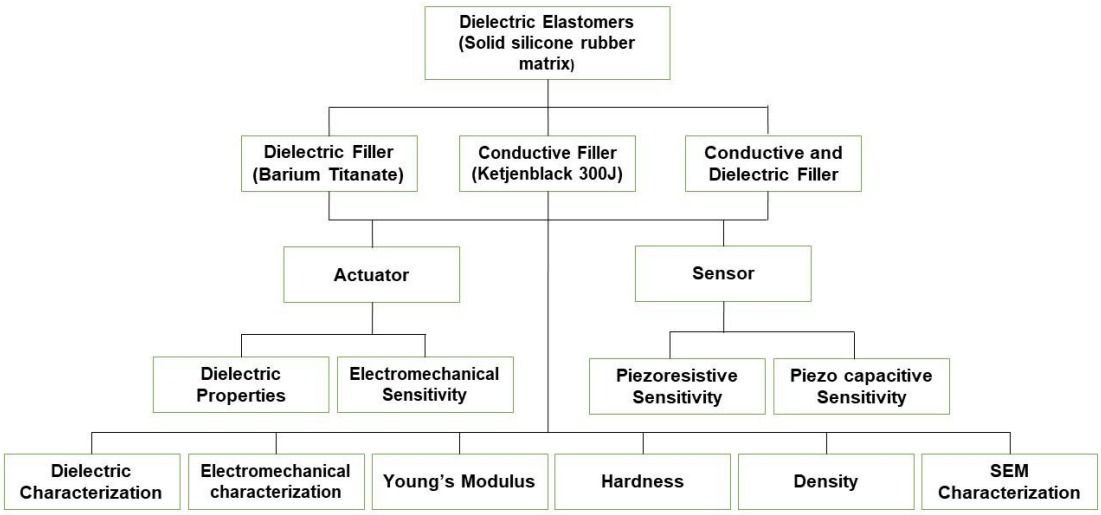

Figure 2.1 Methodology of the study undertaken

2.1 Raw Materials

High temperature vulcanized solid silicone rubber (NE-5140) of shore A hardness 40 in the form of solid block is acquired from DJ Silicones, China (Table 2.1). Barium titanate in powder form is obtained from Sigma Aldrich India (product 338842). Curing agent (Dicup 98, India) used is Dicumyl peroxide (DCP) of 98 % purity. Super conducting carbon black (SCCB) used is Ketjenblack EC 300J, in the form of pellets having surface area of 800 m^2/gms and is sourced from AkzoNobel India.

Table 2-1 Materials used for development of dielectric elastomer composites

Product	**Barium Titanate (IV)**	**Ketjenblack EC 300 J**	**Solid silicone rubber NE-5140**
Make	Sigma-Aldrich	AkzoNobel	DJ Silicone
Product Number	338842	EC 300 J	NE-5140
Density	6.08 g/cm^3	130 Kg/m^3	1.13 g/cm^3
Surface area	NA	800 m^2/g	NA

The matrix employed for this study is solid silicone rubber of shore A hardness 40, sourced from DJ Silicones. It is a peroxide cure system that is compression moulded at high temperature.

Dicumyl peroxide is used as the curing agent. It is an organic peroxide that has the ability to form free radicals at specific temperature. These radicals then initiate the polymerisation of monomers to form polymer through an exothermic reaction. Due to the exothermic combustion limits, the peroxide concentrations in practice ranges from 0.05 to 5 phr. Hence the curing agent loading for the present study is varied from 1 to 5 phr.

The two fillers employed are barium titanate (BT) as dielectric filler and Ketjenblack as conductive filler. As per the literature survey, a minimum of 3.5 phr of BT loading was used for the DDC composites, hence this was the minimum loading that was selected for both the fillers. From the preliminary investigation it was observed that with filler loading at greater than 12 phr, proper wetting was not observed with the given mixing time of a minimum of 10 mins, hence the maximum filler loadings were restricted to 12 phr.

Barium titanate ($BaTiO_3$) is a well-known ferroelectric ceramic that exists in tetragonal phase. It shows spontaneous polarization, with the dipole moments arising due to movement of Ti atoms with respect to O atoms(Bele et al. 2015a). Barium titanate offers high permittivity (>1000) even at room temperatures. It is commercially available in different sizes from μm to nm and is relatively cheap.

The superconducting carbon black used is Akzo Nobel's Ketjenblack EC-300 J that consists mainly of elemental carbon in the form of spherically shaped particles that are fused together to form aggregates. It has a highly branched structure that enables electrical networks to be formed across the polymer matrix at relatively low concentrations. Due to its unique morphology, only 1/3 of the amount is required in order to achieve the same conductivity as with other carbon blacks(Krieg et al. 2018).

2.2 Taguchi Design of Experiments

The Taguchi method is used to design and evaluate the experiments for testing the performance of composites for various properties, in order to quantify the effects of

each of the factors on the properties. The design includes four unique variables, each at two levels.

Preliminary investigations into the properties of these composites provided the factor levels that are adopted for the detailed investigations. Also, initial experimentation revealed the curing temperatures of 160 °C was required with 1 phr of curing agent loading. With a higher curing temperature beyond 210 °C problems such as air locks and cracking were encountered for the given curing agent loading. Hence in order to prevent these defects in the specimens, the curing temperature s limited to 210 °C.

The design is referred to as L_8 design, since it requires eight different combinations to evaluate four variables (filler loading, curing agent loading, mixing time and curing temperature), with two levels each. The two level assumes linear trends for all the variables and also reduces the number of factor combinations required to complete the testing matrix. This design was selected to decrease the testing time and combinations, allowing for the effect of factors to be evaluated for a large number of different testing combinations.

For testing the hybrid conductive-dielectric filler composites, Taguchi L_9 design is employed. This design involves 2 factors (conductive and dielectric filler loading) each at three levels giving nine combinations of factors. This design brings out any synergistic effects among the factors involved.

Since the experimental designs are orthogonal, it is possible to separate out the effects of each of the factors at different levels, affecting the characteristics. The analysis of results obtained using Taguchi method is presented in the form of main effects plots and interactions plots for each of the properties investigated with respect to the four factors namely filler and curing agent loading, mixing time and curing temperature.

2.3 Processing of Composites

Solid silicone rubber composites are processed as per the schematic shown in Figure 2.2. Solid silicone rubber in the form of block is masticated in the roll mill till a fine texture is obtained, then curing agent is added to the silicone rubber in roll mill, while continuing mixing. Fillers are added in parts per hundred rubber (phr) to the roll mill to obtain the DDC, CDC and CDDC composites respectively. This precure is laid out

as sheets. Using appropriate dies as required for various characterization standards, composites are obtained using compression molding at appropriate curing temperatures.

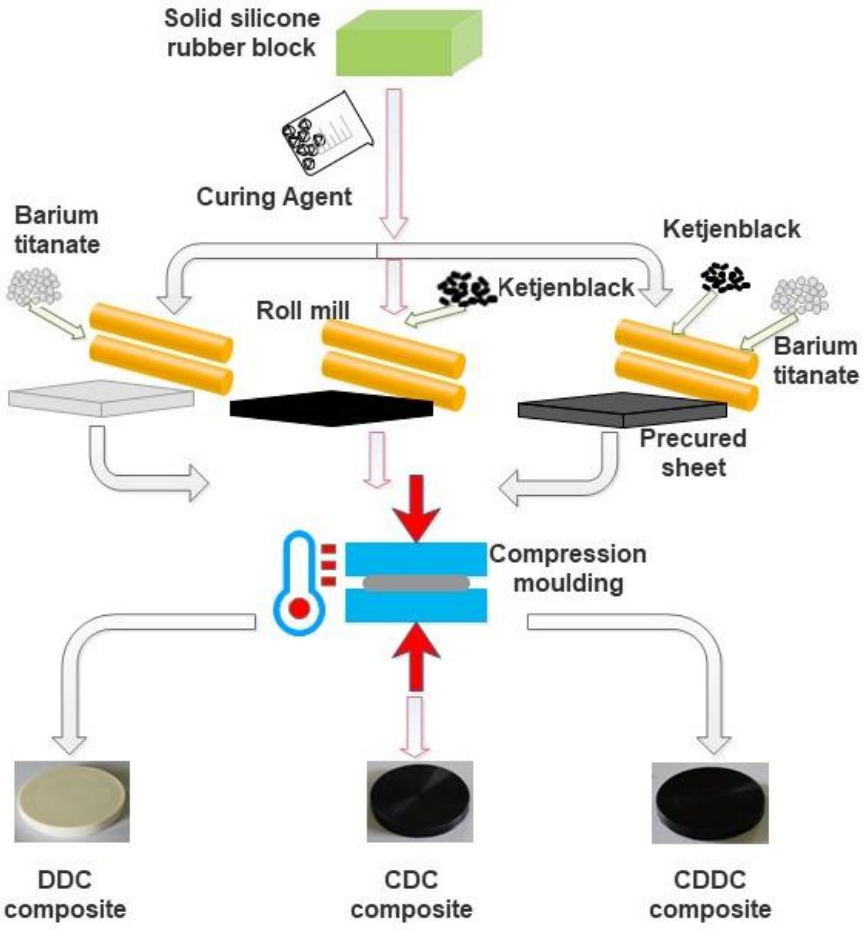

Figure 2.2 Processing of solid silicone rubber composites

2.3.1 Dielectric filler composites

Samples for testing properties of DDC composites are prepared as per L_8 Taguchi orthogonal array as shown in Table 2.2. Pre-established amounts of solid silicone rubber are homogenized in a roll mill (Modern Engineering Works, India) till a fine homogenous texture is obtained. Curing agent and barium titanate in the proportions of parts per hundred rubber (phr) as given in Table 2.2 are mixed and masticated for the specified time periods (MT) in the roll mill, followed by high temperature curing

(CT) using compression molding machine (Modern Engineering Works, India) as shown in Figure 2.3.

Table 2-2 Factors and levels selected for study as per L_8 orthogonal array for DDC composites

Factors	Values		Units
Amount of Barium titanate (BT)	3.5	12	phr
Amount of Curing agent (DCP)	1	5	phr
Mixing Time (MT)	10	30	min
Curing Temperature (CT)	160	180	^{o}C

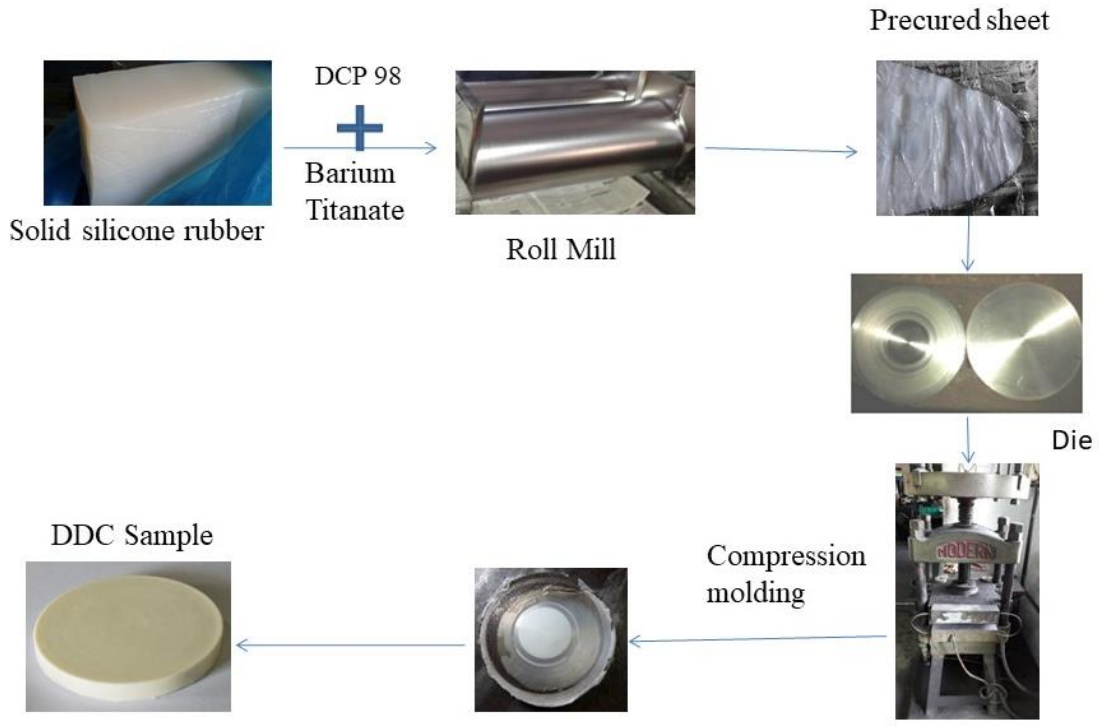

Figure 2.3 Processing of DDC composites

2.3.2 Conductive filler composites

Samples for conductive dielectric composites (CDC) are prepared as follows: Pieces cut from silicone rubber block along with curing agent, are thoroughly mixed in a roll mill. Conductive filler is added to the roll mill while continuing mixing along with

curing agent in the required proportions and for appropriate duration as given in Table 2.3. The obtained mix is packed in a die and cured at 160 and 210°C in a compression molding machine (Figure 2.4).

Table 2-3 Factors and levels selected for study as per L_8 orthogonal array for CDC composites

Factors	Values		Units
Amount of Ketjenblack (SCCB)	3.5	12	phr
Amount of Curing Agent (DCP)	1	5	phr
Mixing Time (MT)	10	30	min
Curing Temperature (CT)	160	210	°C

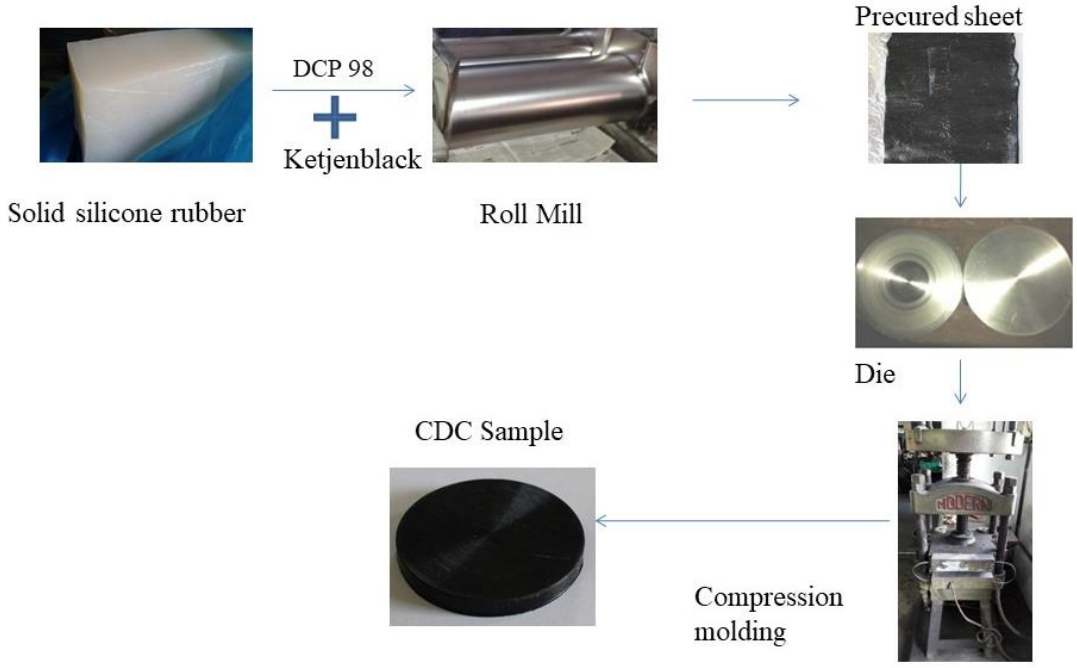

Figure 2.4 Processing of CDC composites

2.3.3 Conductive-dielectric filler composites

Another set of composites are prepared by adding conductive (SCCB) and dielectric fillers (BT) to solid silicone rubber matrix to obtain conductor-dielectric solid silicone rubber composites (CDDC). Taguchi L_9 orthogonal array is used to conduct the

experiments. Solid silicone rubber is weighed in requisite proportion and homogenized thoroughly in the roll mill. Curing agent is dispersed and continued with mixing on the roll mill. Appropriate quantities of SCCB and BT as shown in Table 2.4 are dispersed and mixed well with the rubber. The samples are obtained by compression molding at 160°C (Figure 2.5).

Table 2-4 Factors and levels selected for study as per L_9 orthogonal array for CDDC composites

Factors	Coded Values		
	-1	0	1
SCCB (phr)	3.5	7.75	12
BT (phr)	3.5	7.75	12

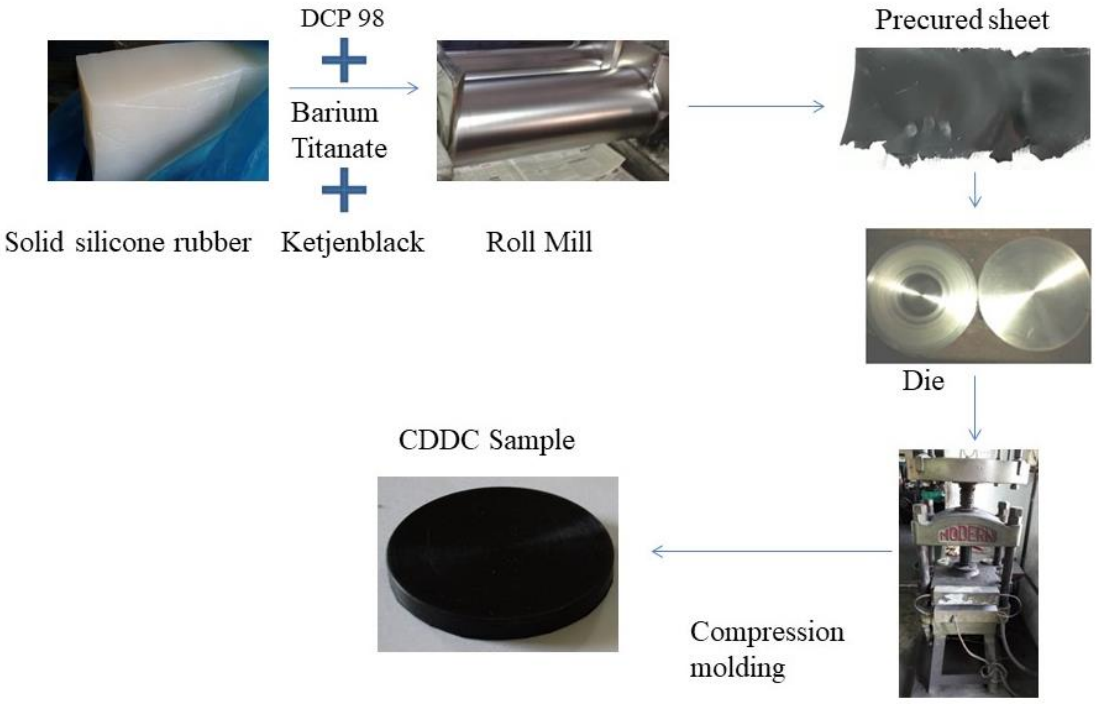

Figure 2.5 Processing of CDDC composites

2.3.4 Samples for dielectric relaxation and comparative studies

For investigating the dielectric relaxation behavior of solid silicone rubber composites and for the purpose of comparison; DDC, CDC and CDDC composites were

additionally prepared with similar filler loadings of 3.5, 7.75 and 12 phr respectively. Curing agent was fixed at 1 phr, mixed for 10 mins and cured at 160 °C.

2.3.5. Sample preparation and coding

Cylindrical samples (Figures 2.6 A, B & C) are prepared as per ASTM D575-91 standard of thickness 12.5 mm and diameter 28.6 mm for physical and mechanical tests.

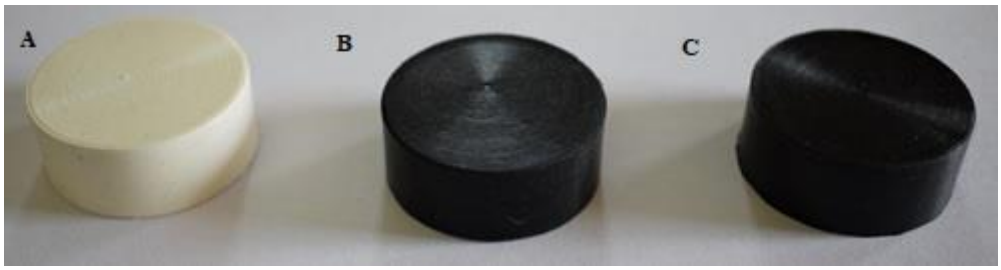

Figure 2.6 Composite samples for physical and mechanical tests (A: DDC, B: CDC and C: CDDC)

Cylindrical samples (Figures 2.7 A, B & C) are prepared for dielectric and electromechanical testing as per ASTM D150-11 standard of 5 mm thickness and 50 mm diameter. Samples were coded as BT-NM, SCCB-NM and SB-NM; where N is the sample number (run) from the Taguchi orthogonal array table and M is sample repetition number for each run. Initials BT, SCCB and SB refer to DDC, CDC and CDDC composites. Schematic dimensions of specimens are shown in Appendix.

Figure 2.7 Composite samples for dielectric and electromechanical tests (A: DDC, B: CDC and C: CDDC)

2.4 Testing of Composites

Solid silicone rubber composites are tested for their physical, mechanical, dielectric and electromechanical properties to determine their suitability for dielectric elastomer applications.

2.4.1 Physical properties

With the addition of fillers to the matrix the density of the composite changes. Also, the inclusion of fillers into the matrix have to be investigated for their distribution and wetting. Hence the physical properties investigated for the DDC, CDC and CDDC composites include density and SEM characterisation.

Density

The density of the specimens was tested using Archimedes method. Weight and volume of the specimens were recorded, from which the density of the specimens was evaluated.

SEM characterization

Scanning Electron Microscope (SEM) images of razor cut surfaces are taken with Carl Zeiss (model EVO 18 special edition, UK) electron microscope (Figure 2.8), operating until 20kV with secondary and backscattering electrons. The samples are razor cut across the thickness direction and mounted by means of double-sided adhesive tapes on the sample studs. A thin layer of gold (80%) and palladium (20%) is sputtered on the sample surface prior to the measurements. These micrographs provide information on the degree of filler dispersion in the matrix.

Figure 2.8 Set up for SEM characterisation of the composites

2.4.2 Mechanical properties

Mechanical properties of the composite samples investigated include Young's modulus and shore A hardness. Young's modulus determines the stiffness of the composites which is a measure of the flexibility of the composites; hence Young's modulus is investigated.

Young's modulus

Young's modulus is evaluated from compressive stress-strain data obtained using Shimadzu UTM (model AG-X plus 100 kN, Japan) following the ASTM D575-91 standard, (Figure 2.9) and reported values are at 10 % strain. A strain rate of 12 mm/min is employed.

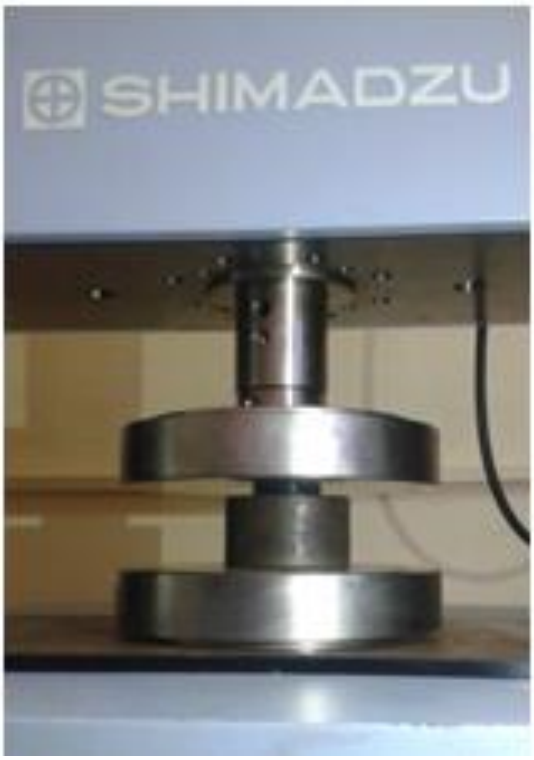

Figure 2.9 Set up for testing Young's modulus in compression

Hardness

The shore A hardness of the specimens was tested with a rubber shore A hardness degree tester (EDHT A11, Stech Engineers, India) as per ASTM D2240 standard (Figure 2.10).

Figure 2.10 Shore A hardness tester

2.4.3 Dielectric properties

Test setup for determining electrical properties consists of LCR meter (Agilent E4980A make) along with Agilent 16451B dielectric test fixture (Figure 2.11) as per ASTM D150-11 standard in the frequency range of 20 Hz to 2 MHz at room temperature. From these data the permittivity (ε') and dielectric loss (ε") are calculated at a given frequency. From the dielectric loss and frequency, conductivity (σ_{AC}) of the specimen are calculated. Relaxation behaviours are obtained through plots of permittivity, dielectric loss and conductivity with frequency. Also effective resistivity (ER)(Princy et al. 1998) of the samples are evaluated from the data obtained using the LCR meter.

Figure 2.11 Test set up for determining dielectric properties of the composite specimens

Permittivity

The capacitance across the specimen is measured using LCR meter. From this data and dimensions of the specimen, the permittivity (ε′) of the specimens is computed using Equation 15.

$$C = \varepsilon' \varepsilon_0 \frac{A}{t} \tag{15}$$

Where A and t are area and thickness of the specimen.

Dielectric loss

The loss tangent (tanδ) across the specimen is measured using the LCR meter. From this data dielectric loss (ε″) of the specimen is computed as (Equation 16).

$$\varepsilon'' = \varepsilon' \tan \delta \tag{16}$$

Effective resistivity

The effective resistivity (ρ) of the composites is determined from the following formula (Equation 17).

$$\rho = \frac{R*A}{t} \text{ ;}\Omega\text{-}m \tag{17}$$

Where resistance R = V/I, A is the area of the electrodes(38mm), t is the thickness of the sample(5mm)(Princy et al. 1998)(Tangboriboon et al. 2013).

2.4.4 Electromechanical properties

Electromechanical properties investigated are electromechanical sensitivity, piezoresistive and piezo capacitive sensitivity. These properties determine its suitability as dielectric elastomer materials.

Electromechanical sensitivity Characterization

Electromechanical sensitivity is determined as the ratio of permittivity at 1 kHz and Young's modulus at 10% strain(Bele et al. 2015a).

Figure 2.12 Setup for determining the piezoresistive and piezo capacitive characteristics

Piezoresistive characterization

The resistance across the specimens were measured using LCR meter (Agilent, E4980A) along with test fixture (Agilent, 16451B) at different pressures according to ASTM D150-11 standard. The pressure was varied from 0 to 20 kPa, that was applied through known weights on the specimen (Figure 2.12). Test fixture used has 38 mm diameter guarded electrodes.

Piezo capacitive characterization

Samples were tested for piezo capacitive properties according to ASTM D150-11 standard using Agilent E4980A, LCR meter at 1 kHz frequency (Figure 2.12). Piezo capacitive measurements are performed under uniaxial pressures (0-20 kPa), that are produced by loading known weights on the specimens, while noting the corresponding capacitance. Test fixture used has 38 mm diameter guarded electrodes.

Properties of the solid silicone rubber composites are tested as per the above methods to determine its suitability for use as dielectric elastomers. Properties investigated include density, SEM characterization, Young's modulus, shore A hardness, permittivity, dielectric loss, effective resistivity, electromechanical sensitivity, piezoresistive and piezo capacitive sensitivity.

Data obtained from the above tests are analyzed in next chapter to determine the influence of filler types, filler and curing agent loading, mixing time and curing temperature on the properties of each of the three DDC, CDC and CDDC composites. Property-processing relationships for each of the above properties is discussed in the results and discussions chapter.

CHAPTER 3

3. RESULTS AND DISCUSSION

This study is undertaken to investigate the dielectric properties of solid silicone rubber particulate composites. Hence the dielectric properties namely permittivity, dielectric loss, effective resistivity and AC conductivity are sought for the three types of composites that are considered. In order to improve the dielectric properties, dielectric, conductive and conductive-dielectric fillers have been incorporated into the solid silicone rubber matrix. While filler loading improves the dielectric properties, it also has a bearing on the properties such as Young's modulus, shore A hardness, density and the filler matrix interface. Hence these properties have been investigated to ascertain their dependence on these fillers and processing factors. Electromechanical properties such as electromechanical sensitivity, piezoresistive and piezo capacitive sensitivity are a complex interplay of both mechanical and dielectric properties, hence they are experimentally determined to understand the influence of the fillers and processing parameters on the same.

3.1 Dielectric Filler Composites

Dielectric filler composites (DDC) are fabricated using barium titanate as the dielectric filler into the solid silicone rubber dielectric matrix. These composites are tested for physical, mechanical, dielectric and electromechanical properties. Property-processing relationships are determined for each of the factors. Factors include filler and curing agent loading, mixing time and curing temperature. Each of these factors are investigated at two levels, to obtain the L_8 Taguchi orthogonal array giving eight different combinations of factors. Thus, eight different composite samples are tested for each of the above properties. The results are then presented as main effects and interaction plots.

3.1.1 Physical properties

Density

One of the objectives in the development of composites for electromechanical transduction applications is that of achieving lower weight. This is achieved by tuning

the properties of the composites to achieve the stated density constraints imposed by the applications. Hence density of the composites has been investigated for understanding the effects of the factors that contributes towards the same. Table 3.1 shows the density of the DDC composites as per the L_8 Taguchi orthogonal array. Solid silicone rubber has a density of 1130 Kg/m^3.

Table 3-1 Density of DDC composites

BT (phr)	**DCP (phr)**	**MT (min)**	**CT (°C)**	**Density (Kg/m^3)**
3.5	1	10	160	1181
3.5	1	30	180	1179
12	1	10	180	1283
12	1	30	160	1246
3.5	5	10	180	1229
3.5	5	30	160	1130
12	5	10	160	1191
12	5	30	180	1329

From the analysis of the L_8 Taguchi orthogonal array, main effects and interactions plot for density of DDC composites are evaluated and plotted as shown in Figures 3.1 and 3.2. As expected, the density of these composites increases with the dielectric filler loading. The increase of curing temperature helps to compact the specimens further thereby increasing the density.

No interactions are observed between filler loading and curing agent loading or curing temperature. Whereas interactions are observed between filler loading and mixing time. Thus, for a larger filler loading (12 phr) the density of composite increases with mixing time. While with lower filler loading of 3.5 phr density decreases with mixing time. Thus, both factors interact with each other for density. Hence in order to have lower weight composites, we need to employ lower filler loading with longer mixing time or larger filler loading with shorter mixing time.

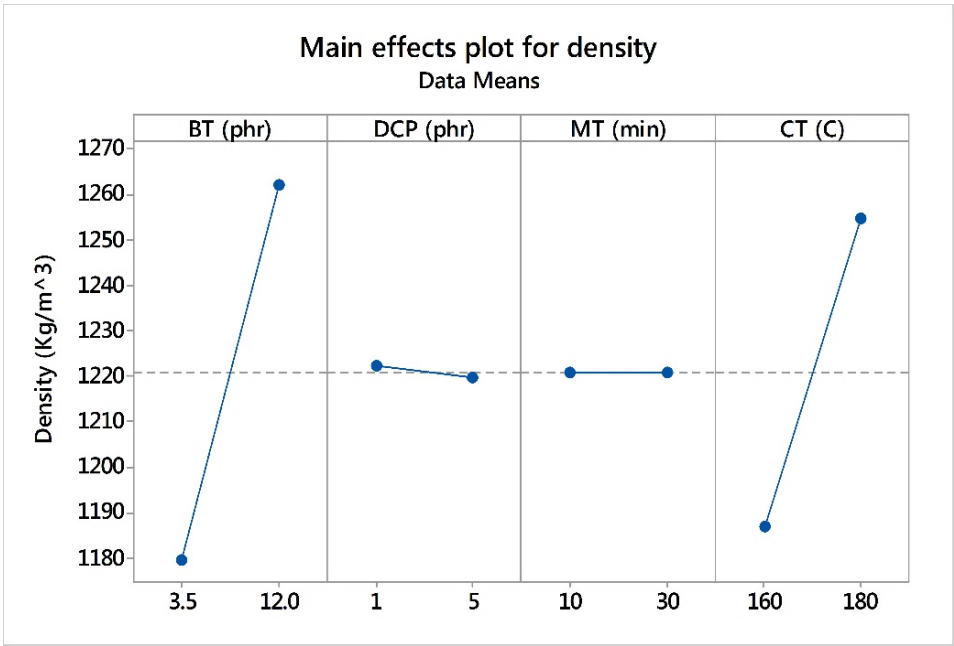

Figure 3.1 Main effects plot for density of DDC composites

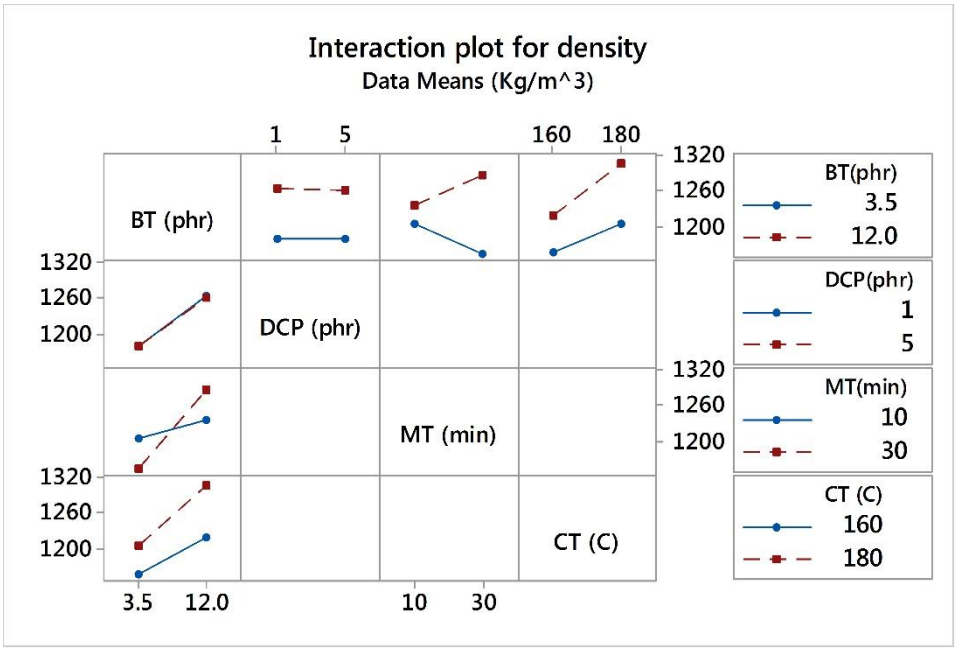

Figure 3.2 Interactions plot for density of DDC composites

SEM characterization

In order to investigate the effectiveness of the roll mill mixing method to obtain better filler distribution and wetting, SEM images of the composites are obtained. The dark phase represents the silicone rubber matrix and the bright phase represents the fillers.

The SEM images of the razor cut surfaces of DDC composites are shown in Figures 3.3, 3.4 and 3.5 for increasing filler content of 3.5, 7.75 and 12 phr respectively. As is evident from the SEM micrographs the uniform distribution of the dielectric filler in the polymer matrix is observed. This will prominently influence the dielectric properties of the composites. From the observation it is clear that there are no aggregates formed of the fillers. After milling, the filler particles are well dispersed(Zhao et al. 2013b) in the solid silicone rubber matrix phase. This is due to lower filler loading which allows proper wetting of the dielectric fillers. Hence the filler particles are neatly coated by silicone matrix, that manifests as excellent interfacial cohesion between the fillers and the solid silicone rubber. Thus due to lower filler loading and the roll mill processing method proper wetting of the fillers and its even distribution is ensured, indicating that processing methods also influence the dispersion of fillers in polymer matrix(Fan et al. 2013). Hence when filler particles are thus wetted and upon cross linking of the chains, the fillers are trapped through mechanical and adsorption mechanisms reflecting in strong attachments to the polymer matrix.

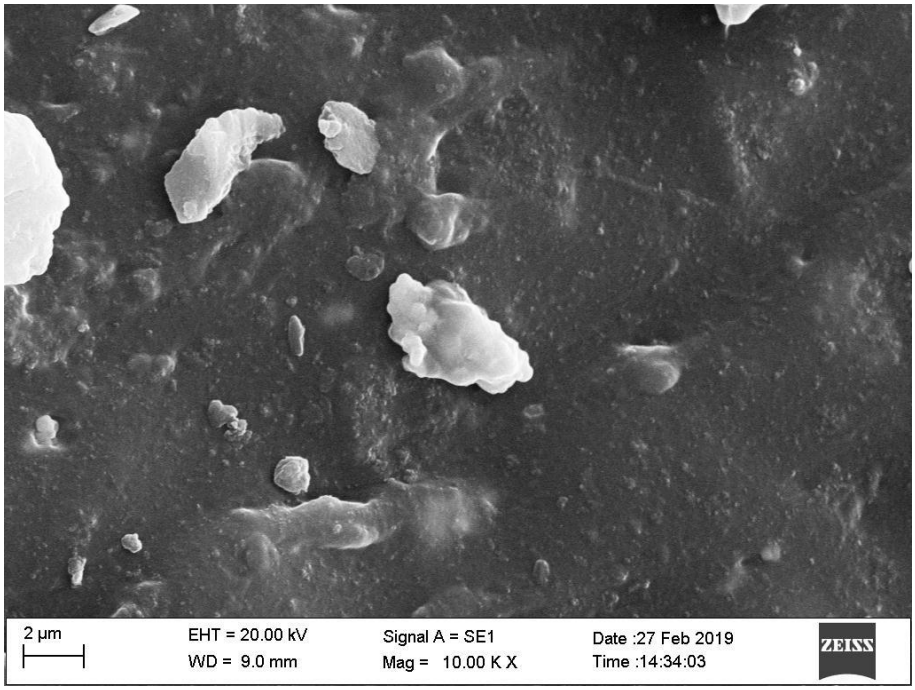

Figure 3.3 SEM micrograph of 3.5 phr DDC composites

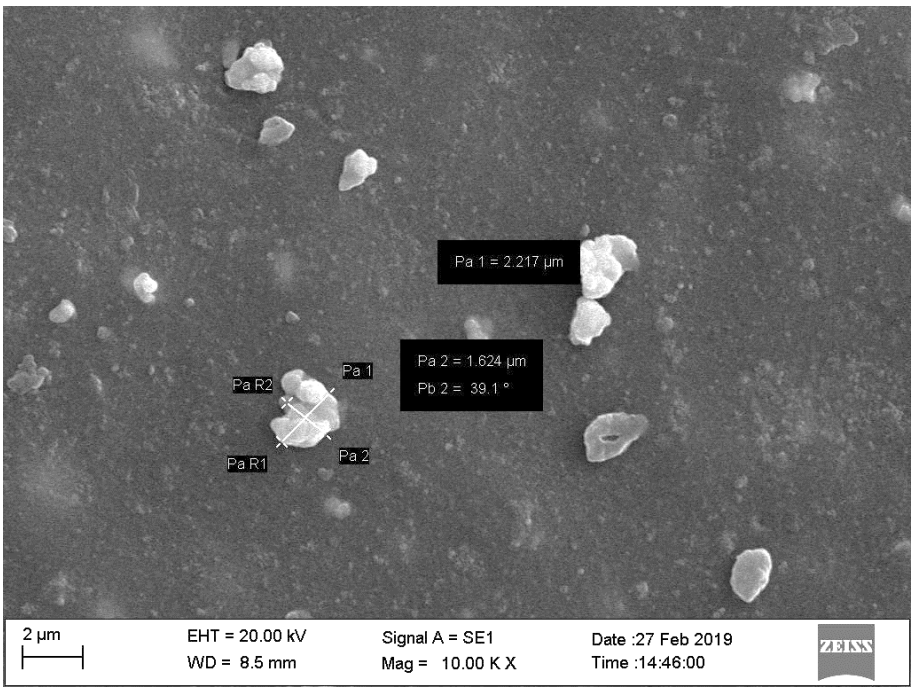

Figure 3.4 SEM micrograph of 7.75 phr DDC composites

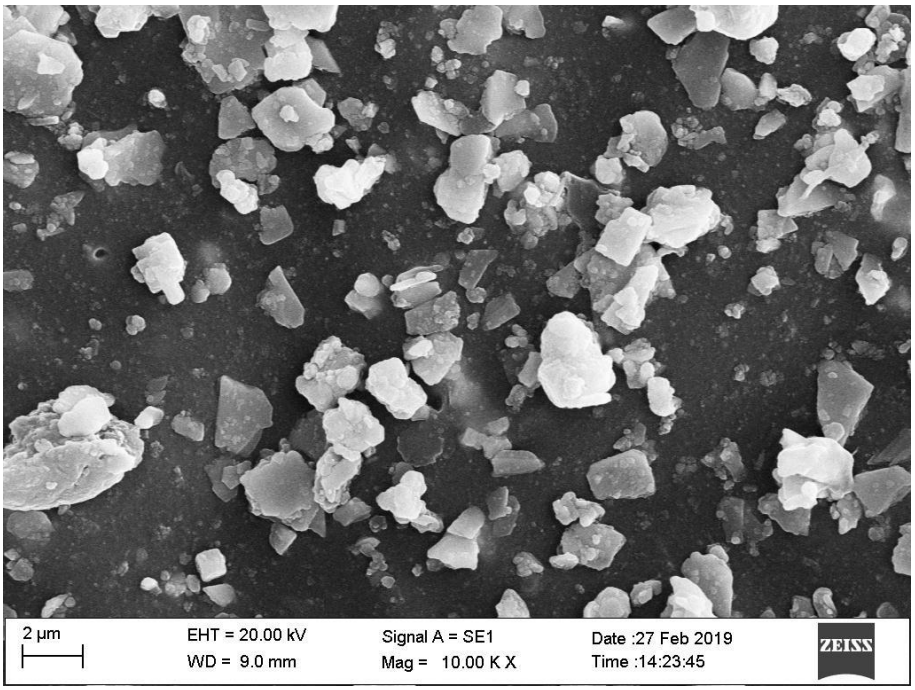

Figure 3.5 SEM micrograph of 12 phr DDC composites

3.1.2 Mechanical properties

With the addition of fillers to improve the dielectric properties of the composites, a corresponding change in the mechanical properties of the composites manifests itself. Thus, an improvement in dielectric properties should not be underscored by reduction in other properties. Hence mechanical properties of the composites are investigated.

Mechanical properties of the DDC composites as per L_8 Taguchi orthogonal array is presented in Table 3.2. Solid silicone rubber has Young's modulus and shore A hardness of 3.2 MPa and 40 respectively.

Table 3-2 Mechanical properties of DDC composites

BT (phr)	DCP (phr)	MT (min)	CT (°C)	Young's modulus (MPa)	Shore A hardness
3.5	1	10	160	3.7	43
3.5	1	30	180	3.5	43
12	1	10	180	3.7	44
12	1	30	160	3.5	42
3.5	5	10	180	2.7	44
3.5	5	30	160	3.3	43
12	5	10	160	3.6	44
12	5	30	180	3.2	45

Young's modulus

Young's modulus has to be lower for actuator applications involving large strains with lower forces, whereas for use as dielectric elastomer generators Young's modulus can be significantly higher. Young's modulus of the composites has been reported at 10 % strain in compression.

From the compressive stress strain plot of Figure 3.6 it is seen that the linear region is ensured up to 30% strain beyond which it displays nonlinearity a typical characteristic of elastomers. Solid silicone rubber having 3.2 MPa Young's modulus increased to 3.7 MPa for 12 phr loading of BT fillers. The method utilized for mixing is through roll mill, that ensures good distribution of fillers using shear forces. Due to improved distribution of fillers and improved wetting fillers don't form clusters. This will

manifest as better interfacial cohesion between fillers and matrix, improving the Young's modulus. The Young's modulus increases with increasing dielectric filler loadings as expected (Figure 3.7), displaying the reinforcing nature of dielectric fillers and strong filler matrix interaction. Young's modulus also increases with decreasing amount of curing agent, mixing time and curing temperature. Lesser curing agent along with lower curing temperature offers better cross linking of the matrix, thereby increased resistance to strain resulting in higher Young's modulus. Mixing time has two-fold influence in the fabrication of DDC. Firstly they help to distribute the BT filler particles uniformly and secondly they try to elongated the long macromolecular chains, thereby also prevent entanglements(Larsen et al. 2003). Larger entanglements give rise to harder and stiffer composites. Figure 3.8 shows interactions exists among the factors, predominant being between dielectric filler and mixing time.

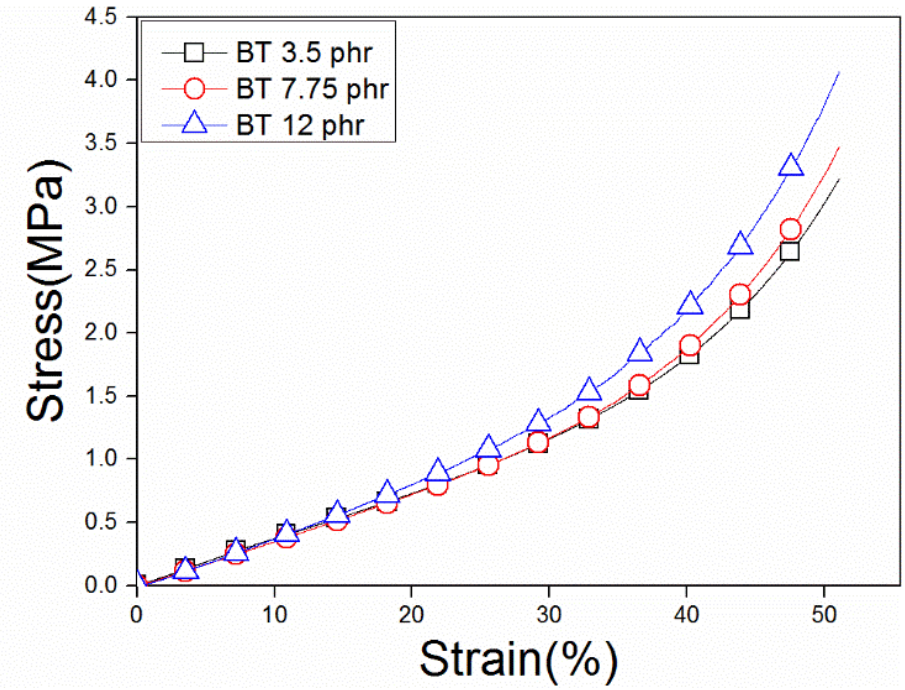

Figure 3.6 Stress strain plots of DDC composites

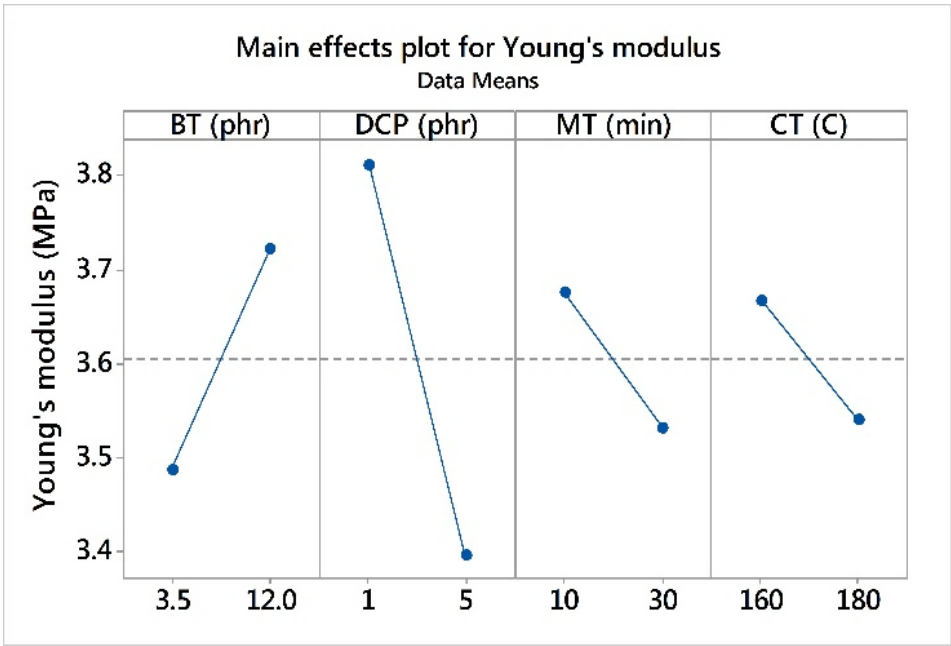

Figure 3.7 Main effects plot for Young's modulus of DDC composites

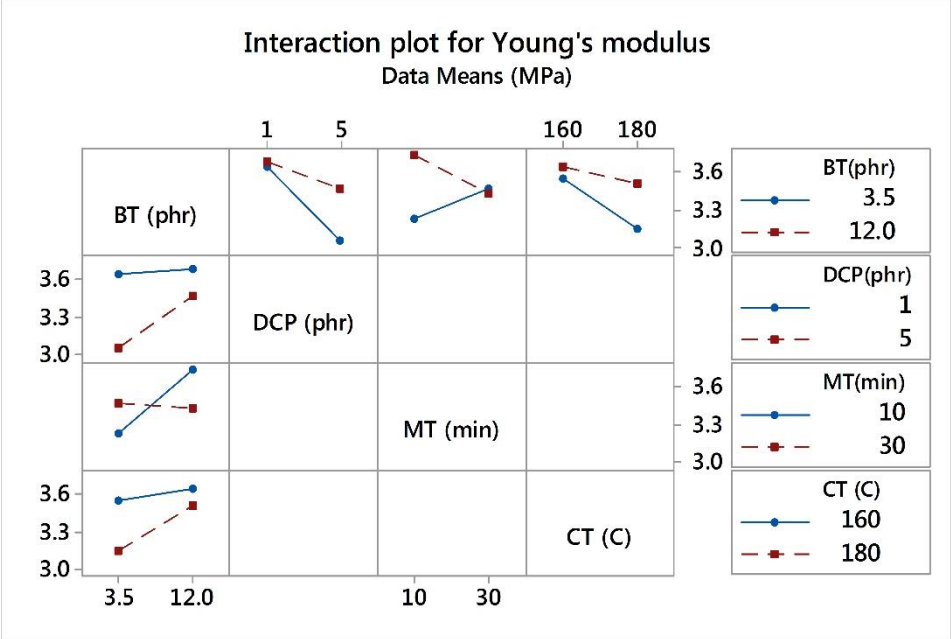

Figure 3.8 Interactions plot for Young's modulus of DDC composites

Hardness

Shore A hardness is often used as a proxy to flexibility, as it scales inversely with the flexibility of the composites(Jayalakshmy and Philip 2015). Hence shore A hardness gives an estimate of the flexibility of these composites for flexible pressure applications. The hardness of the composite may be considered as low strain modulus.

The influences of filler and processing parameters on the shore A hardness of the composites is investigated.

The addition of dielectric filler increases the hardness of the composites as the BT particles are rigid. Further with increase in filler loading restriction is imposed on the movement of polymer chains(Nayak et al. 2014a). Hence, solid silicone rubber having 40 Shore A hardness increased to 45 Shore A hardness with 12 phr loading of BT filler. Shore A hardness also increases (Figure 3.9) with curing agent and curing temperature. With the increase in curing agent along with curing temperature there is improved cross linking, this offers restriction on the movement of polymer chains, thereby increasing hardness. It also increases with reduced mixing time in the roll mill. With reduced MT the polymer molecules will be randomly distributed with greater entanglements. Since the concentration of entanglements are higher with lesser mixing, hence the composites are cured with harder network. One of the ways to minimize the trapped entanglements is to align the molecules during cross linking(Larsen et al. 2003) by shearing on a roll mill for longer time period, thus achieving aligned molecules offering lesser hardness upon curing. Interactions exists among factors for shore A hardness (Figure 3.10).

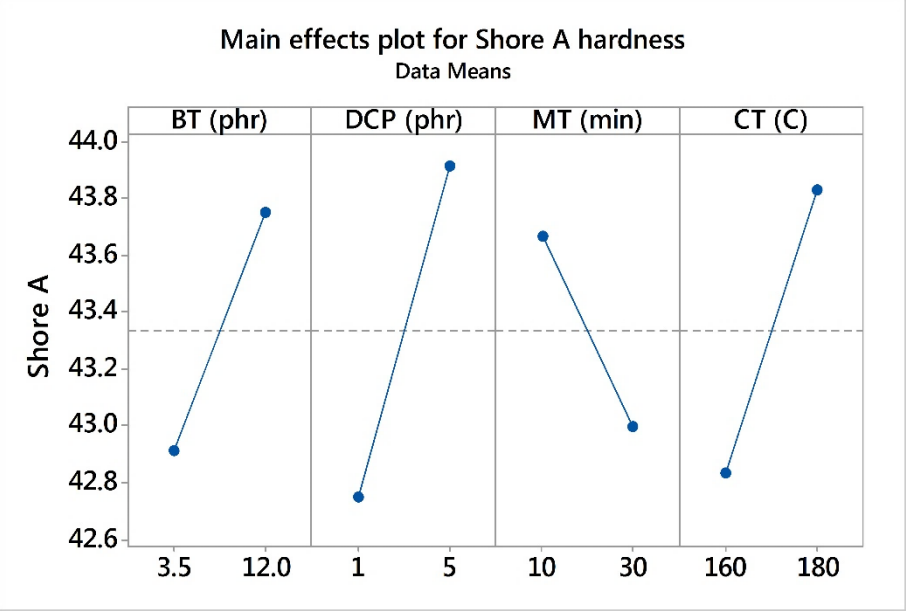

Figure 3.9 Main effects plot for shore A hardness of DDC composites

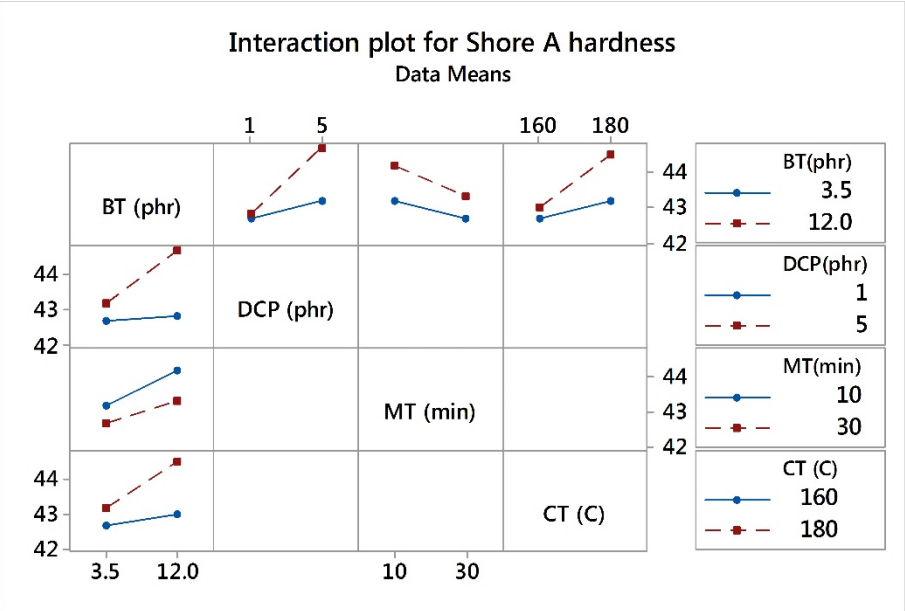

Figure 3.10 Interactions plot for shore A hardness of DDC composites

3.1.3 Dielectric properties

The polarization mechanism in silicone elastomer can be explained as follows: As silicone elastomer is an insulator, it consists of small dipoles with separate internal charges. Electrons and anions constitute the negative charge, while the atomic nuclei and cations form the positive charges of this dipoles. When an electric field is applied the dipoles will align with the field, thus polarising the material(Madsen et al. 2016b).

Complex relative permittivity consists of real part (permittivity, ε') and imaginary part (dielectric loss, ε''). Real part of permittivity is obtained from Equation 15 using the capacitance values from the LCR meter and the dimensions of the specimen along with the test fixture. Dielectric loss tangent is obtained from the LCR meter for the specimens. From this value dielectric loss (ε'') for the specimens is evaluated using Equation 16.

The insulating property of the composites have been expressed in literature in terms of effective resistivity (Equation 17) and AC conductivity.

As AC conductivity is frequency dependent and follows the AC universality law (Equation 18), the same is investigated for the three types of composites in order to determine the frequency exponent, s for each of the three composites. The total

electrical conductivity consists of DC (σ_{DC}) and AC (σ_{AC}) conductivity components. AC conductivity σ_{AC} of the prepared samples have been measured in the frequency range of 20 Hz to 2 MHz. Data thus obtained reveals that the AC conductivity is frequency dependent and thus follow the AC universality law (Equation 18).

$$\sigma_{AC}(\omega) = \sigma_{DC} + A(\omega)^s \quad (18)$$

The frequency exponent, s is obtained by the least squares straight line fit of the experimental data.

The dielectric properties of the DDC composites are measured and tabulated in Table 3.3 as per Taguchi L_8 orthogonal array. The Taguchi method is used in order to quantify the effects of the factors on these properties. The L_8 orthogonal array includes four variables, namely barium titanate (BT) filler loading, amount of curing agent (DCP), mixing time (MT) and curing temperature (CT). Each of these factors are at two levels. Since the experimental design is orthogonal, it is possible to separate out the effects of each of the factors at different levels, affecting the properties. From the analysis of L_8 orthogonal array, main effects and interactions plot are presented that show the effects of each of the factors and their interactions on the dielectric properties of the composites. Solid silicone rubber has permittivity, dielectric loss and effective resistivity of 2.9, 0.14 and 6297444 Ω-m respectively.

Table 3-3 Dielectric properties of DDC composites as per L_8 orthogonal array

BT (phr)	DCP (phr)	MT (min)	CT (°C)	Permittivity @ 1kHz	Dielectric loss	Effective resistivity @ 1kHz (Ω-m)
3.5	1	10	160	3.2	0.28	5813026
3.5	1	30	180	2.9	0.20	6667882
12	1	10	180	3.1	0.21	5667700
12	1	30	160	3.3	0.26	5462843
3.5	5	10	180	3.0	0.27	5966000
3.5	5	30	160	3.1	0.25	5813026
12	5	10	160	3.3	0.26	5449712
12	5	30	180	3.2	0.26	5667700

Permittivity

The influence of fillers and processing parameters on the permittivity of the composites are presented. Permittivity enhancement improves the Maxwell pressure applied on the elastomer for the given driving voltage for actuator applications. Permittivity improvement is also sought for in sensor applications involving piezo capacitive sensing. Other applications that look for improved permittivity are capacitors, electronic packaging materials.

Permittivity and dielectric loss both increase with BT loadings. Permittivity improved from 2.9 to 3.3, while dielectric loss increased from 0.14 to 0.28 with the addition of BT fillers.

From the main effects plot of the Taguchi analysis of the L_8 orthogonal array for permittivity of the DDC composites (Figure 3.11), it is observed that permittivity improves with increasing dielectric filler loading as expected. It also increases with increased curing agent loading. Permittivity decreases with increasing mixing time and curing temperatures. BT is a ferroelectric material possessing high permittivity on account of self-polarization due to strong dipole moments. Hence permittivity of the composites improves with BT loading. The cross linking of the DDC reduces the

rotational degree of freedom of BT particles, thereby reducing the permittivity of the composite, with increasing cross linking.

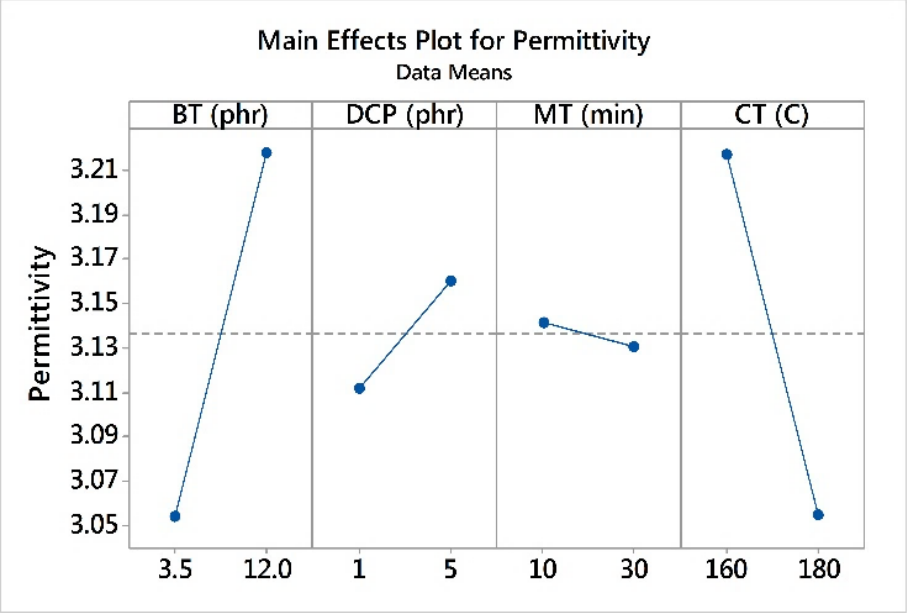

Figure 3.11 Main effects plot for permittivity for DDC composites

From the interactions plot for permittivity (Figure 3.12) it can be seen that only interactions among filler and mixing time is prominent. This suggests that combined influence of both these parameters affect the permittivity.

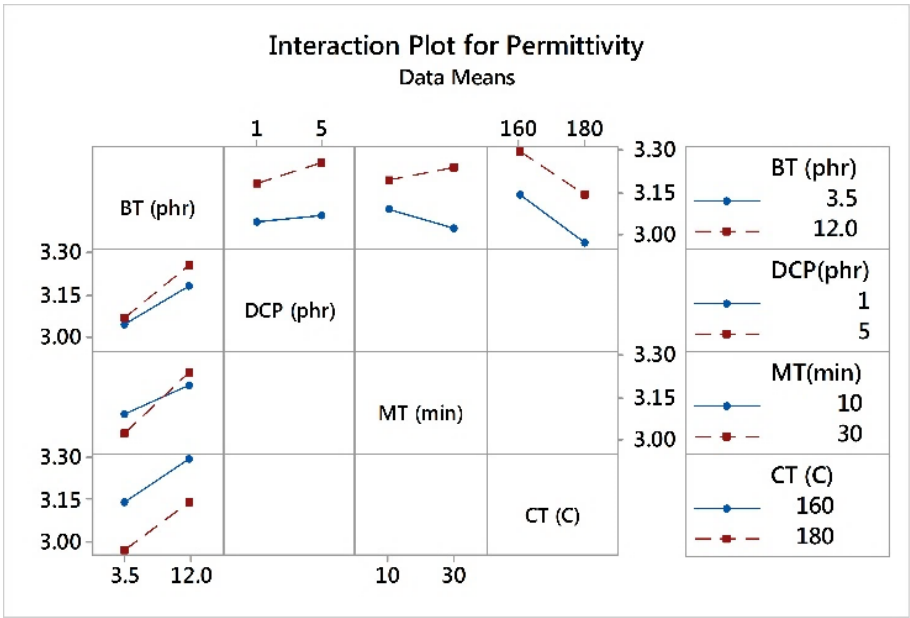

Figure 3.12 Interactions plot for permittivity for DDC composites

At lower filler content of BT and better dispersion, the particles are apart from each other, thus particle-particle interaction is negligible compared to particle matrix interactions. This can be seen as reduced permittivity in composite as compared to the permittivity of the fillers. The polymer molecules are cross linked, entangled, entrapped and physically adsorbed to the BT particles(Blow 1973).

The measured permittivity at 1kHz frequency is compared with theoretical values from well-known mixing rules from literature(Carpi and De Rossi 2005). Each of the mixing rule, based on a different model, predicts the permittivity of the composite ε_c, consisting of a mixture of two components as a function of their permittivity and volume fractions. BT is known to have high permittivity varying from 1000 to 2500(Poikelispää et al. 2016), for the above mixing rules, a value of 1000(Zhao et al. 2013a) is selected as permittivity for the BT filler. For the weight fractions of BT ranging from 0 to 12 phr, the corresponding volume fractions vary from 0 to 0.022. Figure 3.13 shows the comparison between predicted and measured values for the dielectric mixing rules applied to DDC, wherein the permittivity of the composite is plotted as a function of the volume fraction of the BT filler. All the models predict an increase in permittivity with increasing volume fraction. From the Figure 3.13 it is observed that Lichtenecker model predicts the permittivity of the composite more accurately for the DDC composites, yet it does not follow the experimental result accurately. This model does not consider the interactions among the particles nor the interaction between particle and matrix(Araújo et al. 2014).

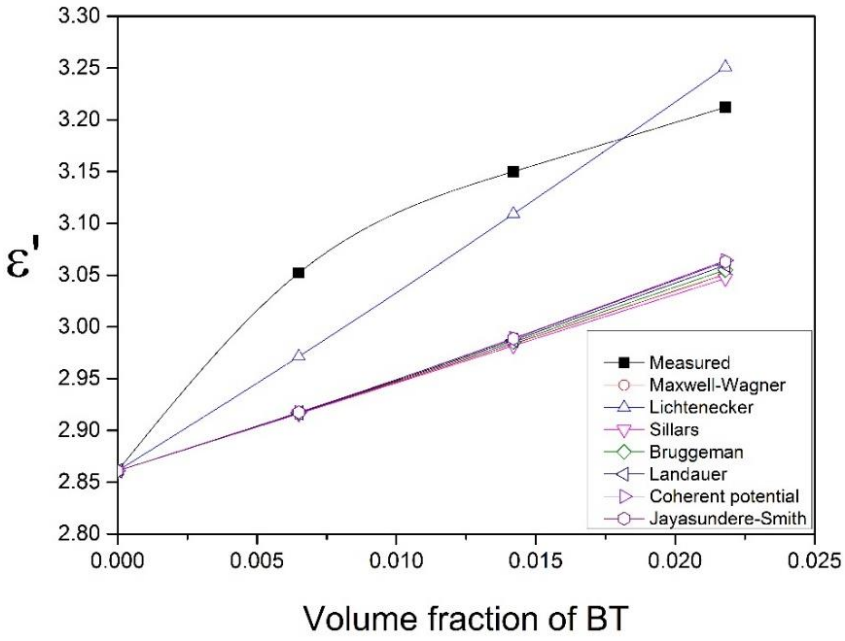

Figure 3.13 Comparison of dielectric mixing rules for DDC composites

In the case of dielectric fillers, an increase in permittivity of the composites is observed with dielectric filler volume fraction. In these composites polarisation of the particles determines the permittivity of the composites due to the large difference in permittivity between the two-phase materials. The local electric field is weakened as proposed by the AC electric field distribution principle(Zhong and Dang 2018). This suppression of the filler polarisation on the permittivity of the composite accounts for the lower permittivity of the composites even with higher loading of high dielectric constant fillers.

Figure 3.14 shows the variation of permittivity with frequency for the DDC composites for three different filler loadings. It can be observed that permittivity decreases with frequency for all filler loadings. In contrast to CDC composites, the decrease for all filler loadings of DDC composites show similar trends. This indicates that in DDC composites relaxation behaviour does not change with filler loadings. Polarization does not show significant increase with filler loadings for DDC composites. Permittivity increases with reducing frequency and reaches a maximum value of 5.6 at 20 Hz frequency for 3.5 and 7.75 phr, while it increases to 5.8 for 12 phr filler loadings. An important observation that is made for these composites is that permittivity reduces to 0.8 at 2 MHz frequency for all filler loadings.

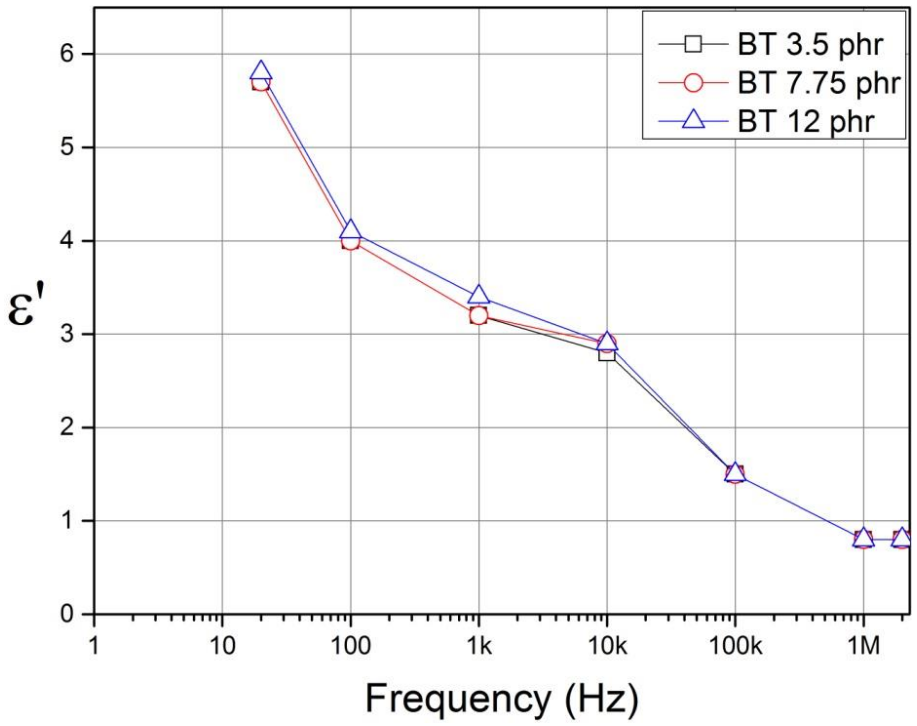

Figure 3.14 Characteristic response of permittivity as a function of frequency for DDC composites

Significant increase in permittivity is seen below the 10 kHz frequency. The factors that lead to this increase is strong interfacial polarization at the low frequency region, as the size of the BT particles are less than 3 μm, it provides enhanced surface areas. This favours the interfacial polarization. Another factor that contributes is the original contribution to increase in permittivity from the high permittivity BT fillers themselves(Fan et al. 2013). However, the permittivity of these composites is still lower than that with conductive fillers as different mechanisms influence the permittivity of conductive and dielectric filler composites. At lower filler loadings of BT fillers, the particles are apart from each other and thus filler-matrix interactions are predominant as compared to filler-filler interactions. This restricts the molecular mobility causing a decrease of polarization and consequently the permittivity of these dielectric filler composites. Two regions of drop in permittivity at 100 Hz and 100 kHz, are evident from the plot, accompanied by peaks in dielectric losses, suggesting the relaxation processes occurring at the matrix-filler interface. The decrease in permittivity with frequency is due to the inability of the dipoles to orient and return to

initial position along with the oscillation electric field(Bele et al. 2015a). Thus, polarization cannot follow the field that results in energy absorption and losses. A similar relaxation mechanism is reported by Gonzalez et. al.(González et al. 2017) for BT composites.

Dielectric loss

The influence of fillers and processing parameters on the dielectric loss of the composites are presented. Dielectric losses result in heat generation that leads to increase in temperature and conductivity. This produces a cascading effect that leads to thermal or electrical breakdown. Hence reduction in dielectric losses is crucial to the development of dielectric elastomers.

Main effects and interaction plots for dielectric loss are shown in Figures 3.15 and 3.16. Major effects on the dielectric loss is from curing agent and curing temperature and not so much from dielectric filler itself. Dielectric loss does increase with dielectric filler loading as expected, however its contribution is much lesser as compared to from curing characteristics of the composites. More mixing as indicated by mixing time leads to better dispersion of the fillers in the matrix hence contributes to lower dielectric losses.

Major interactions are observed only between dielectric filler loading and mixing time. Suggesting that the dispersion of these dielectric fillers along with filler loadings has synergistic effects on dielectric losses.

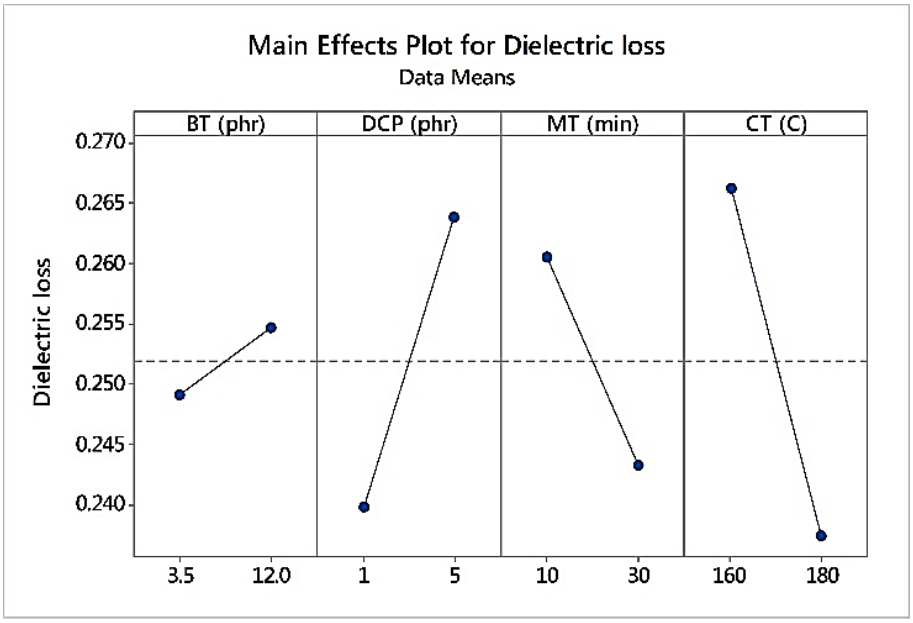

Figure 3.15 Main effects plot for dielectric loss of DDC composites

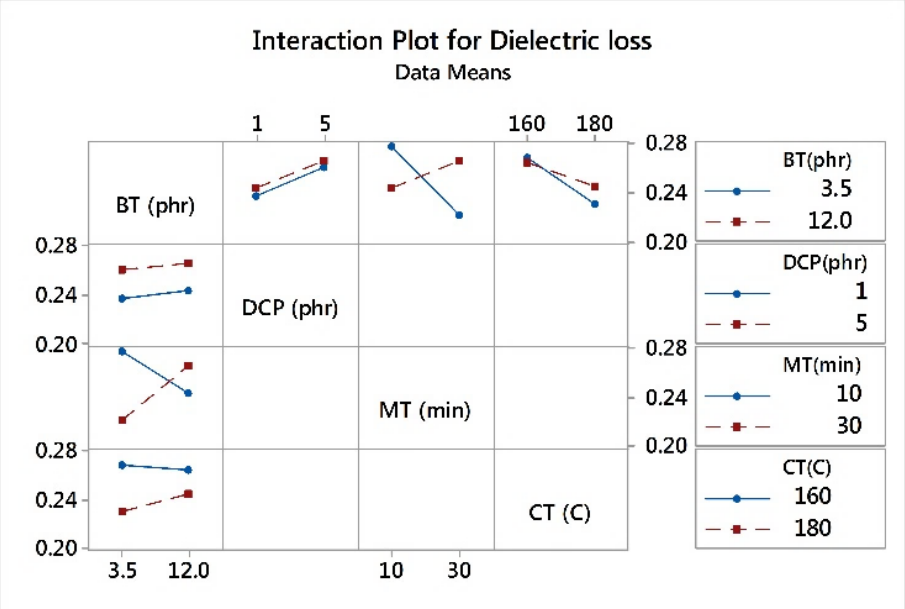

Figure 3.16 Interactions plot for dielectric loss of DDC composites

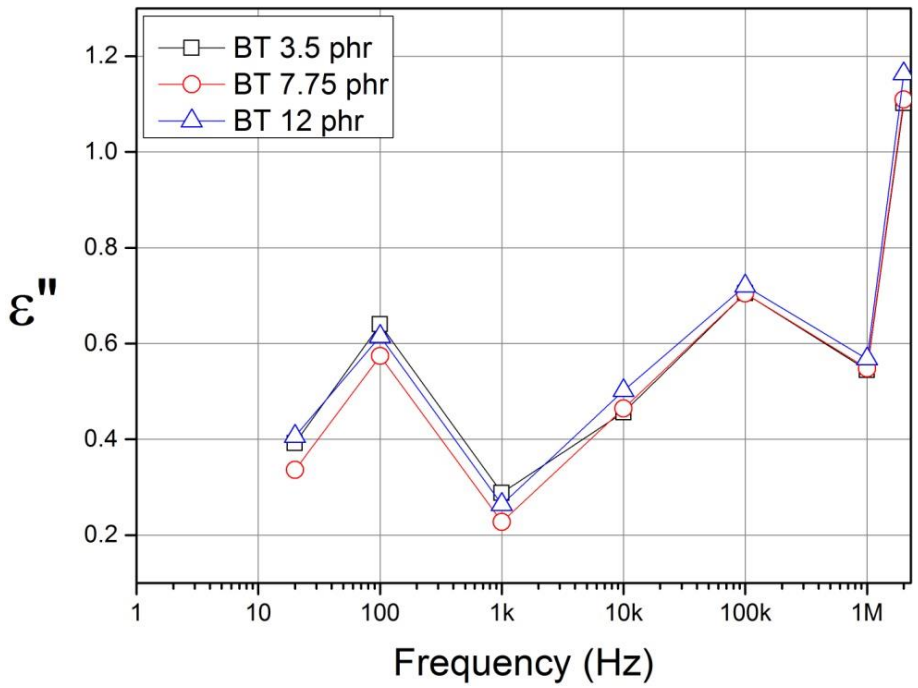

Figure 3.17 Characteristic response of dielectric loss as a function of frequency for DDC composites

The variation of dielectric loss with frequency for the DDC composites is shown in Fig. 3.17. It is observed that all filler loadings show similar trends. The dielectric loss peaks increase with increasing frequency. Two relaxation peaks are observed from the figure, one at 100 Hz and other at 100 kHz frequency. Relaxation peaks for all filler loadings are at the same frequency, indicating that they do not depend on filler loadings. Dielectric loss increases to a maximum of 1.1 at 2 MHz for 3.5 and 7.75 phr, while for 12 phr the maximum achieved is 1.2 at 2 MHz frequency. Two relaxation peaks are clearly evident, that do not change position with the filler loading, suggesting that dielectric filler loading has no consequence on the polarization process. When compared with the dielectric loss relaxations for the dielectric filler composites available in the literature for dielectric elastomer applications such a behaviour is not observed. This suggests that the fabrication process involved in this composite provides for long molecular chain entanglements that lock the dielectric fillers in place could be the reason for such a behaviour. The losses in this composite are seen to increase with increasing frequencies as opposed to the behaviour seen in conductive filler composites that sees a decrease with frequency on account of strong interfacial polarization. The low values of dielectric loss

observed at lower frequencies for these dielectric filler composites offer minimal conversion of electrical energy to heat in the composites, hence there will be less losses of electrical signals in these materials(Cazacu et al. 2014)

Effective resistivity

With the addition of dielectric and conductive fillers to the solid silicone rubber, conductive paths are formed. Even though silicone rubber is an insulator the addition of fillers reduces the effective resistivity of the composites. To be useful as dielectric elastomers these composites have to be in the insulating region even with the addition of fillers. Hence investigation of these properties is crucial to their usage as dielectric elastomers. The influence of filler and processing factors on the effective resistivity of the composites are investigated.

Low conductivity is key to dielectric elastomer performance(Madsen et al. 2016b). Hence effective resistivity of the composites in their operational range should be in the insulator regime. Effective resistivity of the composites depends on the effective resistivity of both, the matrix polymer and dielectric filler. The effect of factors on effective resistivity is presented in Figure 3.18 and is found that effective resistivity of the composite is composition dependent. Upon addition of high permittivity fillers, conductive paths occur thereby providing a means of charge transport through the composite, hence effective resistivity decreases with increasing dielectric BT filler loading as seen from Figure 3.18. With the addition of BT fillers, the effective resistivity of the DDC composites reduced to 5.4×10^6 Ω-m for a maximum filler loading of 12 phr from 6.3×10^6 Ω-m for solid silicone rubber. Effective resistivity also increases with increasing curing temperature and mixing time as per Taguchi analysis of L_8 orthogonal array. Greater mixing time ensures more uniform distribution of BT fillers, hence effective resistivity increases. Also, from Figure 3.19 it can be observed that interactions exist between filler and curing agent and between filler and mixing time for effective resistivity.

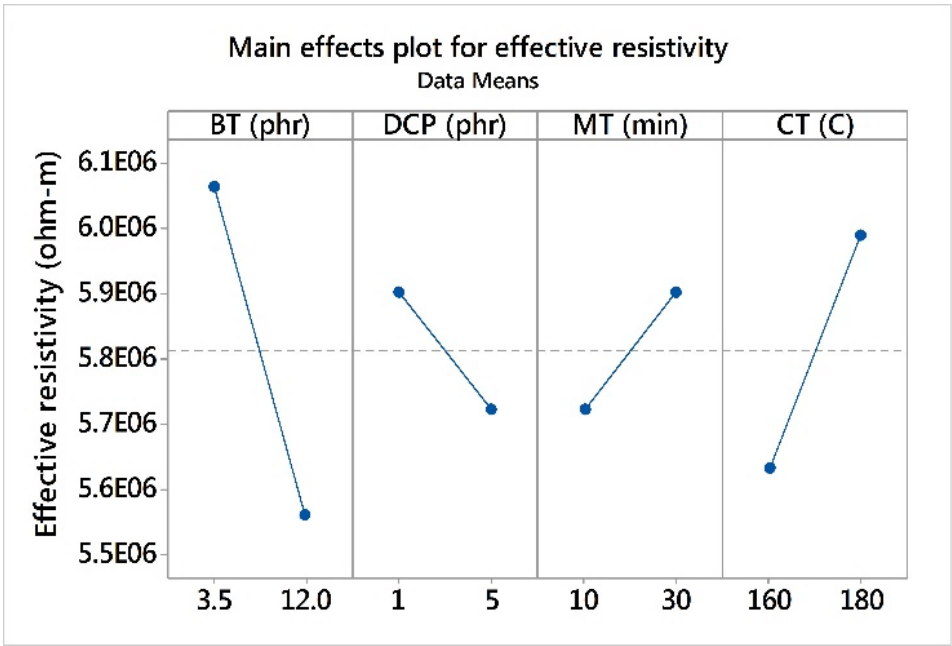

Figure 3.18 Main effects plot for effective resistivity of DDC composites

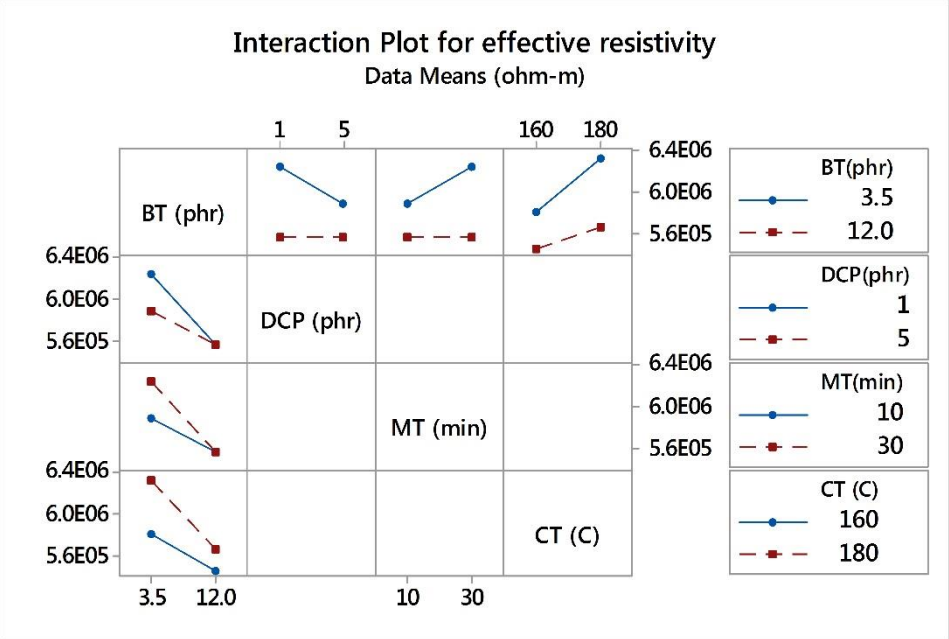

Figure 3.19 Interactions plot for effective resisitivity of DDC composites

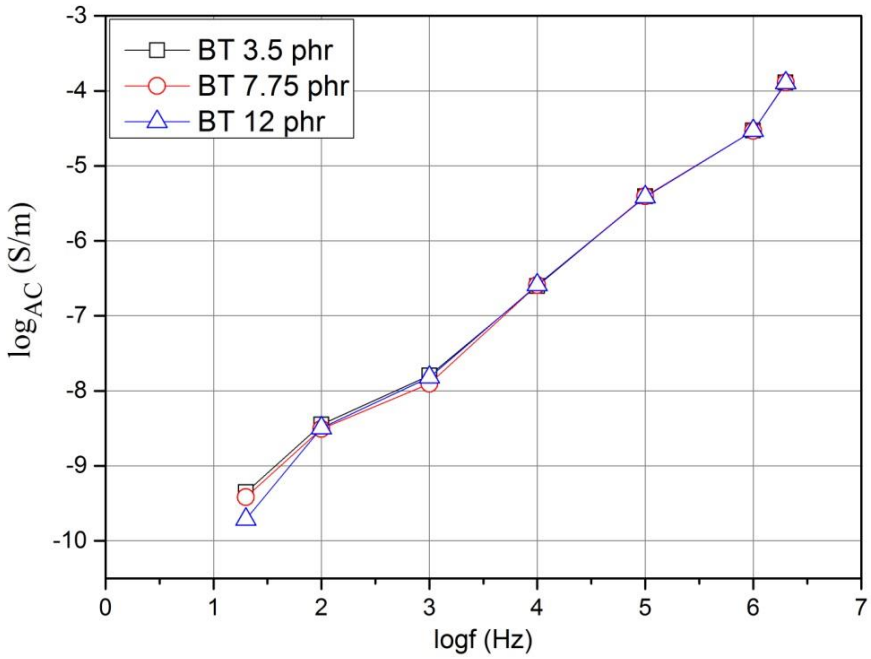

Figure 3.20 Characteristic response of AC conductivity as a function of frequency for DDC composites

Variation of AC conductivity with frequency for the DDC composites is shown in Figure 3.20. Composites with all three filler loadings show similar trends. Even though the conductivity values of composites are different at lower frequencies, however they achieve nearly same values at higher frequencies. The lowest recorded σ_{AC} was around 4.4E-10, 3.7E-10 and 4.5E-10 S/m for 3.5 phr, 7.75 phr and 12 phr filler loadings respectively at 20 Hz and the highest σ_{AC} was around 1.2E-04 S/m at 2MHz for these composites. The slope of the linearly fitted curves for the experimental data provide the exponent value of 1.02 as shown in Table 3.4. The AC universality law satisfactorily describes the experimental data, however the deviations are due to the fact that experimentally determined AC conductivity includes both the contributions from conduction and polarization processes(Psarras et al. 2003). The small deviations from the AC universality law has been attributed to weakly varying values of exponent with frequency(Dyre and Schröder 2000)(Dang et al. 2008)(He et al. 2009).

Table 3-4 Exponent of AC universality law of DDC composites

Exponent	3.5 (phr)	7.75 (phr)	12 (phr)
s	1.02	1.02	1.02

3.1.4 Electromechanical properties

When an electric field is applied across the opposite surfaces of the dielectric material, coulomb forces between the charges generate a stress called Maxwell stress, compressing the material in this direction and elongating it in lateral direction. The material is coated with conducting paint, grease or powder to act as compliant electrodes(Pelrine et al. 2000). The strain induced in the material is proportional to the permittivity and square of the electric field. Hence strains can be increased by increasing electric fields that is limited by electric breakdown strength of the material, by improving the permittivity or by reducing its thickness. A figure of merit taking permittivity and Young's modulus into account is the electromechanical sensitivity(Bele et al. 2014). It is the materials ability to provide more deformation at a lower electric field. It is regarded as a significant value in the determination of voltage induced deformation, to achieve high actuation performance in a low electric field. It is defined as ratio of permittivity to Young's modulus(Zhao et al. 2013a)(Yang et al. 2015a)(Bele et al. 2015a).

This method of enhancing electromechanical properties of off-the-shelf materials increases the toolset available to researchers for developing sensors and actuators.

Sensors for aircraft applications require high accuracy and working ranges of up to 2 kPa, whereas for automotive applications pressure ranges of around 10 to 30 kPa have to be measured. The electromechanical transduction performance for this study are measured for pressures up to 20 kPa, for both resistive and capacitive sensing mechanisms.

The pressure applied on the sensor is obtained by calibrating the mechanical deformation of the sensing dielectric material with the resistance and capacitance across the material. This behavior is referred to as piezoresistive and piezo capacitive

effect(Fan et al. 2017) respectively. The permittivity of the dielectric layer does not change during compression. Conventionally complicated micromachining processes are required for fabricating these sensors. A simpler approach would be to replace the sensing structures with flexible dielectric polymer as undertaken in this study.

Electromechanical sensitivity characterization

Electromechanical sensitivity is an important figure of merit of materials that are to be used as dielectric elastomer actuators. It gives an indication of the improvement in permittivity achieved without compromising the flexibility of the composites. The electromechanical sensitivity of the composites is analyzed using Taguchi techniques to understand its dependence on various processing parameters, such as filler and curing agent loadings, curing temperature and mixing time in the roll mill.

Table 3.5 shows the electromechanical sensitivity (β**)** of DDC composites obtained as per L_8 Taguchi orthogonal array. Solid silicone rubber has an electromechanical sensitivity of 0.89E-3 $(kPa)^{-1}$.

Table 3-5 Electromechanical sensitivity of DDC composites

BT (phr)	**DCP (phr)**	**MT (min)**	**CT (°C)**	**β (E-3) $(kPa)^{-1}$**
3.5	1	10	160	0.85
3.5	1	30	180	0.82
12	1	10	180	0.81
12	1	30	160	0.91
3.5	5	10	180	1.10
3.5	5	30	160	0.92
12	5	10	160	0.89
12	5	30	180	0.98

Electromechanical sensitivity of the composite depends largely on curing agent loading, followed by other factors as indicated from Figure 3.21. For the DDC composites electromechanical sensitivity increases with lesser dielectric filler, larger amount of curing agent, longer mixing time and cured at a lower curing temperature.

As the effects of curing agent and curing temperature is significant, it indicates that for the dielectric elastomer composites, contribution from Young's modulus towards electromechanical sensitivity is predominant compared to contributions from permittivity.

Electromechanical sensitivity of the composite depends on significant interaction between filler and mixing time (Figure 3.22).

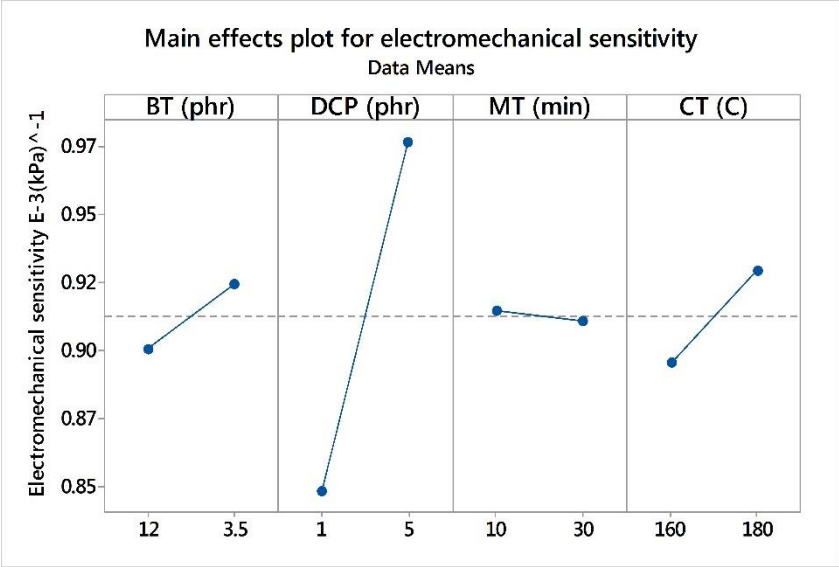

Figure 3.21 Main effects plot for electromechanical sensitivity of DDC composites

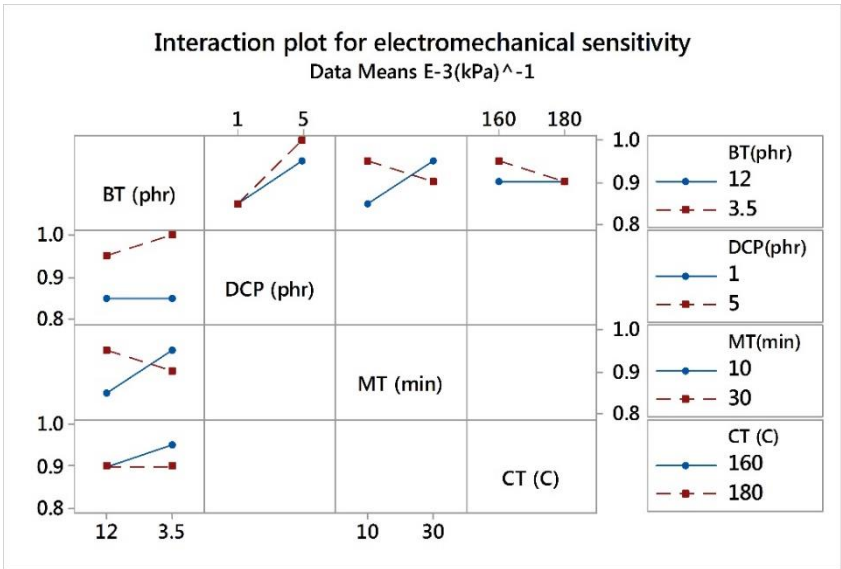

Figure 3.22 Interactions plot for electromechanical sensitivity of DDC composites

Piezoresistive characterization

In the case of piezoresistive materials, a change in electrical resistance is observed as a result of application of pressure. This change can be quantified by piezoresistive sensitivity. It relates normalized change in resistance with applied pressure. ΔR is the change in resistance across the specimen with pressure and R_0 is the resistance at no pressure. Solid silicone rubber composites are tested for piezoresistive (PR) properties. In order to investigate the effects of filler loading, curing agent, mixing time and curing temperature on the PR sensitivity of the composites, Taguchi analysis of the L_8 orthogonal array is conducted and the results are expressed as main effects and interaction plots. These plots provide the variation of mean values of PR sensitivity with different levels of factors. As the array is orthogonal, the effect of different levels of factors on the output response can be separated. The resistance value of solid silicone rubber with no fillers added was 28 MΩ.

Normalized change in resistance is plotted with pressure. Figure 3.23 shows the relationship as linearly fitted curves between the normalized change in resistance and pressure obtained experimentally for the DDC composites. The piezo resistance change with pressure for pure silicone rubber is linear up to 12 kPa, beyond which it flattens off. The resistance decreased with the applied pressures, showing a linear trend for all the composites in the tested range. PR sensitivity is obtained from the slopes of the linearly fitted curves of Figure 3.23 and is tabulated in Table 3.6. From the Table 3.6, it is observed that PR sensitivity is maximum for the composite sample of composition: BT of 3.5 phr, curing agent of 1 phr, mixed for 30 mins and cured at 180°C. The piezoresistive sensitivity of solid silicone rubber is 4.10E-3 $(kPa)^{-1}$, measured for pressure up to 9 kPa beyond which it becomes nonlinear (Figure 3.23).

The reduction in resistance of the composites with pressure can be explained by the reduction in the distance between the dielectric filler particles thus facilitating the conduction of charges.

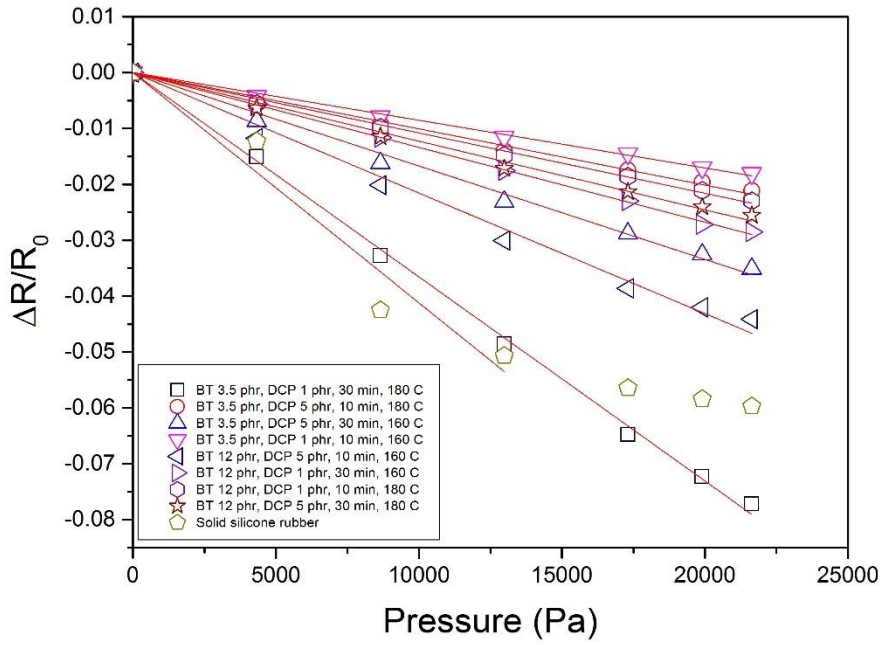

Figure 3.23 Piezoresistive characteristics of DDC composites

Table 3-6 Piezoresistive sensitivity of DDC composites

BT (phr)	**DCP (phr)**	**MT (min)**	**CT (°C)**	**Piezoresistive sensitivity (E-3) $(kPa)^{-1}$**
3.5	1	30	180	3.65
3.5	1	10	160	1.15
3.5	5	10	180	1.01
3.5	5	30	160	1.67
12	1	10	180	1.08
12	1	30	160	1.34
12	5	10	160	2.15
12	5	30	180	1.23

The main effects plot for piezoresistive sensitivity is shown in Figure 3.24. Sensitivity improves with lower BT filler and curing agent, whereas it improves with increased mixing time and curing temperature. From the interaction plot (Figure 3.25), it is evident that interactions among factors exist. Hence the effects of individual factors on the sensitivity depends on the nominal values of other factors.

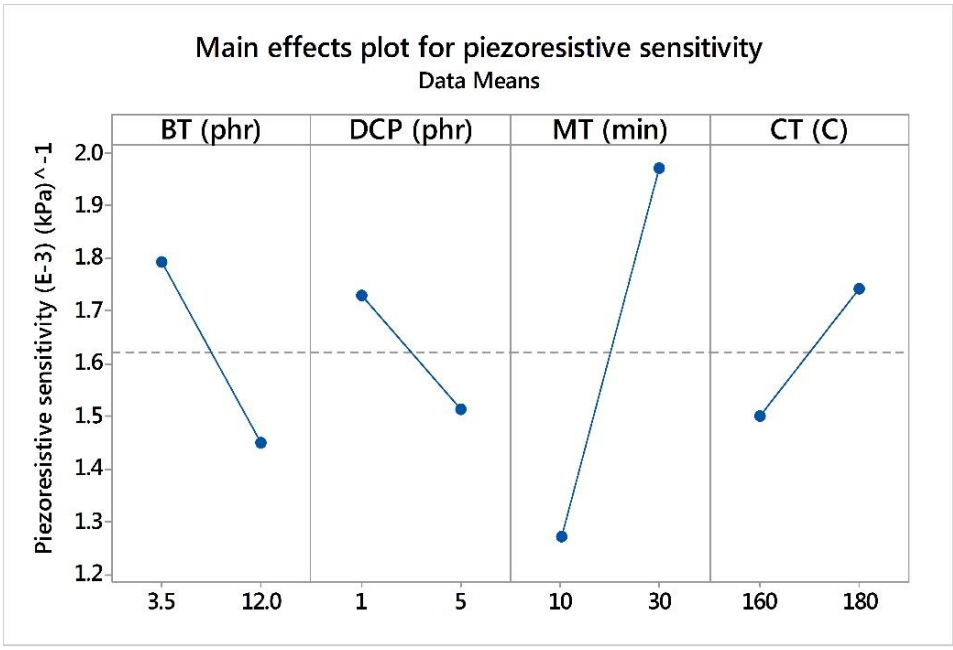

Figure 3.24 Main effects plot for piezoresistive sensitivity of DDC composites

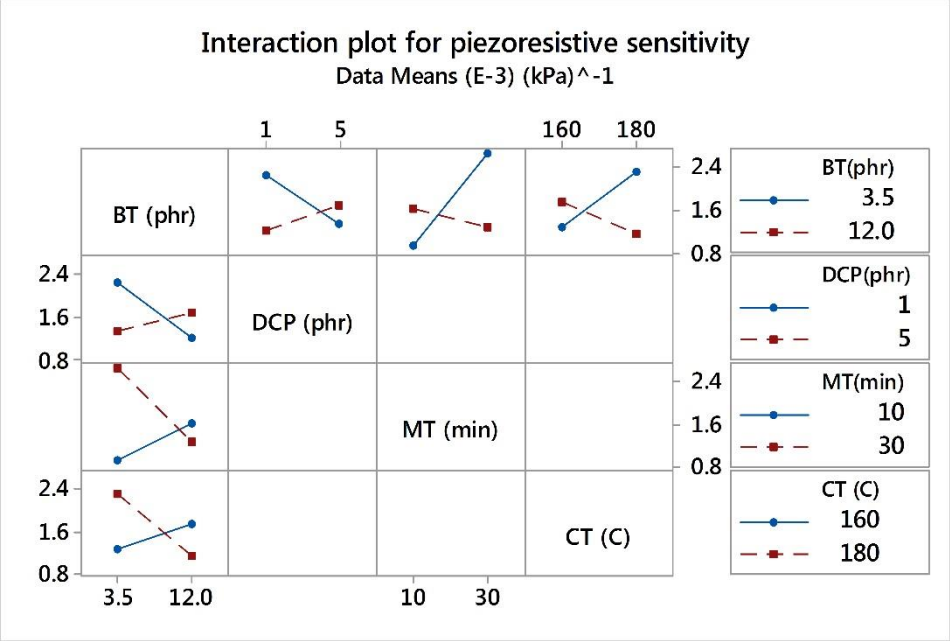

Figure 3.25 Interactions plot for piezoresistive sensitivity of DDC composites

Piezo capacitive characterization

Flexible pressure sensors for aircraft applications require high accuracy and working ranges of up to 2 kPa, whereas for automotive applications pressure range of around 10 to 30 kPa have to be measured(Zagnoni et al. 2005). For robotic applications two

broad classes of contact are identified based on pressure range(Maiolino et al. 2015). Gentle touch class for pressures in the range of 0-10 kPa, while manipulation touch class for 10-100 kPa range.

This study reports piezo capacitive properties for pressures of up to 20 kPa, beyond which the response shows nonlinearity. The pressure applied on the material is obtained by calibrating the mechanical deformation of the composite with normalized capacitance change across the material. This behavior is referred to as piezo capacitive effect(Fan et al. 2017). ΔC is the change in capacitance across the specimen with pressure and C_0 is the capacitance at no pressure.

A figure of merit that relates dielectric, mechanical and geometric properties to the overall response of a tactile sensor is the piezo capacitive sensitivity. DDC composites exhibit a nearly linear trend for the tested range of pressure.

The normalized capacitance changes with pressure change for various DDC samples as per L_8 Taguchi orthogonal array are plotted as shown in Figure 3.26. The slope of these linearly fitted curves gives the piezo capacitive sensitivity. Solid silicone rubber with no fillers shows linearity up to 12 kPa and then flattens off after a critical pressure, this trend is also correlated in literature(Cheng et al. 2017). The piezo capacitive sensitivity of solid silicone rubber is 3.93E-3 $(kPa)^{-1}$. Table 3.7 shows the linear fit values for sensor sensitivity up to 20 kPa. The maximum sensitivity obtained for the DDC samples is 3.69E-3 $(kPa)^{-1}$. A general observation for the capacitive pressure sensor response curves in the literature shows two quasi-linear sections, that have remarkably different slopes (sensitivity)(Fan et al. 2017).

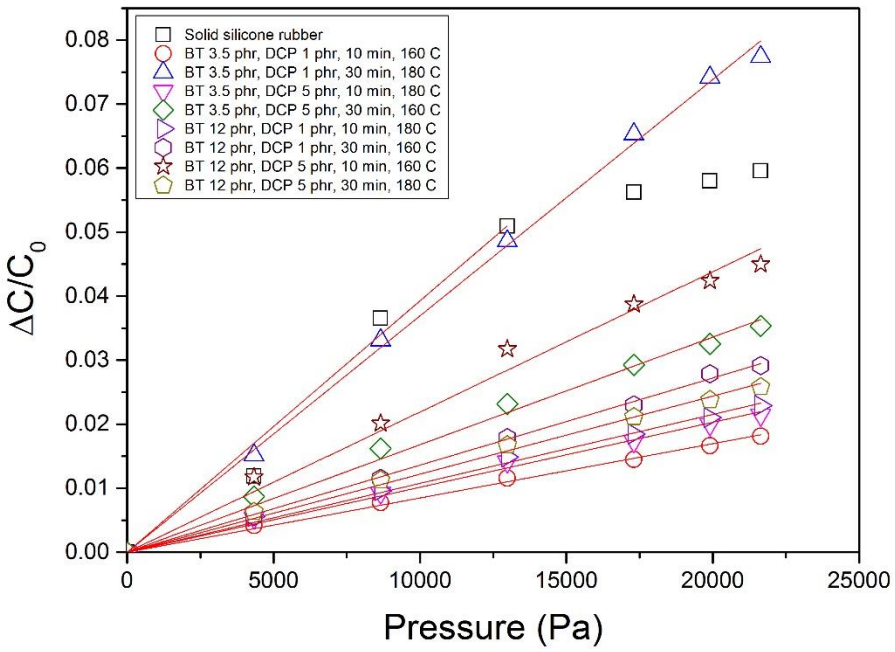

Figure 3.26 Piezo capacitive characteristics of DDC composites.

Table 3-7 Piezo capacitive sensitivity of DDC composites.

BT (phr)	**DCP (phr)**	**MT (min)**	**CT (°C)**	**Piezo capacitive sensitivity (E-3) $(kPa)^{-1}$**
3.5	1	10	160	1.15
3.5	1	30	180	3.69
3.5	5	10	180	1.01
3.5	5	30	160	1.68
12	1	10	180	1.08
12	1	30	160	1.36
12	5	10	160	2.19
12	5	30	180	1.22

Piezo capacitive sensitivity data thus obtained is analyzed using Taguchi analysis to ascertain the effects of the factors on the sensor sensitivity response of the composites. Main effects and interaction plots for sensor sensitivity display the mean values of sensitivity obtained at each of the factor levels, while varying all other factors. This analysis reveals that sensitivity is improved with lower level of BT loading, lower amount of curing agent, mixed for larger MT and cured at higher CT

(Figure 3.27). Lower BT filler loading contributes to reduced permittivity, however that also leads to lower elastic resistance. Lower curing agent leads to lesser cross linking thereby lower elastic resistance. Greater mixing time allows uniform dispersion of the fillers thereby improving the permittivity, while on the other hand reducing the entanglements in the silicone elastomer thereby reducing the elastic modulus. Higher curing temperature along with lower curing agent leads to lower curing with lesser elastic resistance. Hence the piezo capacitive sensitivity is an interplay between the permittivity and the elastic resistance. However, there are interactions observed among all the factors (Figure 3.28).

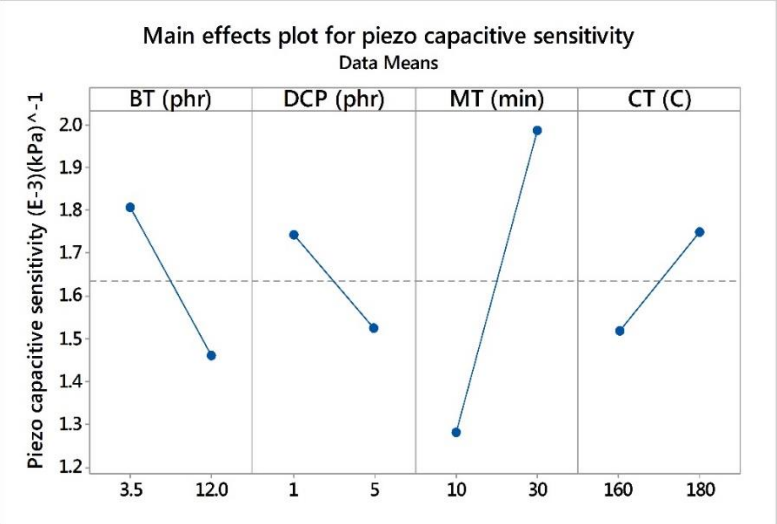

Figure 3.27 Main effects plot for piezo capacitive sensitivity of DDC composites

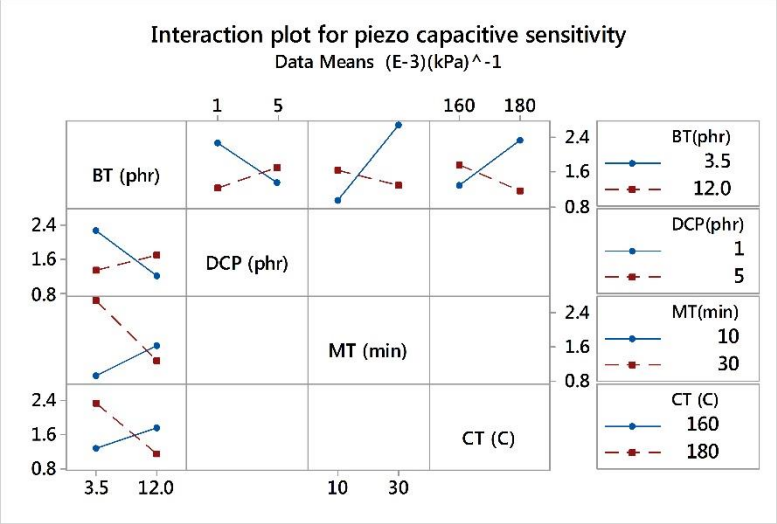

Figure 3.28 Interactions plot for piezo capacitive sensitivity of DDC composites.

3.2 Conductive Filler Composites

Conductive filler composites (CDC) are fabricated using Ketjenblack 300J as the conductive filler into the solid silicone rubber dielectric matrix. These composites are tested for physical, mechanical, dielectric and electromechanical properties. Property-processing relationships are determined for each of the factors. Factors include filler and curing agent loading, mixing time and curing temperature. Each of these factors are investigated at two levels, to obtain the L_8 Taguchi orthogonal array giving eight different combinations of factors. Thus, eight different composite samples are tested for each of the above properties. The results are then presented as main effects and interaction plots.

3.2.1 Physical properties

The density and SEM characterization for CDC composites are presented.

Density

Density of the CDC composites as per L_8 Taguchi orthogonal array is presented in Table 3.8.

Table 3-8 Density of CDC Composites.

SCCB (phr)	DCP (phr)	MT (min)	CT (°C)	Density (Kg/m^3)
3.5	1	10	160	1199
3.5	5	10	210	1118
3.5	5	30	160	1077
3.5	1	30	210	1150
12	1	30	160	1174
12	5	30	210	1126
12	5	10	160	1210
12	1	10	210	1116

The main effects and interactions plot for CDC composites are shown in Figures 3.29 and 3.30 respectively. The density of the CDC composites increases with increasing conductive filler loadings; however, it is lesser as compared to the contribution from dielectric fillers to DDC composites. This is on account of the structure of the

Ketjenblack filler as against BT filler. Density also increases with reduction in curing agent, curing temperature and mixing time. However, interactions among the factors exists.

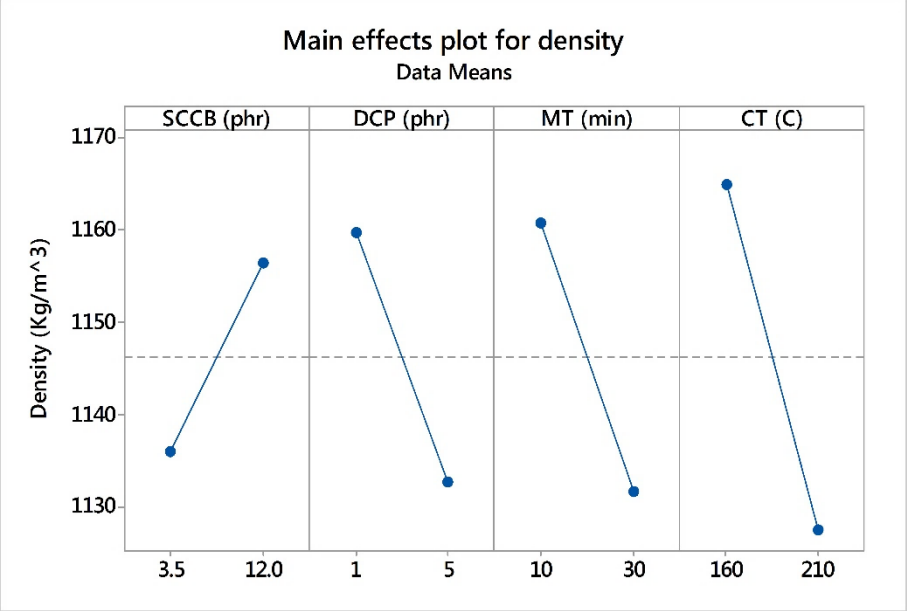

Figure 3.29 Main effects plot for density of CDC composites

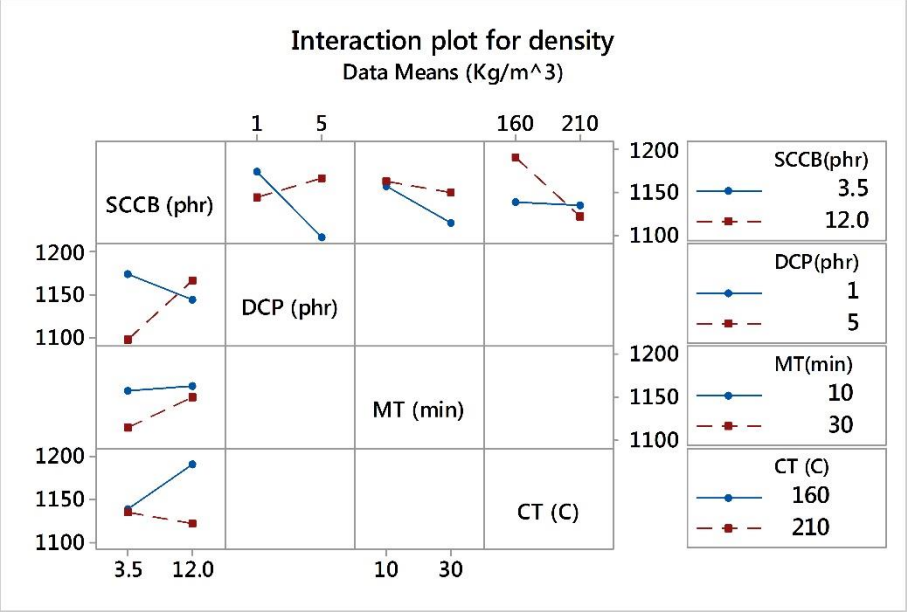

Figure 3.30 Interactions plot for density of CDC composites

SEM Characterization

The SEM micrographs for conductive filler composites confirm the uniform distribution of the Ketjenblack superconducting carbon black into the solid silicone

rubber elastomer matrix as shown in Figures 3.31, 3.32 and 3.33 for different filler loadings. The particles are seen to be neatly coated with the elastomer, suggesting good wetting by the matrix. There is no agglomeration of the carbon black particles as reported for many CDC composites in the literature. This also suggests that the roll mill mixing method is appropriate for the production of these composites.

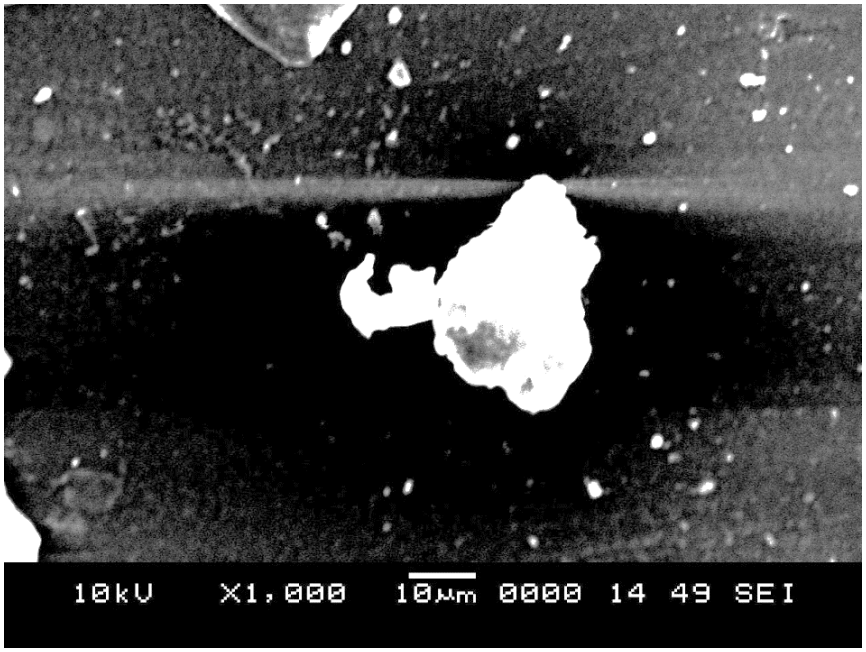

Figure 3.31 SEM micrograph of 3.5 phr CDC composites

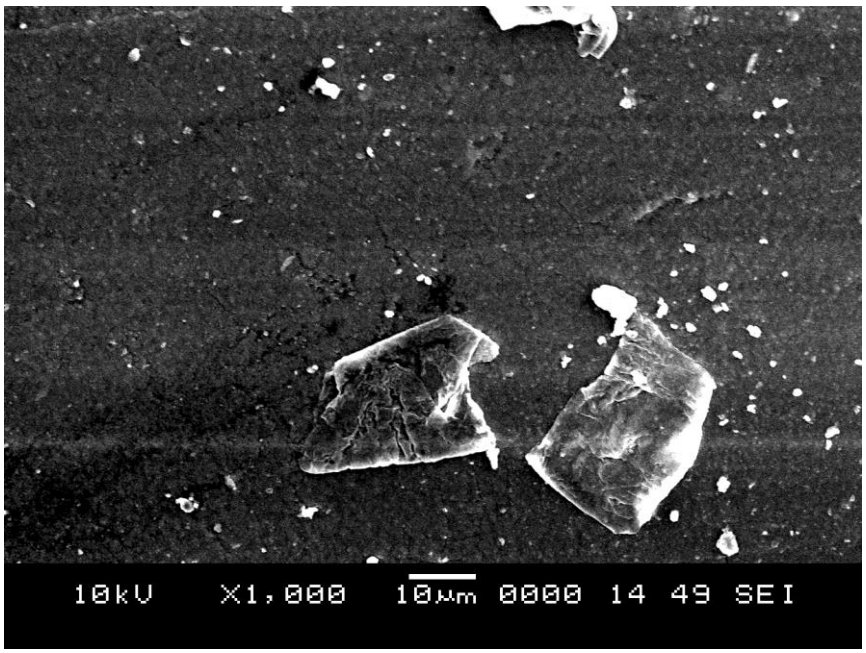

Figure 3.32 SEM micrograph of 7.75 phr CDC composites

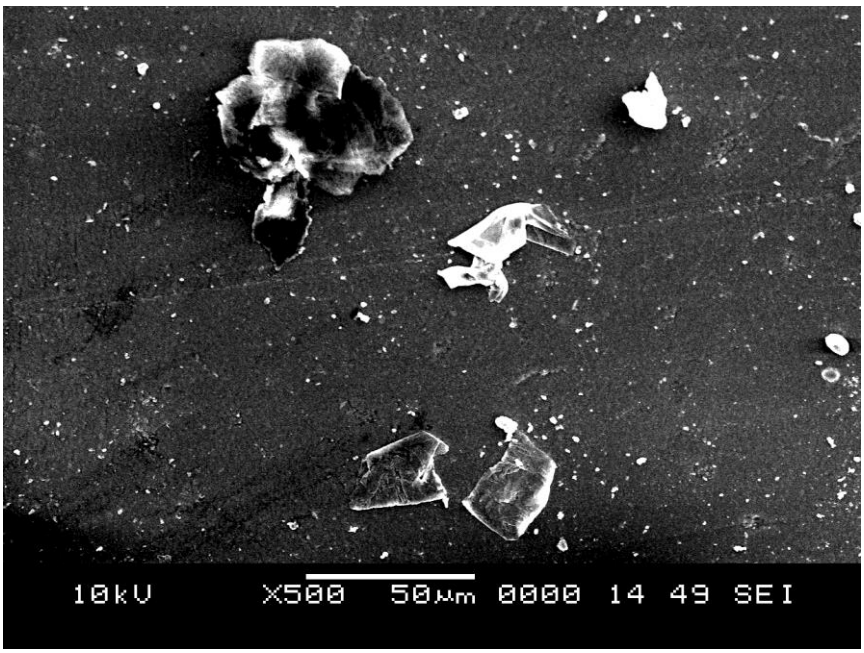

Figure 3.33 SEM micrograph of 12 phr CDC composites

3.2.2 Mechanical properties

Mechanical properties of the CDC composites as per L_8 Taguchi orthogonal array is presented in Table 3.9.

Table 3-9 Mechanical properties of CDC Composites.

SCCB (phr)	DCP (phr)	MT (min)	CT (°C)	Young's modulus (MPa)	Shore A hardness
3.5	1	10	160	10.4	57
3.5	5	10	210	9.8	58
3.5	5	30	160	11.0	68
3.5	1	30	210	4.1	64
12	1	30	160	9.7	65
12	5	30	210	17.0	83
12	5	10	160	25.2	86
12	1	10	210	12.1	71

Young's modulus

The conducting carbon black namely, Ketjenblack in the form of pellets is incorporated into the matrix in order to improve its permittivity. This alters the mechanical properties of the composite(Su and Zhang 2015). The Young's modulus of the composites varies from 4.1 to 25.2 MPa depending on the levels of various factors. This suggests that the process parameters have influence on the Young's modulus. Figure 3.34 shows the compressive stress strain plots for the conductive filler composites for different filler loadings.

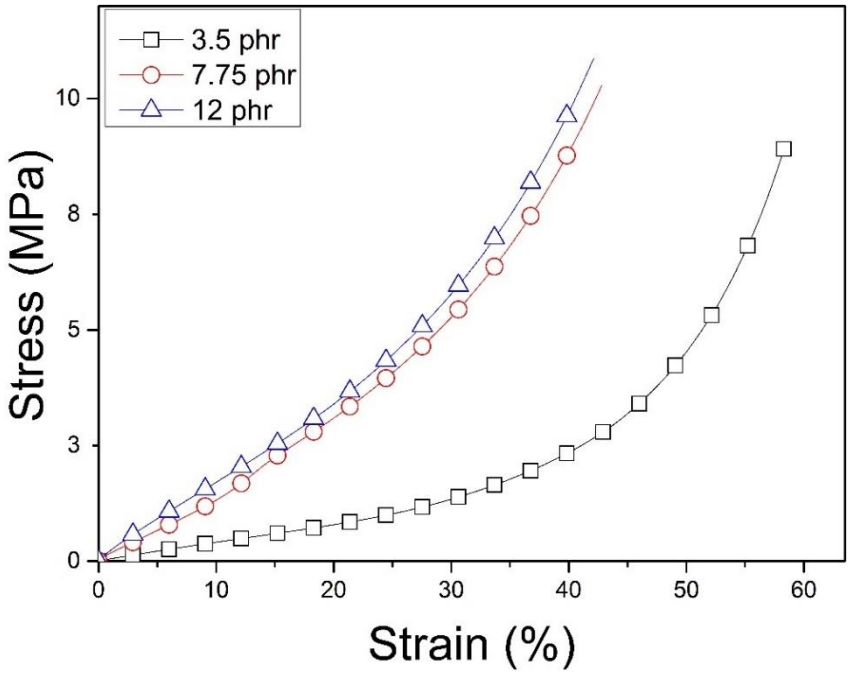

Figure 3.34 Stress strain plots of CDC composites

The reinforcing nature of the filler can be observed as increasing filler loadings leads to increase in Young's modulus. The curves show an initial linear region followed by nonlinear plot, a typical characteristic of elastomers(Stiubianu et al. 2016).

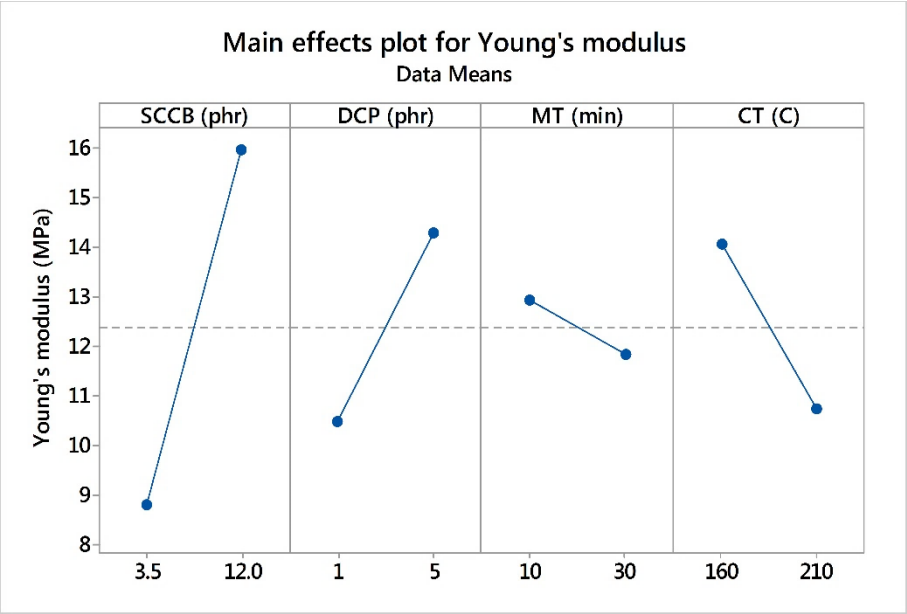

Figure 3.35 Main effects plot for Young's modulus of CDC composites

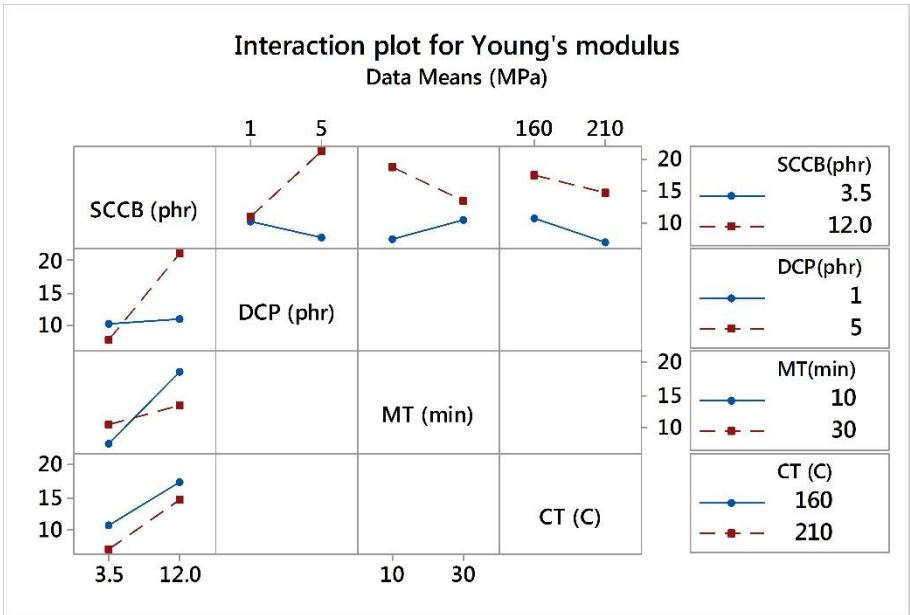

Figure 3.36 Interactions plot for Young's modulus of CDC composites

Main effects plot (Figure 3.35) for Young's modulus indicates that it increases with increasing conductive filler, curing agent and with decreasing mixing time and curing temperatures. Increasing filler content increases Young's modulus, indicating its reinforcing nature. Curing agent improves the crosslinking among the elastomer chains thereby improving in Young's modulus. Interactions are observed among filler

and curing agent, while no interactions are observed among filler and curing temperature (Figure 3.36). Mixing time has interaction with filler loading as mixing time gives an estimate of the distribution of the conductive filler.

Hardness

With the inclusion of conductive filler into the solid silicone rubber matrix of 40 shore A hardness, the hardness of the composites increases suggesting its reinforcing nature(Sahoo et al. 2012)(Nayak et al. 2013). Main effects plot for hardness is shown in Figure 3.37. Curing temperature has no effect on the change in hardness, while hardness improves with increasing values of other factors.

Interactions are observed among the filler and curing agent and among the filler and mixing time (Figure 3.38).

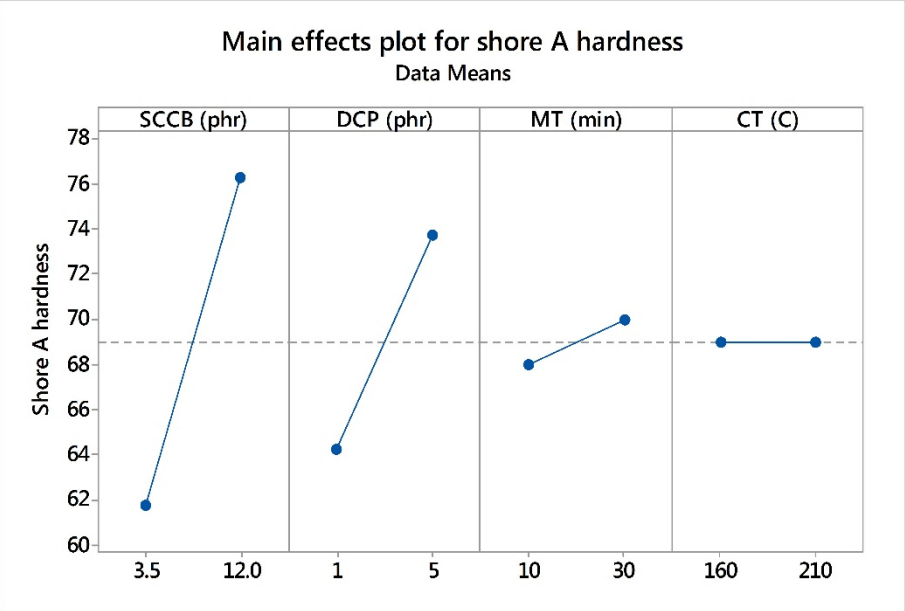

Figure 3.37 Main effects plot for shore A hardness of CDC composites

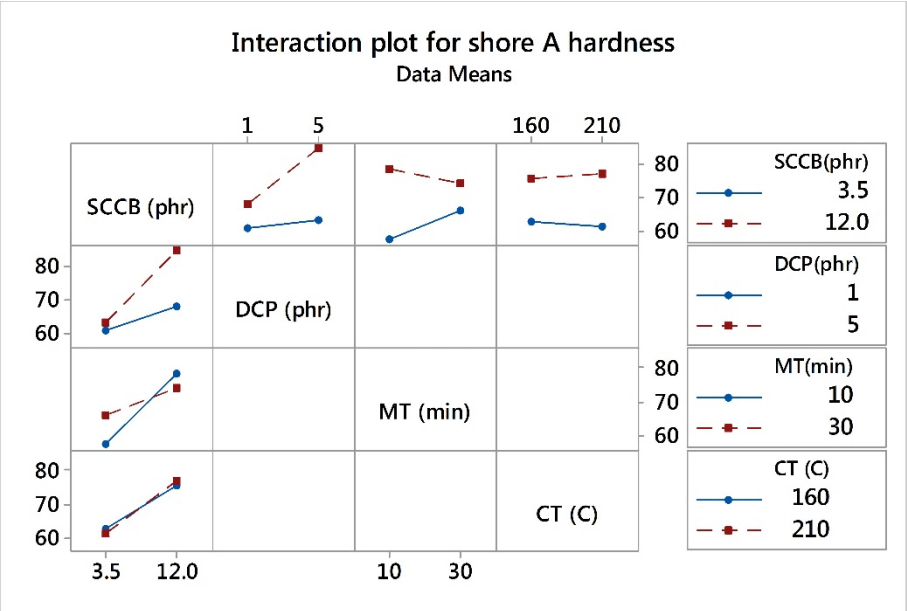

Figure 3.38 Interactions plot for shore A hardness of CDC composites

3.2.3 Dielectric properties

The dielectric properties for the CDC composites are recorded at 1 kHz and presented in Table 3.10.

Table 3-10 Dielectric properties of CDC composites as per L_8 orthogonal array

SCCB (phr)	DCP (phr)	MT (min)	CT (°C)	Permittivity @ 1kHz	Dielectric loss	Effective resistivity @ 1kHz (Ω-m)
3.5	1	10	160	4.6	0.14	3977333
3.5	5	10	210	4.0	0.12	4803136
3.5	5	30	160	4.3	0.13	4359769
3.5	1	30	210	3.8	0.11	4864979
12	1	30	160	14.1	1.27	1273392
12	5	30	210	14.1	1.27	1280385
12	5	10	160	14.1	1.27	1279929
12	1	10	210	14.1	1.27	1283104

Permittivity

Permittivity of the CDC composites is seen to vary from 3.8 to 14.1. While dielectric loss varies from 0.11 to 1.27. These values are higher as compared to the DDC composites for similar filler loadings. The permittivity of the CDC composites is analysed using Taguchi analysis and the results are presented as main effects and interaction plots as shown in Figures 3.39 and 3.40.

From the main effects plot it is observed that the permittivity of the conductive filler solid silicone rubber composites depends primarily on the influence of conductive filler loading. Other factors don't influence the permittivity as much as the filler loading. As expected, the permittivity of the composites increases with increase in conductive filler loading. This is on account of the superconducting nature of the ketjenblack particles that contribute to greater increase in permittivity with small amount of filler loadings(Yoshimura et al. 2012), which arises from its unique morphology.

The composites containing conductive fillers exhibit greater permittivity with lower filler loadings as compared to the dielectric filler loaded composites. This is on account of the interfacial polarization displayed by these heterogenous systems that are made up of materials having large differences in permittivity. The interfacial polarization is caused on account of the charges getting blocked at the interface between materials with largely different polarities(Gonzalez et al. 2017). The conductive carbon black fillers are completely enveloped by the solid silicone rubber matrix, thus developing into an appreciable increase in polarization. Interactions are not observed for this study as seen from the interactions plot for permittivity. Hence, the major contribution to the permittivity of the composites comes from the conductive filler loading only.

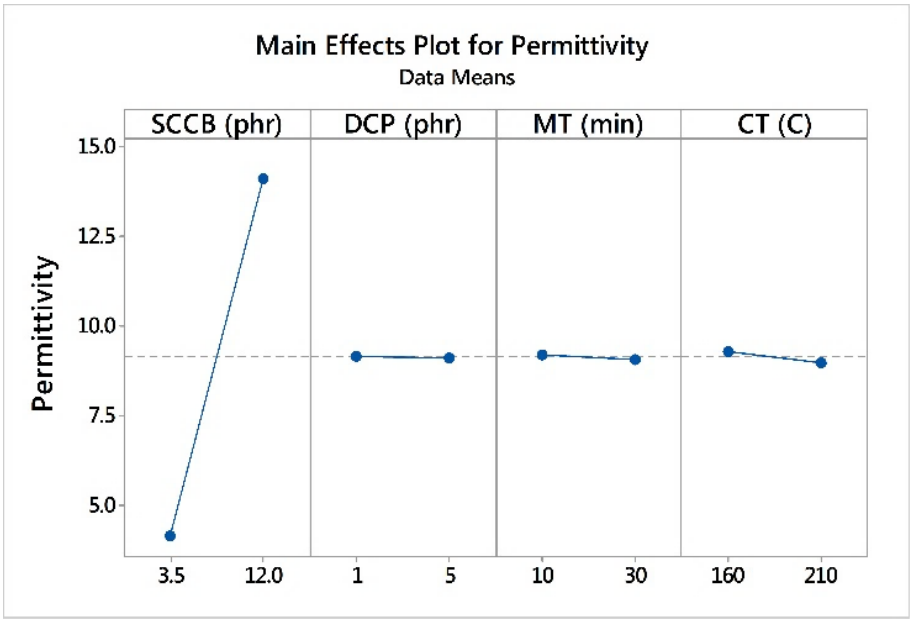

Figure 3.39 Main effects plot for permittivity of CDC composites

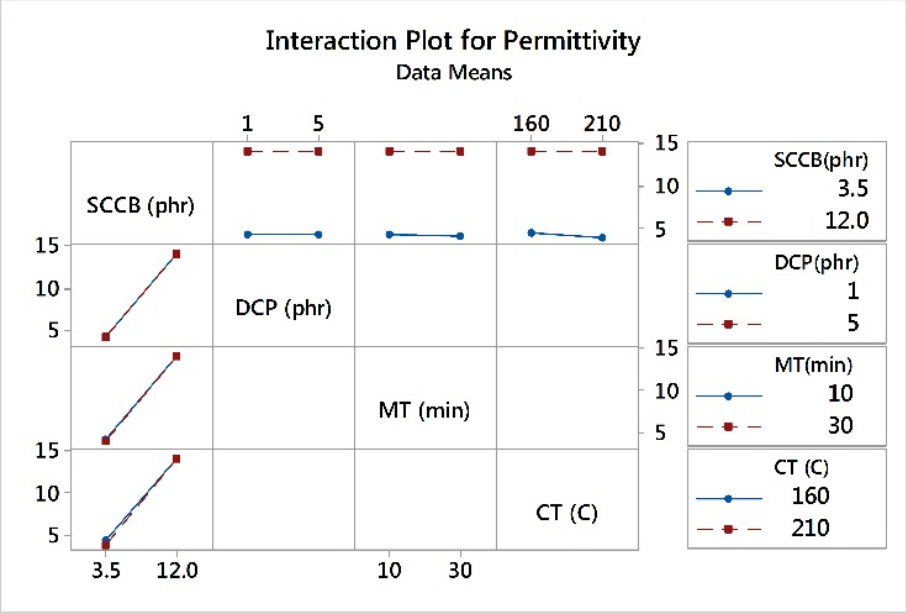

Figure 3.40 Interactions plot for permittivity of CDC composites

Figure 3.41 shows the variation of permittivity with frequency for the CDC composites for three different filler loadings. It can be observed that permittivity decreases with frequency for all filler loadings. The decrease for higher filler loaded composites being sharper than for lower filler loadings. Also composites with filler loadings of 7.75 phr and 12 phr show almost similar trends. This indicates that in

CDC composites relaxation behaviour does not change for loadings beyond 7.75 phr. As polarization is encouraged with higher filler loadings hence permittivity also increases and reaches a maximum value of 46 at 20 Hz frequency. The maximum permittivity value of 7 is achieved at 20 Hz for 3.5 phr composite. It is observed that permittivity reduces to 0.3 at 2 MHz frequency for composites with 7.75 phr and above, whereas it reduces to 0.6 at 2 MHz frequency for 3.5 phr composite.

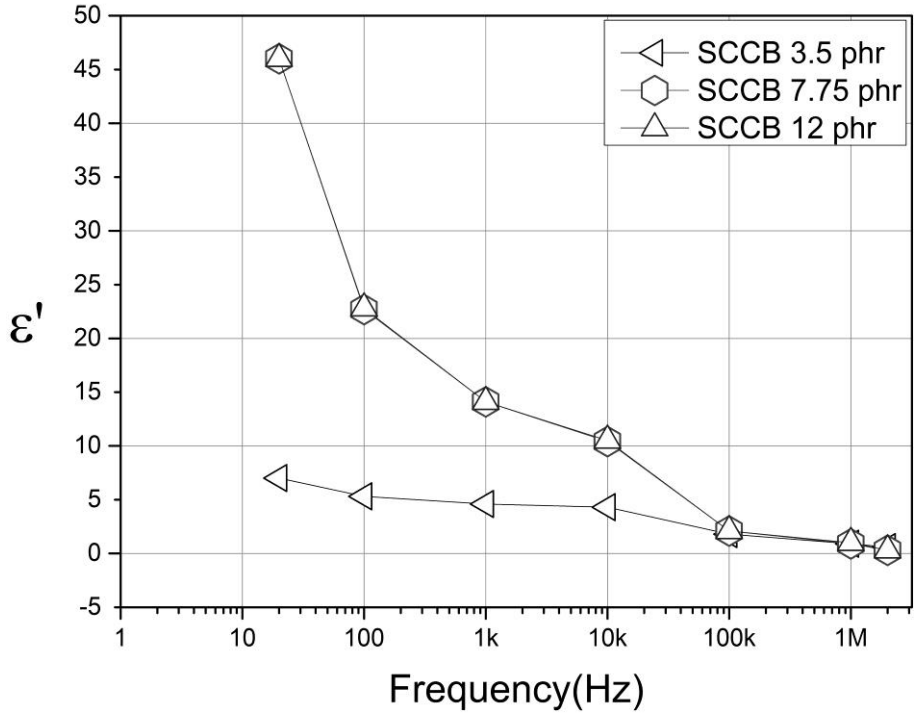

Figure 3.41 Characteristic response of permittivity as a function of frequency for CDC composites

The addition of conductive carbon black fillers to the solid silicone rubber matrix to obtain CDC composites makes these composites heterogeneous. This gives rise to interfaces between materials that possess significantly different permittivity. This gives rise to Maxwell-Wagner polarization at lower frequencies. There is accumulation of the free charges at these interfaces. This polarization mechanism results in high permittivity values at lower frequencies that decrease with frequency. The carbon black fillers thus enveloped by silicone matrix develop significant increase in permittivity due to appreciable interfacial polarization. These composites are polarized in response to applied electric fields(Renukappa et al. 2009). The

concentration of the filler influences the polarization as well as the conduction. It can be observed that permittivity drops off beyond 10 KHz as the electric field is too fast to influence the dipole rotation and the orientation polarization disappears. The decrease in permittivity with frequency is due to the inability of the dipoles to orient and return to initial position in accordance with the oscillating electric field. This happens when the time taken for the dipoles to return to its original random orientation is larger than that of oscillating electric field, indicating the existence of a dielectric relaxation. Hence the polarization cannot follow the oscillating frequency, resulting in the energy absorption and dissipation as heat. Other conductive filler composites with carbon black(Renukappa et al. 2009), nanographite(Saji et al. 2016) and multiwalled carbon nanotube(Saji et al. 2015) composites also demonstrate similar relaxation behaviour in the literature.

Dielectric loss

The dielectric loss analysis using Taguchi method for the various composites are presented as main effects and interactions plot as shown in Figures 3.42 and 3.43.

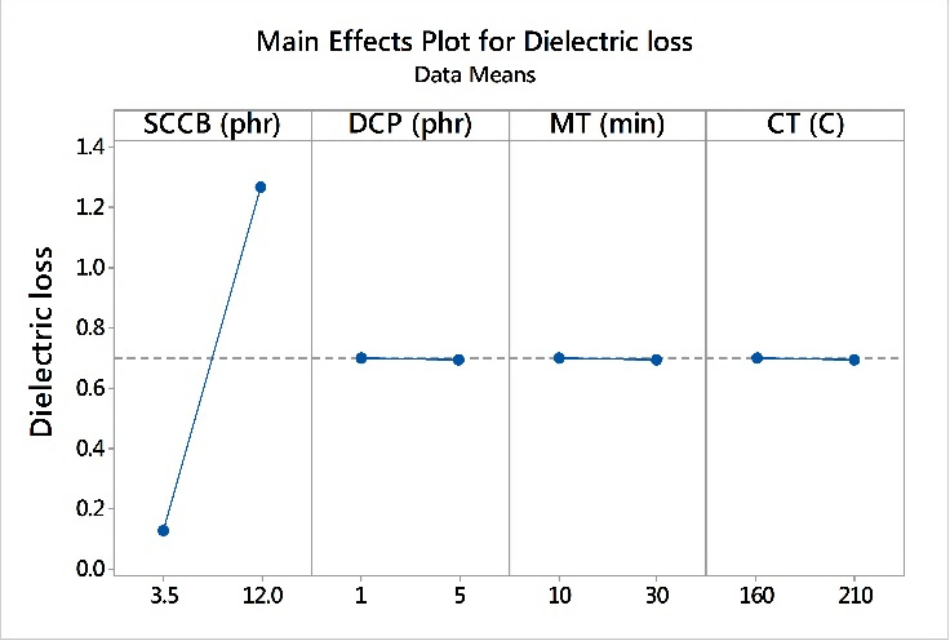

Figure 3.42 Main effects plot for dielectric loss of CDC composites

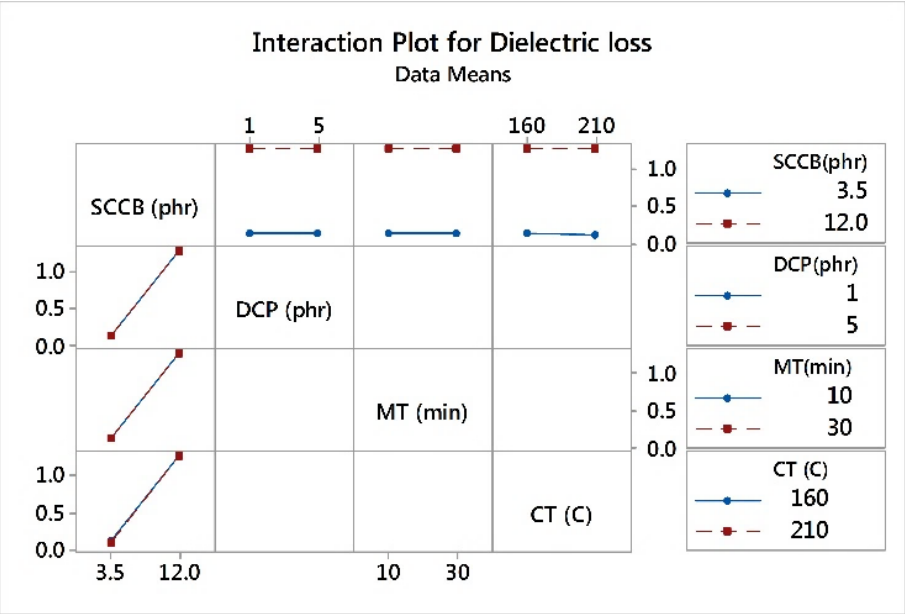

Figure 3.43 Interactions plot for dielectric loss of CDC composites

The dielectric loss depends primarily on the conductive filler loading. As expected of conductive fillers, the dielectric loss increases with increasing conductive filler loading(Wu et al. 2018). However, they are still lower as compared to the values reported in the literature. The low values of dielectric loss are on account of the good compatibility of fillers with the polymer matrix. From the interactions plot for dielectric loss it can been seen that there are no interactions among the factors. Hence the factors can be individually varied, without any contrary effects from the other factors.

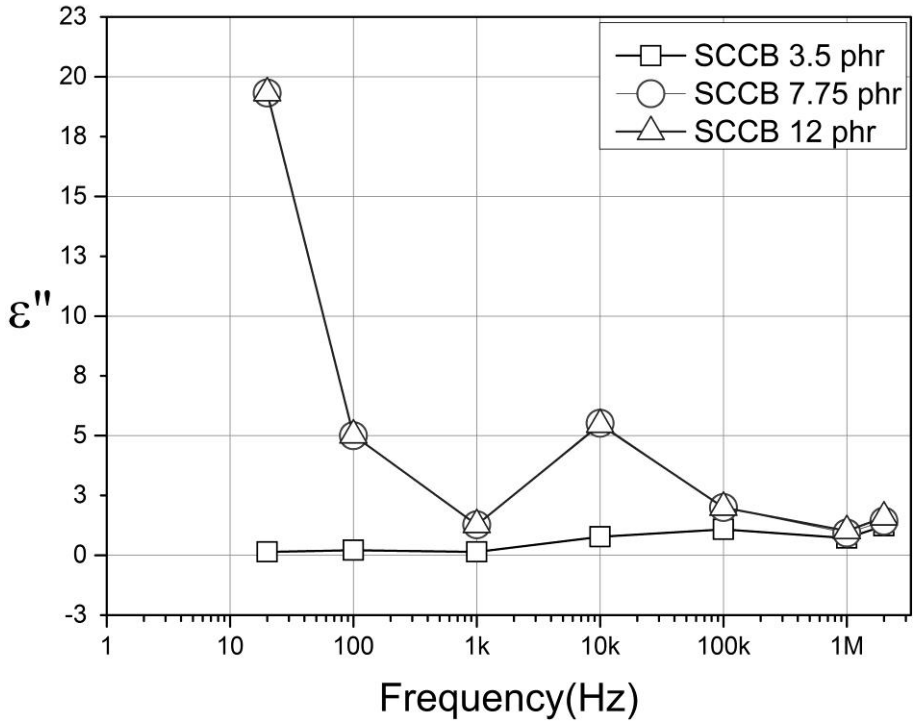

Figure 3.44 Characteristic response of dielectric loss as a function of frequency for CDC composites

The variation of dielectric loss with frequency for the CDC composites is shown in Figure 3.44. It is observed that composites with filler loading of 7.75 phr and above show similar trends. Relaxation peaks as well as dielectric loss are predominant in these filler loadings as compared with 3.5 phr composites. As evident from literature relaxation peaks move towards lower frequency with increasing filler loading from 3.5 to 7.75 phr. However, this trend is not seen from 7.75 to 12 phr increase in filler loadings. Dielectric loss increases to a maximum of 19.3 at 20 Hz for 7.75 phr and beyond filler loadings. The maximum dielectric loss for 3.5 phr is 1.2 at 2 MHz frequency. The dielectric losses increase with increased SCCB filler as also with decreasing frequency. This is a typical characteristic of conductive filler composites.

Effective resistivity

Main effects and interactions plot for effective resistivity of conductive filler composites are shown in Figures 3.45 and 3.46 respectively. Effective resistivity of the CDC composites depends primarily on the loading of the conductive filler, while other factors have negligible effects on the same. With the increase in conductive filler loading the conductive paths increase thus reducing the effective resistivity of the composites. Also, no substantial interaction effects are observed for the factors, suggesting that conductive fillers contribute substantially to the effective resistivity as compared to other processing factors.

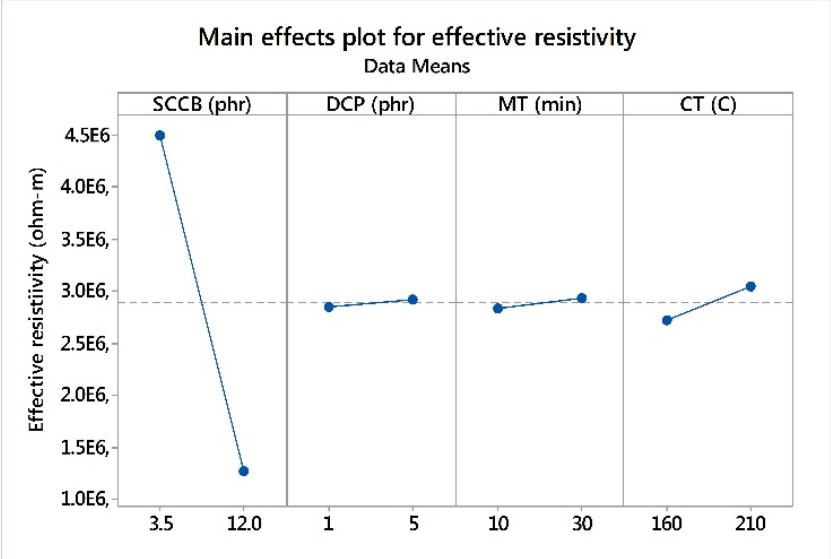

Figure 3.45 Main effects plot for effective resistivity of CDC composites

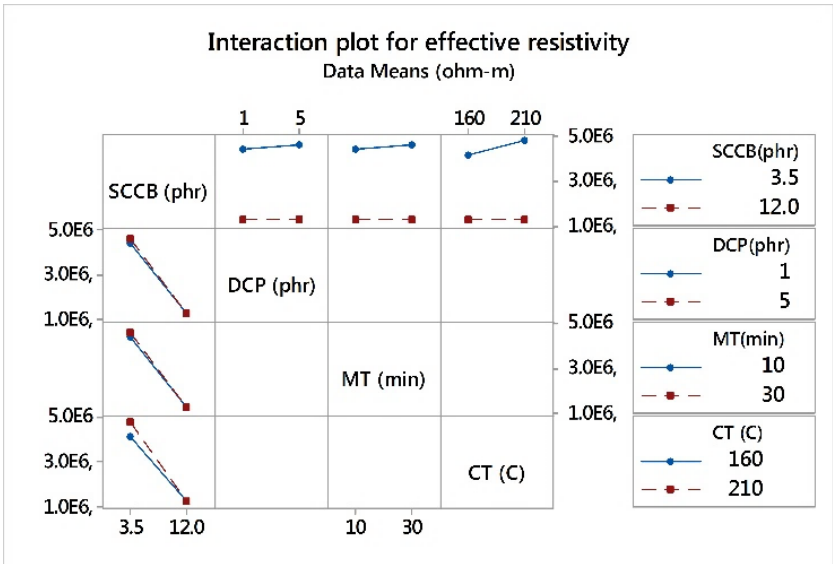

Figure 3.46 Interactions plot for effective resistivity of CDC composites

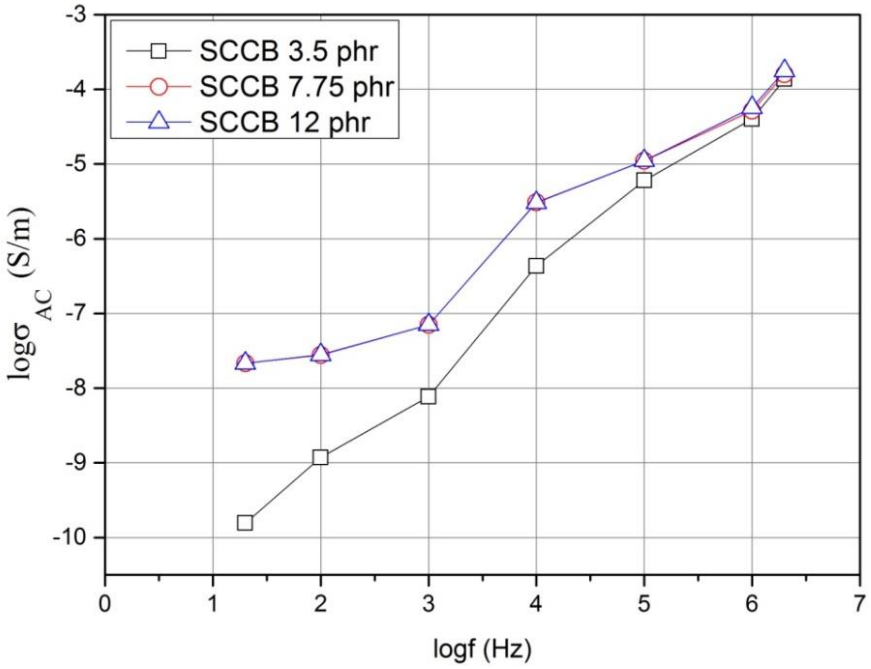

Figure 3.47 Characteristic response of AC conductivity as a function of frequency for CDC composites

Variation of AC conductivity with frequency for the CDC composites is shown in Figure 3.47. Composites with filler loadings of 7.75 phr and above show similar trends. Two distinct slopes are evident from the figure. A lesser slope for frequencies upto 1 kHz, while other with increased slope beyond 1 kHz. Composite with filler loading of 3.5 phr shows lower σ_{AC} as expected with conductive fillers. The lowest recorded σ_{AC} was around 1.6E-10 S/m for 3.5 phr while it was 2.1E-10 S/m for 7.75 phr and above at 20 Hz. The highest σ_{AC} observed was around 1.4E-04, 1.6E-04 and 1.8E-04 S/m for 3.5 phr, 7.75 phr and 12 phr filler loadings respectively for these composites at 2MHz.

The values of exponent of AC universality law range between 0.82 to 1 for different filler loading (Table 3.11). The conductivity is proportional to frequency at high frequencies due to the capacitance of the host medium between the fillers. At lower frequencies, the charge carriers drift over large distances, while these distances are reduced at higher frequencies. Hopping mode of conduction is characterized when exponent lie between 0 and 1. Lower conductivity is observed at lower frequencies for

the composites with conductive fillers. Also, lower filler content enables lower charge transport losses in the composites.

Table 3-11 Exponent of AC universality law of CDC composites

Exponent	**3.5 (phr)**	**7.75 (phr)**	**12 (phr)**
s	1	0.82	0.82

3.2.4 Electromechanical properties

Electromechanical properties of the CDC composites namely, electromechanical, piezoresistive and piezo capacitive sensitivity are presented.

Electromechanical sensitivity characterization

Table 3.12 shows the electromechanical sensitivity (β) of CDC composites obtained as per L_8 Taguchi orthogonal array. Electromechanical sensitivity varies from 0.89E-3 $(kPa)^{-1}$ for solid silicone rubber to 1.44E-3 $(kPa)^{-1}$ for the sample with 12 phr conductive filler, cured at higher temperature with lower curing agent.

Table 3-12 Electromechanical sensitivity of CDC composites

SCCB (phr)	**DCP (phr)**	**MT (min)**	**CT (°C)**	**β (E-3) $(kPa)^{-1}$**
3.5	1	10	160	0.44
3.5	5	10	210	0.98
3.5	5	30	160	0.39
3.5	1	30	210	0.39
12	1	30	160	1.16
12	5	30	210	0.82
12	5	10	160	0.55
12	1	10	210	1.44

From the analysis of results obtained for electromechanical sensitivity, it is observed that it improves with increasing conductive filler, reducing curing agent, reducing mixing time and increasing curing temperature (Figure 3.48). However, interactions exist among all the factors (Figure 3.49).

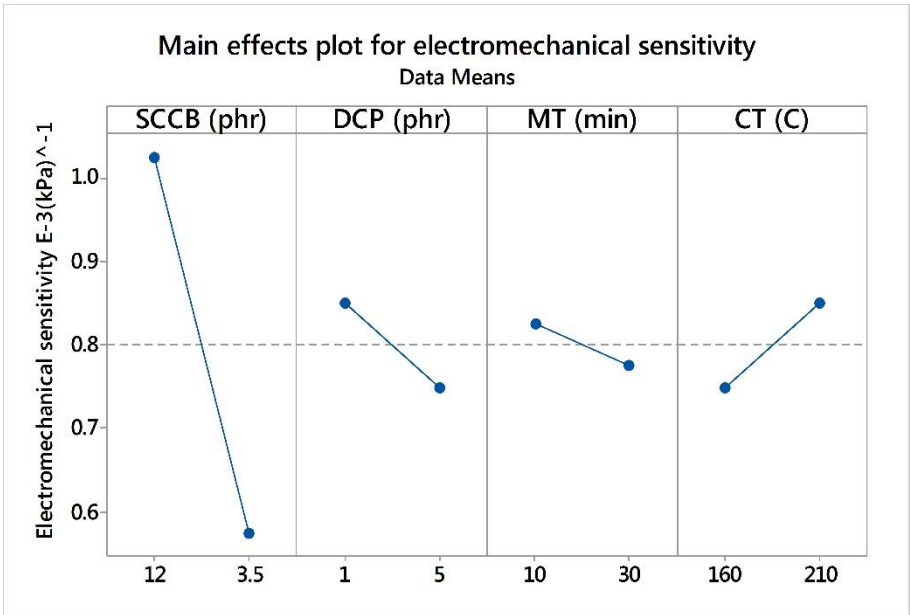

Figure 3.48 Main effects plot for electromechanical sensitivity of CDC composites.

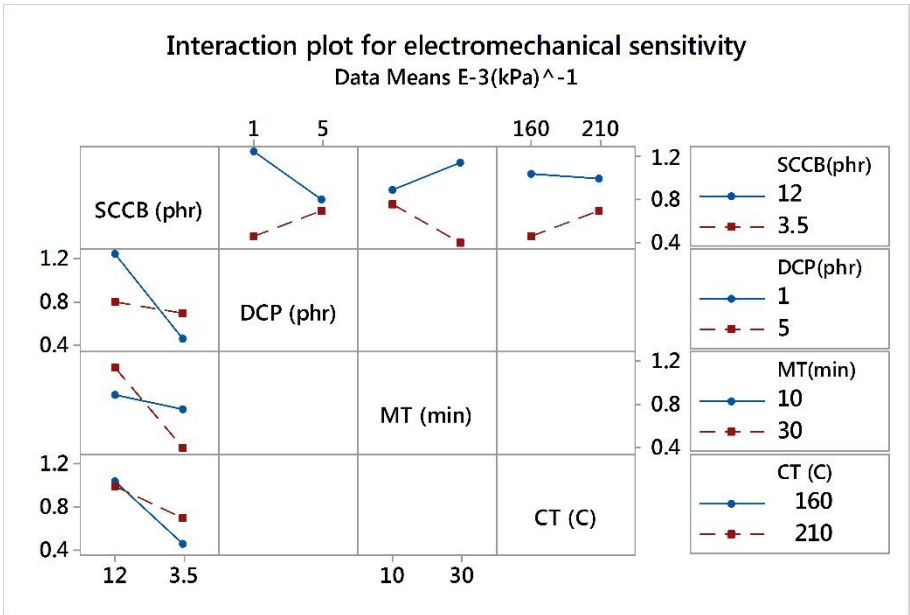

Figure 3.49 Interactions plot for electromechanical sensitivity of CDC composites.

Piezoresistive characterization

Resistance across the composite specimens varies with the pressure applied; the increase or decrease in resistance values depends on the specific composite compositions(Ding et al. 2019). In the literature it is observed that electrically conducting polymer composites under uniaxial compression showed increase of resistance with pressure, while resistance of thin PP films decreased with increasing pressure(Aneli et al. 1999).

In this study it is observed that the resistance decreases with increasing pressure, for all the compositions, indicating the predominance of electron transport mechanism. The resistance of the composite is the sum of resistance offered across conductive fillers and that of the matrix. In the case of uniaxial compression as in pressure sensing, the conductive fillers are brought near to each other thereby reducing the hopping path between them and consequently the resistance decreases.

Figure 3.50 shows the plot of normalized resistance change with pressure applied. ΔR is the resistance change across the composite sample at a particular pressure, while R_0 is the initial resistance at no pressure.

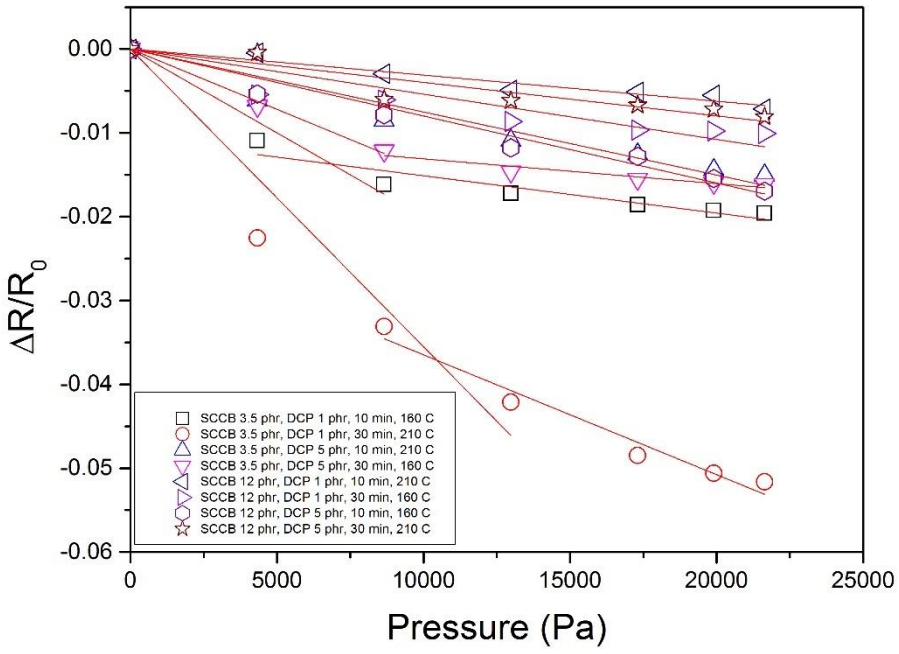

Figure 3.50 Piezoresistive characteristics of CDC composites

The piezoresistive sensitivity is obtained from Figure 3.50 as slopes of the linear fit of the curves and tabulated in Table 3.13. Main effects and interactions plot for piezoresistive sensitivity are shown in Figure 3.51 and Figure 3.52.

Table 3-13 Piezoresistive sensitivity of CDC composites

SCCB (phr)	DCP (phr)	MT (min)	CT (°C)	Piezoresistive sensitivity (E-3) $(kPa)^{-1}$
3.5	1	10	160	2.00
3.5	1	30	210	3.55
3.5	5	10	210	0.75
3.5	5	30	160	1.44
12	1	10	210	0.31
12	1	30	160	0.54
12	5	10	160	0.80
12	5	30	210	0.40

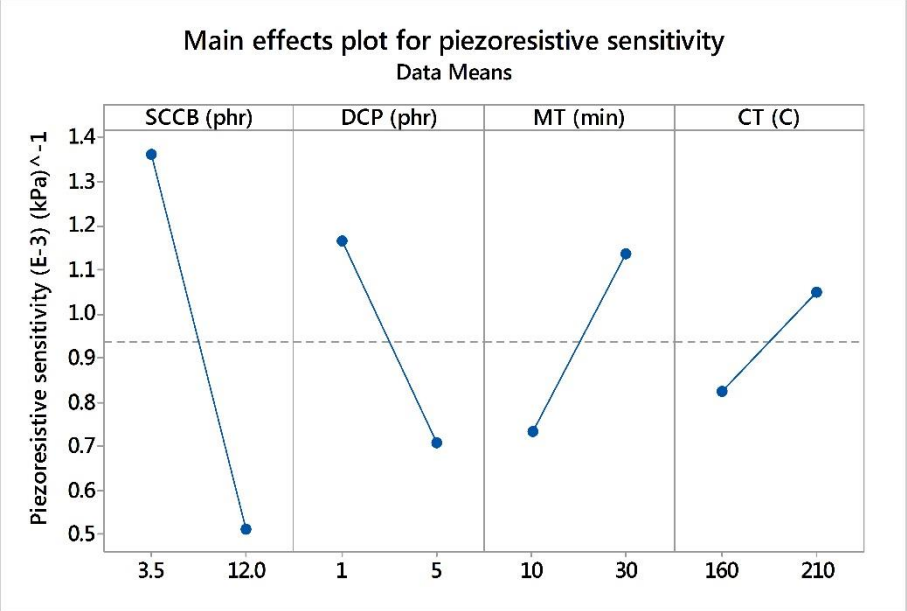

Figure 3.51 Main effects plot for piezoresistive sensitivity of CDC composites

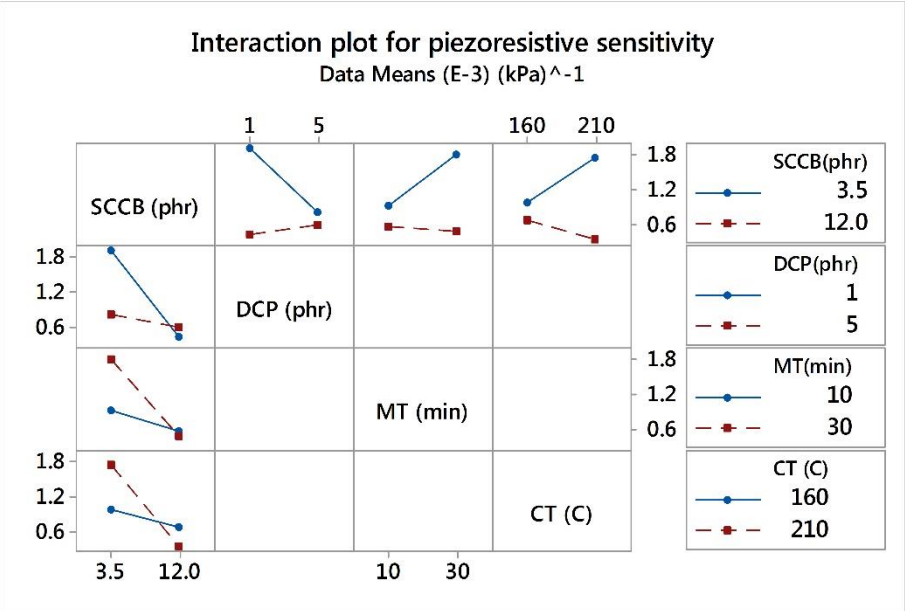

Figure 3.52 Interactions plot for piezoresistive sensitivity of CDC composites

The piezoresistive sensitivity for the composites can be improved by lowering the conductive filler and curing agent loadings, while increasing the mixing time and the curing temperature. However, interactions among the factors exist that influence the overall effect on the piezoresistive sensitivity.

Piezo capacitive characterization

The piezo capacitance effect can be visualized by the capacitance equation of a parallel plate capacitor. The capacitance increases with permittivity, area and decreases with thickness of the composite. With the application of pressure, thickness of the sample reduces thereby increasing the capacitance across the same. Samples with various compositions are characterized for piezo capacitive properties. Figure 3.53 shows the normalized capacitance change with applied pressure for the various compositions. Linearity is retained up to pressures of 9 kPa, beyond which the sensor sensitivity reduces to being almost horizontal. Thus, the CDC composites can effectively sense the change in pressure up to 9 kPa.

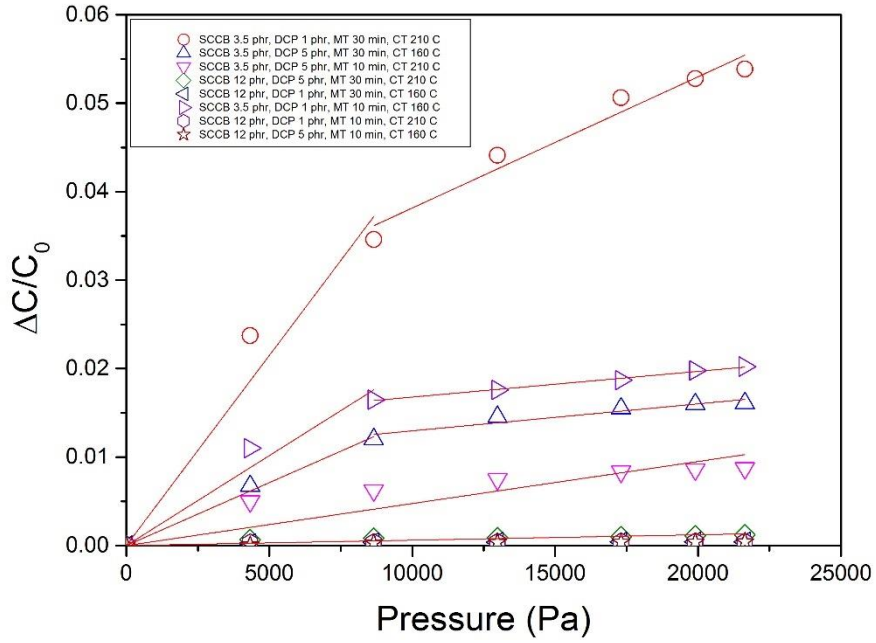

Figure 3.53 Piezo capacitive characteristics of CDC composites

The piezo capacitive sensitivity presented in the Table 3.14 are evaluated for pressures up to 9 kPa (linear range of curve). From the table (Table 3.14) it is observed that the composite with the following composition (SCCB 3.5 phr, DCP 1 phr, 30 minutes mixing time (MT) and 210 °C curing temperature (CT)) achieved the highest value of piezo capacitive sensitivity.

Table 3-14 Piezo capacitive sensitivity of CDC composites

SCCB (phr)	DCP (phr)	MT (min)	CT (°C)	Piezo capacitive sensitivity (E-3) $(kPa)^{-1}$
3.5	1	30	210	4.30
3.5	5	30	160	1.42
3.5	5	10	210	0.47
12	5	30	210	0.06
12	1	30	160	0.02
3.5	1	10	160	2.03
12	1	10	210	0.02
12	5	10	160	0.02

Taguchi analysis is carried out for the piezo capacitive sensitivity values of the composites and the main effects and interaction plots of the factors affecting the sensitivity are plotted as in Figure 3.54 and Figure 3.55. From the main effects plot it is clear that sensitivity of the composites can be maximized when the factor level settings are: Lower amount of conductive filler and curing agent, higher curing temperature and mixing times. From the interactions plot, interactions among the factors are seen, hence factors interact among themselves for the sensitivity response.

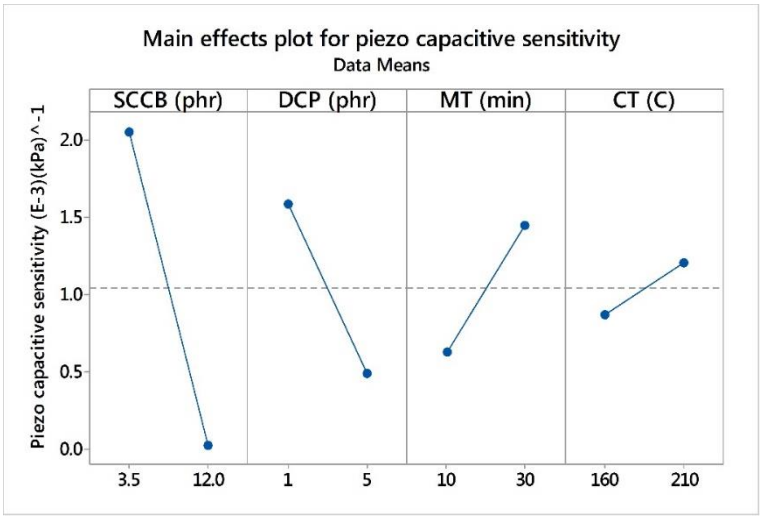

Figure 3.54 Main effects plot for piezo capacitive sensitivity of CDC composites

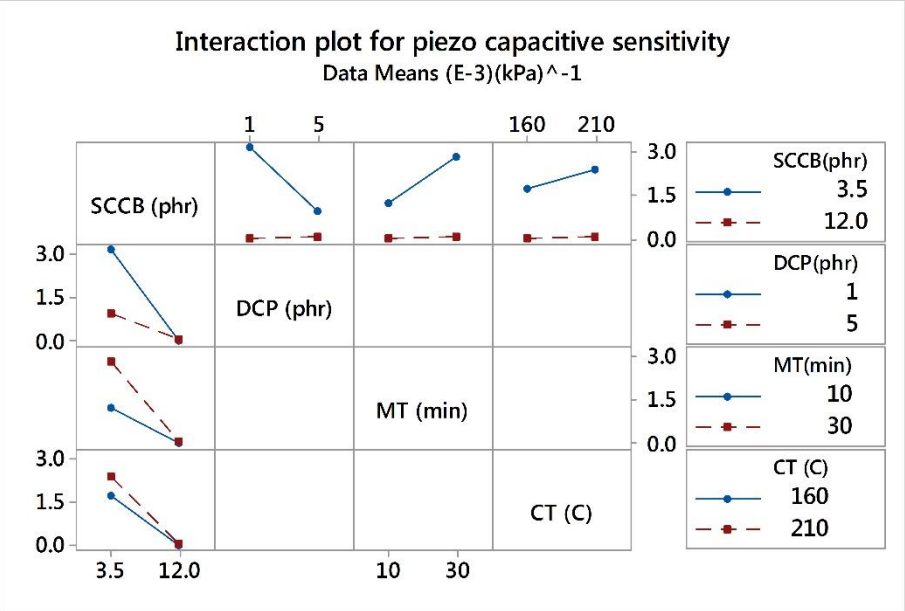

Figure 3.55 Interactions plot for piezo capacitive sensitivity of CDC composites

3.3 Conductive-Dielectric Filler Composites

Conductive-dielectric filler composites (CDDC) are fabricated using Ketjenblack 300J and barium titanate as the conductive and dielectric filler respectively into the solid silicone rubber dielectric matrix. These composites are tested for physical, mechanical, dielectric and electromechanical properties. Property-processing relationships are determined for each of the two factors. Factors include conductive and dielectric filler loading. Each of these factors are investigated at three levels, to obtain the L_9 Taguchi orthogonal array giving nine different combinations of factors. Thus, nine different composite samples are tested for each of the above properties. The results are then presented as main effects and interaction plots.

3.3.1 Physical properties

The density and SEM characterization of the CDDC composites are presented.

Density

Table 3.15 shows the density of CDDC composites as per L_9 Taguchi orthogonal array.

Table 3-15 Density of CDDC composites

BT (phr)	SCCB (phr)	Density (Kg/m^3)
3.5	3.5	1204
3.5	7.75	1155
3.5	12	1102
7.75	3.5	1067
7.75	7.75	1100
7.75	12	1209
12	3.5	1100
12	7.75	1350
12	12	1343

From the main effects plot for density (Figure 3.56) it is observed that contribution of BT filler to density dramatically improves after 7.75 phr dielectric filler loading, whereas it increases with conductive filler for loading upto 7.75 phr. This signifies the

existence of synergy between the dielectric and conductive fillers. However, contribution of the dielectric filler towards density is larger as compared to that from conductive filler. Large interactions among the factors towards density are observed (Figure 3.57).

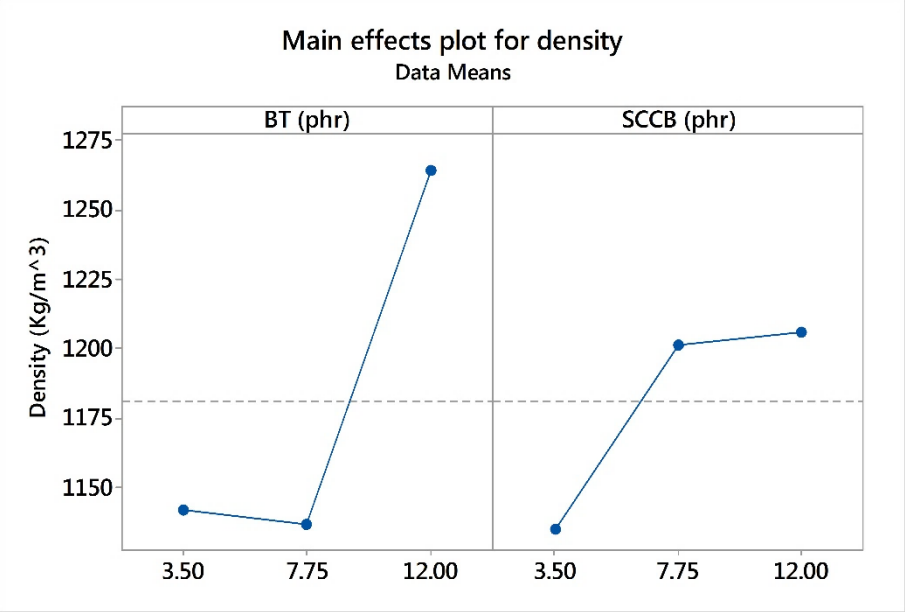

Figure 3.56 Main effects plot for density of CDDC composites

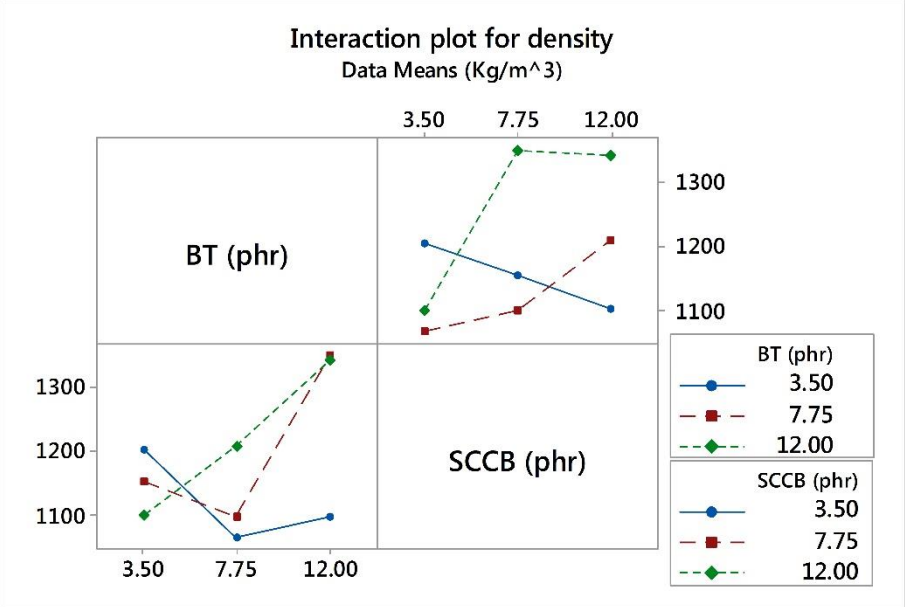

Figure 3.57 Interactions plot for density of CDDC composites

SEM Characterization

Figures 3.58, 3.59 and 3.60 shows the SEM micrographs of the CDDC composites with filler loadings of both SCCB and BT each at 3.5, 7.75 and 12 phr loading respectively. The micrographs show that both fillers are evenly distributed for all the loadings, without any agglomeration. This is on account of lower filler loadings, the high viscous solid silicone rubber matrix and the roll mixing process adopted for dispersion. Lower filler content offers better dispersion and are prone to agglomeration only when BT and SCCB filler concentration are high(González et al. 2017). Also, as the filler concentrations are lower, better wetting and thereby coating by the matrix elastomer is visible. This also contributes to improved particle matrix interactions, which reflects in improved Young's modulus. Due to roll milling, homogeneous dispersion of the fillers is obtained, suggesting that this process is suitable for production of CDDC composites.

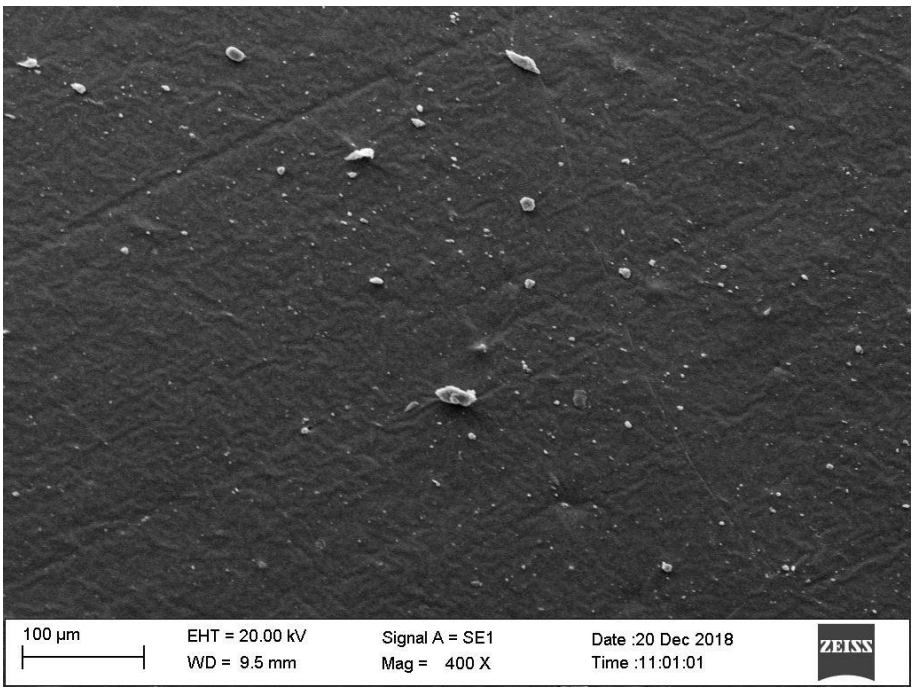

Figure 3.58 SEM micrographs for 3.5 phr CDDC composites

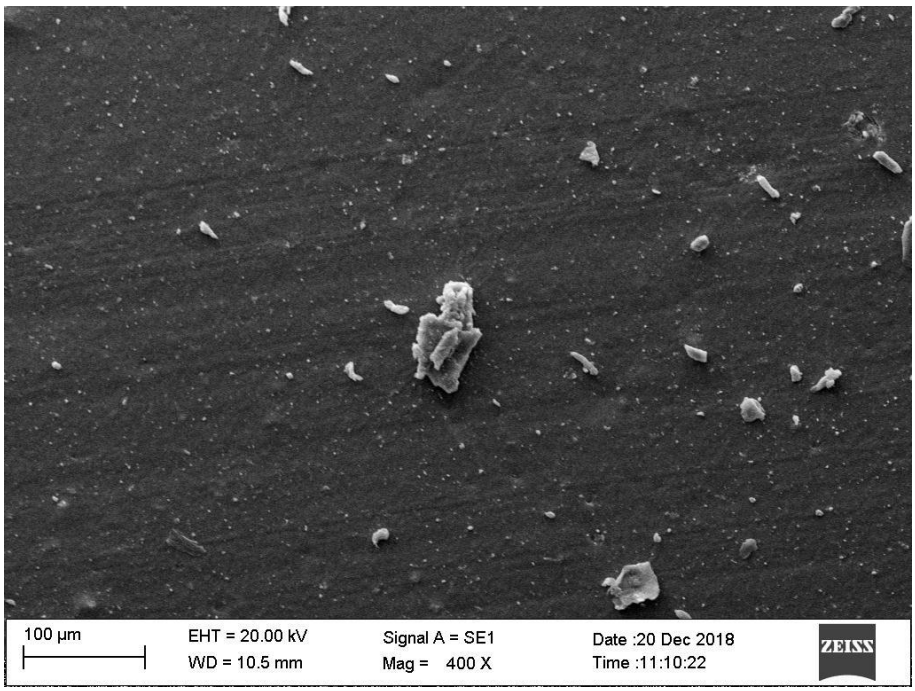

Figure 3.59 SEM micrographs for 7.75 phr CDDC composites

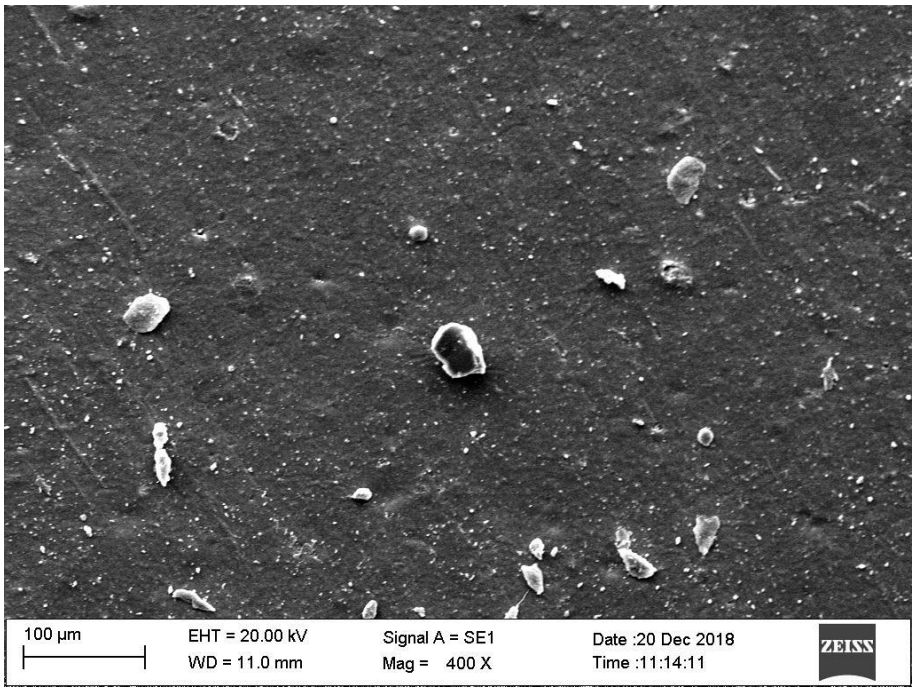

Figure 3.60 SEM micrographs for 12 phr CDDC composites

3.3.2 Mechanical properties

Mechanical properties of the CDDC composites as per L_9 Taguchi orthogonal array is presented in Table 3.16.

Table 3-16 Mechanical properties of CDDC composites

BT (phr)	SCCB (phr)	Young's modulus (MPa)	Shore A Hardness
3.5	3.5	7.2	55
3.5	7.75	10.1	67
3.5	12	12.3	70
7.75	3.5	10.1	58
7.75	7.75	12.4	69
7.75	12	13.1	75
12	3.5	7.2	56
12	7.75	12.2	70
12	12	15.3	76

Young's modulus

Young's modulus of the composites sees a rise compared to DDC, indicating that the conductive carbon filler is more reinforcing than the dielectric filler. As in the case of DDC, the linearity is maintained up to 30 % strain (Figure 3.61).

Young's modulus increases with conductive fillers as is also seen in literature. However, in these composites at a given SCCB filler loading Young's modulus shows an increase with BT fillers initially which subsequently decreases with increasing BT filler loading (Figure 3.62). The decrease in Young's modulus from 7.75 phr BT loading is on account of the enlargement in packing volume fraction of the fillers as the particles are of different sizes(Zhao et al. 2013b). This is in contrast to observations made by Zhao et. al.(Zhao et al. 2013b) who observed that Young's modulus initially decreased with carbon black and then subsequently increased, while it increased with increase in BT loading. The differences in behavior is attributed to acetylene carbon black as against ketjenblack, which has a different structure and

conductivity. Secondly, they investigated very high weight fractions of BT filler (from 23 to 60 phr) in their work as compared to low weight fractions of up to 12 phr in our work. Also, the matrix material was room temperature vulcanized as against the HTV high molecular weight solid silicone rubber used for the present study. In our study, the Young's modulus shows an increase with increasing SCCB filler. Increase in insertion of SCCB particles builds the SCCB network, increasing the Young's modulus. Interactions among fillers at SCCB loadings of 7.75 and 12 phr are evident from Figure 3.63.

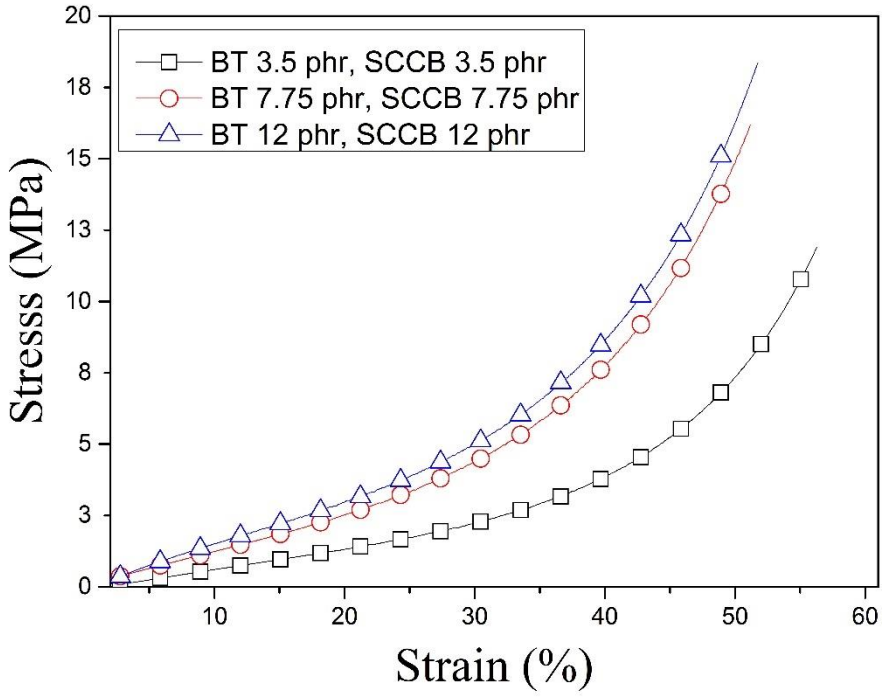

Figure 3.61 Stress strain plots of CDDC composites

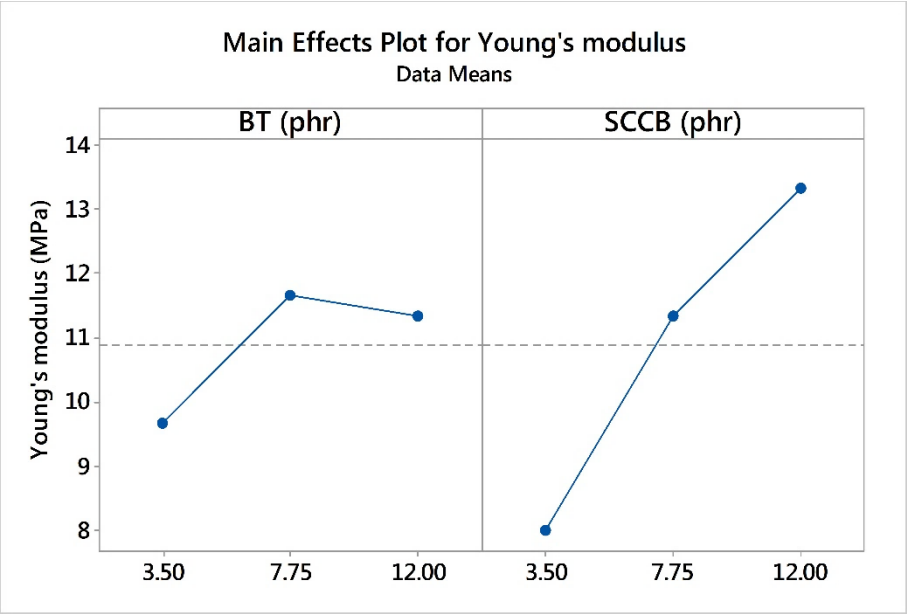

Figure 3.62 Main effects plot for Young's modulus of CDDC composites

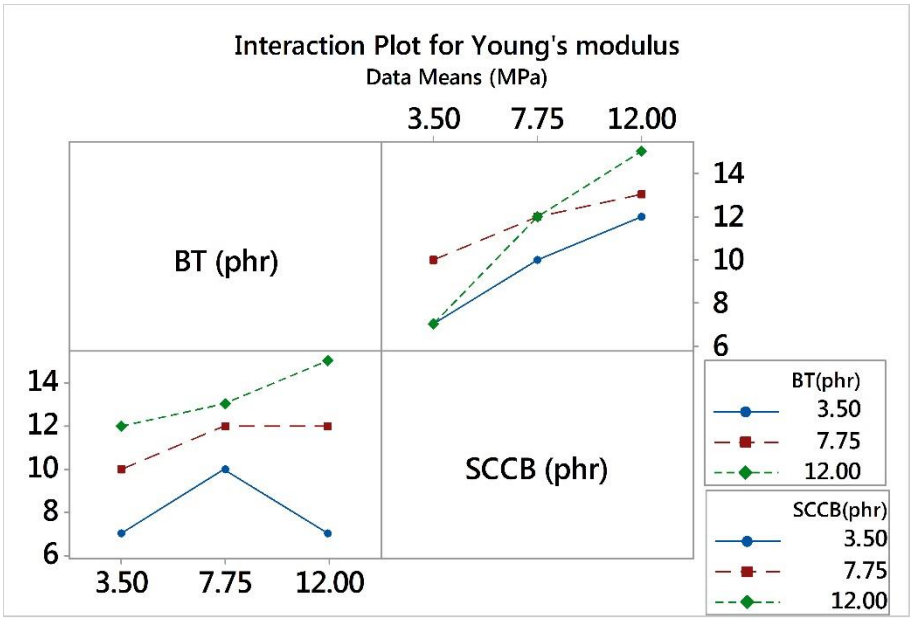

Figure 3.63 Interactions plot for Young's modulus of CDDC composites

Hardness

With the addition of fillers, Shore A hardness increases to 76. From Figure 3.64 it can be observed that both the conductive and dielectric fillers contribute to the hardness of the CDDC composites, increasing with increasing filler content. The contribution of conductive filler being larger compared to that of dielectric filler, indicating that the conductive filler hardens the composite more than dielectric filler, as carbon black is well known for this property. The contribution of dielectric filler towards increasing

hardness plateaus out beyond 7.75 phr loading, for all levels of conductive filler loadings. The interactions between filler and matrix is responsible for the restriction in the mobility of polymer molecules leading to an increase in hardness. No significant interaction is observed among the fillers (Figure 3.65).

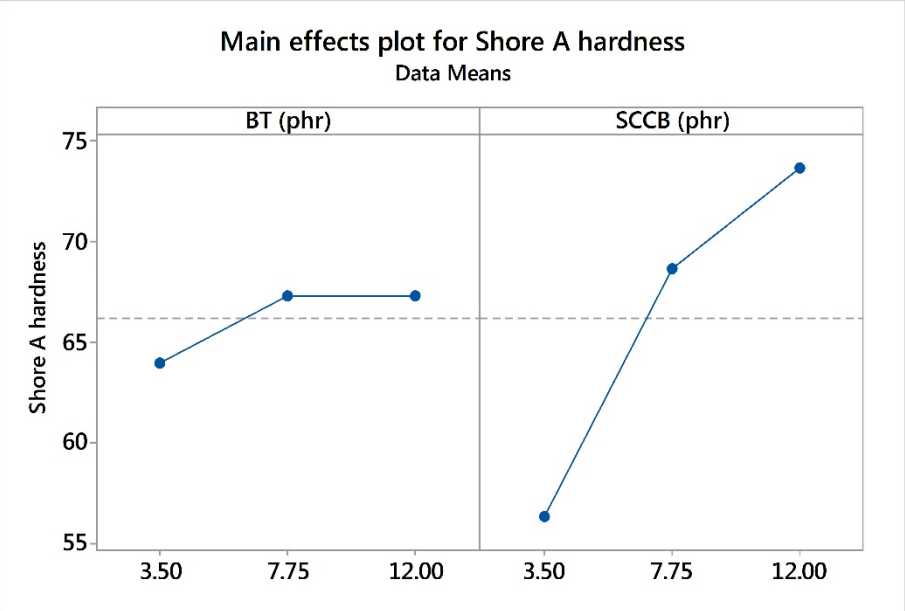

Figure 3.64 Main effects plot for shore A hardness of CDDC composites

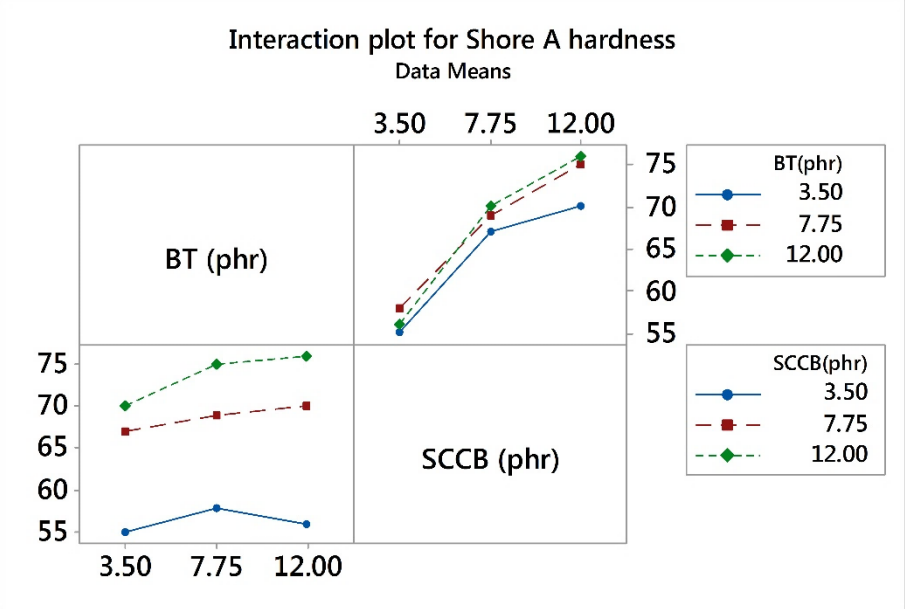

Figure 3.65 Interactions plot for shore A hardness of CDDC composites

3.3.3 Dielectric properties

The dielectric properties for the CDDC composites are recorded at 1 kHz and presented in Table 3.17.

Table 3-17 Dielectric properties of CDDC composites as per L_9 orthogonal array

BT (phr)	SCCB (phr)	Permittivity @ 1kHz	Dielectric loss	Effective resistivity @ 1kHz (Ω-m)
3.5	3.5	12.0	1.80	1491500
3.5	7.75	14.1	1.12	1280836
3.5	12	14.0	1.12	1271287
7.75	3.5	10.5	1.50	1704571
7.75	7.75	14.1	1.12	1271870
7.75	12	14.1	1.12	1279097
12	3.5	10.5	1.65	1585371
12	7.75	14.1	1.12	1280385
12	12	14.1	1.12	1278164

Permittivity

Permittivity is seen to vary from 10.5 to 14.1, while the dielectric loss varies from 1.12 to 1.80. Interactions among the conductive and dielectric fillers play an important role in the CDDC composites(Yao et al. 2008). In the region of the filler polymer interactions for CDDC composites, the contact is a combination of mechanical and chemisorptions processes. While the conductive and dielectric particles are wetted in the polymer, the cross linking ensures that they are entrapped physically and chemically adsorbed by the cross-linked polymers.

The permittivity of the conductor-dielectric composites improved as compared to the pure solid silicone rubber. This is on account of the conductive filler that provides interfacial polarization to the composites. This effect of increasing permittivity with low concentrations of conductive filler is called Maxwell-Wagner polarization, seen on account of interface between materials having widely different permittivity values. The dielectric loss shows greater values as expected from these composites due to the

conductive nature of the filler. The existence of BT fillers hinders the network formed between SCCB particles(Zhao et al. 2013b). With the CDDC, which is also referred to as three component composites in literature, a network of micro capacitors is formed by polymer, SCCB and BT. The interfaces increase with the increase of BT loading. Hence permittivity increases as compared with DDC composites. Also, the dielectric loss increases with the increasing concentration of BT as conductive paths increase. It can be seen that for 3.5 phr BT loading the permittivity increased 4 times as that with DDC for same BT loading.

The permittivity initially decreases slightly with BT up to 7.75 phr, which subsequently increases with BT filler as seen from Figure 3.66, which is in contrast to Zhao et.al.(Zhao et al. 2013b) who reported the reverse behavior for carbon black-BT nanocomposites. The differences in behavior is attributed to acetylene carbon black as against ketjenblack, which has a different structure and conductivity. Secondly, they investigated very high weight fractions of BT filler (from 23 to 60 phr) in their work as compared to low weight fractions of up to 12 phr in our work. Also, the matrix material was room temperature vulcanized as against the HTV high molecular weight solid silicone rubber used for the present study. In the present study the behavior of permittivity with SCCB fillers shows an initial steep increase followed by decrease, beyond 7.75 phr loading. This behavior can be explained by the interactions among network structures formed by dielectric and conductive fillers along with the type of matrix elastomer. With the addition of BT up to 7.75 phr, it prevents charge buildup among SCCB fillers thereby reducing the Maxwell-Wagner polarization, hence showing a decrease in permittivity. Probably at higher BT filler loadings the SCCB particles are forming more compact network(Poikelispää et al. 2016) thus improving the permittivity. From Figure 3.67, it can be observed that interactions among the fillers exist for SCCB loadings of 7.75 and 12 phr respectively.

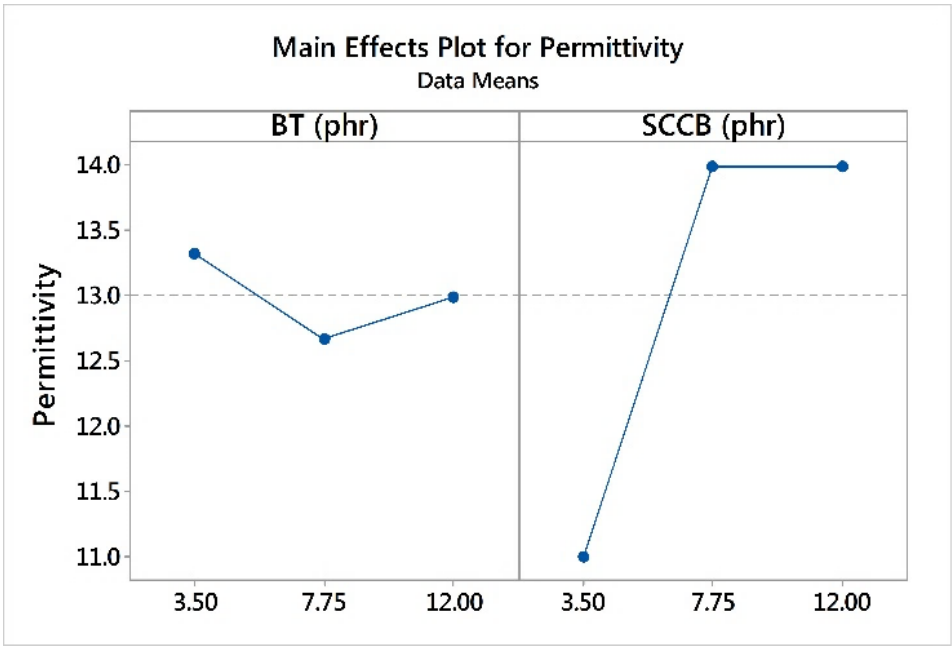

Figure 3.66 Main effects plot for permittivity of CDDC composites

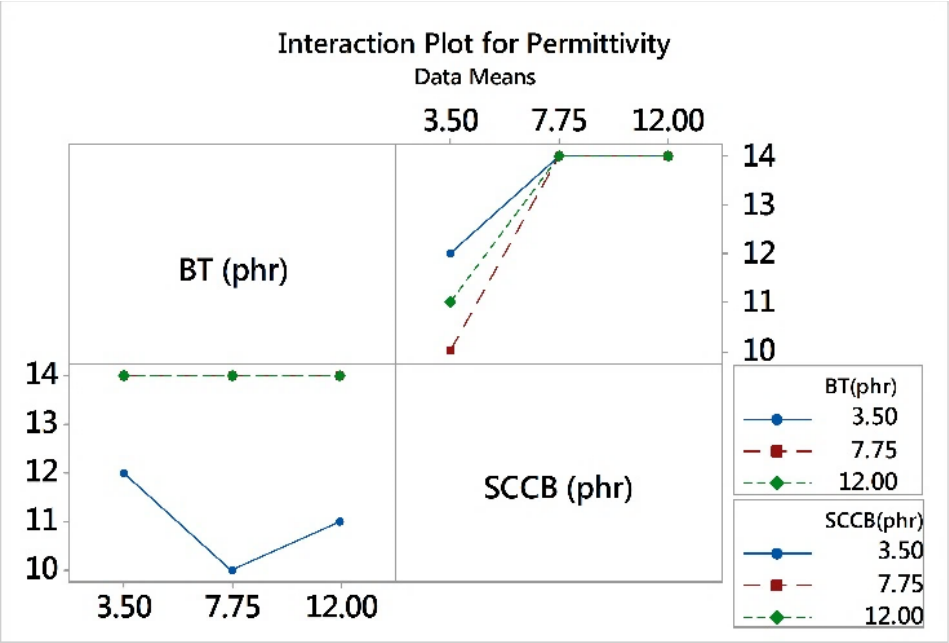

Figure 3.67 Interactions plot for permittivity of CDDC composites

Figure 3.68 shows the variation of permittivity with frequency for the CDDC composites for three different filler loadings. It can be observed that permittivity decreases with frequency for all filler loadings. In contrast to CDC composites, the decrease for all filler loadings of CDDC composites show similar trends. This indicates that in CDDC composites relaxation behaviour does not change with filler

loadings. Polarization does not show significant increase with increased filler loadings for CDDC composites. Permittivity increases with reducing frequency and reaches a maximum value of 42 at 20 Hz frequency for 3.5 phr filler loading. It increases to 46 for 7.75 and 12 phr filler loadings. It is seen that permittivity reduces to 0.5 at 2 MHz frequency for 3.5 phr filler loading while it reduces to 0.3 for 7.75 phr and beyond.

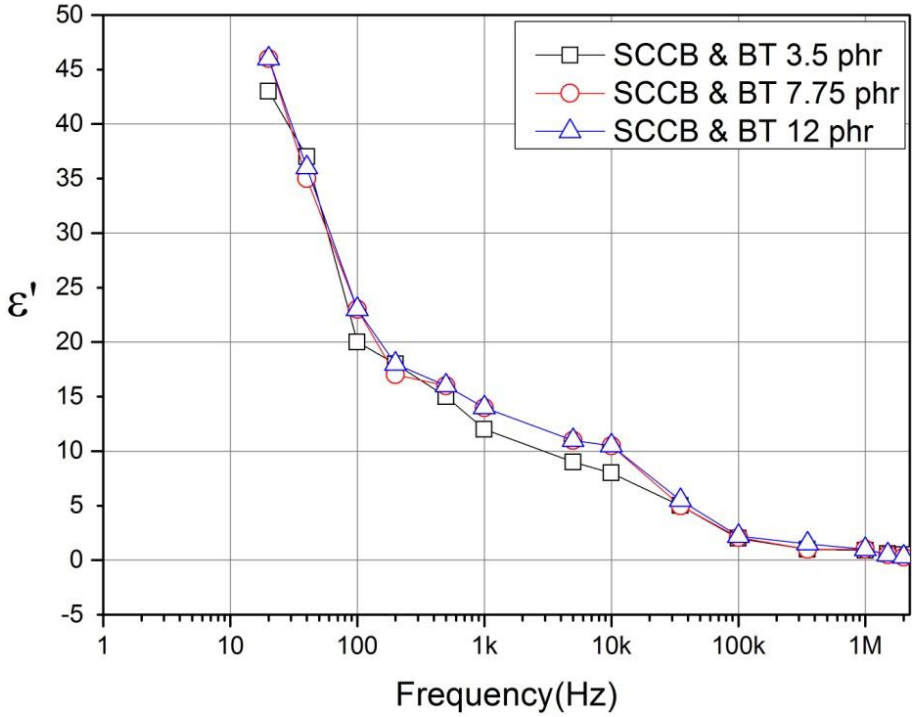

Figure 3.68 Characteristic response of permittivity as a function of frequency for CDDC composites

At low frequencies the relaxation times are greater, hence an increase in permittivity is observed due to increased mobility of charge carriers(Iacob et al. 2014). The relaxation time corresponding to Maxwell-Wagner effect is very small, hence this mechanism does not affect the permittivity of the composite at higher frequencies(Zhang et al. 2014). Yao et. al. observed rapid decrease of permittivity with frequency for three phase composites with BT filler at 0.15 volume fraction, while at other filler loadings this variation was not remarkable(Yao et al. 2008). They attributed this increase in permittivity at lower frequencies to Maxwell-Wagner relaxation mechanisms.

Dielectric loss

The main effects and interactions plot for dielectric loss of CDDC composites are shown in Figures 3.69 and 3.70 respectively. Influence of dielectric filler loading towards dielectric loss is negligible as compared with conductive filler loading. Increasing amount of conductive filler actually sees a reduction in dielectric loss. This is on account of the synergistic interactions among the dielectric and conductive fillers above 3.5 phr loading. However, from 7.75 to 12 phr conductive filler loading the dielectric loss remains constant. Interactions plot also suggests a different behaviour at conductive filler loading of 3.5 phr.

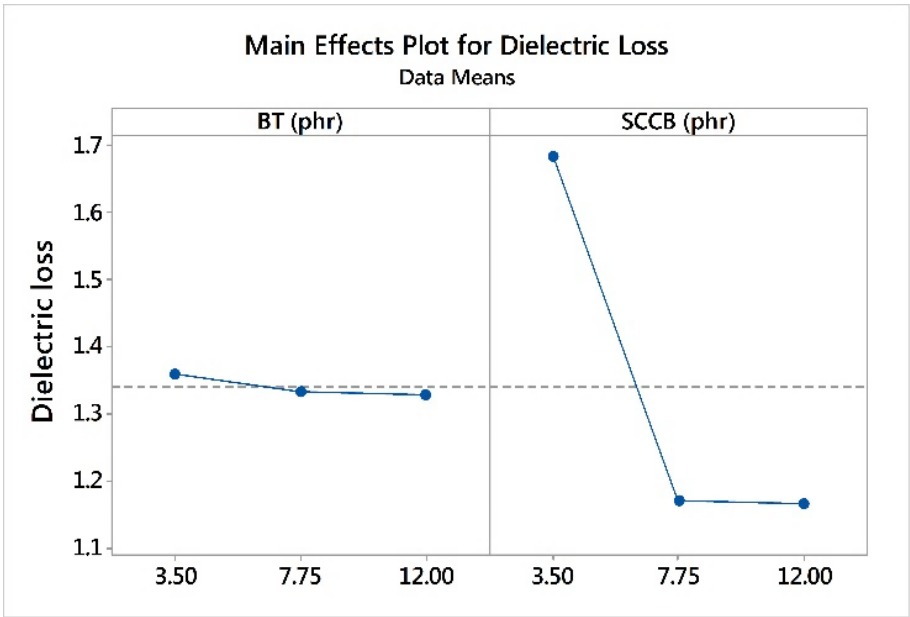

Figure 3.69 Main effects plot for dielectric loss of CDDC composites

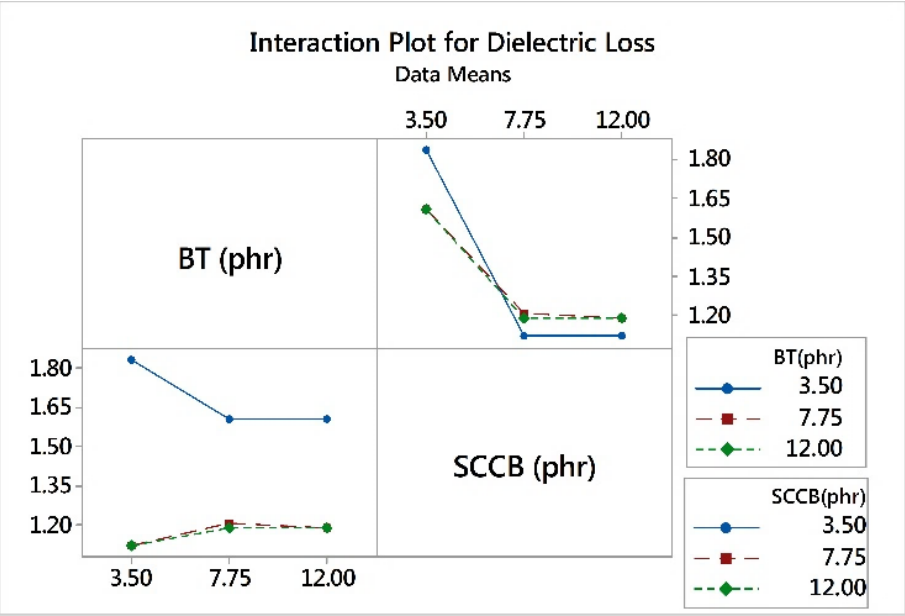

Figure 3.70 Interactions plot for dielectric loss of CDDC composites

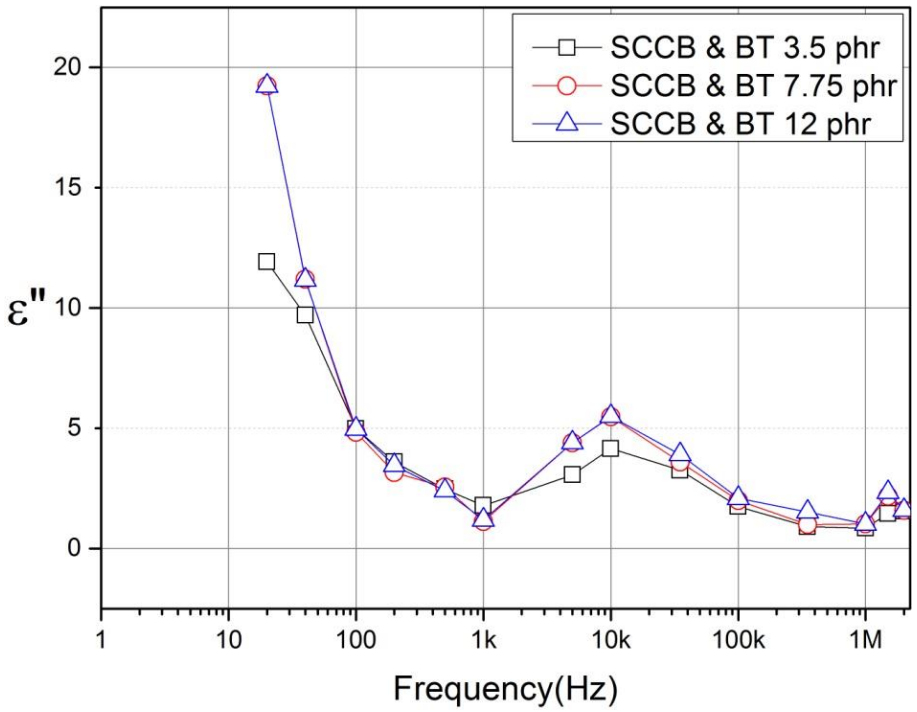

Figure 3.71 Characteristic response of dielectric loss as a function of frequency for CDDC composites

The variation of dielectric loss with frequency for the CDDC composites is shown in Figure 3.71. It is observed that composites with filler loading of 7.75 phr and above

show similar trends. Relaxation peaks as well as dielectric loss are predominant in these filler loadings as compared with 3.5 phr composites. All filler loadings have relaxation peaks appearing at the same frequency unlike as seen in literature that move towards lower frequency with increasing filler loading(Gallone et al. 2010). Dielectric loss increases to a maximum of 10.9 at 20 Hz for 3.5 phr and 19.2 at 20 Hz for filler loadings of 7.75 and 12 phr. The losses decrease with increase in frequency suggesting that conductive fillers have a dominant role as compared to the dielectric fillers even at same filler loadings.

Effective resistivity

HTV solid silicone rubber matrix is an insulator with effective resistivity of 6.3E6 Ω-m. With the addition of conductive fillers, the effective resistivity of the composites decreases and it can become conducting. To be dielectric the effective resistivity of the material should be in the range(Poikelispää et al. 2016) of 10^6 Ω-m. SCCB loading drastically lowers the effective resistivity of the composites. However, the effective resistivity of the CDDC composites with both types of fillers even at higher level loading is still in the insulator regime. Main effects plot for effective resistivity of the CDDC composites is shown in Figure 3.72. It is observed that for a given SCCB filler loading, the effective resistivity initially increases with BT fillers up to 7.75 phr and then decreases with further BT loading. As the BT filler loading increases, the effective resistivity improves for the CDDC composites. However, after a threshold of 7.75 phr along with the SCCB fillers they form charge carrier networks, hence the reduction in effective resistivity. Whereas for a given BT filler loading the effective resistivity of the composite drastically decreases with SCCB filler up to around 7.75 phr, beyond which it shows an increasing trend. The dielectric fillers interrupt the possible percolation paths created by SCCB filler beyond 7.75 phr BT loading, reducing the leakage current. Hence synergistic interaction among the conductive and dielectric fillers is observed on the effective resistivity of the CDDC composites (Figure 3.73).

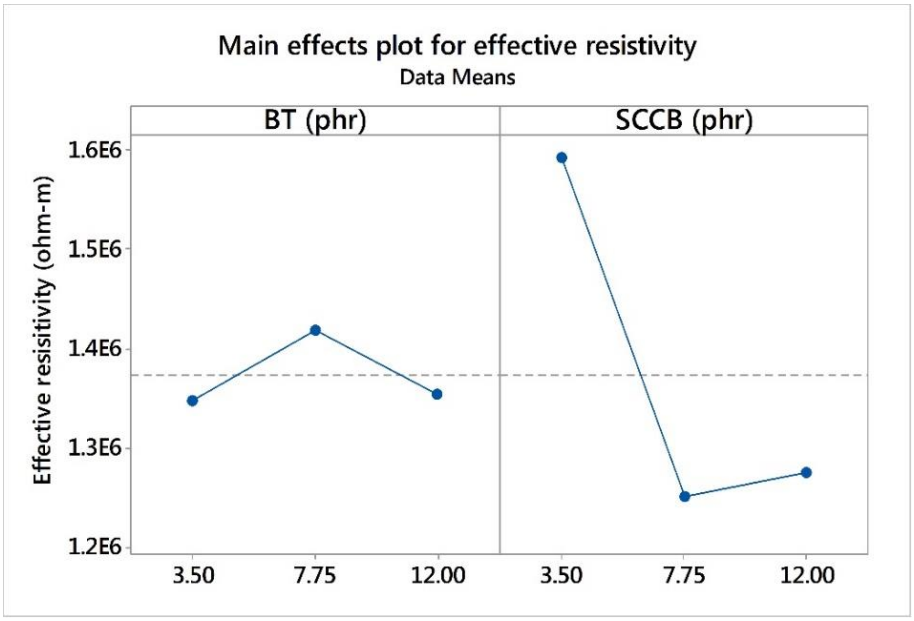

Figure 3.72 Main effects plot for effective resistivity of CDDC composites

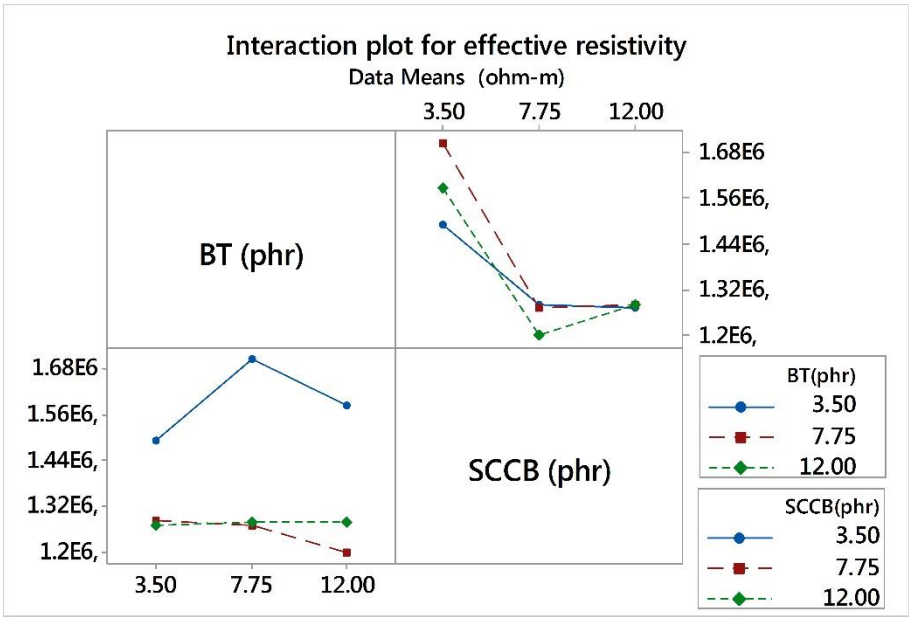

Figure 3.73 Interactions plot for effective resistivity of CDDC composites

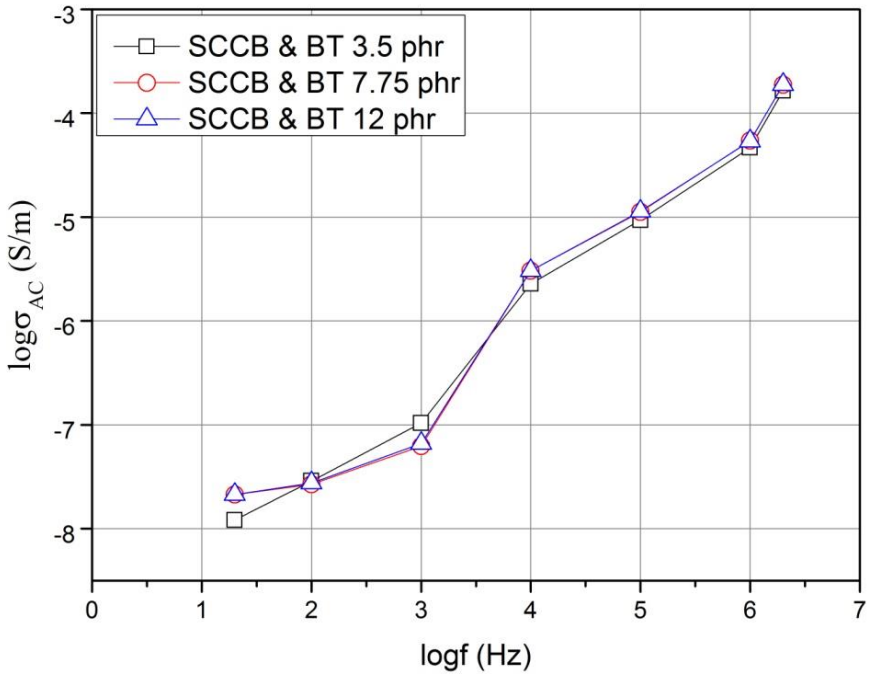

Figure 3.74 Characteristic response of AC conductivity as a function of frequency for CDDC composites

Variation of AC conductivity with frequency for the CDDC composites is shown in Figure 3.74. Composites with filler loadings of 7.75 phr and above show similar trends. Two distinct slopes are evident from the figure. A lesser slope for frequencies upto 1 kHz, while other with increased slope beyond 1 kHz. Even though the conductivity values of 3.5 and 7.75 phr composites are different at lower frequencies, however they achieve nearly same values at higher frequencies for these composites. The lowest recorded σ_{AC} was around 2.9E-08 S/m for these composites at 100 Hz and the highest σ_{AC} was around 1.7E-04 S/m at 2MHz for these composites. The slope of the linearly fitted curve for the experimental data provides the value of the exponent of the AC universality law. It is observed that the value of the exponent (Table 3.18) remains constant at 0.83 even for varying amounts of both conductive and dielectric fillers, suggesting that frequency exponent is independent of the filler loadings. The conduction mechanism is frequency dependent with the value of exponent being lesser than 1. Hence hopping model of conduction mechanism explains the AC conductivity observed in these composites(Güler et al. 2019).

Table 3-18 Exponent of AC universality law of CDDC composites

Exponent	**3.5 (phr)**	**7.75 (phr)**	**12 (phr)**
s	0.83	0.83	0.83

3.3.4 Electromechanical properties

Electromechanical properties of the CDDC composites namely; electromechanical, piezoresistive and piezo capacitive sensitivity are presented.

Electromechanical sensitivity characterization

The electromechanical sensitivity(β) of the CDDC composites is shown in Table 3.19, as per L_9 orthogonal array. It is seen that electromechanical sensitivity varies from 0.93E-3 $(kPa)^{-1}$ to 1.79E-3 $(kPa)^{-1}$ for the given range of filler loadings. When compared with either the DDC or CDC composites, CDDC composites provide greater electromechanical sensitivity for the same level of filler loadings. This is on account of synergistic interactions among the fillers.

Table 3-19 Electromechanical sensitivity of CDDC composites

BT (phr)	**SCCB (phr)**	**β (E-3) $(kPa)^{-1}$**
7.75	7.75	1.12
12	12	0.93
3.5	7.75	1.40
3.5	3.5	1.79
12	7.75	1.16
12	3.5	1.79
7.75	12	1.05
7.75	3.5	1.10
3.5	12	1.16

Main effects plot as shown in Figure 3.75, indicates the significance of the factors on electromechanical sensitivity of CDDC composites. It initially decreases with increase

in dielectric filler loading till 7.75 phr. Beyond 7.75 phr, electromechanical sensitivity increases with dielectric filler loading till 12 phr. Electromechanical sensitivity however continues to decrease with increasing conductive filler loading.

Interactions among the conductive and dielectric behaviours is evident from Figure 3.76. For dielectric filler loadings at 3.5 phr and 12 phr, decrease of conductive filler loading improves electromechanical sensitivity. However, with dielectric filler loading at 7.75 phr, electromechanical sensitivity first registers an increase and then a decrease with increasing conductive filler loadings.

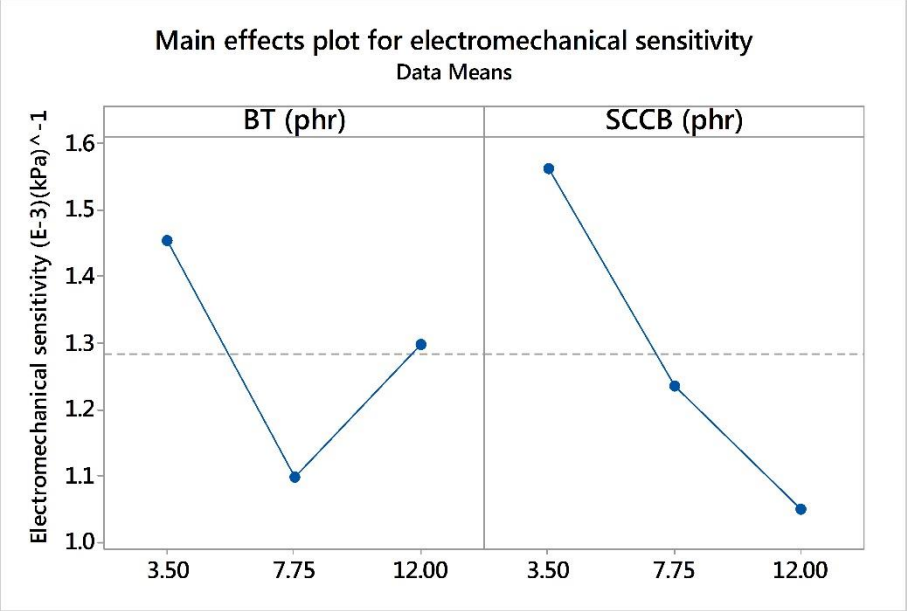

Figure 3.75 Main effects plot for electromechanical sensitivity of CDDC composites

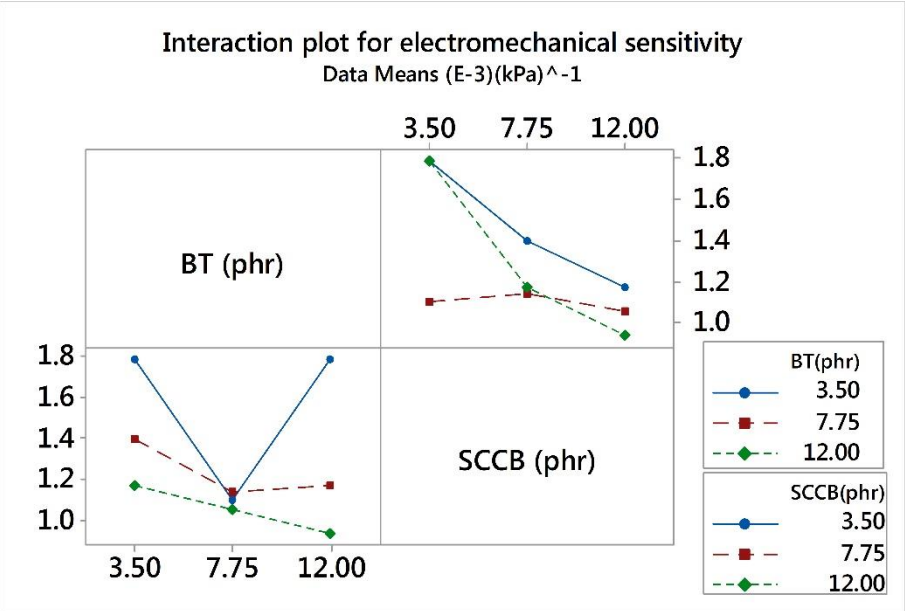

Figure 3.76 Interactions plot for electromechanical sensitivity of CDDC composites

Piezoresistive characterization

Results of piezoresistive tests for CDDC composites are shown in Figure 3.77. For each of the composites, normalized resistance change is plotted as a function of applied pressure. Linear fit is performed for each of the curves for obtaining the value of piezoresistive sensitivity. From the figure it is observed that a good linear fit is achieved in the pressure ranges tested, indicating the suitability of materials for pressure sensor applications. Negative piezo resistance of the composites is observed. The distance between conductive carbon black particles changes under the influence of pressure, reducing the density of the particles per unit area of composite. The conduction through the composite is mainly determined by the conductive paths formed by the carbon particles, interlaced by BT particles Also, the electrons jump across the gap of carbon particles as described by the tunnelling effect. As pressure is applied on the composite, the volume of composite is compressed thereby, SCCB volume fraction increases. So, the elastic polymer matrix deforms to the extent that conductive filler particles are forced closer together to form conduction paths, resulting in reduction of resistance. Hence either new conductive paths are formed or the resistance of the effective conductive path's decreases, giving rise to negative piezoresistive effect.

The resistivity of carbon particles is very less as compared to the dielectric filler and solid silicone rubber. So upon compression and subsequent reduction in the inter particle gap, the tunneling effect occurs, that lead to the formation of conductive path(Luheng et al. 2007), thereby a reduction in resistance of the composite with increase in pressure.

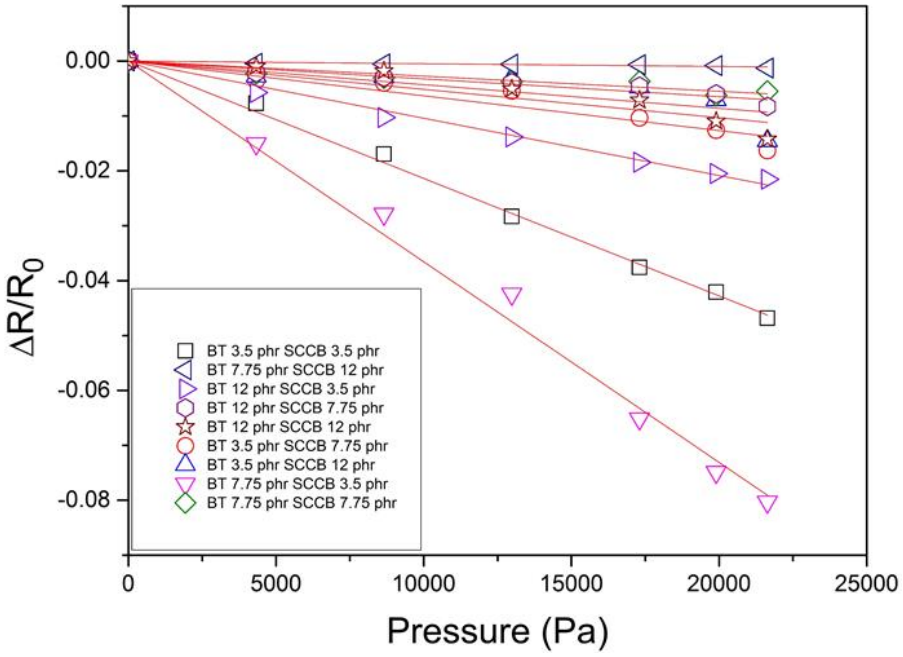

Figure 3.77 Piezoresistive characteristics of CDDC composites

Table 3-20 Piezoresistive sensitivity of CDDC composites

BT (phr)	**SCCB (phr)**	**Piezoresistive Sensitivity (E-3) (kPa)$^{-1}$**
3.5	3.5	2.14
3.5	7.75	0.63
3.5	12	0.43
7.75	3.5	3.70
7.75	7.75	0.28
7.75	12	0.05
12	3.5	1.04
12	7.75	0.32
12	12	0.52

Piezoresistive sensitivity are obtained from the slopes of the linearly fitted curves to the Figure 3.77 and they are tabulated in Table 3.20. Variation in piezoresistive sensitivity of these composites is from 0.05E-3 to 3.70E-3 $(kPa)^{-1}$ which compares well with the sensitivity of 6.4E-3 $(kPa)^{-1}$ reported for micro structured PR sensors(Santos et al. 2019). Maximum sensitivity is achieved for the composite composed of 7.75 phr BT and 3.5 phr SCCB. The improvement in resistance ratio for CDDC composites is due to the interaction of Ketjenblack and BT fillers in silicone rubber matrix.

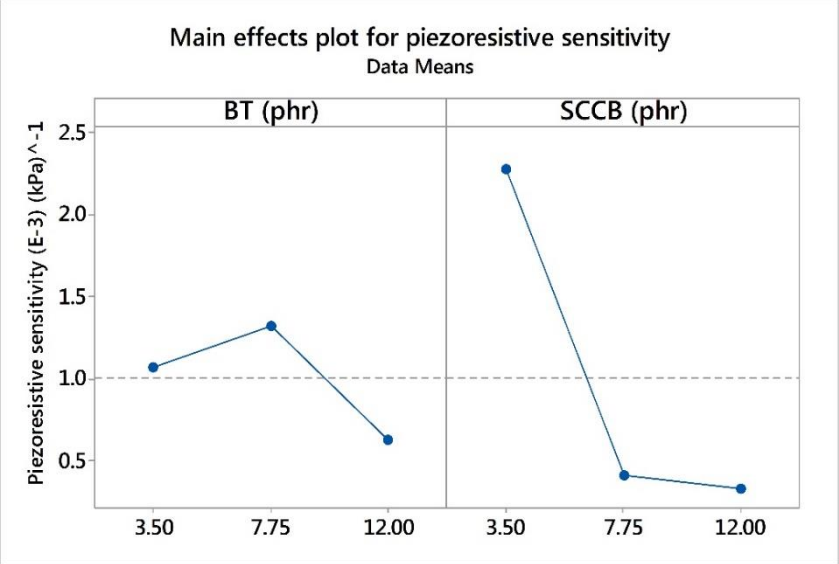

Figure 3.78 Main effects plot for piezoresistive sensitivity of CDDC composites

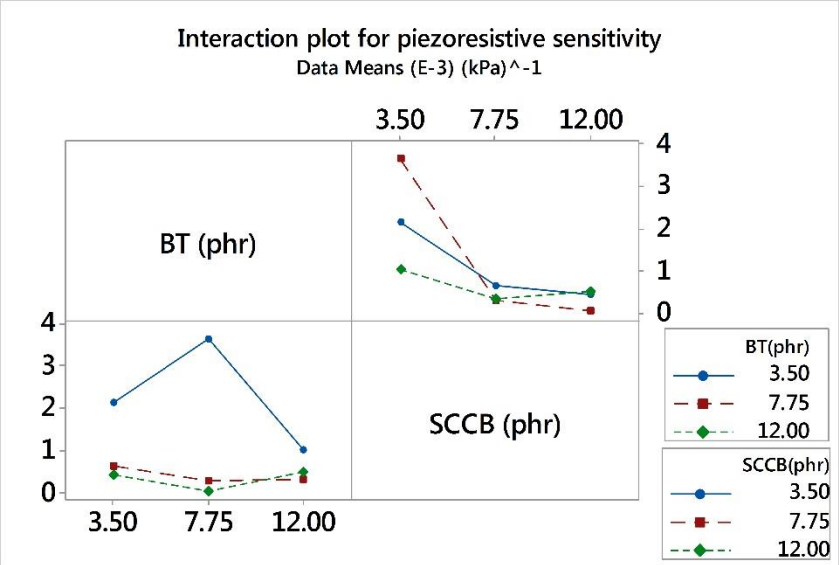

Figure 3.79 Interactions plot for piezoresistive sensitivity of CDDC composites

From the main effects plot (Figure 3.78), it is observed that sensitivity continuously improves with decrease in SCCB filler loading, while decreasing filler loading of BT up to 7.75 phr. Further reduction in BT shows a fall in sensitivity. This is explained on account of interactions among the conductive and dielectric fillers. With increase of dielectric filler, the resistance decreases at a lesser rate as compared to the resistance decrease for the same amount for conductive filler. Also loading of dielectric fillers interrupt the conductive channels that are formed by SCCB fillers.

The interaction plot for the CDDC composites (Figure 3.79) shows that 3.5 phr SCCB filler shows greater interaction as compared to other loading. Hence piezoresistive sensitivity is a maximum at 3.5 phr SCCB with 7.75 phr BT loading. This interaction is on account of synergistic effect among the dielectric and conductive fillers.

Piezo capacitive characterization

For a pressure sensor, it is necessary to make a trade-off between piezo capacitive sensitivity and detection range(Maiolino et al. 2015). Improved sensitivity easies data processing by reducing the relative noise levels.

The capacitance of the CDDC composites is formed by a series of nano-capacitors that are developed within the composite on account of these conductor-dielectric filler dielectric matrix interactions. Upon pressure loading of the composite, the individual capacitances increases, thereby improving the overall capacitive effect of the composites, providing the positive piezo capacitive effects(Mei et al. 2015a).

Figure 3.80 shows the normalized capacitance change with pressure change for various CDDC samples as per the L_9 Taguchi orthogonal array. Linearity is an important characteristic to describe the static performance of pressure sensitive materials. The normalized capacitance change varies linearly with pressure change as is evident from the graph. The slope of these linearly fitted curves gives the sensor sensitivity up to 20 kPa as presented in Table 3.21. The maximum piezo capacitive sensitivity obtained for the CDDC samples is 3.92E-3 $(kPa)^{-1}$ for BT at 7.75 phr and SCCB at 3.5 phr weight fractions.

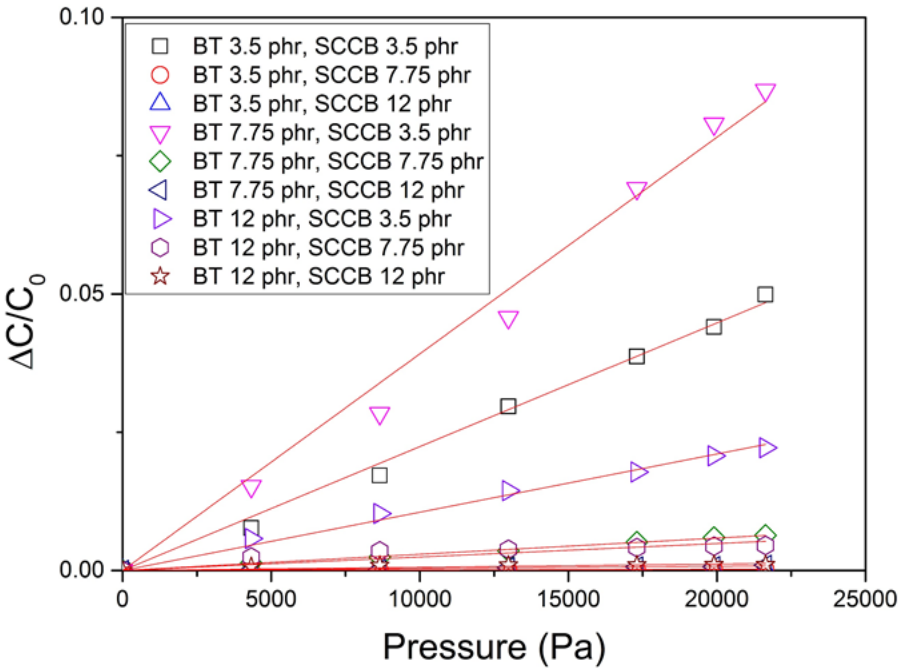

Figure 3.80 Piezo capacitive characteristics of CDDC composites.

Table 3-21 Piezo capacitive sensitivity of CDDC composites

BT (phr)	SCCB (phr)	Piezo capacitive sensitivity (E-3) $(kPa)^{-1}$
3.5	3.5	2.24
3.5	7.75	0.01
3.5	12	0.01
7.75	3.5	3.92
7.75	7.75	0.29
7.75	12	0.04
12	3.5	1.05
12	7.75	0.24
12	12	0.06

The sensor sensitivity data thus obtained are analyzed and results presented as main effects and interaction plots. Analysis of the results reveals that piezo capacitive sensitivity improves with decrease of SCCB filler loading. SCCB is a reinforcing filler for rubber, hence lower filler loadings will produce lesser elastic resistance,

however it also reduces permittivity. Hence from the Taguchi analysis, it is clear that reduction of elastic resistance is more profound than decrease in permittivity for SCCB filler, which reflects as improved piezo capacitive sensitivity (Figure 3.81). Hence lower SCCB filler loadings show improved piezo capacitive sensitivity. Another observation that can be made is improvement in sensitivity with reduction in SCCB from 12 to 7.75 phr is lower compared to that from 7.75 to 3.5 phr. This behavior is explained by the synergistic interaction among the dielectric and conductive fillers. This synergy is exploited by using conductive and dielectric fillers. A peculiar behavior is observed for effect of BT loadings, that is piezo capacitive sensitivity improves with BT loading for weight fractions up to 7.75 phr. Further loading of BT fillers leads to decrease in piezo capacitive sensitivity. At higher filler loadings of BT, the SCCB particles along with BT form a compact conducting network. Also, above 7.75 phr the reinforcing nature of BT is predominant over its contribution to permittivity.

Predominant interactions are observed for SCCB weight fraction at 3.5 phr (Figure 3.82).

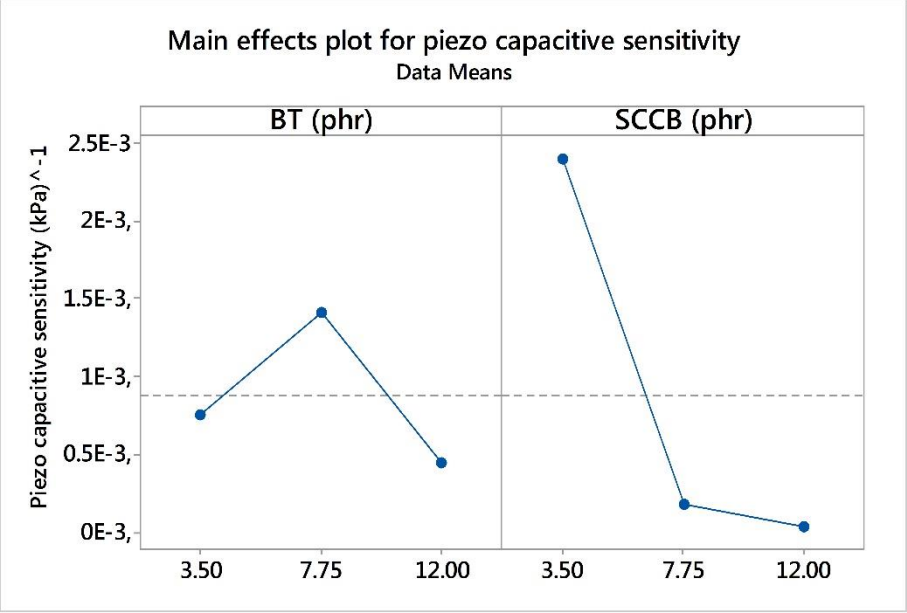

Figure 3.81 Main effects plot for piezo capacitive sensitivity of CDDC composites

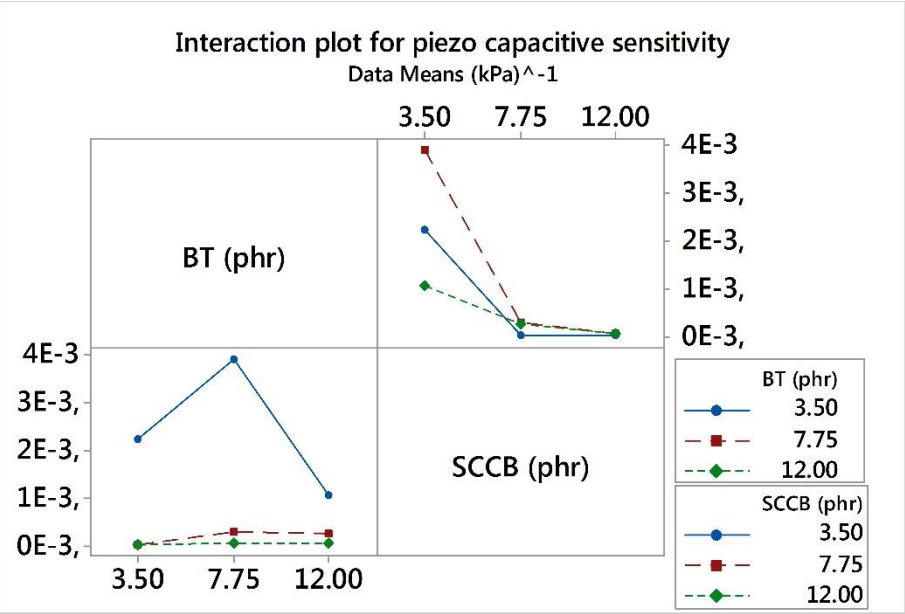

Figure 3.82 Interactions plot for piezo capacitive sensitivity of CDDC composites

Table 3-22 Piezo capacitive sensitivity values of unstructured capacitive sensors from literature

Author	Piezo capacitive sensitivity
Chen,2016(Chen et al. 2016)	0.0003 $(kPa)^{-1}$
Guo, 2016(Guo et al. 2016)	0.00025 $(kPa)^{-1}$
Cheng, 2017(Cheng et al. 2017)	0.0011$(kPa)^{-1}$
Fan,2017(Fan et al. 2017)	0.004 $(kPa)^{-1}$
Fan, 2018(Fan et al. 2018)	0.0036 to 0.029 $(kPa)^{-1}$
Liu,2018(Liu et al. 2018a)	0.0014 $(kPa)^{-1}$
This work	0.0039 $(kPa)^{-1}$

Table 3.22 compares the piezo capacitive sensitivity for unstructured piezo capacitive sensors from literature. From this data it is evident that the proposed HTV solid silicone rubber composites are promising candidates for capacitive sensor applications.

3.4 Confirmatory Tests

Once the trends for the solid silicone rubber composite material properties are investigated as above using the Taguchi analysis and reported as main effects and

interaction plots, confirmatory tests are carried out only for those factor combinations that provide the desired outcome for a given property. The properties that are sought to increase are permittivity, effective resistivity, electromechanical sensitivity, piezoresistive and piezo capacitive sensitivity. While properties such as dielectric loss, Young's modulus, density and Shore A hardness are desired to be decreased. Thus, for the DDC composites permittivity is maximum for the factor settings of 12 phr BT, 5 phr DCP, 10 minutes MT and 160°C curing temperature. The same combination of factors provides the maximum values for both piezoresistive and piezo capacitive sensitivity for the DDC composites as seen from Table 3.23.

Table 3-23 Confirmatory tests of DDC composites

BT (phr)	**DCP (phr)**	**MT (min)**	**CT (°C)**	**Property**	**Desired Value**
3.5	5	30	160	Density	1130 Kg/m^3 (Min.)
3.5	5	30	180	Young's modulus	2.70 MPa (Min.)
3.5	1	30	160	Shore A hardness	42 (Min.)
12	5	10	160	Permittivity	3.3 (Max.)
3.5	1	30	180	Dielectric loss	0.19 (Min.)
3.5	1	30	180	Effective resistivity	6.67E+6 Ω-m(Max.)
3.5	5	10	180	Electromechanical sensitivity	1.09E-3 $(kPa)^{-1}$ Max.)
3.5	1	30	180	Piezoresistive sensitivity	3.65E-3 $(kPa)^{-1}$ (Max.)
3.5	1	30	180	Piezo capacitive sensitivity	3.69E-3 $(kPa)^{-1}$ (Max.)

The confirmatory tests conducted on the CDC composites for those factor levels that provide the desired values for the properties are tabulated in Table 3.24. The combination of factors that give the desired value for permittivity are different from the combination of factors that give the best value for dielectric loss.

Table 3-24 Confirmatory tests of CDC composites

SCCB (phr)	DCP (phr)	MT (min)	CT (°C)	Property	Desired Value
3.5	5	30	210	Density	1070 Kg/m^3 (Min.)
3.5	1	30	210	Young's modulus	4.1 MPa (Min.)
3.5	1	10	160	Shore A hardness	57 (Min.)
12	1	10	160	Permittivity	14.1 (Max.)
3.5	1	30	210	Dielectric loss	0.11 (Min.)
3.5	5	30	210	Effective resistivity	4.87E+6 Ω-m(Max.)
12	1	10	210	Electromechanical sensitivity	1.44E-3 $(kPa)^{-1}$ (Max.)
3.5	1	30	210	Piezoresistive sensitivity	3.55E-3 $(kPa)^{-1}$ (Max.)
3.5	1	30	210	Piezo capacitive sensitivity	4.30E-3 $(kPa)^{-1}$ (Max.)

Similarly, the desired values of the properties obtained through confirmatory tests on the CDDC composites are tabulated in Table 3.25. Same combinations of factor settings provide the best values for both piezoresistive and piezo capacitive sensitivities.

Table 3-25 Confirmatory tests of CDDC composites

BT (phr)	SCCB (phr)	Property	Desired Value
7.75	3.5	Density	1067 Kg/m^3 (Min.)
3.5	3.5	Young's modulus	7 MPa. (Min.)
3.5	3.5	Shore A hardness	55 (Min.)
3.5	7.75	Permittivity	14.1 (Max.)
12	12	Dielectric loss	1.12 (Min.)
7.75	3.5	Effective resistivity	1.70E+6 Ω-m(Max.)
3.5	3.5	Electromechanical sensitivity	1.80E-3 $(kPa)^{-1}$ (Max.)
7.75	3.5	Piezoresistive sensitivity	3.70E-3 $(kPa)^{-1}$ (Max.)
7.75	3.5	Piezo capacitive sensitivity	3.94E-3 $(kPa)^{-1}$ (Max.)

3.5 Comparison of Performance

The earlier discussions were on the influence of factors such as filler and curing agent loading, mixing time and curing temperature on the various properties of composites. This section compares the DDC, CDC and CDDC composites on the basis of the influence of the filler type and filler loading on the properties of the composites. For this purpose, samples were fabricated by only varying filler and filler loading. While other factors such as curing agent loading, mixing time and curing temperature were fixed at 1 phr, 10 mins and 160 C respectively for each of these composites. Error bars of ± 1 SD is shown on these graphs for each of the properties compared.

Comparison of physical properties of composites

DDC composites provide higher density as compared to CDC composites on account of the structure of the ketjenblack fillers (Figure 3.83). CDDC provides the lowest density at a combination of conductive and dielectric fillers at 7.75 phr respectively. The slight decrease in density at 7.75 phr for CDDC composites is on account of the synergistic combination at this filler loading. The enlargement of packing density on account of different sized fillers is predominant at this loading. With further increase in filler loadings however, the density increases for CDDC composites. The increase in density of the composites with filler loading is corroborated in literature as seen for BT fillers (Ramajo et al. 2005) and Titania fillers (Nayak et al. 2013).

Also, the SEM micrographs of all the three types of composites show that uniform dispersion and good wetting are observed. This indicates that the fabrication process adopted is well suited for the production of these composites.

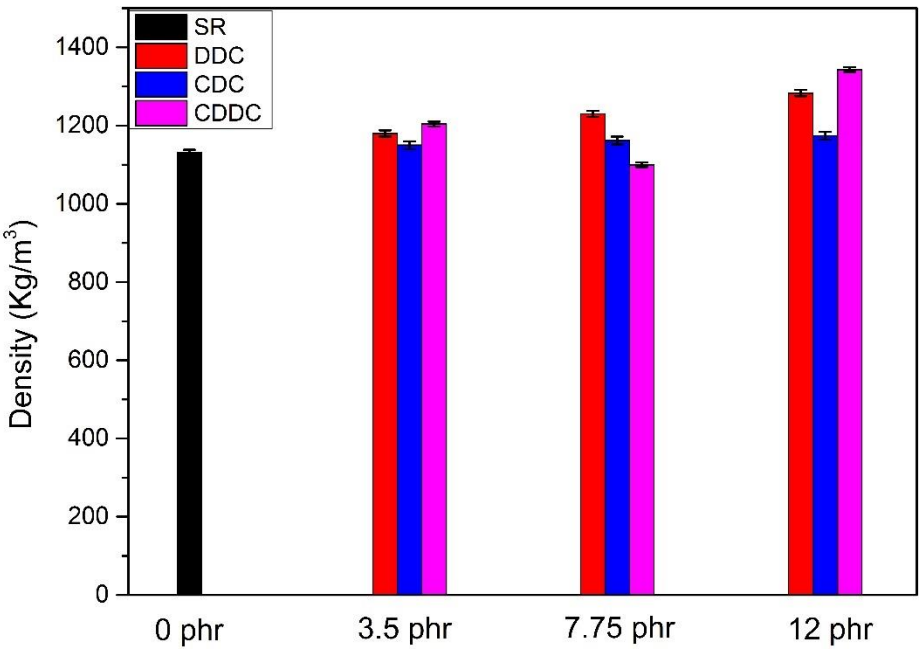

Figure 3.83 Comparison of density of composites for varying filler loading

Comparison of mechanical properties of composites

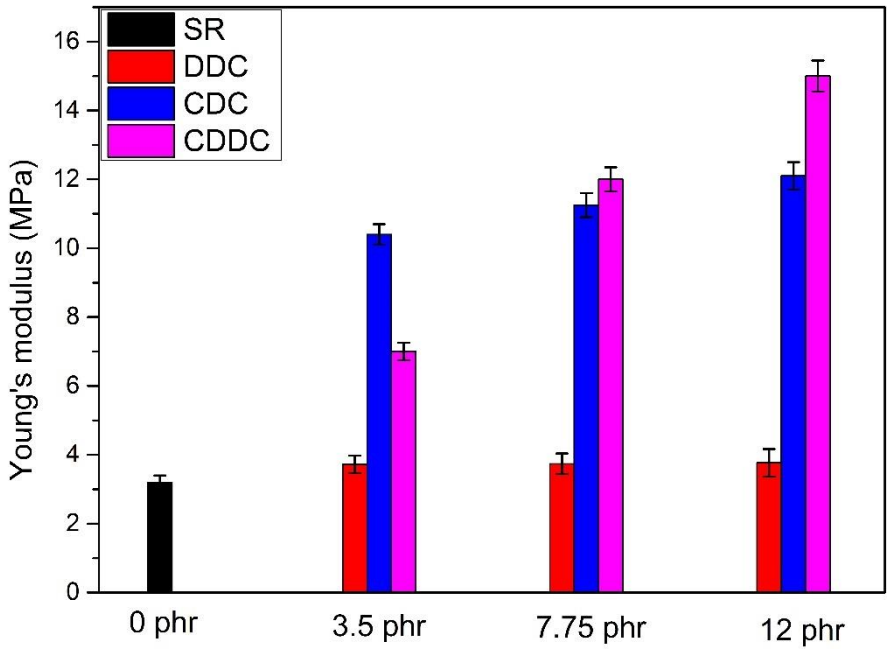

Figure 3.84 Comparison of Young's modulus of composites for varying filler loading

While it is desired to improve the dielectric properties of the composites with addition of dielectric, conductive and conductive-dielectric fillers, it also contributes to increase in mechanical properties. All three types of composites produce an increase

in Young's modulus with increasing filler loadings this is in agreement with trends available in literature (Figure 3.84). Maximum value of Young's modulus is achieved by synergistic combination of both conductive and dielectric fillers at 12 phr loading for CDDC composites. Dielectric filler is less reinforcing as compared to conductive filler as dielectric filler provides lower Young's modulus as compared to conductive and conductive-dielectric fillers. This observation is consistent with that seen in literature for BT filler loadings, that demonstrate increase in Young's modulus with BT filler loading (Nayak et al. 2014a). The variation of Young's modulus with hybrid fillers as in CDDC composites is in contrast to that observed in literature (Zhao et al. 2013b).

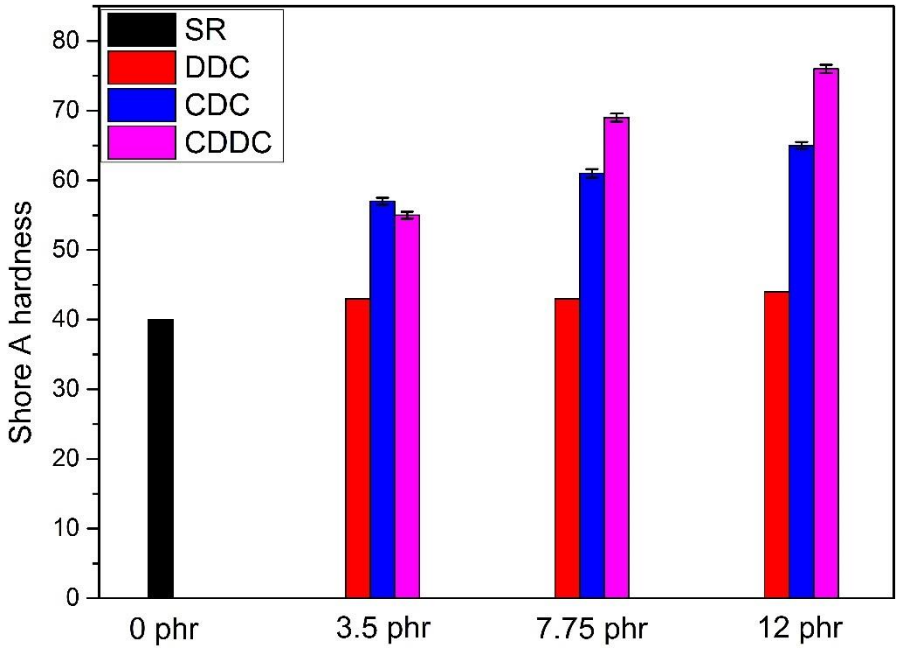

Figure 3.85 Comparison of shore A hardness of composites for varying filler loading

Shore A hardness of all three types of composites increases with filler loadings (Figure 3.85). This trend is in agreement with results seen in literature (Renukappa et al. 2009). The synergistic combination of conductive and dielectric fillers provides the highest hardness values at 12 phr filler loading.

Comparison of dielectric properties of composites

Dielectric properties such as permittivity, dielectric loss and conductivity are compared for the three types of composites. These composites are developed with an

aim of improving permittivity and effective resistivity, reducing dielectric loss and AC conductivity for use as dielectric elastomer materials.

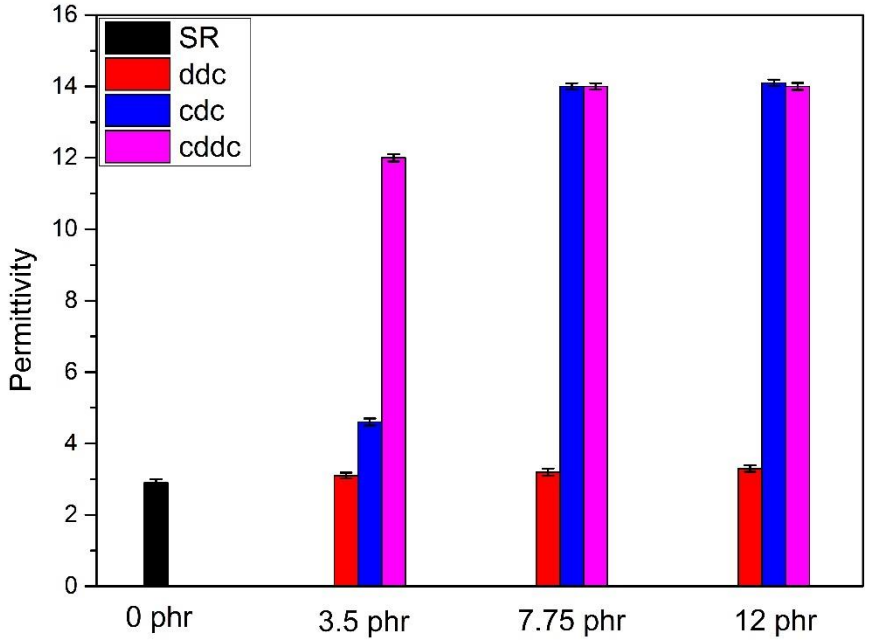

Figure 3.86 Comparison of permittivity of composites for varying filler loading

From Figure 3.86 it is observed that permittivity of solid silicone rubber composites increases with filler loadings for all three types of composites. The quantum of increase being dependent on the type of filler. Conductive fillers provide a major rise in permittivity up to 7.75 phr beyond which the increase is not predominant. High permittivity for CDC composites is achieved at lower conductive filler loadings at the cost of higher dielectric loss while DDC composites can achieve the same values only with very high dielectric filler loadings. BT filler was shown to improve the permittivity with increased filler loadings. Jiang et. al., showed that PDMS/BT composite achieving permittivity of 6.3 at 50 % wt. fraction. However as seen from literature hybrid composites demonstrate larger rise in permittivity with filler loading (Ardimas et al. 2018)

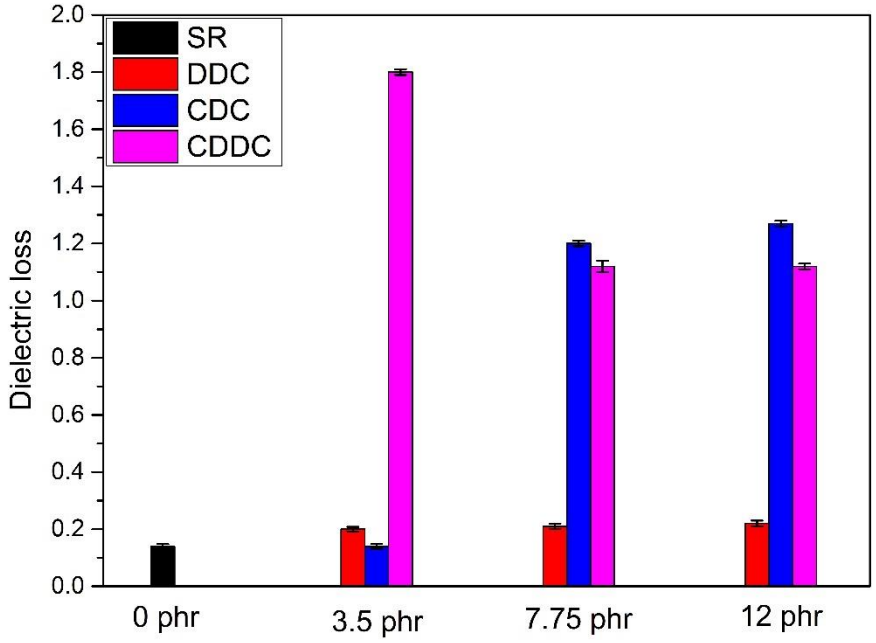

Figure 3.87 Comparison of dielectric loss of composites for varying filler loading

The dielectric loss sees a marginal increase with dielectric fillers, while it shows a major rise with conductive filler. Synergistic combination of conductive and dielectric fillers is evident from Figure 3.87 for CDDC composites wherein the dielectric loss decreases with increase in filler loadings beyond 3.5 phr. Dielectric loss is seen to increase with conducting fillers such as carbon black (Leyva et al. 2003) at a greater rate than with dielectric fillers (Ruan et al. 2018).

Effective resistivity of the composites decreases with filler loadings for all types of composites (Figure 3.88). The dielectric filler loadings provide a marginal decrease in effective resistivity for the range of filler loading tested. CDC composites show a larger reduction in resistivity with conductive filler loading (Yoshimura et al. 2016) as compared to DDC composites with BT filler loading (Nayak et al. 2012). Compared to DDC and CDC composites CDDC composites sees a large drop in effective resistivity. However, variation with increasing filler loadings is marginal for CDDC composites.

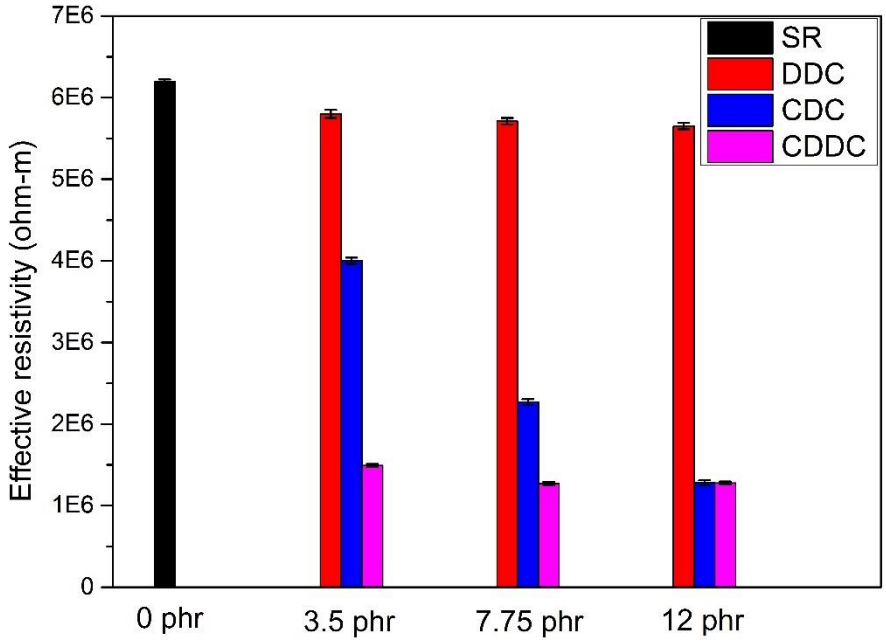

Figure 3.88 Comparison of effective resistivity of composites for varying filler loading

In summary, the permittivity of CDC and CDDC composites are higher, while lower value of permittivity is achieved for DDC composites. Higher dielectric loss is observed for CDC and CDDC composites, while it is lower for DDC composites. Higher effective resistivity is obtained for DDC composites, while it is lower for both CDC and CDDC composites. The objectives of the development of dielectric elastomers involve improving permittivity and effective resistivity while lowering dielectric loss.

Comparison of electromechanical properties of composites

Compared to solid silicone rubber, CDDC composites provide a higher value of electromechanical sensitivity (Figure 3.89). CDC composites improve the sensitivity with increasing conductive filler loadings as against the DDC composites that sees a decrease in sensitivity with increasing dielectric filler loadings. Similarly, CDDC composites also show a decrease in electromechanical sensitivity with increased filler

loadings. The electromechanical sensitivity was shown to initially increase with BT filler up to 10 phr, beyond which it decreased with filler (Ruan et al. 2017).

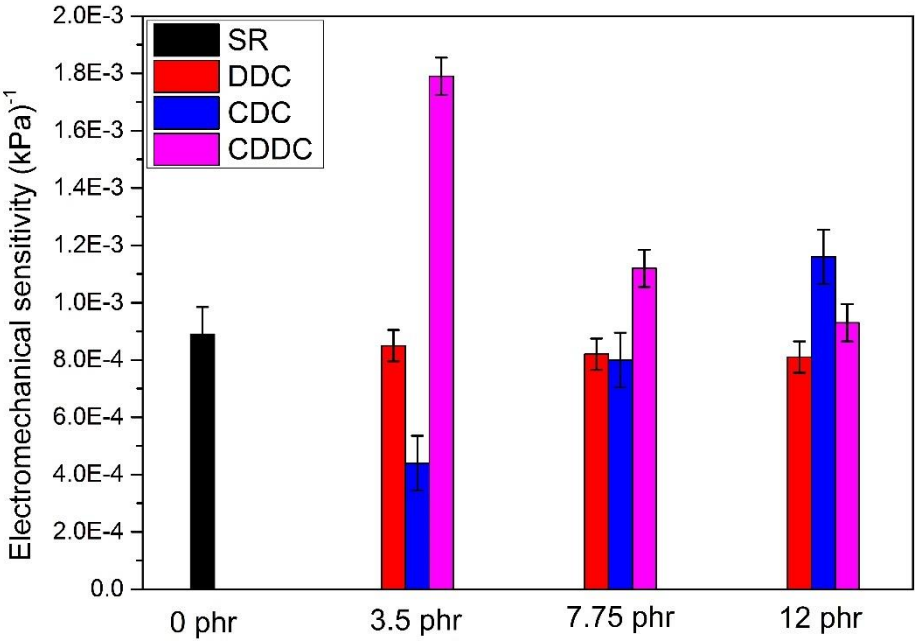

Figure 3.89 Comparison of electromechanical sensitivity of composites for varying filler loading

Solid silicone rubber displays the highest piezoresistive sensitivity however with lower pressure range of up to 9 kPa (Figure 3.90). CDC composites provide a larger piezoresistive sensitivity compared to DDC. Increasing conductive filler produces a decrease in sensitivity. CDDC composites provide a maximum value of piezoresistive sensitivity only at 3.5 phr filler loading of conductive and dielectric filler respectively. Further loading decreases the sensitivity of CDDC composites. Knite et.al. demonstrated a three-order change in resistance with 0.3 MPa increase of pressure for polyisoprene-CB (10 wt%) composites. While, Yoshimura et. al. showed a 60 % decrease in resistivity with 10% compressive strain, for SR-CB (6.5 wt%) composites.

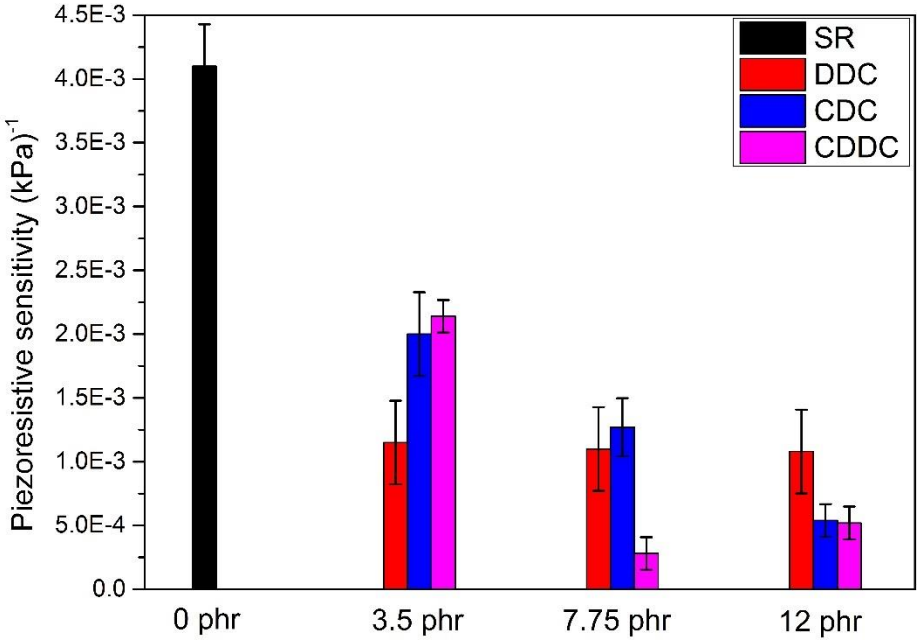

Figure 3.90 Comparison of piezoresistive sensitivity of composites for varying filler loading

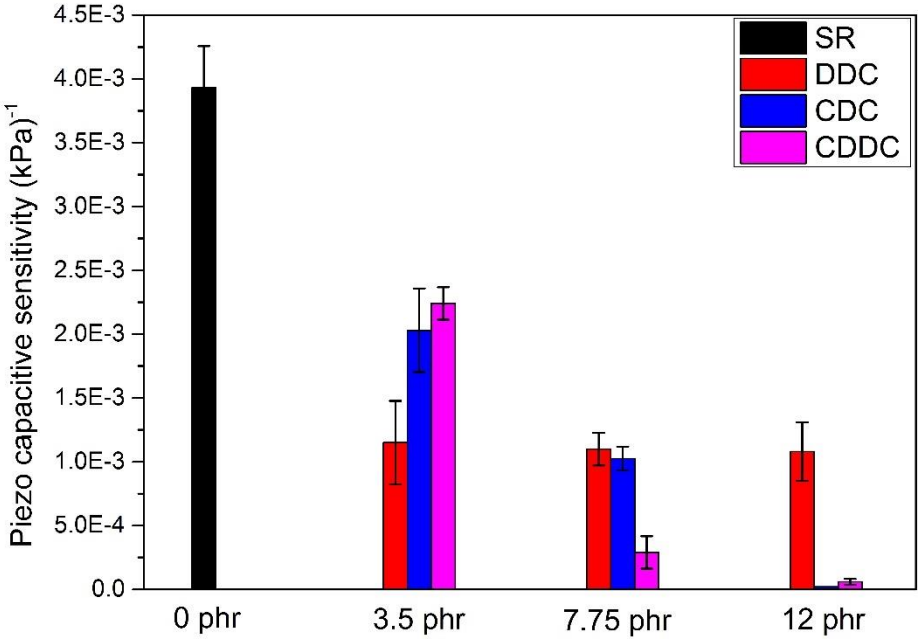

Figure 3.91 Comparison of piezo capacitive sensitivity of composites for varying filler loading

Solid silicone rubber displays the highest piezo capacitive sensitivity as compared to the composites however for a limited pressure range of 9 kPa (Figure 3.91). Both working range and sensitivity are important parameters for tactile sensing. However, from the literature it is seen that there usually exists a trade-off(Fan et al. 2018). CDDC composites provide the highest sensitivity compared to the other two types of composites with an extended pressure range as compared to pure solid silicone rubber. Both CDC and CDDC composites sees a decrease in piezo capacitive sensitivity with increased filler loadings. PDMS was shown to have piezo capacitive sensitivity of 0.0014 $(kPa)^{-1}$ (Liu et al. 2018a). SR-CB (6 wt%) composites was shown to possess piezo capacitive sensitivity of 0.00025 $(kPa)^{-1}$ (Guo et al. 2016).

In summary, the properties of the solid silicone rubber composites are tested to determine its suitability for use as dielectric elastomers. Properties investigated include density, SEM characterization, Young's modulus, shore A hardness, permittivity, dielectric loss, effective resistivity, AC conductivity, electromechanical sensitivity, piezoresistive and piezo capacitive sensitivity. The aim of development of composites for electromechanical transduction applications seek materials that provide improved electromechanical, piezoresistive and piezo capacitive sensitivities.

In the next chapter conclusions based on the variation of properties that are important for dielectric elastomer applications are summarized. Scope for further research is proposed based on the insights obtained in this research work.

CHAPTER 4

4. CONCLUSION

Solid silicone rubber-based composites are successfully fabricated using high temperature compression molding method. These composites are fabricated using dielectric, conductive and dielectric-conductive fillers, by varying the processing parameters such as filler loadings, mixing time (MT), curing agent and curing temperature (CT).

These composites are tested for their physical, mechanical, dielectric and electromechanical properties and the results analyzed using Taguchi techniques. Property-processing relationships are investigated for these composites to determine their suitability for use as dielectric elastomers.

4.1 Dielectric Filler Composites

DDC composites were successfully fabricated using the high temperature vulcanization process and tested for suitability as dielectric elastomer materials.

4.1.1 Physical properties

With the addition of dielectric fillers, the density of the composites increased by 17.6%. SEM characterisation of these composites demonstrate that good wetting and uniform dispersion of fillers is achieved by the processing method adopted.

4.1.2 Mechanical properties

In order to improve the dielectric properties of the solid silicone rubber composites, fillers were added to the solid silicone rubber matrix and were fabricated through high temperature vulcanisation method. A corresponding increase in the mechanical properties is observed for these composites. However, the increase is comparable to those proposed in the literature.

Solid silicone rubber has Young's modulus and shore A hardness of 3.2 MPa and 40 respectively. Young's modulus increases by 17.7 %, hardness increases by 12.5% as compared to the pure elastomer. Linearity in stress strain plots is maintained up to

30% strain. Young's modulus increases with dielectric filler, while it decreases with curing agent, MT and CT. Shore A hardness increases with filler, curing agent and CT, while it decreases with MT.

4.1.3 Dielectric properties

From the study undertaken to investigate the dielectric properties of solid silicone rubber particulate composites, it is observed that the methodology employed provides an improvement in the permittivity of the composites. This is achieved without undue increase in dielectric loss or effective resistivity.

For the DDC composites, permittivity increased with the increase of dielectric filler. A 14% increase in permittivity was achieved for 12 phr filler loading. Various dielectric mixing rules were applied to DDC composites and compared with experimental values. It was found that Lichtenecker model predicts the permittivity of these composite that are in good agreement with experimental values. Dielectric loss increased from 0.14 to 0.28 showing an increase of 100 %. Effective resistivity of the composite decreased with the filler loading by 13.5%. These composites follow the AC universality law for conductivity with exponent equal to 1. Permittivity increases with filler and curing agent loading and decreases with MT and CT. Dielectric loss increases with filler and curing agent loading, while reducing with MT and CT. Effective resistivity decreases with filler and curing agent, while increasing with MT and CT.

4.1.4 Electromechanical properties

Electromechanical sensitivity is a characteristic sought out for actuator applications of dielectric elastomers. With the proposed methodology, it is observed that it increases for all the three types of composites over the solid silicone rubber matrix. It is also dependent on the processing parameters as well.

Piezoresistive and piezo capacitive sensitivities are sought for in sensor and energy harvesting applications of dielectric elastomer materials. For the proposed composites, it is observed that these characteristics increased as compared to the solid silicone rubber matrix. Also, these characteristics are influenced by the processing parameters.

Electromechanical sensitivity for DDC composites increased to 1.10E-3 $(kPa)^{-1}$ from a value of 0.89E-3 $(kPa)^{-1}$ observed for pure solid silicone rubber,

The piezoresistive sensitivity of DDC composites increases with increased mixing time and curing temperature, while it increases with lesser dielectric filler and curing agent loading. It shows a maximum value of 3.65E-3 $(kPa)^{-1}$.

Solid silicone rubber achieves piezo capacitive sensitivity of 3.93E-3 $(kPa)^{-1}$ for pressures up to 12 kPa after which it is almost horizontal.

DDC composites achieved a maximum piezo capacitive sensitivity of 3.69E-3 $(kPa)^{-1}$ for the entire pressure range tested. It increases with lesser filler and curing agent loading, while it increases with increased mixing time and curing temperature.

4.2 Conductive Filler Composites

CDC composites were successfully fabricated using the high temperature vulcanization process and tested for suitability as dielectric elastomer materials.

4.2.1 Physical properties

The density increases by 7.1%. Density increases with filler and decreases with curing agent, MT and CT. SEM characterisation of these composites demonstrate that good wetting and uniform dispersion of fillers is achieved by the processing method adopted.

4.2.2 Mechanical properties

Conductive filler used is Ketjenblack EC 300 which is a well-known reinforcing agent. Hence, Young's modulus and shore A increases by 687 % and 115 % respectively. Linearity in stress strain plots is observed up to 30% strain. Young's modulus of these composites increases with conductive filler and curing agent, while it decreases with MT and CT. Shore A hardness increases with filler and DCP.

4.2.3 Dielectric properties

The permittivity of the CDC composites increased by 390% with the addition of filler loadings of up to 12 phr. Dielectric loss however increased by 800 % from 0.14 to 1.27, which is a characteristic feature of CDC composites. Composites are still in the insulator regime even though the effective resistivity of these composites decreased

by 80%. From the dielectric relaxation studies the discrepancy in the relaxation behaviours between the conductive filler and dielectric filler solid silicone rubber composites has been observed. Even though both of them have been loaded with the same filler loadings, they show different dielectric behaviours on account of the type of filler. In the case of conductive filler composites, a large increase of permittivity is observed at low frequencies as compared to that with dielectric fillers for same filler loadings. The power exponent for the AC universality law was 0.82, suggesting that the charge carrier transport inside the material supports correlated barrier hopping mechanism.

4.2.4 Electromechanical properties

Electromechanical sensitivity of CDC composites increased to 1.44E-3 $(kPa)^{-1}$.

For CDC composites maximum achieved piezoresistive sensitivity is 3.55E-3 $(kPa)^{-1}$. It increases with lesser conductive filler loading along with curing agent, while it increases with increased mixing time and curing temperature.

CDC composites achieved a maximum piezo capacitive sensitivity of 4.30E-3 $(kPa)^{-1}$. It increases with lesser filler loading and curing agent, while increasing with increased mixing time and curing temperature.

4.3 Conductive-Dielectric Filler Composites

CDDC composites were successfully fabricated using the high temperature vulcanization process and tested for suitability as dielectric elastomer materials.

4.3.1 Physical properties

Density of the CDDC composites increased by 20%. SEM characterisation of these composites demonstrate that good wetting and uniform dispersion of fillers is achieved by the processing method adopted.

4.3.2 Mechanical properties

Young's modulus and hardness of the CDDC composites increased by 370% and 90% respectively. Linearity is observed up to 30 % strain. Young's modulus initially increases with dielectric filler up to 7.75 phr then drops down, while it increases with

conductive filler loading. Increase in Shore A hardness with conductive filler is more profound than with dielectric filler loading.

4.3.3 Dielectric properties

In the case of CDDC composites, the permittivity increased by 390%. While dielectric loss increased by 700%. Effective resistivity decreased by 80%. For these composites, it is observed that conductive filler dominates the polarization mechanisms of the composite compared to dielectric fillers even at the same filler loadings. The power exponent for the AC universality law was 0.83, suggesting that the charge carrier transport inside the material supports correlated barrier hopping mechanism.

4.3.4 Electromechanical properties

Electromechanical sensitivity of the CDDC composites was the largest at 1.79E-3 $(kPa)^{-1}$, suggesting that synergistic interaction between both types of fillers contributed towards the same.

Piezoresistive sensitivity of CDDC composites reaches a maximum value of 3.70E-3 $(kPa)^{-1}$. CDDC composites shows larger resistance change as compared to DDC composites.

A maximum piezo capacitive sensitivity of 3.92E-3 $(kPa)^{-1}$ was achieved.

The sensitivity of composites depends on permittivity and Young's modulus. With the increase in active filler content, the permittivity of the composites increases. However, this gets offset by the corresponding increase in Young's modulus. Hence sensitivity of these types of composites depend on the interplay between permittivity and Young's modulus.

Hence, we propose that solid silicone rubber can be tailored as composites for capacitive sensing applications, that target flexible and large area deployable applications obtained through low cost, simple and mature fabrication processes.

In summary, CDDC composite (both fillers at 3.5 phr loading) is proposed for use as dielectric elastomer actuators on account of its electromechanical sensitivity value. Solid silicone rubber has demonstrated to be a candidate material for capacitive

sensing applications but over a limited pressure range. This range has been enhanced by developing the composites. CDC composite (3.5 phr filler, 1 phr curing agent, 30 min MT, 210°C CT) demonstrating highest value of piezo capacitive sensitivity is proposed for capacitive pressure sensing applications. CDDC composite (7.75 phr BT, 3.5 phr SCCB) is proposed for piezoresistive pressure sensing application.

The study reveals that solid silicone rubber particulate composites fabricated through high temperature vulcanization process using dielectric, conductive and conductive-dielectric fillers can be tailored for use as dielectric elastomer materials. Their properties can be tuned by adjusting the type, composition of the fillers and varying the processing parameters to particularly suit flexible pressure sensing applications.

4.4 Scope for Further Research

This study demonstrates the feasibility of using the solid silicone rubber composites for use as dielectric elastomers specifically as flexible pressure sensors using both piezoresistive and piezo capacitive mechanisms. This work can be further expanded to investigate the sensitivity of these composites through modifications including developing micro structured and porous composites.

In order to determine the effectiveness of these composites for actuating and sensing, dynamic properties of these composites could be investigated after encapsulating these materials with suitable packaging and signal conditioning.

Many attributes such as permittivity, dielectric loss, effective resistivity, AC conductivity, Young's modulus, Shore A hardness, density, electromechanical, piezoresistive and piezo capacitive sensitivity have to be considered in the development of these composites. Further these attributes are influenced by various factors such as filler type, filler loading, amount of curing agent, mixing time and curing temperature. Thus, multi-attribute decision making techniques can be applied to obtain the best combination of factors that could give the best levels for each of the attributes.

A. APPENDIX

Table A-1 Volume fraction equivalent to phr

Filler amount (phr)	Volume fraction
3.5	0.006
7.75	0.014
12	0.022

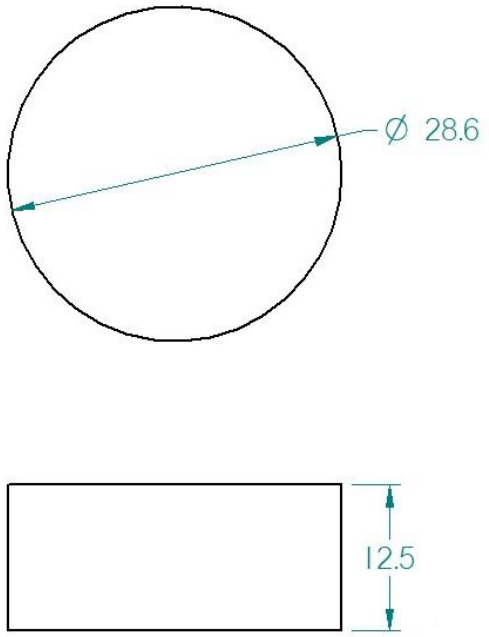

Figure A.1 Schematic of the specimen with dimensions for evaluating mechanical properties (Dimensions in mm).

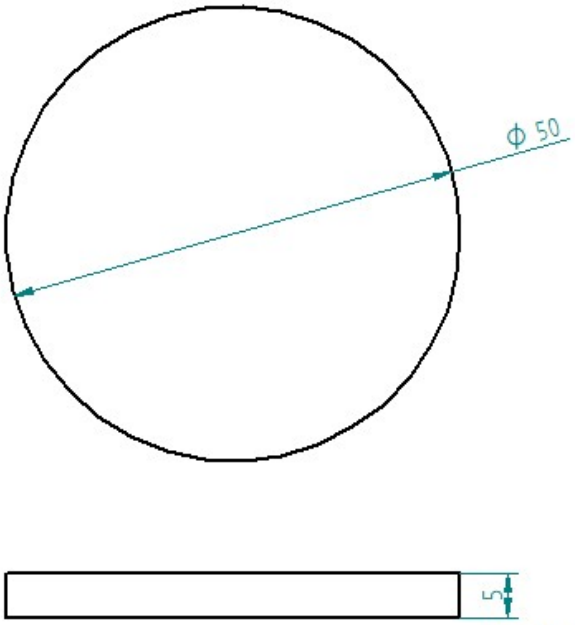

Figure A.2 Schematic of the specimen with dimensions for evaluating dielectric and electromechanical properties (Dimensions in mm).

RESEARCH OUTCOMES

Sr. No	Title of Paper	Authors (in the same order as in the paper)	Name of the Journal/Conference, Vol. no., Pages.	Month & Year of Publication.	Category
1	Influences of dielectric and conductive fillers on dielectric and mechanical properties of solid silicone rubber composites	B. S. Manohar Shankar& S. M. Kulkarni	Iranian Polymer Journal, 28, 7, 563-573	June 2019	1
2	Influence of conductive and dielectric fillers on the relaxation of solid silicone rubber composites	B.S. Manohar Shankar, Shivashankar Hiremath & S. M. Kulkarni	Materials Research Express, 6, 125308	Nov 2019	1
3	Investigation on Electromechanical Properties of Solid Silicone Rubber Composites with Conductive Carbon Filler	B.S. Manohar Shankar& S.M. Kulkarni	Materials Science Forum, 969, 409-414	Aug 2019	3
4	Investigation of piezo-capacitance and piezo-resistance properties of solid silicone rubber-conductive carbon black composites	B. S. Manohar Shankar& S. M. Kulkarni	AIP Conference Proceedings **2057**, 020034	Jan 2019	3
5	Experimental Investigation on Dielectric Properties of Composites using Taguchi Technique	B.S. Manohar Shankar, Kevin Amith Mathias & S.M. Kulkarni	Materials Today: Proceedings Doi: 10.1016/j.matpr.2019.09.095	Sept 2019	3

6	Influence of filler and processing parameters on the mechanical properties of dielectric elastomer composites	B.S. Manohar Shankar, Kevin Amith Mathias & S.M. Kulkarni	Materials Today: Proceedings Doi: 10.1016/j.matpr.2019.10.058	Oct 2019	3

Category*

1: Journal paper, full paper reviewed
2: Journal paper, Abstract reviewed
3: Conference/Symposium paper, full paper reviewed
4: Conference/Symposium paper, abstract reviewed
5: others (including papers in Workshops, NITK Research Bulletins, Short notes, etc.)
(If the paper has been accepted for publication but yet to be published, the supporting documents must be attached.)

REFERENCES

Abu-Abdeen, M., Hamza, S. S., Elwy, A. A., and Abd El-Wahab, S. M. (2007). "Dielectric properties of SBR vulcanizates loaded with HAF carbon black and $BaTiO_3$ ceramics." *J. Appl. Polym. Sci.*, 103(4), 2227–2234.

Ali, S., Maddipatla, D., Narakathu, B. B., Chlaihawi, A. A., Emamian, S., Janabi, F., Bazuin, B. J., and Atashbar, M. Z. (2019). "Flexible Capacitive Pressure Sensor Based on PDMS Substrate and Ga-In Liquid Metal." *IEEE Sens. J.*, 19(1), 97–104.

Alwaan, I. M., Hassan, A., and Piah, M. A. M. (2015). "Effect of zinc borate on mechanical and dielectric properties of metallocene linear low-density polyethylene/rubbers/magnesium oxide composite for wire and cable applications." *Iran. Polym. J.*, 24(4), 279–288.

Aneli, J. N., Zaikov, G. E., and Khananashvili, L. M. (1999). "Effects of mechanical deformations on the structurization and electric conductivity of electric conducting polymer composites." *J. Appl. Polym. Sci.*, 74(3), 601–621.

Araújo, M. C., Costa, C. M., and Lanceros-Méndez, S. (2014). "Evaluation of dielectric models for ceramic/polymer composites: Effect of filler size and concentration." *J. Non. Cryst. Solids*, 387, 6–15.

Ardimas, Putson, C., and Muensit, N. (2018). "High electromechanical performance of modified electrostrictive polyurethane three-phase composites." *Compos. Sci. Technol.*, 158, 164–174.

Balasubramanian, K., and Burghard, M. (2008). "Electrochemically functionalized carbon nanotubes for device applications." *J. Mater. Chem.*, 18(26), 3071–3083.

Bele, A., Cazacu, M., Stiubianu, G., and Vlad, S. (2014). "Silicone-barium titanate composites with increased electromechanical sensitivity. the effects of the filler morphology." *RSC Adv.*, 4(102), 58522–58529.

Bele, A., Cazacu, M., Stiubianu, G., Vlad, S., and Ignat, M. (2015a). "Polydimethylsiloxane-barium titanate composites: Preparation and evaluation of the morphology, moisture, thermal, mechanical and dielectric behavior." *Compos. Part B Eng.*, 68, 237–245.

Bele, A., Stiubianu, G., Varganici, C. D., Ignat, M., and Cazacu, M. (2015b). "Silicone dielectric elastomers based on radical crosslinked high molecular weight polydimethylsiloxane co-filled with silica and barium titanate." *J. Mater. Sci.*, 50(20), 6822–6832.

Bele, A., Tugui, C., Sacarescu, L., Iacob, M., Stiubianu, G., Dascalu, M., Racles, C., and Cazacu, M. (2018). "Ceramic nanotubes-based elastomer composites for applications in electromechanical transducers." *Mater. Des.*, 141, 120–131.

Blow, C. M. (1973). "Polymer/particulate filler interaction-the bound rubber phenomena." *Polymer*, 14(7), 309–323.

Brochu, P., and Pei, Q. (2012). "Dielectric elastomers for actuators and artificial muscles." *Electroact. Polym. Mater.*, 9781461408(5), 1–56.

Brochu, P., Stoyanov, H., Chang, R., Niu, X., Hu, W., and Pei, Q. (2014). "Capacitive energy harvesting using highly stretchable silicone-carbon nanotube composite electrodes." *Adv. Energy Mater.*, 4(3), 1–9.

Cagatay, E., Kohler, P., Lugli, P., and Abdellah, A. (2015). "Flexible capacitive tactile sensors based on carbon nanotube thin films." *IEEE Sens. J.*, 15(6), 3225–3233.

Cai, W., Huang, Y., Wang, D., Liu, C., and Zhang, Y. (2014). "Piezoresistive behavior of graphene nanoplatelets/carbon black/silicone rubber nanocomposite." *J. Appl. Polym. Sci.*, 131(3), 1–6.

Carlson, W. B., Bartkowski, S. F., Schulze, W. A., and Pilgrim, S. M. (2006). "Testing of piezoresistive polyurethane-Fe_3O_4 composites." *Ferroelectrics*, 331, 83–88.

Carpi, F., Gallone, G., Galantini, F., and Rossi, D. De. (2008). "Silicone-poly(hexylthiophene) blends as elastomers with enhanced electromechanical transduction properties." *Adv. Funct. Mater.*, 18(2), 235–241.

Carpi, F., and Rossi, D. De. (2005). "Improvement of electromechanical actuating performances of a silicone dielectric elastomer by dispersion of titanium dioxide powder." *IEEE Trans. Dielectr. Electr. Insul.*, 12(4), 835–843.

Castano, L. M., and Flatau, A. B. (2014). "Smart fabric sensors and e-textile technologies: A review." *Smart Mater. Struct.*, 23(5), 53001.

Cazacu, M., Ignat, M., Racles, C., Cristea, M., Musteata, V., Ovezea, D., and Lipcinski, D. (2014). "Well-defined silicone-titania composites with good performances in actuation and energy harvesting." *J. Compos. Mater.*, 48(13), 1533–1545.

Cha, S. W., Song, C., Cho, Y. H., and Choi, S. (2014). "Piezoresistive properties of CNT reinforced cementitious composites." *Mater. Res. Innov.*, 18, S2716–S2721.

Chakraborti, P., Toprakci, H. A. K., Yang, P., Spigna, N. Di, Franzon, P., and Ghosh, T. (2012). "A compact dielectric elastomer tubular actuator for refreshable Braille displays." *Sensors Actuators, A Phys.*, 179, 151–157.

Chen, S., Zhuo, B., and Guo, X. (2016). "Large Area One-Step Facile Processing of Microstructured Elastomeric Dielectric Film for High Sensitivity and Durable Sensing over Wide Pressure Range." *ACS Appl. Mater. Interfaces*, 8(31), 20364–20370.

Cheng, J., Jia, Z., and Li, T. (2018). "Dielectric-elastomer-based capacitive force sensing with tunable and enhanced sensitivity." *Extrem. Mech. Lett.*, 21, 49–56.

Cheng, Y., Wang, R., Zhai, H., and Sun, J. (2017). "Stretchable electronic skin based on silver nanowire composite fiber electrodes for sensing pressure, proximity, and multidirectional strain." *Nanoscale*, 9(11), 3834–3842.

Chi, Q. G., Li, Z., Zhang, T. D., and Zhang, C. H. (2019). "Study on nonlinear conductivity of copper-titanate-calcium/liquid silicone rubber composites." *IEEE Trans. Dielectr. Electr. Insul.*, 26(3), 681–688.

Chiba, S., Waki, M., Kornbluh, R., and Pelrine, R. (2011). “Current status and future prospects of power generators using dielectric elastomers.” *Smart Mater. Struct.*, 20(12).

Chowdhury, S. A., Saha, M. C., Patterson, S., Robison, T., and Liu, Y. (2019). “Highly Conductive Polydimethylsiloxane/Carbon Nanofiber Composites for Flexible Sensor Applications.” *Adv. Mater. Technol.*, 4(1), 1–10.

Dabros, M., Dennewald, D., Currie, D. J., Lee, M. H., Todd, R. W., Marison, I. W., and Stockar, U. Von. (2009). “Cole-Cole, linear and multivariate modeling of capacitance data for on-line monitoring of biomass.” *Bioprocess Biosyst. Eng.*, 32(2), 161–173.

Dahiya, R. S., Metta, G., Valle, M., and Sandini, G. (2010). “Tactile sensing-from humans to humanoids.” *IEEE Trans. Robot.*, 26(1), 1–20.

Dang, Z. M., Peng, B., Xie, D., Yao, S. H., Jiang, M. J., and Bai, J. (2008). “High dielectric permittivity silver/polyimide composite films with excellent thermal stability.” *Appl. Phys. Lett.*, 92(11), 23–25.

Dang, Z. M., Shen, Y., and Nan, C. W. (2003). “Dielectric behavior of three-phase percolative Ni-$BaTiO_3$/polyvinylidene fluoride composites.” *Appl. Phys. Lett.*, 81(25), 4814–4816.

Dang, Z. M., Xia, B., Yao, S. H., Jiang, M. J., Song, H. T., Zhang, L. Q., and Xie, D. (2009). “High-dielectric-permittivity high-elasticity three-component nanocomposites with low percolation threshold and low dielectric loss.” *Appl. Phys. Lett.*, 94(4), 28–31.

Dang, Z. M., Yuan, J. K., Zha, J. W., Zhou, T., Li, S. T., and Hu, G. H. (2012). “Fundamentals, processes and applications of high-permittivity polymer-matrix composites.” *Prog. Mater. Sci.*, 57(4), 660–723.

Dimiev, A., Zakhidov, D., Genorio, B., Oladimeji, K., Crowgey, B., Kempel, L., Rothwell, E. J., and Tour, J. M. (2013). “Permittivity of dielectric composite materials comprising graphene nanoribbons. the effect of nanostructure.” *ACS Appl. Mater. Interfaces*, 5(15), 7567–7573.

Ding, X., Wang, J., Zhang, S., Wang, J., and Li, S. (2015). “Composites based on CB/CF/Ag filled EPDM/NBR rubber blends with high conductivity.” *J. Appl. Polym. Sci.*, 132(4), 1–7.

Ding, Y., Xu, T., Onyilagha, O., Fong, H., and Zhu, Z. (2019). “Recent advances in flexible and wearable pressure sensors based on piezoresistive 3D monolithic conductive sponges.” *ACS Appl. Mater. Interfaces*, 11(7), 6685–6704.

Dyre, J., and Schröder, T. B. (2000). “Universality of ac conduction in disordered solids.” *Rev. Mod. Phys.*, 72(C), 873–892.

Ellingford, C., Zhang, R., Wemyss, A. M., Bowen, C., McNally, T., Figiel, Ł., and Wan, C. (2018). “Intrinsic Tuning of Poly(styrene-butadiene-styrene)-Based Self-Healing Dielectric Elastomer Actuators with Enhanced Electromechanical Properties.” *ACS Appl. Mater. Interfaces*, 10(44), 38438–38448.

Fan, B. H., Zha, J. W., Wang, D. R., Zhao, J., Zhang, Z. F., and Dang, Z. M. (2013). "Preparation and dielectric behaviors of thermoplastic and thermosetting polymer nanocomposite films containing $BaTiO_3$ nanoparticles with different diameters." *Compos. Sci. Technol.*, 80, 66–72.

Fan, Q., Zhang, X., and Qin, Z. (2012). "Preparation of polyaniline/polyurethane fibers and their piezoresistive property." *J. Macromol. Sci. Part B Phys.*, 51(4), 736–746.

Fan, Y., Liao, C., Liao, G., Tan, R., and Xie, L. (2017). "Capacitive pressure-sensitive composites using nickel-silicone rubber: Experiments and modeling." *Smart Mater. Struct.*, 26(7), 75003.

Fan, Y., Liao, C., Xie, L., and Chen, X. (2018). "Piezo-capacitive behavior of a magnetically structured particle-based conductive polymer with high sensitivity and a wide working range." *J. Mater. Chem. C*, 6(20), 5401–5411.

Fang, F., Yang, W., Yu, S., Luo, S., and Sun, R. (2014). "Mechanism of high dielectric performance of polymer composites induced by $BaTiO_3$ -supporting Ag hybrid fillers." *Appl. Phys. Lett.*, 104(13), 132909-1–4.

Gallone, G., Carpi, F., Rossi, D. De, Levita, G., and Marchetti, A. (2007). "Dielectric constant enhancement in a silicone elastomer filled with lead magnesium niobate-lead titanate." *Mater. Sci. Eng. C*, 27(1), 110–116.

Gallone, G., Galantini, F., and Carpi, F. (2010). "Perspectives for new dielectric elastomers with improved electromechanical actuation performance: Composites versus blends." *Polym. Int.*, 59(3), 400–406.

Giousouf, M., and Kovacs, G. (2013). "Dielectric elastomer actuators used for pneumatic valve technology." *Smart Mater. Struct.*, 22(10).

González, N., Custal, M. dels À., Tomara, G. N., Psarras, G. C., Riba, J. R., and Armelin, E. (2017). "Dielectric response of vulcanized natural rubber containing $BaTiO_3$ filler: The role of particle functionalization." *Eur. Polym. J.*, 97, 57–67.

Gonzalez, N., Riba, J. R., Dels Angels Custal, M., and Armelin, E. (2017). "Improvement of insulation effectiveness of natural rubber by adding hydroxyl-functionalized barium titanate nanoparticles." *IEEE Trans. Dielectr. Electr. Insul.*, 24(5), 2881–2889.

Guan, S., Li, H., Zhao, S., and Guo, L. (2018). "Novel three-component nanocomposites with high dielectric permittivity and low dielectric loss co-filled by carboxyl-functionalized multi-walled nanotube and $BaTiO_3$." *Compos. Sci. Technol.*, 158, 79–85.

Güler, A. C., Dindar, B., and Orücü, H. (2019). "Effect of B or N doping on the dielectric and electrical properties of ZnO at room temperature." *Mater. Res. Express*, 6(6), 65017.

Guo, C., Kondo, Y., Takai, C., and Fuji, M. (2017). "Piezoresistivities of vapor-grown carbon fiber/silicone foams for tactile sensor applications." *Polym. Int.*, 66(3), 418–427.

Guo, X., Huang, Y., Cai, X., Liu, C., and Liu, P. (2016). “Capacitive wearable tactile sensor based on smart textile substrate with carbon black /silicone rubber composite dielectric.” *Meas. Sci. Technol.*, 27(4), 1–2.

Guo, Y., Ma, H., Liu, G., Zhang, H., Sun, Y., Wang, Y., Ren, Y., and Fu, M. (2018). “Enhanced dielectric properties of conductive-dielectric composites by reducing particle size and core@shell method.” *Funct. Mater. Lett.*, 11(1), 1850010.

Hassan, H. H., Nasr, G. M., and El-Waily, M. A. (2013). “Electrical and mechanical properties of aluminum-loaded NBR composites.” *J. Elastomers Plast.*, 45(2), 121–141.

He, F., Lau, S., Chan, H. L., and Fan, J. (2009). “High dielectric permittivity and low percolation threshold in nanocomposites based on poly(vinylidene fluoride) and exfoliated graphite nanoplates.” *Adv. Mater.*, 21(6), 710–715.

Heydt, R., Pelrine, R., Joseph, J., J, E., and R, K. (2000). “Acoustical performance of an electrostrictive polymer film loudspeaker.” *J. Acoust. Soc. Am.*, 107(2), 833–9.

Horne, J., Mcloughlin, L., Bury, E., Koh, A. S., and Wujcik, E. K. (2020). “Interfacial Phenomena of Advanced Composite Materials toward Wearable Platforms for Biological and Environmental Monitoring Sensors , Armor , and Soft Robotics.” *Adv. Mater. interfaces*, 7, 1901851-1–25.

Huang, C., Zhang, Q. M., DeBotton, G., and Bhattacharya, K. (2004). “All-organic dielectric-percolative three-component composite materials with high electromechanical response.” *Appl. Phys. Lett.*, 84(22), 4391–4393.

Huang, Y., Wang, W., Wang, Y., Liu, P., Liu, C., and Tian, H. (2016). “Synergistic effects and piezoresistive characteristics of carbon nanofillers/silicone rubber composites.” *Mater. Technol.*, 31(4), 229–233.

Iacob, M., Bele, A., Patras, X., Pasca, S., Butnaru, M., Alexandru, M., Ovezea, D., and Cazacu, M. (2014). “Preparation of electromechanically active silicone composites and some evaluations of their suitability for biomedical applications.” *Mater. Sci. Eng. C*, 43, 392–402.

Jaschin, P. W., Bhimireddi, R., and Varma, K. B. R. (2018). “Enhanced Dielectric Properties of $LaNiO_3$/$BaTiO_3$/PVDF: A Three-Phase Percolative Polymer Nanocrystal Composite.” *ACS Appl. Mater. Interfaces*, 10(32), 27278–27286.

Javadi, S., Panahi-Sarmad, M., and Razzaghi-Kashani, M. (2018). “Interfacial and dielectric behavior of polymer nano-composites: Effects of chain stiffness and cohesive energy density.” *Polymer*, 145, 31–40.

Jayalakshmy, M. S., and Philip, J. (2015). “Enhancement in pyroelectric detection sensitivity for flexible $LiNbO_3$/PVDF nanocomposite films by inclusion content control.” *J. Polym. Res.*, 22(3), 1–11.

Jiang, S. L., Yu, Y., and Zeng, Y. K. (2009). “Novel Ag-$BaTiO_3$/PVDF three-component nanocomposites with high energy density and the influence of nano-Ag on the dielectric properties.” *Curr. Appl. Phys.*, 9(5), 956–959.

Jin, Y., Xia, N., and Gerhardt, R. A. (2016). “Enhanced dielectric properties of polymer matrix composites with $BaTiO_3$ and MWCNT hybrid fillers using simple phase separation.” *Nano Energy*, 30, 407–416.

Jordi, C., Schmidt, A., Kovacs, G., Michel, S., and Ermanni, P. (2011). “Performance evaluation of cutting-edge dielectric elastomers for large-scale actuator applications.” *Smart Mater. Struct.*, 20(7).

Kappassov, Z., Corrales, J. A., and Perdereau, V. (2015). “Tactile sensing in dexterous robot hands - Review.” *Rob. Auton. Syst.*, 74, 195–220.

Khastgir, D., and Adachi, K. (1999). “Piezoelectric and dielectric properties of siloxane elastomers filled with bariumtitanate.” *J. Polym. Sci. Part B Polym. Phys.*, 37(21), 3065–3070.

Kim, D. C., Shim, H. J., Lee, W., Koo, J. H., and Kim, D. H. (2019). “Material-Based Approaches for the Fabrication of Stretchable Electronics.” *Adv. Mater.*, 1902743, 1902743.

Kim, H., Kim, G., Kim, T., Lee, S., Kang, D., Hwang, M. S., Chae, Y., Kang, S., Lee, H., Park, H. G., and Shim, W. (2018). “Transparent, Flexible, Conformal Capacitive Pressure Sensors with Nanoparticles.” *Small*, 14(8), 1–10.

Kim, K. J., and Tadokoro, S. (2007). *Electroactive polymers for robotic applications: Artificial muscles and sensors*, (K. J. Kim and S. Tadokoto, eds.), London: Springer-Verlag.

Klonos, P. A., Tegopoulos, S. N., Koutsiara, C. S., Kontou, E., Pissis, P., and Kyritsis, A. (2019). “Effects of CNTs on thermal transitions, thermal diffusivity and electrical conductivity in nanocomposites: comparison between an amorphous and a semicrystalline polymer matrix.” *Soft Matter*, 15(8), 1813–1824.

Knite, M., Teteris, V., Kiploka, A., and Kaupuzs, J. (2004). “Polyisoprene-carbon black nanocomposites as tensile strain and pressure sensor materials.” *Sensors Actuators, A Phys.*, 110(1–3), 142–149.

Kollosche, M., Stoyanov, H., Laflamme, S., and Kofod, G. (2011). “Strongly enhanced sensitivity in elastic capacitive strain sensors.” *J. Mater. Chem.*, 21(23), 8292–8294.

Kornbluh, R. (2004). “Dielectric elastomer artificial muscle for actuation, sensing, generation, and intelligent structures.” *Mater. Technol.*, 19(4), 216–224.

Kovacs, G., Düring, L., Michel, S., and Terrasi, G. (2009). “Stacked dielectric elastomer actuator for tensile force transmission.” *Sensors Actuators, A Phys.*, 155(2), 299–307.

Krieg, A. S., King, J. A., Jaszczak, D. C., Miskoglu, I., Mills, O. P., and Odegard, G. M. (2018). “Tensile and conductivity properties of epoxy composites containing carbon black and graphene nanoplatelets.” *J. Compos. Mater.*, 52(28), 3909–3918.

Laflamme, S., Kollosche, M., Connor, J. J., and Kofod, G. (2013). “Robust Flexible Capacitive Surface Sensor for Structural Health Monitoring Applications.” *J. Eng.*

Mech., 139(7), 879–885.

Larsen, A. L., Hansen, K., Sommer-Larsen, P., Hassager, O., Bach, A., Ndoni, S., and Jørgensen, M. (2003). "Elastic properties of nonstoichiometric reacted PDMS networks." *Macromolecules*, 36(26), 10063–10070.

Leyva, M. E., Barra, G. M. O., Moreira, A. C. F., Soares, B. G., and Khastgir, D. (2003). "Electric, dielectric, and dynamic mechanical behavior of carbon black/styrene-butadiene-styrene composites." *J. Polym. Sci. Part B Polym. Phys.*, 41(23), 2983–2997.

Li, T., Luo, H., Qin, L., Wang, X., Xiong, Z., Ding, H., Gu, Y., Liu, Z., and Zhang, T. (2016). "Flexible Capacitive Tactile Sensor Based on Micropatterned Dielectric Layer." *Small*, 12(36), 5042–5048.

Li, W., Song, Z., Qian, J., Chu, H., Wu, X., Tan, Z., and Nie, W. (2018a). "Surface modification-based three-phase nanocomposites with low percolation threshold for optimized dielectric constant and loss." *Ceram. Int.*, 44(5), 4835–4844.

Li, Y. J., Xu, M., Feng, J. Q., and Dang, Z. M. (2006). "Dielectric behavior of a metal-polymer composite with low percolation threshold." *Appl. Phys. Lett.*, 89(7), 72902.

Li, Y., Samad, Y. A., and Liao, K. (2015). "From cotton to wearable pressure sensor." *J. Mater. Chem. A*, 3(5), 2181–2187.

Li, Y., Yang, W., Ding, S., Fu, X. Z., Sun, R., Liao, W. H., and Wong, C. P. (2018b). "Tuning dielectric properties and energy density of poly(vinylidene fluoride) nanocomposites by quasi core–shell structured BaTiO3@graphene oxide hybrids." *J. Mater. Sci. Mater. Electron.*, 29(2), 1082–1092.

Lin, Y., Wang, L., Yin, F., Farzaneh, M., Liu, Y., and Gao, S. (2019). "Comparison of four commonly used high temperature vulcanized silicone rubber formulas for outdoor insulator and their regional adaptability." *J. Appl. Polym. Sci.*, 136(19), 1–12.

Liu, S. Y., Lu, J. G., and Shieh, H. P. D. (2018a). "Influence of Permittivity on the Sensitivity of Porous Elastomer-Based Capacitive Pressure Sensors." *IEEE Sens. J.*, 18(5), 1870–1876.

Liu, W., Liu, N., Yue, Y., Rao, J., Luo, C., Zhang, H., Yang, C., Su, J., Liu, Z., and Gao, Y. (2018b). "A flexible and highly sensitive pressure sensor based on elastic carbon foam." *J. Mater. Chem. C*, 6(6), 1451–1458.

Liu, Y.-J., Lan, X., Lu, H.-B., And Leng, J.-S. (2010). "Recent Progresses in Polymeric Smart Materials." *Int. J. Mod. Phys. B*, 24, 2351–2356.

Liu, Y. F., Li, Y. Q., Huang, P., Hu, N., and Fu, S. Y. (2018c). "On the Evaluation of the Sensitivity Coefficient of Strain Sensors." *Adv. Electron. Mater.*, 4(12), 1–6.

Liu, Z. D., Feng, Y., and Li, W. L. (2015). "High dielectric constant and low loss of polymeric dielectric composites filled by carbon nanotubes adhering $BaTiO_3$ hybrid particles." *RSC Adv.*, 5(37), 29017–29021.

Luheng, W., Tianhuai, D., and Peng, W. (2007). “Effects of conductive phase content on critical pressure of carbon black filled silicone rubber composite.” *Sensors Actuators, A Phys.*, 135(2), 587–592.

Luheng, W., Tianhuai, D., and Peng, W. (2009). “Influence of carbon black concentration on piezoresistivity for carbon-black-filled silicone rubber composite.” *Carbon*, 47(14), 3151–3157.

Ma, R., Chou, S. Y., Xie, Y., and Pei, Q. (2019). “Morphological/nanostructural control toward intrinsically stretchable organic electronics.” *Chem. Soc. Rev.*, 48(6), 1741–1786.

Madhanagopal, J., Singh, O. P., Sornambikai, S., Omar, A. H., Sathasivam, K. V., Fatihhi, S. J., and Abdul Kadir, M. R. (2017). “Enhanced wide-range monotonic piezoresistivity, reliability of Ketjenblack/deproteinized natural rubber nanocomposite, and its biomedical application.” *J. Appl. Polym. Sci.*, 134(25), 1–11.

Madsen, F. B., Daugaard, A. E., Hvilsted, S., and Skov, A. L. (2016a). “The Current State of Silicone-Based Dielectric Elastomer Transducers.” *Macromol. Rapid Commun.*, 37(5), 378–413.

Madsen, F. B., Yu, L., Mazurek, P., and Skov, A. L. (2016b). “A simple method for reducing inevitable dielectric loss in high-permittivity dielectric elastomers.” *Smart Mater. Struct.*, 25(7), 75018.

Maffli, L., Rosset, S., Ghilardi, M., Carpi, F., and Shea, H. (2015). “Ultrafast All-Polymer Electrically Tunable Silicone Lenses.” *Adv. Funct. Mater.*, 25(11), 1656–1665.

Maheshwari, V., and Saraf, R. (2008). “Tactile devices to sense touch on a par with a human finger.” *Angew. Chemie - Int. Ed.*, 47(41), 7808–7826.

Maiolino, P., Galantini, F., Mastrogiovanni, F., Gallone, G., Cannata, G., and Carpi, F. (2015). “Soft dielectrics for capacitive sensing in robot skins: Performance of different elastomer types.” *Sensors Actuators, A Phys.*, 226, 37–47.

Maiolino, P., Maggiali, M., Cannata, G., Metta, G., and Natale, L. (2013). “A flexible and robust large scale capacitive tactile system for robots.” *IEEE Sens. J.*, 13(10), 3910–3917.

Mannsfeld, S. C. B., Tee, B. C. K., Stoltenberg, R. M., Chen, C. V. H. H., Barman, S., Muir, B. V. O., Sokolov, A. N., Reese, C., and Bao, Z. (2010). “Highly sensitive flexible pressure sensors with microstructured rubber dielectric layers.” *Nat. Mater.*, 9(10), 859–864.

Matsuhisa, N., Chen, X., Bao, Z., and Someya, T. (2019). “Materials and structural designs of stretchable conductors.” *Chem. Soc. Rev.*, 48(11), 2946–2966.

Mei, H., Wang, R., Wang, Z., Feng, J., Xia, Y., and Zhang, T. (2015a). “A flexible pressure-sensitive array based on soft substrate.” *Sensors Actuators, A Phys.*, 222, 80–86.

Mei, H., Zhang, C., Wang, R., Feng, J., and Zhang, T. (2015b). “Impedance

characteristics of surface pressure-sensitive carbon black/silicone rubber composites." *Sensors Actuators, A Phys.*, 233, 118–124.

Metzger, C., Fleisch, E., Meyer, J., Dansachmüller, M., Graz, I., Kaltenbrunner, M., Keplinger, C., Schwödiauer, R., and Bauer, S. (2008). "Flexible-foam-based capacitive sensor arrays for object detection at low cost." *Appl. Phys. Lett.*, 92(1), 1–4.

Molberg, M., Crespy, D., Rupper, P., Nüesch, F., Manson, J. A. E., Löwe, C., and Opris, D. M. (2010). "High breakdown field dielectric elastomer actuators using encapsulated polyaniline as high dielectric constant filler." *Adv. Funct. Mater.*, 20(19), 3280–3291.

Nayak, S., Chaki, T. K., and Khastgir, D. (2014a). "Development of flexible piezoelectric poly(dimethylsiloxane)-$BaTiO_3$ nanocomposites for electrical energy harvesting." *Ind. Eng. Chem. Res.*, 53(39), 14982–14992.

Nayak, S., Kumar Chaki, T., and Khastgir, D. (2012). "Development of Poly(dimethylsiloxane)/$BaTiO_3$ Nanocomposites as Dielectric Material." *Adv. Mater. Res.*, 622–623, 897–900.

Nayak, S., Rahaman, M., Pandey, A. K., Setua, D. K., Chaki, T. K., and Khastgir, D. (2013). "Development of poly(dimethylsiloxane)-titania nanocomposites with controlled dielectric properties: Effect of heat treatment of titania on electrical properties." *J. Appl. Polym. Sci.*, 127(1), 784–796.

Nayak, S., Sahoo, B., Chaki, T. K., and Khastgir, D. (2014b). "Facile preparation of uniform barium titanate ($BaTiO_3$) multipods with high permittivity: Impedance and temperature dependent dielectric behavior." *RSC Adv.*, 4(3), 1212–1224.

Newnham, R. E. (1986). "Composite electroceramics." *Ferroelectrics*, 68(1), 1–32.

Nguyen, T. D., Nguyen, C. T., Lee, D. hyuk, Kim, U., Lee, C., Nam, J. do, and Choi, H. R. (2014). "Highly stretchable dielectric elastomer material based on acrylonitrile butadiene rubber." *Macromol. Res.*, 22(11), 1170–1177.

Panahi-Sarmad, M., Abrisham, M., Noroozi, M., Amirkiai, A., Dehghan, P., Goodarzi, V., and Zahiri, B. (2019a). "Deep focusing on the role of microstructures in shape memory properties of polymer composites: A critical review." *Eur. Polym. J.*, 117, 280–303.

Panahi-Sarmad, M., Chehrazi, E., Noroozi, M., Raef, M., Razzaghi-Kashani, M., and Haghighat Baian, M. A. (2019b). "Tuning the Surface Chemistry of Graphene Oxide for Enhanced Dielectric and Actuated Performance of Silicone Rubber Composites." *ACS Appl. Electron. Mater.*, 1(2), 198–209.

Panahi-Sarmad, M., Goodarzi, V., Amirkiai, A., Noroozi, M., Abrisham, M., Dehghan, P., Shakeri, Y., Karimpour-Motlagh, N., Poudineh Hajipoor, F., Ali Khonakdar, H., and Asefnejad, A. (2019c). "Programing polyurethane with systematic presence of graphene-oxide (GO) and reduced graphene-oxide (rGO) platelets for adjusting of heat-actuated shape memory properties." *Eur. Polym. J.*, 118, 619–632.

Panahi-Sarmad, M., and Razzaghi-Kashani, M. (2018). “Actuation behavior of PDMS dielectric elastomer composites containing optimized graphene oxide.” *Smart Mater. Struct.*, 27(8), 85021-1–15.

Panahi-Sarmad, M., Zahiri, B., and Noroozi, M. (2019d). “Graphene-based composite for dielectric elastomer actuator: A comprehensive review.” *Sensors Actuators, A Phys.*, 293, 222–241.

Park, M., Kim, H., and Youngblood, J. P. (2008). “Strain-dependent electrical resistance of multi-walled carbon nanotube/polymer composite films.” *Nanotechnology*, 19(5).

Park, S. W., Das, P. S., and Park, J. Y. (2018). “Development of wearable and flexible insole type capacitive pressure sensor for continuous gait signal analysis.” *Org. Electron. physics, Mater. Appl.*, 53, 213–220.

Pelrine, R., Kornbluh, R., Joseph, J., Heydt, R., Pei, Q., and Chiba, S. (2000). “High-field deformation of elastomeric dielectrics for actuators.” *Mater. Sci. Eng. C*, 11(2), 89–100.

Pignanelli, J., Schlingman, K., Carmichael, T. B., Rondeau-Gagné, S., and Ahamed, M. J. (2019). “A comparative analysis of capacitive-based flexible PDMS pressure sensors.” *Sensors Actuators, A Phys.*, 285, 427–436.

Poikelispää, M., Shakun, A., Das, A., and Vuorinen, J. (2016). “Improvement of actuation performance of dielectric elastomers by barium titanate and carbon black fillers.” *J. Appl. Polym. Sci.*, 133(42), 44116-1–9.

Poudel, A., Walsh, P., Kennedy, J., Thomas, K., Lyons, J. G., and Coffey, A. (2019). “Thermal, mechanical, dielectric, and morphological study of dielectric filler–based thermoplastic nanocomposites for electromechanical applications.” *J. Thermoplast. Compos. Mater.*, 32(2), 178–204.

Princy, K. G., Joseph, R., and Kartha, C. S. (1998). “Studies on conductive silicone rubber compounds.” *J. Appl. Polym. Sci.*, 69(5), 1043–1050.

Psarras, G. C., Manolakaki, E., and Tsangaris, G. M. (2003). “Dielectric dispersion and ac conductivity in - Iron particles loaded: Polymer composites.” *Compos. Part A Appl. Sci. Manuf.*, 34(12), 1187–1198.

Pyo, S., Choi, J., and Kim, J. (2018). “Flexible, Transparent, Sensitive, and Crosstalk-Free Capacitive Tactile Sensor Array Based on Graphene Electrodes and Air Dielectric.” *Adv. Electron. Mater.*, 4(1), 1–8.

Ramajo, L., Reboredo, M., and Castro, M. (2005). “Dielectric response and relaxation phenomena in composites of epoxy resin with $BaTiO_3$ particles.” *Compos. Part A Appl. Sci. Manuf.*, 36(9), 1267–1274.

Rana, A., Roberge, J. P., and Duchaine, V. (2016). “An Improved Soft Dielectric for a Highly Sensitive Capacitive Tactile Sensor.” *IEEE Sens. J.*, 16(22), 7853–7863.

Raptis, C. G., Patsidis, A., and Psarras, G. C. (2010). “Electrical response and functionality of polymer matrix-titanium carbide composites.” *Express Polym. Lett.*,

4(4), 234–243.

Renard, C., Wang, D., Yang, Y., Xiong, S., Shi, C. Y., and Dang, Z. M. (2017). “Plasticized thermoplastic polyurethanes for dielectric elastomers with improved electromechanical actuation.” *J. Appl. Polym. Sci.*, 134(30), 1–10.

Renukappa, N. M., Siddaramaiah, Sudhaker Samuel, R. D., Sundara Rajan, J., and Lee, J. H. (2009). “Dielectric properties of carbon black: SBR composites.” *J. Mater. Sci. Mater. Electron.*, 20(7), 648–656.

Romasanta, L. J., Hernández, M., López-Manchado, M. A., and Verdejo, R. (2011). “Functionalised graphene sheets as effective high dielectric constant fillers.” *Nanoscale Res. Lett.*, 6, 1–6.

Romasanta, L. J., Leret, P., Casaban, L., Hernández, M., La Rubia, M. A. De, Fernández, J. F., Kenny, J. M., Lopez-Manchado, M. A., and Verdejo, R. (2012). “Towards materials with enhanced electro-mechanical response: $CaCu_3Ti_4O_{12}$-polydimethylsiloxane composites.” *J. Mater. Chem.*, 22(47), 24705–24712.

Romasanta, L. J., Lopez-Manchado, M. A., and Verdejo, R. (2015). “Increasing the performance of dielectric elastomer actuators: A review from the materials perspective.” *Prog. Polym. Sci.*, 51, 188–211.

Ruan, M., Yang, D., Guo, W., Huang, S., Wu, Y., Wang, H., Wang, H., and Zhang, L. (2017). “Improved electromechanical properties of brominated butyl rubber filled with modified barium titanate.” *RSC Adv.*, 7(59), 37148–37157.

Ruan, M., Yang, D., Guo, W., Zhang, L., Li, S., Shang, Y., Wu, Y., Zhang, M., and Wang, H. (2018). “Improved dielectric properties, mechanical properties, and thermal conductivity properties of polymer composites via controlling interfacial compatibility with bio-inspired method.” *Appl. Surf. Sci.*, 439, 186–195.

Sahoo, B. P., Naskar, K., and Tripathy, D. K. (2012). “Conductive carbon black-filled ethylene acrylic elastomer vulcanizates: Physico-mechanical, thermal, and electrical properties.” *J. Mater. Sci.*, 47(5), 2421–2433.

Sahu, D., Sahu, R. K., and Patra, K. (2019). “Effects of crosslink density on the behavior of VHB 4910 dielectric elastomer.” *J. Macromol. Sci. Part A Pure Appl. Chem.*, 56(9), 821–829.

Sahu, R. K., Saini, A., Ahmad, D., Patra, K., and Szpunar, J. (2016). “Estimation and validation of maxwell stress of planar dielectric elastomer actuators.” *J. Mech. Sci. Technol.*, 30(1), 429–436.

Saji, J., Khare, A., Choudhary, R. N. P., and Mahapatra, S. P. (2015). “Impedance analysis, dielectric relaxation, and electrical conductivity of multi-walled carbon nanotube-reinforced silicon elastomer nanocomposites.” *J. Elastomers Plast.*, 47(5), 394–415.

Saji, J., Khare, A., and Mahapatra, S. P. (2016). “Relaxation behavior of nanographite-reinforced silicon elastomer nanocomposites.” *High Perform. Polym.*, 28(1), 3–13.

Santos, A. Dos, Pinela, N., Alves, P., Santos, R., Farinha, R., Fortunato, E., Martins, R., Águas, H., and Igreja, R. (2019). "E-skin bimodal sensors for robotics and prosthesis using PDMS molds engraved by laser." *Sensors (Switzerland)*, 19(4).

Sarban, R., Mace, B. R., Jones, R. W., and Rustighi, E. (2010). "Active vibration isolation using a dielectric electro-active polymer actuator." *MOVIC 2010 - 10th Int. Conf. Motion Vib. Control. Proc.*, 5(5), 643–652.

Sheima, Y., Caspari, P., and Opris, D. M. (2019). "Artificial Muscles: Dielectric Elastomers Responsive to Low Voltages." *Macromol. Rapid Commun.*, 40(16), 1–8.

Sheng, J., Chen, H., Qiang, J., Li, B., and Wang, Y. (2012). "Thermal, Mechanical, and Dielectric Properties of a Dielectric Elastomer for Actuator Applications." *J. Macromol. Sci. Part B*, 51(10), 2093–2104.

Shirinov, A. V., and Schomburg, W. K. (2008). "Pressure sensor from a PVDF film." *Sensors Actuators, A Phys.*, 142(1), 48–55.

Shuai, X., Zhu, P., Zeng, W., Hu, Y., Liang, X., Zhang, Y., Sun, R., and Wong, C. P. (2017). "Highly Sensitive Flexible Pressure Sensor Based on Silver Nanowires-Embedded Polydimethylsiloxane Electrode with Microarray Structure." *ACS Appl. Mater. Interfaces*, 9(31), 26314–26324.

Shukla, N., and Dwivedi, D. K. (2016). "Dielectric relaxation and AC conductivity studies of $Se_{90}Cd_{10-x}In_x$ glassy alloys." *J. Asian Ceram. Soc.*, 4(2), 178–184.

Skov, A. L., and Yu, L. (2018). "Optimization Techniques for Improving the Performance of Silicone-Based Dielectric Elastomers." *Adv. Eng. Mater.*, 20(5), 1–21.

Stiubianu, G., Dumitriu, A. M. C., Varganici, C. D., Tugui, C., Iacob, M., Bele, A., and Cazacu, M. (2016). "Changes induced in the properties of dielectric silicone elastomers by the incorporation of transition metal complexes." *High Perform. Polym.*, 28(8), 915–926.

Stoyanov, H., Brochu, P., Niu, X., Lai, C., Yun, S., and Pei, Q. (2013). "Long lifetime, fault-tolerant freestanding actuators based on a silicone dielectric elastomer and self-clearing carbon nanotube compliant electrodes." *RSC Adv.*, 3(7), 2272–2278.

Su, J., and Zhang, J. (2015). "Remarkable enhancement of mechanical and dielectric properties of flexible ethylene propylene diene monomer (EPDM)/ barium titanate ($BaTiO_3$) dielectric elastomer by chemical modification of particles." *RSC Adv.*, 5(96), 78448–78456.

Sun, Q. J., Zhuang, J., Venkatesh, S., Zhou, Y., Han, S. T., Wu, W., Kong, K. W., Li, W. J., Chen, X., Li, R. K. Y., and Roy, V. A. L. (2018a). "Highly Sensitive and Ultrastable Skin Sensors for Biopressure and Bioforce Measurements Based on Hierarchical Microstructures." *ACS Appl. Mater. Interfaces*, 10(4), 4086–4094.

Sun, X., Wang, C., Chi, C., Xue, N., and Liu, C. (2018b). "A highly-sensitive flexible tactile sensor array utilizing piezoresistive carbon nanotube-polydimethylsiloxane composite." *J. Micromechanics Microengineering*, 28(10), 105011.

Tangboriboon, N., Datsanae, S., Onthong, A., Kunanuruksapong, R., and Sirivat, A.

(2013). “Electromechanical responses of dielectric elastomer composite actuators based on natural rubber and alumina.” *J. Elastomers Plast.*, 45(2), 143–161.

Tolvanen, J., Hannu, J., and Jantunen, H. (2017). “Hybrid foam pressure sensor utilizing piezoresistive and capacitive sensing mechanisms.” *IEEE Sens. J.*, 17(15), 4735–4746.

Tressler, J. F., Alkoy, S., Dogan, A., and Newnham, R. E. (1999). “Functional composites for sensors, actuators and transducers.” *Compos. Part A Appl. Sci. Manuf.*, 30(4), 477–482.

Tsangaris, G. M., and Psarras, G. C. (1999). “Dielectric response of a polymeric three-component composite.” *J. Mater. Sci.*, 34(9), 2151–2157.

Vandeparre, H., Watson, D., and Lacour, S. P. (2013). “Extremely robust and conformable capacitive pressure sensors based on flexible polyurethane foams and stretchable metallization.” *Appl. Phys. Lett.*, 103(20), 204103.

Wang, B., and Facchetti, A. (2019). “Mechanically Flexible Conductors for Stretchable and Wearable E-Skin and E-Textile Devices.” *Adv. Mater.*, 31(28), 1–53.

Wang, J., Jiu, J., Nogi, M., Sugahara, T., Nagao, S., Koga, H., He, P., and Suganuma, K. (2015a). “A highly sensitive and flexible pressure sensor with electrodes and elastomeric interlayer containing silver nanowires.” *Nanoscale*, 7(7), 2926–2932.

Wang, J., Qi, S., Sun, Y., Tian, G., and Wu, D. (2015b). “ Dielectric behavior of a flexible three-phase polyimide/$BaTiO_3$/multi-walled carbon nanotube composite film.” *Funct. Mater. Lett.*, 9(1), 1650006.

Weadon, T. L., Evans, T. H., and Sabolsky, E. M. (2014). “An analytical model for porous polymer-ceramic capacitive pressure sensors.” *IEEE Sens. J.*, 14(12), 4411–4422.

Wolf, M. P., Salieb-Beugelaar, G. B., and Hunziker, P. (2018). “PDMS with designer functionalities—Properties, modifications strategies, and applications.” *Prog. Polym. Sci.*, 83, 97–134.

Wu, S. Q., Wang, J. W., Shao, J., Wei, L., Ge, R. K., and Ren, H. (2018). “An approach to developing enhanced dielectric property nanocomposites based on acrylate elastomer.” *Mater. Des.*, 146, 208–218.

Yang, D., Ge, F., Tian, M., Ning, N., Zhang, L., Zhao, C., Ito, K., Nishi, T., Wang, H., and Luan, Y. (2015a). “Dielectric elastomer actuator with excellent electromechanical performance using slide-ring materials/barium titanate composites.” *J. Mater. Chem. A*, 3(18), 9468–9479.

Yang, D., Huang, S., Ruan, M., Li, S., Wu, Y., Guo, W., and Zhang, L. (2018). “Improved electromechanical properties of silicone dielectric elastomer composites by tuning molecular flexibility.” *Compos. Sci. Technol.*, 155, 160–168.

Yang, G., Pang, G., Pang, Z., Gu, Y., Mantysalo, M., and Yang, H. (2019). “Non-Invasive Flexible and Stretchable Wearable Sensors with Nano-Based Enhancement for Chronic Disease Care.” *IEEE Rev. Biomed. Eng.*, 12, 34–71.

Yang, Y., Sun, H., Zhu, B., Wang, Z., Wei, J., Xiong, R., Shi, J., Liu, Z., and Lei, Q. (2015b). "Enhanced dielectric performance of three phase percolative composites based on thermoplastic-ceramic composites and surface modified carbon nanotube." *Appl. Phys. Lett.*, 106(1), 12902-1–5.

Yao, H. Bin, Ge, J., Wang, C. F., Wang, X., Hu, W., Zheng, Z. J., Ni, Y., and Yu, S. H. (2013). "A flexible and highly pressure-sensitive graphene-polyurethane sponge based on fractured microstructure design." *Adv. Mater.*, 25(46), 6692–6698.

Yao, S. H., Dang, Z. M., Jiang, M. J., and Bai, J. (2008). "$BaTiO_3$-carbon nanotube/polyvinylidene fluoride three-phase composites with high dielectric constant and low dielectric loss." *Appl. Phys. Lett.*, 93(18), 182905-1–3.

Yoshimura, K., Nakano, K., and Hishikawa, Y. (2016). "Flexible tactile sensor materials based on carbon microcoil/silicone-rubber porous composites." *Compos. Sci. Technol.*, 123, 241–249.

Yoshimura, K., Nakano, K., Okamoto, K., and Miyake, T. (2012). "Mechanical and electrical properties in porous structure of Ketjenblack/silicone-rubber composites." *Sensors Actuators, A Phys.*, 180, 55–62.

Yu, L., and Skov, A. L. (2015). "Silicone rubbers for dielectric elastomers with improved dielectric and mechanical properties as a result of substituting silica with titanium dioxide." *Int. J. Smart Nano Mater.*, 6(4), 268–289.

Yu, X. G., Li, Y. Q., Zhu, W. Bin, Huang, P., Wang, T. T., Hu, N., and Fu, S. Y. (2017). "A wearable strain sensor based on a carbonized nano-sponge/silicone composite for human motion detection." *Nanoscale*, 9(20), 6680–6685.

Zagnoni, M., Golfarelli, A., Callegari, S., Talamelli, A., Bonora, V., Sangiorgi, E., and Tartagni, M. (2005). "A non-invasive capacitive sensor strip for aerodynamic pressure measurement." *Sensors Actuators, A Phys.*, 123–124, 240–248.

Zakaria, S., Madsen, F. B., and Skov, A. L. (2017). "Post Curing as an Effective Means of Ensuring the Long-term Reliability of PDMS Thin Films for Dielectric Elastomer Applications." *Polym. - Plast. Technol. Eng.*, 56(1), 83–95.

Zakaria, S., Yu, L., Kofod, G., and Skov, A. L. (2015). "The influence of static pre-stretching on the mechanical ageing of filled silicone rubbers for dielectric elastomer applications." *Mater. Today Commun.*, 4, 204–213.

Zhang, F., Li, T., and Luo, Y. (2018). "A new low moduli dielectric elastomer nano-structured composite with high permittivity exhibiting large actuation strain induced by low electric field." *Compos. Sci. Technol.*, 156, 151–157.

Zhang, H. Z., Tang, Q. Y., and Chan, Y. C. (2012). "Development of a versatile capacitive tactile sensor based on transparent flexible materials integrating an excellent sensitivity and a high resolution." *AIP Adv.*, 2(2).

Zhang, J., and Feng, S. (2003). "Temperature Effects of Electrical Resistivity of Conductive Silicone Rubber Filled with Carbon Blacks." *J. Appl. Polym. Sci.*, 90(14), 3889–3895.

Zhang, L., Bass, P., and Cheng, Z.-Y. (2015). “Physical aspects of 0-3 dielectric composites.” *J. Adv. Dielectr.*, 5(2), 1550012.

Zhang, L., Bass, P., Dang, Z.-M., and Cheng, Z.-Y. (2014). “Characterization of percolation behavior in conductor–dielectric 0-3 composites.” *J. Adv. Dielectr.*, 4(4), 1450035.

Zhang, L., and Cheng, Z.-Y. (2011). “Development of Polymer-Based 0–3 Composites With High Dielectric Constant.” *J. Adv. Dielectr.*, 1(4), 389–406.

Zhang, Q., Liang, J., Huang, Y., Chen, H., and Ma, R. (2019a). “Intrinsically stretchable conductors and interconnects for electronic applications.” *Mater. Chem. Front.*, 3(6), 1032–1051.

Zhang, Z., Zhang, J., Li, S., Liu, J., Dong, M., Li, Y., Lu, N., Lei, S., Tang, J., Fan, J., and Guo, Z. (2019b). “Effect of graphene liquid crystal on dielectric properties of polydimethylsiloxane nanocomposites.” *Compos. Part B Eng.*, 176, 107338-1–9.

Zhao, H., Wang, D. R., Zha, J. W., Zhao, J., and Dang, Z. M. (2013a). “Increased electroaction through a molecular flexibility tuning process in TiO_2-polydimethylsilicone nanocomposites.” *J. Mater. Chem. A*, 1(9), 3140–3145.

Zhao, H., Xia, Y. J., Dang, Z. M., Zha, J. W., and Hu, G. H. (2013b). “Composition dependence of dielectric properties, elastic modulus, and electroactivity in (carbon black-$BaTiO_3$)/silicone rubber nanocomposites.” *J. Appl. Polym. Sci.*, 127(6), 4440–4445.

Zheng, X., Huang, Y., Zheng, S., Liu, Z., and Yang, M. (2019). “Improved dielectric properties of polymer-based composites with carboxylic functionalized multiwalled carbon nanotubes.” *J. Thermoplast. Compos. Mater.*, 32(4), 473–486.

Zhong, S. L., and Dang, Z. M. (2018). “High energy storage dielectric polymer materials with hierarchical microstructures.” *Dielectr. Polym. Mater. High-Density Energy Storage*, Elsevier Inc., 165–197.

Zhu, J., Wang, H., and Zhu, Y. (2018). “A flexible piezoresistive carbon black network in silicone rubber for wide range deformation and strain sensing.” *J. Appl. Phys.*, 123(3).

Zhu, S., and Zhang, J. (2017). “Enhanced dielectric constant of acrylonitrile–butadiene rubber/barium titanate composites with mechanical reinforcement by nanosilica.” *Iran. Polym. J.*, 26(4), 239–251.

Zhuo, B., Chen, S., Zhao, M., and Guo, X. (2017). “High Sensitivity Flexible Capacitive Pressure Sensor Using Polydimethylsiloxane Elastomer Dielectric Layer Micro-Structured by 3-D Printed Mold.” *IEEE J. Electron Devices Soc.*, 5(3), 219–223.

BIO-DATA

Name: B.S. Manohar Shankar

DOB: 19/08/1974

Address:

H.No 217/45 (FF), Goa Housing Board Colony,

Farmagudi, Ponda,Goa 403401.

Ph: +919049269449

Email: manoharshankarbhat@gmail.com

Qualification: BE (Mechanical Engineering) from Goa University

ME (Industrial Engineering) from Goa University

Industry Experience: 1 Year (Ciba Speciality Chemicals)

Teaching Experience: 21 Years (Department of Mechanical Engineering, Goa College of Engineering)

List of publications: Journals: 02

Conferences: 04